

JYU DISSERTATIONS 341

---

**Tuuli Nissinen**

# **Molecular and Physiological Effects of Muscle Wasting and Its Treatment by Blocking Myostatin and Activins**

---



UNIVERSITY OF JYVÄSKYLÄ  
FACULTY OF SPORT AND  
HEALTH SCIENCES

JYU DISSERTATIONS 341

---

**Tuuli Nissinen**

# **Molecular and Physiological Effects of Muscle Wasting and Its Treatment by Blocking Myostatin and Activins**

Esitetään Jyväskylän yliopiston liikuntatieteellisen tiedekunnan suostumuksella  
julkisesti tarkastettavaksi joulukuun 18. päivänä 2020 kello 12.

Academic dissertation to be publicly discussed, by permission of  
the Faculty of Sport and Health Sciences of the University of Jyväskylä,  
on December 18, 2020 at 12 o'clock noon.



UNIVERSITY OF JYVÄSKYLÄ  
FACULTY OF SPORT AND  
HEALTH SCIENCES

JYVÄSKYLÄ 2020

Editors

Simon Walker

Faculty of Sport and Health Sciences, University of Jyväskylä

Timo Hautala

Open Science Centre, University of Jyväskylä

Copyright © 2020, by University of Jyväskylä

Permanent link to this publication: <http://urn.fi/URN:ISBN:978-951-39-8468-7>

ISBN 978-951-39-8468-7 (PDF)

URN:ISBN:978-951-39-8468-7

ISSN 2489-9003

## ABSTRACT

Nissinen, Tuuli

Molecular and physiological effects of muscle wasting and its treatment by blocking myostatin and activins

Jyväskylä: University of Jyväskylä, 2020, 147 p.

(JYU Dissertations

ISSN 2489-9003; 341)

ISBN 978-951-39-8468-7

Muscle wasting, occurring e.g. in cancer, is associated with poor prognosis, and cancer treatments may even exacerbate the wasting. The prevention of muscle wasting has improved survival in preclinical cancer models, but the mechanisms are poorly understood. The purpose of this dissertation was to study the molecular and physiological effects of different wasting conditions and their treatment by myostatin/activin blocking. The effects of myostatin/activin blocking were studied in (1) doxorubicin (DOX) chemotherapy-treated mice, (2) tumour-bearing (TB) mice, and (3) fasted and inactive mice. Myostatin/activin blocking prevented muscle wasting in DOX-treated and TB mice. In TB mice, this was associated with improved survival, but not when myostatin/activin blocking was used to increase muscle mass only before cancer. Myostatin/activin blocking also restored bone density in DOX-treated mice, but did not counteract the impaired running capacity and the decreased physical activity in DOX-treated and TB mice, respectively. Muscle protein synthesis was decreased by DOX and restored by myostatin/activin blocking in skeletal muscle, but not in the heart. The transcriptomic responses to DOX and myostatin/activin blocking were also larger in skeletal muscle than in the heart. Muscle protein synthesis was also decreased in TB mice. This was associated with reduced mTORC1 signalling and decreased colocalization of mTOR with lysosomes, which were restored by myostatin/activin blocking. Myostatin/activin blocking also induced muscle protein synthesis in healthy mice independent of alterations in physical activity and food intake and increased the amount of mTOR colocalised with lysosomes. This study shows that prevention of muscle wasting by myostatin/activin blocking improves survival in experimental cancer and has other beneficial effects beyond skeletal muscle in chemotherapy and cancer. In addition, maintaining muscle mass may be more beneficial in terms of survival than having a larger muscle mass before the cachectic stimulus. Finally, muscle protein synthesis and mTORC1 signalling induced by myostatin/activin blocking may be mediated via increased mTOR-lysosome colocalisation in healthy and cachectic muscles. This dissertation contributes to the cachexia research with novel results that may advance the development of strategies to prevent or treat cachexia.

Keywords: activin, cancer cachexia, chemotherapy, muscle wasting, myostatin, physical activity, protein synthesis, skeletal muscle

**Author's address**

Tuuli Nissinen, MSc  
NeuroMuscular Research Center  
Faculty of Sport and Health Sciences  
University of Jyväskylä  
P.O. Box 35  
FI-40014 University of Jyväskylä, Finland  
tuuli.a.m.nissinen@jyu.fi

**Supervisors**

Associate professor Juha Hulmi, PhD  
NeuroMuscular Research Center  
Faculty of Sport and Health Sciences  
University of Jyväskylä  
Jyväskylä, Finland

Riikka Kivelä, PhD, Academy Research Fellow  
Stem Cells and Metabolism Research Program  
Research Programs Unit  
Faculty of Medicine  
University of Helsinki and  
Wihuri Research Institute  
Helsinki, Finland

Professor Heikki Kainulainen, PhD  
NeuroMuscular Research Center  
Faculty of Sport and Health Sciences  
University of Jyväskylä  
Jyväskylä, Finland

**Reviewers**

Professor Silvia Busquets, PhD  
Department of Biochemistry and Molecular Biology  
University of Barcelona  
Barcelona, Spain

Assistant Professor Andrea Bonetto, PhD  
Department of Surgery  
Indiana University School of Medicine  
Indianapolis, USA

**Opponent**

Professor Karl-Heinz Herzig, MD, PhD  
Research Unit of Biomedicine  
Faculty of Medicine  
University of Oulu  
Oulu, Finland

## TIIVISTELMÄ (FINNISH ABSTRACT)

Nissinen, Tuuli

Lihaskadon ja myostatiini/aktiviini-signaaloinnin eston molekulaariset ja fysiologiset vaikutukset

Jyväskylä: University of Jyväskylä, 2020, 147 s.

(JYU Dissertations

ISSN 2489-9003; 341)

ISBN 978-951-39-8468-7

Moniin sairauksiin, kuten syöpään, liittyvä lihaskato on yhteydessä huonoon ennusteeseen, ja syöpähoidot voivat jopa kiihdyttää lihaskatoa. Lihaskadon esto on pidentänyt selviytymistä kokeellisissa syöpämalleissa, mutta sen mekanismeja ei vielä tunneta. Tämän väitöskirjan tarkoitus oli tutkia lihaskadon ja sen hoidon fysiologiaa ja molekyyli-tason vaikutuksia. Lihaskatoa ehkäisevän myostatiinin/aktiviinien eston vaikutuksia tutkittiin (1) kemoterapiaa saavilla hiirillä, (2) kokeellisella syöpämallilla hiirillä ja (3) passiivisilla ja aktiivisilla sekä paastonneilla ja ei-paastonneilla hiirillä. Myostatiinin/aktiviinien esto ehkäisi sekä kemoterapian että kokeellisen syövän aiheuttaman lihaskadon. Tämä oli yhteydessä parempaan selviytymiseen syövässä, mutta vain silloin, kun lihaskadon hoitoa jatkettiin myös kasvaimen muodostumisen jälkeen. Myostatiinin/aktiviinien esto ehkäisi myös kemoterapian aiheuttaman luuntiheyden laskun, mutta ei vaikuttanut kemoterapian aiheuttamaan juoksukapasiteetin heikkenemiseen eikä fyysisen aktiivisuuden laskuun syövässä. Kemoterapia laski luurankoli-haksen proteiinisynteesiä, ja myostatiinin/aktiviinien esto ehkäisi tämän laskun. Kemoterapian ja myostatiinin/aktiviinien eston vaikutukset proteiinisynteesiin ja geenien ilmentymiseen olivat selvästi suurempia luurankoli-haksessa kuin sydämessä. Luurankoli-haksen proteiinisynteesi laski myös syövässä, mikä oli yhteydessä mTORC1-signaaloinnin laskuun sekä vähentyneeseen mTOR:n ilmenemiseen lysosomien lähellä. Myostatiinin/aktiviinien esto ehkäisi syövän aiheuttamia muutoksia mTOR:n solunsisäisessä sijainnissa ja signaaloinnissa. Myostatiinin/aktiviinien esto lisäsi luurankoli-haksen proteiinisynteesiä terveillä hiirillä riippumatta fyysisen aktiivisuuden tai syömisen määrästä ja lisäsi mTOR:n ilmenemistä lysosomien lähellä. Tulokset osoittavat, että lihaskadon ehkäisy myostatiinia ja aktiviineja estämällä voi pidentää selviytymistä kokeellisessa syövässä ja sillä on edullisia vaikutuksia myös muihin kudoksiin kemoterapiaa saavilla ja syöpää sairastavilla hiirillä. Lihaskoon ylläpito saattaa olla selviytymisen kannalta hyödyllisempää kuin lihasten kasvatus ennen syöpää. Myostatiinin ja aktiviinien eston aikaansaama proteiinisynteesin ja mTORC1-signaaloinnin nousu saattavat osittain selittyä mTOR:n solunsisäisellä sijainnilla. Tulokset lisäävät ymmärrystä luurankoli-haskudoksen tärkeydestä, lihaskadon mekanismeista ja mahdollisista uusista lihaskadon hoitomuodoista.

Avainsanat: aktiviini, fyysinen aktiivisuus, kakeksia, kemoterapia, lihaskato, luurankolihas, myostatiini, proteiinisynteesi

## ACKNOWLEDGEMENTS

Majority of the work presented in this thesis was carried out at the Faculty of Sport and Health Sciences at the University of Jyväskylä. The faculty provided excellent facilities for research and a skilled staff to work with, for which I am grateful. Some of the work was carried out at the Department of Physiology as well as at the Translational Cancer Biology laboratory and Wihuri Research Institute, led by Academy Professor Kari Alitalo, at the Faculty of Medicine, University of Helsinki. I would like to express my gratitude for the opportunity to conduct a crucial part of my research there. The Academy of Finland, the Cancer Society of Finland, Jenny and Antti Wihuri Foundation, Ellen and Artturi Nyyssönen Foundation, the Finnish Concordia Fund, the Finnish Physiological Society, the Association of Researchers and Teachers of Jyväskylä, and the Faculty of Sport and Health Sciences are acknowledged for the financial support.

I wish to express my deepest gratitude to my supervisor Dr. Juha Hulmi for all the guidance, encouragement and trust during this project. It is thanks to you that I first got into doing research, as you pushed me into the right direction during my bachelor's studies. It was a dream come true to get the opportunity to do my PhD in this project, and I want to thank you for believing in me and for giving me that opportunity. I am thankful for everything that I have learned from you. In addition to the common research interests, we share the same taste in music, which has made working in this project even more fun and special. I am not sure whether musical taste was a contributing factor when you were recruiting PhD students to your project. Finally, I appreciate your patience with my perhaps excessive attention to detail. Maybe I have learned to tone it down at least a little bit during this project. I hope our paths will cross in the future in a form of some kind of collaboration.

Secondly, I would sincerely like to thank my second supervisor, Dr. Riikka Kivelä, for all her support and expertise that improved not only the quality of the research but also my growth as a researcher. Every time I had some kind of a problem or question, you were able and willing to help me with it, and every time after talking with you I felt like the weight was lifted from my shoulders (at least for a moment). I feel very lucky to have had you as my second supervisor and I sincerely hope that we can collaborate somehow in the future as well. Thirdly, I wish to thank my third supervisor, Professor Heikki Kainulainen. You have always been interested in how everything is going with my research and willingly shared your expertise when I have needed advice. You have also influenced the beginning of my research career by being an inspiring teacher and by helping me get my foot in the door to start doing research.

I wish to thank the official reviewers of my dissertation, Professor Silvia Busquets and Assistant Professor Andrea Bonetto, for their constructive criticism and valuable comments. I also thank Professor Karl-Heinz Herzig for accepting the invitation to be my opponent.

I would like to acknowledge all the collaborators and co-authors, who have had an invaluable contribution to this project. Firstly, I would like to ex-

press my sincere gratitude to Dr. Olli Ritvos and Dr. Arja Pasternack, who have provided this project with valuable tools without which the work would not have been possible. I thank both of you for sharing your expertise in this project and also for wishing me welcome to learn new and exciting things in your lab during this project. Arja, I enjoyed a lot working with you and I am thankful for everything that I learned under your supervision.

I thank Dr. Markus Räsänen and Mr. Joni Degerman for the collaboration during the chemotherapy experiments. Joni, it was a real pleasure to start my PhD project by working with you. I would like to thank Dr. Fabio Penna for his important contribution to the cancer cachexia experiments by enabling the use of the cachexia model and by sharing his expertise in the cancer cachexia research. I also thank Dr. Satu Pekkala and Dr. Tanja Holopainen for providing valuable assistance in setting up the cancer model at our facility. I would also like to express my gratitude to Dr. Anita Kopperi, Mr. Vasco Fachada and Dr. Satu Koskinen for the indispensable help with immunohistochemistry and microscopy, without which the project would not have been as successful. I thank Dr. Mika Silvennoinen for the valuable contribution to this project, and also for being a great supervisor for my bachelor and master's theses, and thus inspiring me to continue with the PhD studies. I wish to acknowledge the bright and dedicated master's students, Ms. Aino Poikonen, Ms. Juulia Lautaoja and Mr. Jouni Härkönen, who worked in this project. I am sure I learned more from working with you than you learned from me. I would also like to thank Dr. Sanna Lensu not only for the invaluable help and guidance with the animal experiments, but also for being my "roommate" with whom I have shared the everyday life at work during the past years. You have been a huge help and support for me during this project.

There are not enough words to express my gratitude to Dr. Jaakko Hentilä, a fellow PhD student and my brother-in-arms in this project. I am lucky that I got to conduct most of the experiments with such an inspiring and analytical person. I am especially thankful for your help and company during the toughest times of this project, while conducting the survival experiment and working nocturnal hours in another experiment. I always felt that I could count on you, and I would not have managed without you. We have shared all the ups and downs during our PhD journey, and you have become one of my closest friends during this time, for which I am truly grateful. I sincerely believe that our friendship will last, wherever life takes us. I also hope that we can still shred and jam together at some point in the future.

Next, I would like to thank Ms. Juulia Lautaoja. Firstly, my PhD project would have taken even longer than it took if it had not been for you and your incredible efficiency. I cannot thank you enough for all your help and assistance during this project. Secondly, I wish to thank you for your friendship and for the dog therapy during these years. The long walks in the forest with you and our furry friends have played an important role in keeping me as sane as I am. Finally, I wish we can laugh together at Manu's crazy set-ups also in the future.



I would like to express my gratitude to Dr. Enni Hietavala for all the support, laughter and friendship during the past years. Words cannot describe how much your company, whether it was at the gym, at band rehearsals, at summer festivals or rock concerts, at a scientific conference, or in the next office when we were working late, has meant to me. I am also thankful for our intense scientific discussions, mostly about lactic acid. You are a real superwoman and it is an honor to be a godmother to one of your wonderful children, Ahti.

I would also like to collectively thank our Maca group, Jaakko, Juulia, Enni and Anita, for the pleasant company both at and outside of work. Our lunch breaks filled with laughter have been very enjoyable and a great way to relax in the middle of a busy and stressful day. Without you, my life would have been very different during these years, and probably not in a good way.

It has been a privilege to be a part of the Biology of Physical Activity team. I want to thank all the brilliant fellow PhD students for the company and discussions during these years. I thank Katja Pylkkänen and Minna Herpola for their assistance with all the practical matters. I wish to thank Dr. Maarit Lehti for having been an inspiring mentor for me during the past years. I also thank Dr. Sira Karvinen for all the help and support. Sira, you have been a role model for me and I really admire your efficiency and passion for science.

I would also like to express my sincere gratitude to the skilled and helpful laboratory staff, Mervi Matero, Bettina Hutz, Leena Tulla, Hanne Tähti, Aila Ollikainen, Risto Puurtinen and Jukka Hintikka. I had fun working in the lab with you and you had an important contribution to the successful completion of this project. Mervi, in addition to your valuable help in the lab, I also thank you for all the fun I have had chatting with you and for the support I got from you when I was not at my best. I also want to thank Eliisa Kiukkanen and the rest of the staff at the laboratory center for the excellent animal care and Jouni Tukiainen for the assistance with all the technical matters. I would also like to thank Maria Arrano de Kivikko from Alitalo laboratory for the amazing expertise in the animal work and for the fun we had while working together.

I wish to thank Noora, my best friend since third grade, for her endless support. Words cannot describe how lucky I am to have a friend like you. I also thank Lauri for all the support during the past years. I would not have been able to finish this dissertation without your indispensable help. I wish to thank my godparents, who have been my family here in Jyväskylä. I am grateful for all your help and support as well as for the time we have got to spend together. Last but not least, I would like to express my deepest gratitude to my parents who have always encouraged me to follow my dreams and supported all the choices that I have made. I want to thank you for your endless love and support that have helped me get through this project.

Jyväskylä 22.11.2020

Tuuli Nissinen

## LIST OF ORIGINAL PUBLICATIONS

This dissertation is based on the following original research articles, which will be referred to in the text by their Roman numerals:

- I **Nissinen, T.A.**, Degerman, J., Räsänen, M., Poikonen, A.R., Koskinen, S., Mervaala, E., Pasternack, A., Ritvos, O., Kivelä, R. & Hulmi, J.J. 2016. Systemic blockade of ACVR2B ligands prevents chemotherapy-induced muscle wasting by restoring muscle protein synthesis without affecting oxidative capacity or atrogenes. *Scientific reports* 6, 32695.
- II Hulmi, J.J.\*, **Nissinen, T.A.\***, Räsänen, M., Degerman, J., Lautaoja, J.H., Hemanthakumar, K.A., Backman, J.T., Ritvos, O., Silvennoinen, M. & Kivelä, R. 2018. Prevention of chemotherapy-induced cachexia by ACVR2B ligand blocking has different effects on heart and skeletal muscle *Journal of Cachexia, Sarcopenia and Muscle* 9 (2), 417–432. \*Equal contribution.
- III **Nissinen, T.A.**, Hentilä, J., Penna, F., Lampinen, A., Lautaoja, J.H., Fachada, V., Holopainen, T., Ritvos, O., Kivelä, R. & Hulmi, J.J. 2018. Treating cachexia using soluble ACVR2B improves survival, alters mTOR localization, and attenuates liver and spleen responses. *Journal of Cachexia, Sarcopenia and Muscle* 9 (3), 514–529.
- IV **Nissinen, T.A.**, Hentilä, J., Fachada, V., Lautaoja, J.H., Pasternack, A., Ritvos, O., Kivelä, R. & Hulmi, J.J. Muscle Follistatin gene delivery increases muscle protein synthesis independent of periodical physical inactivity and fasting. *In revision*.

The studies included in this dissertation were planned by me and my supervisors Juha Hulmi and Riikka Kivelä. I participated in designing the experiments for publications I and II, and designed the experiments for publications III and IV together with Juha Hulmi, Riikka Kivelä (III, IV) and Jaakko Hentilä (III). I performed the experiments and the sample collection in publications I–IV together with Joni Degerman and Markus Räsänen (I, II), and Jaakko Hentilä (III, IV), with the help of Juulia Lautaoja (IV). I performed the tissue preparation for protein and RNA analyses in publications I, II and IV, and together with Juulia Lautaoja in publication III. I conducted most (I, II) or all (III, IV) of the Western blot analyses and some of the qPCR analyses (I–III). I conducted the histological analyses in publication I, with the help of Satu Koskinen and Vasco Fachada. I also participated in cloning of the follistatin gene construct for AAV production in IV and cultured the C26 cancer cells in III. I conducted most (I, III) or all (IV) of the data handling and statistical analyses. I prepared the figures for publications I, III and IV, except for the microscope images in publications III and IV, and together with Juha Hulmi for publication II. I had the main responsibility of writing articles I, III and IV, and I wrote article II together with Juha J. Hulmi.

## ABBREVIATIONS

4E-BP1	4E binding protein 1
AAV	Adeno-associated virus
(s)ACVR2B	(Soluble) Activin receptor type IIB
Akt	Protein kinase B
BMC	Bone mineral content
BMD	Bone mineral density
BMP	Bone morphogenetic protein
C26	Colon-26 carcinoma
CD31/PECAM-1	Platelet endothelial cell adhesion molecule-1
CS	Citrate synthase
DNA	Deoxyribonucleic acid
DOX	Doxorubicin
ERK1/2	Extracellular signal-regulated kinase 1/2
eWAT	Epididymal white adipose tissue
FoxO1	Forkhead box protein O1
FS288	Follistatin-288
GA	Gastrocnemius
GAPDH	Glyceraldehyde 3-phosphate dehydrogenase
GDF	Growth and differentiation factor
IL	Interleukin
JNK	c-Jun NH <sub>2</sub> -terminal kinase
LAMP2	Lysosome-associated membrane protein 2
LC3	Microtubule-associated protein 1A/1B-light chain 3
LLC	Lewis lung carcinoma
MCP-1	Monocyte chemoattractant protein-1
MuRF1	Muscle RING-finger protein-1
mTOR(C1)	Mechanistic target of rapamycin (complex 1)
Myod1	Myogenic Differentiation 1/Myoblast Determination Protein 1
OXPHOS	Oxidative phosphorylation
p21/Cdkn1a	Cyclin Dependent Kinase Inhibitor 1A
p38 MAPK	p38 mitogen-activated protein kinase
p53	Cellular tumor antigen p53
p70 S6K	p70 ribosomal protein S6 kinase
PBS	Phosphate-buffered saline
RANTES	Regulated upon activation, normal T cell expressed and secreted (also known as CCL5)
REDD1/Ddit4	Regulated in development and DNA damage responses 1/DNA Damage Inducible Transcript 4
RNA	Ribonucleic acid
rpS6	ribosomal protein S6
SD	Standard deviation
SEM	Standard error of the mean

Smad	Mothers against decapentaplegic
Stat3	Signal transducer and activator of transcription 3
TA	Tibialis anterior
TB	Tumour-bearing
TGF- $\beta$	Transforming growth factor $\beta$
UPS	Ubiquitin-proteasome system



# CONTENTS

ABSTRACT	
TIIVISTELMÄ (FINNISH ABSTRACT)	
ACKNOWLEDGEMENTS	
LIST OF ORIGINAL PUBLICATIONS	
ABBREVIATIONS	
CONTENTS	

1	INTRODUCTION .....	17
2	LITERATURE REVIEW.....	20
2.1	Cancer cachexia.....	20
2.1.1	History and definition.....	20
2.1.2	Physiology of cachexia .....	21
2.1.2.1	Skeletal muscle.....	21
2.1.2.2	Other factors and tissues in cachexia.....	26
2.1.3	Experimental models of cancer cachexia .....	30
2.1.4	Chemotherapy and muscle loss .....	32
2.1.5	Cachexia and survival .....	33
2.1.6	Cancer, chemotherapy and physical exercise .....	36
2.2	Myostatin, activins and their receptors .....	39
2.2.1	Discovery and function .....	39
2.2.2	Blocking of myostatin and activins in muscle atrophy .....	42
3	AIMS AND HYPOTHESES .....	45
4	MATERIALS AND METHODS .....	47
4.1	Animals .....	47
4.1.1	Ethics statement.....	47
4.1.2	Humane endpoint criteria (III).....	47
4.2	Experimental design.....	48
4.2.1	Randomization of the mice (I-IV).....	48
4.2.2	Chemotherapy experiments (I, II).....	48
4.2.3	C26 cancer experiments (III).....	49
4.2.4	Follistatin experiments (IV) .....	50
4.3	Blocking of myostatin and activins .....	51
4.3.1	Production of the soluble Activin receptor type IIB (I-III) .....	51
4.3.2	Production of the adeno-associated virus vectors (IV).....	52
4.4	Tumour cell lines and cultures (I, III) .....	53
4.4.1	Lewis lung carcinoma cells (I).....	53
4.4.2	Colon-26 adenocarcinoma cells (III) .....	53
4.4.3	Cell harvesting for injection (I, III).....	53

4.5	Analysis of running capacity, behavior and body composition.....	53
4.5.1	Treadmill running test (I).....	53
4.5.2	Physical activity (III, IV).....	54
4.5.3	Dual-energy X-ray absorptiometry (DXA) (I).....	54
4.5.4	Food intake (I, III, IV) .....	55
4.5.5	Respirometry (IV).....	55
4.6	Tissue collection and processing .....	55
4.6.1	Sample collection (I-IV).....	55
4.6.2	Analysis of protein synthesis (I-IV) .....	56
4.6.3	Mitochondrial function (I) .....	56
4.6.4	Measurement of doxorubicin content (II).....	57
4.7	Blood analyses.....	57
4.7.1	Basic haematology (I, III) .....	57
4.7.2	Serum cytokine analysis (III) .....	57
4.8	Messenger RNA analyses .....	57
4.8.1	RNA extraction (I, II, III) .....	57
4.8.2	Microarray analysis (I, II).....	57
4.8.3	Pathway analysis (I, II) .....	58
4.8.4	Transcription factor analysis (II).....	58
4.8.5	Reverse transcription and quantitative real-time PCR (I-III) ...	58
4.9	Protein analyses .....	59
4.9.1	Protein extraction and total protein content (I-IV).....	59
4.9.2	Citrate synthase activity (I, III).....	60
4.9.3	Western blotting (I-IV).....	60
4.10	Immunohistochemistry.....	62
4.10.1	Preparation of cryosections (I, III, IV) .....	62
4.10.2	Muscle immunohistochemistry (I, III, IV) .....	62
4.11	Statistical analyses .....	63
5	RESULTS .....	65
5.1	Cachexia and myostatin/activin blocking in chemotherapy and cancer.....	65
5.1.1	Body mass, body composition and tissue masses (I-IV).....	65
5.1.2	Physical activity, running performance and food consumption (I, III, IV) .....	69
5.1.3	Oxidative properties of skeletal muscle (I, III).....	70
5.1.4	Comparison of the effects on the heart and skeletal muscle in chemotherapy (II) .....	72
5.2	Effects of cachexia and its treatment on survival and other tissues in cancer and after chemotherapy (I, III) .....	75
5.2.1	Survival time (III) .....	75
5.2.2	Inflammation (III) and haematological parameters (I, III) .....	75
5.2.3	Bone parameters (I).....	78

5.3	Regulation of muscle size in chemotherapy, cancer and reduced physical activity and fasting - effects of myostatin/activin blocking.....	79
5.3.1	Muscle protein synthesis and its regulation (I-IV) .....	79
5.3.2	Protein degradation pathways in skeletal muscle (I-III) .....	84
6	DISCUSSION .....	86
6.1	Muscle size and its regulation in different wasting conditions with myostatin/activin blocking.....	87
6.2	Physical activity and exercise capacity in different wasting conditions and the effects of myostatin/activin blocking .....	98
6.3	Importance of skeletal muscle tissue in the wasting conditions and the role of myostatin/activin blocking .....	103
6.4	Strengths and limitations.....	112
6.5	Future directions.....	114
7	MAIN FINDINGS AND CONCLUSIONS.....	115
	YHTEENVETO (FINNISH SUMMARY).....	117
	REFERENCES.....	119

ORIGINAL PUBLICATIONS





# 1 INTRODUCTION

Skeletal muscle tissue comprises around 40% of total body mass (Frontera & Ochala 2015), making it the most abundant tissue of the body (Fanzani et al. 2012). It is essential for locomotion, thus being important for performing daily tasks and exercising (Frontera & Ochala 2015). Moreover, skeletal muscle action is required for breathing, as well as for maintaining bone mass and strength (Wolfe 2006). Comprising such a large part of total body mass, skeletal muscle tissue also plays a central role in whole body metabolism, acting as a target for glucose disposal and serving as an amino acid reservoir (Fanzani et al. 2012; Wolfe 2006). Despite all this, the role of skeletal muscle tissue has been underappreciated in health and disease (Wolfe 2006).

Decline in muscle mass, i.e. muscle atrophy or muscle wasting, occurs in many diseases, aging, and conditions associated with decreased muscle activity or nutrient intake (Fanzani et al. 2012; Thomas 2007). Wasting syndrome associated with disease states, such as cancer, is referred to as cachexia, originating from Greek words, *kakos* and *hexis*, meaning 'bad condition' (Argiles et al. 2014). Cachexia is a multifactorial syndrome that is characterized by loss of body mass due to wasting of muscle, and often also adipose tissue, and increased inflammation (Fearon et al. 2011). Cancer cachexia induces substantial alterations in many tissues, organs and metabolic pathways (Argiles et al. 2014). Many of the alterations are compensatory adaptations to restore homeostasis disrupted by the tumour and the antitumour treatments, but some of them may actually be harmful to the patient, resulting in energetic inefficiency and ultimately wasting (Argiles et al. 2014).

Cachexia is associated with poor prognosis and reduced physical function (Fearon et al. 2011; Fearon, Arends & Baracos 2013), and it has been suggested to account for up to 20% of all cancer deaths (Argiles et al. 2014; Warren 1932). Furthermore, cancer therapies, such as chemotherapy, may in some cases aggravate muscle wasting, and low muscle mass may be associated with increased treatment toxicity, potentially contributing to the poor prognosis (Fearon, Arends & Baracos 2013). Even though cancer cachexia as a wasting syndrome has been recognized since the time of Hippocrates (Fearon, Arends &

Baracos 2013) and the poor prognosis associated with it has been acknowledged for almost a century (Warren 1932), it has been only quite recently that more research has focused on the importance of skeletal muscle tissue in cancer cachexia, and on the potential therapies targeting skeletal muscle tissue to counteract cachexia.

A potent strategy to increase muscle mass and/or prevent muscle wasting is the blocking of myostatin and activins (Lee et al. 2005). Myostatin and activins belong to the transforming growth factor (TGF)- $\beta$  superfamily of proteins and inhibit muscle growth via signalling through activin receptor type II B (ACVR2B) (Chen et al. 2016; Lee et al. 2005). Their blockade can be achieved via different strategies, such as administration of a soluble form of the ligand binding domain of ACVR2B (sACVR2B) (Lee et al. 2005) or overexpression of follistatin (Lee & McPherron 2001; Winbanks et al. 2012). A hallmark study by Zhou et al. (2010) demonstrated that the blocking of myostatin and activins by sACVR2B administration successfully prevented cachexia in tumour-bearing mice and was also able to reverse already developed advanced cachexia via prevention of muscle wasting (Zhou et al. 2010). Interestingly, prevention and reversal of cachexia were associated with improved survival in tumour-bearing mice without effects on tumour growth (Zhou et al. 2010). This finding highlighted the importance of maintaining muscle mass in experimental cancer cachexia and proposed the blocking of myostatin and activins as a potential therapeutic strategy to counteract cachexia and thus to prolong survival. These findings of improved survival by preventing muscle wasting in tumour-bearing mice have been since replicated by others (Hatakeyama et al. 2016; Toledo et al. 2016b) and are supported by substantial body of epidemiological evidence in cancer patients (Kazemi-Bajestani, Mazurak & Baracos 2016). However, despite rigorous investigation, an effective therapy to counteract cachexia is still missing. Finding such therapy would be crucial, as maintenance of muscle mass could give more time to treat the underlying disease and also result in better tolerance to treatment and improved treatment outcomes (Fearon, Arends & Baracos 2013).

However, the mechanisms underlying the improved survival with myostatin/activin blocking and prevention of muscle wasting still remain poorly understood. Moreover, it has not been investigated in non-genetic models, if increasing muscle size via myostatin/activin blocking before the cachectic stimulus has similar survival benefits as the treatment of muscle wasting. Furthermore, the effects of myostatin/activin blocking and the resulting muscle maintenance on tissues other than skeletal muscle have been inadequately studied in experimental cancer cachexia, and the elucidation of the potential effects beyond skeletal muscle might give more insight into the mechanisms underlying the improved survival. Finally, the effects of myostatin/activin blocking in chemotherapy-induced muscle wasting have not been extensively studied in non-tumour-bearing animals, and the mechanisms of muscle maintenance by myostatin/activin blocking in cancer cachexia and chemotherapy have not yet been completely elucidated.

Thus, the purpose of this dissertation was to study the effects of (1) different wasting conditions, namely, chemotherapy, cancer cachexia as well as reduced physical activity and fasting, and (2) the concomitant blocking of myostatin and activins on muscle size and its regulation, and (3) the importance of maintaining adequate muscle mass in these wasting conditions. In addition, the aim was to investigate (4) the effect of increasing muscle mass only before the cachectic stimulus, meaning tumour formation, on survival, and to explore the effects of myostatin/activin blocking beyond skeletal muscle tissue in experimental cancer cachexia and chemotherapy. This dissertation also aimed to investigate (5) the effects of these wasting conditions on physical activity, exercise capacity and oxidative properties of skeletal muscle.

## 2 LITERATURE REVIEW

### 2.1 Cancer cachexia

#### 2.1.1 History and definition

Cancer cachexia has been acknowledged since the time of Hippocrates (Fearon, Arends & Baracos 2013), and the importance of cachexia as a potential cause of death in cancer has been known for almost a century (Warren 1932). It is defined as “a multifactorial syndrome characterized by an ongoing loss of skeletal muscle mass (with or without loss of fat mass) that cannot be fully reversed by conventional nutritional support and leads to progressive functional impairment” (Fearon et al. 2011). Cachexia arises from a negative protein and energy balance resulting from a variable combination of reduced food intake and abnormal metabolism. The progression of cachexia can be divided into three stages: precachexia, cachexia and refractory cachexia.

The diagnosis of cancer cachexia is based on body weight change, or body mass index (BMI) combined with weight loss, or a direct measure of muscularity combined with weight loss. Cachexia can thus be diagnosed if (1) involuntary weight loss exceeds 5% over a six-month period, (2) BMI is below 20 and is accompanied by weight loss exceeding 2%, or (3) the appendicular skeletal muscle index is equivalent to sarcopenia (males < 7.26 kg/m<sup>2</sup>; females < 5.45 kg/m<sup>2</sup>) and is accompanied by weight loss exceeding 2%. Cachexia is also often accompanied by reduced food intake and systemic inflammation. The patient is considered precachectic if weight loss is under 5% and is accompanied by anorexia and altered metabolism. The most advanced stage of cachexia, known as refractory cachexia, is characterized by progressive catabolism, and unresponsiveness to anticancer treatment, as well as a low performance score with varying degrees of wasting, and it is associated with survival expectance of less than three months. Unlike patients with precachexia, patients that have entered the refractory stage of cachexia are unlikely to benefit from interventions targeted at reversing the muscle wasting (Fearon et al. 2011).

The incidence of cachexia in cancer patients is 30% to 80% depending on the tumour type. The highest prevalence of cachexia is observed in patients with pancreatic or gastric cancer (83%–87%), intermediate in colon, prostate, lung cancer, and unfavorable non-Hodgkin's lymphoma (48%–61%), and the lowest in patients with favorable subtypes of non-Hodgkin's lymphoma, breast cancer, acute nonlymphocytic leukemia, and sarcomas (31%–40%) (Loberg et al. 2007; Tisdale 2009). The presence of cachexia is associated with poor prognosis and reduced survival, and cachexia is estimated to account for about 20% of all cancer deaths, death usually occurring when weight loss approaches 30% (Argiles et al. 2014; Loberg et al. 2007; Tisdale 2009). Considering the number of patients affected by cachexia, the poor prognosis related to it, and the fact that no effective therapies are currently available, cancer cachexia is an important target for investigation.

As indicated by the diagnostic criteria above, cachexia can be detected from involuntary weight loss, or low BMI associated with weight loss (Fearon et al. 2011; Fearon, Arends & Baracos 2013). With these criteria, cachexia may be unnoticed in obese patients, or in patients with ascites or peripheral oedema that may result in weight gain rather than weight loss despite a severe level of cachexia (Fearon, Arends & Baracos 2013). However, obese and overweight patients may also be undergoing severe muscle wasting at the time of cancer diagnosis, and low muscularity is an independent risk factor for impaired survival in both obese and non-obese cancer patients (Fearon et al. 2011; Fearon, Arends & Baracos 2013; Prado et al. 2008; Tan et al. 2009). This is why direct assessment of muscle mass needs to be included in the diagnosis of cachexia at least in these patient populations. In addition, muscle function can decline independent of changes in muscle mass in cachexia, and thus evaluation of muscle function should also be included. However, relatively few studies directly assessing skeletal muscle size at baseline or especially the change in muscle size during disease progression exist, and this assessment is not yet part of standard clinical practice despite the accumulating evidence of its importance (Kazemi-Bajestani, Mazurak & Baracos 2016; Pichard, Baracos & Attaix 2011).

## **2.1.2 Physiology of cachexia**

### **2.1.2.1 Skeletal muscle**

Skeletal muscle has arisen as one of the main targets for investigation and for the development of cachexia therapies. Cachexia is associated with progressive wasting in many human cancers and pre-clinical cancer cachexia models in rodents (Aulino et al. 2010; Bonetto et al. 2016; Murphy et al. 2012; Tisdale 2009). It has been found that low muscle mass is an independent risk factor for mortality as well as chemotherapy-related toxicity (Fearon, Arends & Baracos 2013; Kazemi-Bajestani, Mazurak & Baracos 2016; Prado et al. 2007; Prado et al. 2009). In addition to negative effects on prognosis and tolerance of anti-cancer therapies, muscle wasting associated with cancer cachexia drastically impairs the quality of life and functional capacity of cancer patients and induces weakness,

fatigue and exercise intolerance (Penna et al. 2019). In addition to muscles involved in locomotion, cachexia also affects other vital muscle groups, such as respiratory muscles. Indeed, atrophy and weakness of the diaphragm (Murphy et al. 2012; Roberts et al. 2013), the major respiratory muscle, accompanied by ventilatory dysfunction (Roberts et al. 2013) have been observed in a murine model of cancer cachexia. This may potentially contribute to the impaired survival associated with muscle wasting (Azoulay et al. 2004; Schapira et al. 1993), but this hypothesis requires further investigation.

**Regulation of muscle mass.** In general, muscle mass is regulated by the balance between muscle protein synthesis and degradation, hypertrophy occurring when net synthesis exceeds net degradation and, vice versa, atrophy occurring when net degradation exceeds net synthesis. Consistent with this, the negative protein balance and muscle wasting observed in cancer cachexia can be attributed to decreased protein synthesis (Horstman et al. 2016; Penna et al. 2019; Samuels et al. 2001; Smith & Tisdale 1993; White et al. 2011) and/or increased protein degradation (Penna et al. 2019; Samuels et al. 2001; Smith & Tisdale 1993; Toledo et al. 2016b; White et al. 2011), and potentially also to impaired regeneration (Talbert & Guttridge 2016) in skeletal muscle. The relative contribution of each of these mechanisms may depend on the stage of cachexia, for instance (Smith & Tisdale 1993; White et al. 2011).

**Protein synthesis.** Protein synthesis is a process in which messenger RNA (mRNA) is translated into protein by ribosomes in three steps: initiation, elongation, and termination (Gordon, Kelleher & Kimball 2013). The initiation step consists of the assembly of the 43S preinitiation complex containing the initiator methionyl-transfer RNA (tRNA) and the binding of mRNA to the 43S preinitiation complex (Gordon, Kelleher & Kimball 2013). In the elongation phase, a polypeptide chain is synthesized by the addition of amino acids by tRNAs based on the mRNA template, and in the termination step, the formed polypeptide chain is released when the ribosome phases the stop codon on the mRNA (Hershey, Sonenberg & Mathews 2012). Most of the regulation targets the initiation step (Gordon, Kelleher & Kimball 2013). A master regulator of protein synthesis is a mechanistic target of rapamycin complex 1 (mTORC1), which has many important functions in the control of cell growth and metabolism, that is, the synthesis of proteins, lipids and nucleotides, glucose metabolism, and autophagy (McCarthy & Esser 2010; Saxton & Sabatini 2017). mTORC1 promotes protein synthesis through phosphorylation of its downstream targets, such as p70S6 kinase 1 (S6K1) and eukaryotic initiation factor (eIF) 4E binding protein 1 (4E-BP1). The phosphorylation of S6K1 by mTORC1 (and subsequently by PDK1) activates the kinase and results in phosphorylation of multiple downstream targets, such as eIF4B and ribosomal protein S6 (rpS6). These changes promote e.g. the initiation of translation, elongation, mRNA biogenesis, and ribosomal biogenesis. In contrast, 4E-BP1 inhibits translation through binding to eIF4E, and phosphorylation by mTORC1 relieves this inhibition thus promoting the initiation of translation (Laplante & Sabatini 2009; Saxton & Sabatini 2017).

Multiple upstream signals regulate the activation of mTORC1 signalling, including growth factors, amino acids, cellular energy status and oxygen levels, DNA damage, as well as mechanical stimuli (such as muscle contraction) (Goodman 2019; Jacobs, Goodman & Hornberger 2014; Laplante & Sabatini 2009; Saxton & Sabatini 2017; Sengupta, Peterson & Sabatini 2010.). In addition, it has been shown that subcellular localization influences the activity of mTORC1, and its localization to the lysosomal/late endosomal surface has been associated with enhanced mTORC1 activation (Jacobs et al. 2013; Sancak et al. 2010), also in skeletal muscle (Goodman 2019).

The number of stimuli regulating mTORC1 signalling suggests that muscle protein synthesis may be regulated by multiple physiological and pathological conditions or factors, such as physical exercise or the lack of it, nutrient intake, or different wasting conditions, including ageing/sarcopenia, disuse, and several diseases, such as cancer (Gordon, Kelleher & Kimball 2013). Muscle protein synthesis has been found to be either lower (Dworzak et al. 1998; Emery et al. 1984; Rennie et al. 1983), higher (Shaw et al. 1991), or similar (Williams et al. 2012) in cachectic cancer patients as compared to control levels (Williams et al. 2012) or non-weight losing cancer patients (Shaw et al. 1991). In experimental models of cancer cachexia, muscle protein synthesis has usually been decreased compared with healthy controls (Emery, Lovell & Rennie 1984; Lopes et al. 1989; Pain & Garlick 1980; Samuels et al. 2001; Smith & Tisdale 1993; Toledo et al. 2016b; White et al. 2011), although some studies have reported levels comparable to controls (Costelli et al. 1993, Llovera et al. 1998, Tessitore et al. 1993). The inconsistent results in human patients may be at least in part due to differences in feeding status, as elevated muscle protein synthesis has been found in fasted states (Shaw et al. 1991), whereas depressed levels have been found in fed states (Emery et al. 1984). This may be due to anabolic resistance in cachectic cancer patients (Engelen, van der Meij & Deutz 2016; Penna et al. 2019). Indeed, even though some studies report similar (Williams et al. 2012) or even increased (Shaw et al. 1991) levels of muscle protein synthesis in the fasted state, the anabolic response to nutrient intake may be compromised in cancer cachexia (Deutz et al. 2011; Williams et al. 2012). However, optimized levels and content of protein and amino acids may induce the anabolic response in cachectic cancer patients (Deutz et al. 2011; Engelen, van der Meij & Deutz 2016) and in mouse models of cancer cachexia (Eley, Russell & Tisdale 2007), and different nutrient compositions may thus in part explain the inconsistent results.

In animal models of cancer cachexia, muscle wasting and decreased protein synthesis have been associated with decreased markers of mTORC1 signalling, such as decreased phosphorylation of S6K1 and 4E-BP1, and increased (inactivating) phosphorylation of eukaryotic elongation factor 2 (eEF2) (Eley, Russell & Tisdale 2007; White et al. 2011). In addition to depressed mTORC1 signalling, it has been suggested that assembly of the 43S preinitiation complex might be inhibited in cancer cachexia, potentially impeding protein synthesis (Gordon, Kelleher & Kimball 2013). However, at the time of planning this dissertation, the mechanisms underlying decreased protein synthesis and mTORC1 signal-



ling in cancer cachexia are still not fully understood, and it is not known, for example, if the localization of mTORC1 is altered in cancer cachexia. In addition, closely related to cancer, the effects of chemotherapy, such as doxorubicin, on muscle protein synthesis and its regulation remain largely unknown. Moreover, the contribution of potentially altered levels of physical activity and food intake to protein synthesis and its regulation in these conditions still needs further investigation. Finally, the interaction of protein synthesis and its regulation in these conditions with signalling through Transforming growth factor  $\beta$  (TGF- $\beta$ ) family members is poorly understood, and is an attractive target for investigation due to its therapeutic potential in muscle wasting (see section 2.2).

**Protein degradation.** Proteins can be degraded via different catabolic pathways, and the four main proteolytic pathways in skeletal muscle fibres include the ubiquitin-proteasome system (UPS), autophagy, and the calpain and caspase systems (McCarthy & Esser 2010; Penna et al. 2019). In the UPS, proteins are polyubiquitinated by specific classes of enzymes (E1, E2 and E3) and then degraded by the 26S proteasome. The rate-limiting step of UPS is the transfer of ubiquitin from E2 enzyme to the protein to be degraded, which is catalyzed by E3 ubiquitin ligases. Multiple E3s exist and each of them targets specific groups of proteins (Sandri 2016). Autophagy is a catabolic process in which damaged organelles and macromolecules are degraded in lysosomes, and thus recycled in the cells (Sandri 2016). In muscle wasting, calpain and caspase systems are involved in, for instance, apoptosis and the cleavage of myofilaments and proteins that anchor myofilaments to the Z-disc, and thus release them to be degraded by the UPS (Argiles et al. 2014; Sandri 2008).

The proteolytic systems may be activated by different stimuli, such as mechanical unloading, growth factors (such as myostatin), hormones (such as glucocorticoids), inflammatory cytokines (such as interleukin (IL)-6 and tumour necrosis factor (TNF)- $\alpha$ ), oxidative stress, metabolic stress (ATP levels and production), and nutrient (i.e. amino acid and glucose) availability (McCarthy & Esser 2010). These stimuli activate intracellular signalling pathways that regulate proteolysis. At the center of the regulation is protein kinase B/Akt-Forkhead box O (FoxO) signalling, which interacts with other pathways, and also with the regulation of protein synthesis (McCarthy & Esser 2010; Sandri 2016). Briefly, Akt inhibits FoxOs via phosphorylation, and when this inhibition is relieved, FoxOs translocate to nucleus inducing expression of target genes, including ubiquitin and ubiquitin ligases, proteasomal subunits, and autophagy-related genes (McCarthy & Esser 2010; Sandri 2016). Other pathways potentially activating proteolytic systems include (inhibitor of kappa B kinase) IKK-Nuclear Factor (NF)- $\kappa$ B signalling (McCarthy & Esser 2010; Sandri 2016), Janus kinase (JAK)-Stat3 (signal transducer and activator of transcription) signalling that is activated by proinflammatory cytokines (Zimmers, Fishel & Bonetto 2016), and Smad2/3 signalling activated by TGF- $\beta$  superfamily members, such as myostatin and activin A (McCarthy & Esser 2010; Sandri 2016).

The rate of muscle protein degradation has been investigated in very few human studies, and the majority of the studies have assessed whole body pro-

tein degradation, which does not necessarily represent the rate of skeletal muscle protein degradation (Tipton, Hamilton & Gallagher 2018). In cachectic human cancer patients, whole body protein degradation has been found to be elevated (Shaw et al. 1991), or unchanged (Dworzak et al. 1998; Emery et al. 1984) as compared to healthy subjects (Dworzak et al. 1998; Emery et al. 1984) or non-weight-losing cancer patients (Shaw et al. 1991). In animal models, muscle protein degradation has mostly been found to increase in cachectic tumour-bearing animals compared with healthy (Costelli et al. 1993; Llovera et al. 1998; Lopes et al. 1989; Samuels et al. 2001; Smith & Tisdale 1993; Tessitore et al. 1993; Toledo et al. 2016b) or weight-stable (White et al. 2011) counterparts.

However, despite the limited number of studies assessing the rate of muscle protein degradation, established markers of different proteolytic pathways have been extensively studied in the context of cancer cachexia. Based on these markers, the proteolytic pathways seem to be consistently activated in cachectic cancer patients and in experimental cachexia models (Penna et al. 2019; White et al. 2011). Of the main proteolytic pathways in skeletal muscle, the UPS and autophagy seem particularly important in cancer cachexia (Penna et al. 2019). Activation of protein breakdown via the UPS is typically assessed from the gene expression of the muscle-specific E3 ubiquitin ligases, enzymes that catalyze the ligation of ubiquitin to proteins targeted to degradation via the UPS (Penna et al. 2019). The two most studied muscle-specific ubiquitin ligases are muscle RING finger-containing protein 1 (MuRF1/TRIM63) and muscle atrophy F-box protein (MAFbx/atrogin-1), but many others also exist and continue to be discovered (Sandri 2016, Penna et al. 2019). However, despite being an important component of the UPS, atrogin-1 is a poor marker for proteolysis, because it mainly affects protein synthesis through breakdown of proteins involved in the regulation of protein synthesis (Attaix & Baracos 2010). The level of UPS activation can also be assessed from, for example, the amount of ubiquitinated proteins, the expression of other UPS genes, such as proteasome components, and from the analysis of proteasome activity (Melvin et al. 2013). These above-mentioned markers of UPS have been found to be elevated in experimental models of cancer cachexia (Aulino et al. 2010; Busquets et al. 2012; Johnston et al. 2015; Llovera et al. 1998; Toledo et al. 2016b; Tseng et al. 2015; White et al. 2011; Zhou et al. 2010) and also in human cancer patients (Bossola et al. 2003; Penna et al. 2019) in many studies, but not all (Op den Kamp et al. 2012; Tardif et al. 2013; Williams et al. 2012). However, even though proteasome inhibitors have been able to partially prevent immobilization-induced muscle atrophy (Krawiec et al. 2005), they have not been successful in experimental models of cancer cachexia (Penna et al. 2016), suggesting a potential compensatory activation in other proteolytic pathways and supporting the idea that protein breakdown may actually be an adaptive response to handle the accumulation of damaged or dysfunctional proteins (Penna et al. 2019).

Autophagy, a mechanism to degrade different cellular components (Penna et al. 2019), has also been shown to be induced in skeletal muscle in experimental models of cancer cachexia (Penna et al. 2013a; Pigna et al. 2016) as well

as in cachectic cancer patients (Aversa et al. 2016; Pigna et al. 2016; Tardif et al. 2013), as shown by increased levels of marker proteins of autophagy, such as LC3B-II (Penna et al. 2019; Klionsky et al. 2016). However, it seems that in cancer cachexia, autophagy is not only excessive but may also be defective, as capacity for lysosomal clearance of autophagosomes seems to be decreased. Even though autophagy is a vital process in skeletal muscle, the pathological nature of autophagy in cancer cachexia may contribute to muscle wasting. Thus, potential treatments might be aimed to modulate autophagy via its upstream mediators instead of inhibition of the autophagy process itself (Penna, Baccino & Costelli 2014).

As many factors contribute to muscle atrophy in different wasting conditions, an omics or systems biology approach might give a better understanding of and new insight into the underlying mechanisms (Gallagher et al. 2016; Twelkmeyer, Tardif & Rooyackers 2017). This approach has been adopted in some muscle wasting and cachexia studies (Gallagher et al. 2016; Twelkmeyer, Tardif & Rooyackers 2017), and in fact, transcriptomic analyses have revealed that there is a set of genes, termed “atrogenes”, that is coordinately regulated in different wasting conditions (Lecker et al. 2004; Satchek et al. 2007). However, especially in the context of chemotherapy-associated muscle wasting, studies using omics techniques are lacking at the time of planning this dissertation.

#### **2.1.2.2 Other factors and tissues in cachexia**

Cancer cachexia is a multifactorial and multi-organ syndrome that is characterized by negative energy balance and energetic inefficiency. In addition to skeletal muscle, many other tissues are also affected by and contribute to cancer cachexia, and may also be linked to muscle wasting (Figure 1). These tissues and systems include at least brain, heart, liver, white and brown adipose tissue, gut, blood, spleen and the immune system (Argiles et al. 2014).

Systemic inflammation is a key feature of cancer cachexia and potentially plays a pivotal role in the development of cachexia syndrome. It is induced by the release of pro-inflammatory cytokines, such as interleukin (IL)-6, IL-1, tumour necrosis factor (TNF)- $\alpha$ , or interferon (IFN)- $\gamma$  from activated host immune cells (e.g. macrophages) that are recruited to the tumour, or from the tumour itself (Argiles, Lopez-Soriano & Busquets 2019; Fearon, Glass & Guttridge 2012; Stephens, Skipworth & Fearon 2008). Increased levels of pro-inflammatory cytokines are found in cancer patients undergoing weight loss. Additionally, elevated IL-6 and monocyte chemoattractant protein (MCP)-1 have been associated with cachectic phenotype as well as reduced survival in human cancer patients, making them possible biomarkers and potential therapeutic targets in cachexia (Fearon, Glass & Guttridge 2012; Stephens, Skipworth & Fearon 2008). However, the effectiveness of antagonizing pro-inflammatory cytokines in treatment of cachexia have yielded variable results (Argiles et al. 2019; Fearon, Glass & Guttridge 2012; White et al. 2011), suggesting that blocking of only one cytokine may not be effective and multimodal treatment is needed (Argiles, Lopez-Soriano & Busquets 2019; Argiles et al. 2019).

The pro-inflammatory cytokines may directly or indirectly activate protein degradation pathways in skeletal muscle and thus contribute to muscle wasting (Argiles, Lopez-Soriano & Busquets 2019; Fearon, Glass & Guttridge 2012). In addition, elevated levels of pro-inflammatory cytokines activate hepatic acute phase response (APR), which is an early-defence system that aims to limit tissue injury (Stephens, Skipworth & Fearon 2008). However, if APR is prolonged or severe in nature, it may have detrimental instead of protective effects. Indeed, APR has been suggested to play a role in the development of cachexia and to be associated with impaired survival (Stephens, Skipworth & Fearon 2008). In addition, APR is related to increased hepatic protein synthesis, and thus increased need for amino acids that may potentially be provided by catabolism of skeletal muscle proteins (Stephens, Skipworth & Fearon 2008). Thus, activation of APR may contribute to the loss of muscle mass in cachexia (Fearon, Glass & Guttridge 2012; Stephens, Skipworth & Fearon 2008). Moreover, spleen size has been shown to increase in human cancer patients (Lieffers et al. 2009) and in experimental models of cancer cachexia (Aulino et al. 2010; Bonetto et al. 2016; Cuenca et al. 2014; Mundy-Bosse et al. 2011; Pin et al. 2015) and may contribute to the development of cachexia (Fearon, Glass & Guttridge 2012; Lieffers et al. 2009). This splenomegaly may be accompanied by an expansion of a cell population called myeloid-derived suppressor cells (MDSC), which is a heterogeneous population of metabolically active and immune suppressive immature myeloid cells (Winfield et al. 2008). The function and importance of MDSCs in cancer cachexia still remains relatively unknown, but the expansion of MDSC population has been associated with the development of cachexia, the induction of acute phase response, and impaired survival in the presence of infection or sepsis in tumour-bearing mice (Cuenca et al. 2014; Winfield et al. 2008).

In addition to proinflammatory cytokines, also other tumour- or host-derived circulating factors may contribute to the development of cachexia. Some of these factors are specific to tumours, including lipid mobilizing factor [LMF, also known as zinc- $\alpha$ 2-glycoprotein (ZAG)], and proteolysis-inducing factor (PIF), that cause adipose tissue and skeletal muscle depletion, respectively (Argiles et al. 2014; Fearon, Glass & Guttridge 2012). Others are not specific to tumours, but are secreted also from other tissues, such as skeletal muscle, in normal physiological conditions. These factors include for example the TGF- $\beta$  superfamily members, including activins (Chen et al. 2014), myostatin (Han, Y. Q. et al. 2018), GDF11 (Liu et al. 2019) and GDF15 (Fearon, Glass & Guttridge 2012; Loumaye & Thissen 2017; Mimeault & Batra 2010). For example, the expression of activin A by the tumour as well as high circulating levels of activin A have been found in human cancer patients and are associated with more malignant phenotype and poor prognosis in (colorectal and lung cancer) patients (Hoda et al. 2016; Loumaye et al. 2017). Both myostatin and activins are negative regulators of muscle size (reviewed in section 2.2) and thus may act as drivers of skeletal muscle wasting in cancer cachexia (Chen et al. 2014; Chen et al. 2016). Indeed, blocking of these factors has shown beneficial effects in counteracting cancer cachexia (Benny Klimek et al. 2010; Busquets et al. 2012; Gallot

et al. 2014; Hatakeyama et al. 2016; Li et al. 2007; Murphy et al. 2011b; Toledo et al. 2016b, Zhou et al. 2010,).

As mentioned above, skeletal muscle loss is usually accompanied by marked depletion of fat mass in cachexia. This is due to increased lipolysis, impaired lipid uptake, and decreased *de novo* lipogenesis in white adipose tissue (Argiles et al. 2014). A connection between adipose tissue and skeletal muscle has been proposed, as prevention of lipolysis has been shown to result in the preservation of not only adipose tissue but also skeletal muscle mass in a murine model of cancer cachexia (Das et al. 2011). It has therefore been suggested that signals from adipose tissue wasting may contribute to the activation of proteolysis in skeletal muscle. Supporting this, increased lipid deposition in skeletal muscle has been found in human cancer patients and this has been related to the body weight loss (Stephens et al. 2011). In addition, the phenomenon of white adipose tissue browning as well as the activation of brown adipose tissue have been associated with cancer cachexia, and may contribute to wasting via increased energy expenditure and lipid mobilization (Argiles et al. 2014).

In addition to skeletal muscle tissue, cardiac muscle is also affected by cancer cachexia. As skeletal muscle, the heart has also been shown to undergo significant atrophy, which may be accompanied by fibrosis, disrupted myocardial ultrastructure, and alterations in the contractile proteins, as well as impairment in heart function and ultimately heart failure (Murphy 2016). This has been shown in human cancer patients as well as in experimental rodent models of cancer cachexia (Springer et al. 2014; Tian et al. 2010). Cardiovascular complications are common in cancer patients and they may even be a major cause of death (Murphy 2016). In addition, the incidence of arrhythmias is increased in cancer cachexia, and they may be causally linked with mortality, arrhythmias being potentially the most common cause of sudden cardiac death in cachectic patients (Kalantar-Zadeh et al. 2013). In addition to cancer itself, also anticancer therapies, including chemotherapeutic agents and targeted anticancer therapies, may have cardiotoxic side effects further aggravating cardiac cachexia and impeding the effectiveness of anticancer therapies (Murphy 2016; Vejpongsa & Yeh 2014). However, much like with skeletal muscle, atrophy and other complications of the heart have been underappreciated by clinicians and scientists and require further investigation (Murphy 2016).

Cachexia is also frequently associated with haematologic changes, including increased platelet count, i.e. thrombocytosis, potentially accompanied by enhanced platelet activation and increased platelet volume (Kalantar-Zadeh et al. 2013). This predisposes to thromboembolism and resulting cardiovascular or cerebrovascular events and sudden death (Kalantar-Zadeh et al. 2013). In addition, anemia is a common feature in cachectic cancer patients (Caro et al. 2001) and in animal models of cancer cachexia (Penna et al. 2013b; Pin et al. 2015; Toledo et al. 2014). It has been suggested to contribute to fatigue (Bruera & Sweeney 2000), in addition to being an independent prognostic factor for impaired survival (Caro et al. 2001).

As a regulator of food intake, brain may also be affected by and contribute to cancer cachexia, as appetite, satiation, taste and smell are controlled by the brain. In cancer cachexia, anorexigenic brain pathways are activated and orexi-genic inhibited resulting in decreased food intake. In addition, cancer may alter the patient's ability to taste and smell the food thus affecting the appetite (Argiles et al. 2014). The resulting decrease in food intake may contribute to, but does not fully explain the cachexia associated wasting (Fearon et al. 2011; Murphy et al. 2012). However, the contribution of decreased food intake to muscle wasting and its regulation in cachexia is not fully understood.

Cachectic cancer patients may also suffer from malabsorption, potentially contributing to malnutrition (Argiles et al. 2018). Moreover, altered gut microbiota (Bindels et al. 2016; Bindels et al. 2018; Herremans et al. 2019) and gut barrier dysfunction (Bindels et al. 2018; Jiang et al. 2014; Puppa et al. 2011) have been associated with cancer cachexia and impaired survival in preclinical animal models and in human patients (Bindels et al. 2018), and interventions targeting gut microbiota have been found to reduce cancer and cachexia progression and to improve survival in mice (Bindels et al. 2016).

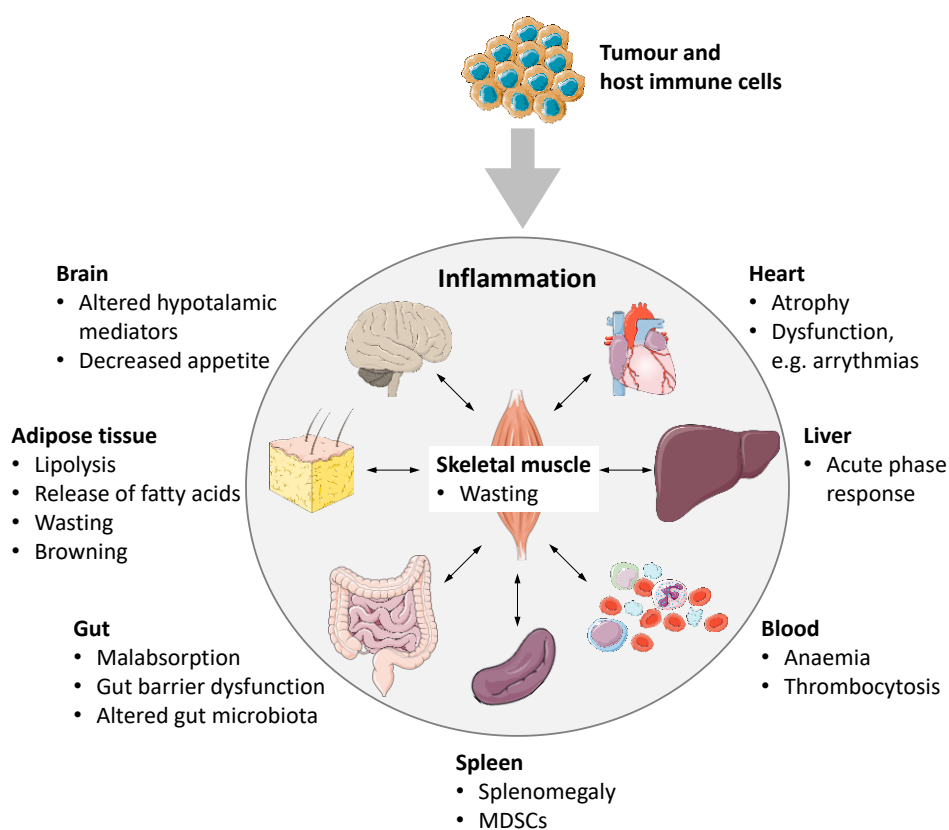


FIGURE 1 Representation of the multi-organ effects of cancer cachexia. Many tissues are affected by and contribute to the development of cachexia, pro-inflammatory environment potentially playing a major role in different alterations seen in cachexia. Individual images were obtained and modified from <https://smart.servier.com>. (Modified from Argiles, Busquets, Stemmler & Lopez-Soriano 2014)

### 2.1.3 Experimental models of cancer cachexia

Due to the heterogeneity of cancer and cancer cachexia syndrome in humans as well as the limitations and difficulties of clinical trials, different pre-clinical experimental models have been developed to allow better exploration of the underlying mechanisms and potential therapies to counteract cancer cachexia. Cell and animal models are simpler and more uniform as compared to cachexia in humans, which reduces the cost and the time to produce meaningful results. The drawback, however, is that they can never fully represent all the features of human cancer cachexia (Penna, Busquets & Argiles 2016). In this dissertation, the murine models of cancer cachexia are in focus, and different types of murine models are briefly presented below.

The experimental models can be divided in different categories based on the origin and location of the tumour, each with different advantages and limitations. Firstly, there are several well-established syngeneic rodent models for cancer cachexia, both in mice and rats. In syngeneic models, cancer cachexia is induced by ectopic injection, i.e. subcutaneous (s.c.), intraperitoneal (i.p.), or intramuscular (i.m.), of cancer cells derived from the same genetic background as the recipient animal (Ballaro, Costelli & Penna 2016). The major advantages of syngeneic models are that immune-competent animals can be used in the experiments and that they produce a rapid, reproducible and easily synchronized tumour growth and cachexia (Ballaro, Costelli & Penna 2016). However, the ectopic location of the tumour may alter the “natural” behaviour of the tumour since it is taken out of its original stroma and microenvironment (Ballaro, Costelli & Penna 2016). Probably the most well characterized and extensively used syngeneic murine models of cancer cachexia are the colon-26 (C26) carcinoma in BALB/c or CD2F1 mice (Aulino et al. 2010; Bonetto et al. 2016), and the Lewis lung carcinoma (LLC) in C57Bl/6 mice (Ballaro, Costelli & Penna 2016; Penna, Busquets & Argiles 2016).

Secondly, some studies have successfully used orthotopically injected human cancer cells to mimic human cancer and to produce cachexia (Chen et al. 2015; Shukla et al. 2015; Yanagihara et al. 2019). The advantage of the orthotopic location is that the tumour grows in its original stroma and microenvironment, making it potentially closer to human scenario. However, the translational potential of these models is limited by the requirement of immuno-compromised animals, and the fact that many of the human cell lines have not been previously used *in vivo* to model cachexia, for instance (Ballaro, Costelli & Penna 2016).

Thirdly, patient derived xenografts (fragments of tumours) implanted ectopically or orthotopically have been used to find the most effective drug for a given tumour (Ballaro, Costelli & Penna 2016), but have recently been adopted to cachexia research as well (Delitto et al. 2017; Go et al. 2017). The advantage is the close resemblance to human cancer, with the limitation of the requirement of immuno-compromised host animals.

Finally, genetic engineered mouse models that spontaneously develop tumours due to mutation or knockout of specific genes potentially best repro-

duce human cancer as to structure, behaviour and development (Ballaro, Costelli & Penna 2016). In addition, their advantage is the orthotopic location and low growth rate of the tumours, allowing time for interventions (Ballaro, Costelli & Penna 2016). Examples of genetic cancer cachexia models include *Apc*<sup>Min/+</sup> model of colon cancer (Mehl et al. 2005) and inhibin- $\alpha$  deficient model producing gonadal tumours (Matzuk et al. 1994). Drawbacks of these models include e.g. difficulties in synchronization of tumour development and cachexia and in assessing the exact timing and rate of tumour growth (Ballaro, Costelli & Penna 2016).

Two different syngeneic murine models of cancer cachexia, the C26 and the LLC model, were used in this dissertation. The LLC model was used in the chemotherapy experiments while the C26 was chosen for the main cancer cachexia experiments. The C26 model was first established in 1975 in an effort to find a transplantable colon cancer model for biological and chemotherapy studies (Aulino et al. 2010). It was originally chemically induced in BALB/c mice and described as an undifferentiated Grade IV carcinoma, which is highly tumourigenic and has a varying tendency for metastasis (Aulino et al. 2010; Corbett et al. 1975; Sato, Michaelides & Wallack 1981). Later, in 1990 inoculation of C26 cells in mice was found to cause significant loss of carcass weight, consisting of depletion of muscle and adipose tissue mass, proving C26 a suitable model for cancer cachexia studies (Tanaka et al. 1990). However, it has been found that the site of inoculation has an effect on C26-induced cachexia (Matsumoto et al. 1999). The LLC cells were isolated from a spontaneous tumour in C57BL/6 mouse in 1951 (Penna, Busquets & Argiles 2016). Both of these models have been extensively used in cachexia studies, and they both have different advantages and limitations. One major difference between these models is the inoculation site: While C26 cells are usually injected subcutaneously in the dorsal region of the mice, LLC cells are often injected intramuscularly (Penna, Busquets & Argiles 2016). One advantage of C26 model is marked cachexia with a relatively small tumour burden (~2 % of the host body mass), which is closer to human scenario as compared to LLC model, for instance, producing a tumour burden of 20–30 % of host body mass (Penna, Busquets & Argiles 2016; Ballaro, Costelli & Penna 2016). A clear limitation of C26 model is the rapid progression of cachexia and the short period of time from the beginning of wasting to death, which leaves a small window of time for interventions (Penna, Busquets & Argiles 2016). Contrary to C26 model, LLC tumour frequently metastasizes, which on the first hand makes it resemble human cancer, but on the other hand adds a potential confounding factor and makes it difficult to assess tumour progression during the experiment (Ballaro, Costelli & Penna 2016). The LLC model is usually used in cachexia studies with transgenic or knockout mice, since C57BL/6, the syngeneic strain for LLC, is the most frequent background of those mice (Penna, Busquets & Argiles 2016). However, a single model cannot represent the heterogeneity of human cancers, which requires studies with different models as well as constant search for more appropriate models (Penna, Busquets & Argiles 2016).



### 2.1.4 Chemotherapy and muscle loss

The interaction between the tumour, the host, and the anti-tumour treatment is important for the overall outcome. If the tumour is responsive to the treatment, the applied anticancer therapy, such as cytotoxic chemotherapy, is likely to alleviate cachexia and to improve the quality of life of the patient (Fearon, Arends & Baracos 2013; Samuels et al. 2001; Tilignac et al. 2002). However, despite not being an actual component of cancer associated cachexia, different anticancer therapies, such as cytotoxic chemotherapy, surgery, radiation therapy, androgen-deprivation therapy, or targeted therapies, may cause muscle wasting and thus aggravate the cachectic phenotype at least initially before tumour regression (Argiles, Lopez-Soriano & Busquets 2019; Fearon, Arends & Baracos 2013; Tilignac et al. 2002). Consequently, it is also important to study the independent effects of the anticancer therapies in the absence of the tumour.

As cytotoxic chemotherapy is a very common anticancer treatment and is in the scope of this dissertation, the effects of chemotherapy on muscle tissue are reviewed more in detail below. Many different chemotherapeutic agents are used alone or in combination with other agents to treat cancer. One of them is doxorubicin, which is a widely used anthracycline chemotherapeutic agent used to treat different cancers (Vejpongsa & Yeh 2014). The antineoplastic effects of doxorubicin include prevention of DNA replication via DNA Topoisomerase II inhibition, DNA damage via formation of reactive oxygen species (ROS), and apoptosis (programmed cell death) (Gilliam & St Clair 2011). Unfortunately, in addition to its antitumour effects, doxorubicin has deleterious effects on noncancerous tissues, cardiotoxicity being its most well-known side effect and limiting its clinical use (Gilliam & St Clair 2011; Vejpongsa & Yeh 2014). However, even with this limited dosage, doxorubicin causes weakness and fatigue potentially in part due to deleterious effects also on skeletal muscle tissue (Doroshov, Tallent & Schechter 1985; Gilliam & St Clair 2011). Indeed, the degree of skeletal muscle dysfunction caused by doxorubicin may be comparable to or even higher than that of heart (Hydock et al. 2011; Min et al. 2015). Studies in both humans (Gilliam & St Clair 2011) and animals (Braun et al. 2014; Ertunc et al. 2009; Gilliam et al. 2009; Gilliam et al. 2011a; Gilliam et al. 2011b; Gouspillou et al. 2015; Hydock et al. 2011; Min et al. 2015) have reported muscle weakness, fatigue, dysfunction, and atrophy after chemotherapy with doxorubicin alone or combined with other cytostatic agents.

The proposed cellular and molecular mechanisms for skeletal muscle toxicity with high doses of doxorubicin include oxidative stress induced by drug accumulation into skeletal muscle, which may lead to contractile and mitochondrial dysfunction associated with activation of proteolytic and apoptotic signalling pathways (Gilliam et al. 2009; Gilliam & St Clair 2011; Gilliam et al. 2011b; Gilliam et al. 2012). For example, increased calpain-1 and caspase-3 activation (Min et al. 2015; Smuder et al. 2011b), decreased actin content and increased myofilament protein release (Smuder et al. 2011b), and increased expression of ubiquitin ligases (Braun et al. 2014) have been observed in muscle

after treatment with doxorubicin or doxorubicin in combination with other chemotherapeutic agents, suggesting increased proteolysis. These findings are supported by an *in vitro* study in C2C12 myotubes (Gilliam et al. 2012). In addition, increased markers of autophagy (Braun et al. 2014; Smuder et al. 2011a), and apoptosis (Braun et al. 2014; Min et al. 2015; Smuder et al. 2011a) have been observed in muscles of rodents treated with doxorubicin or doxorubicin in combination with other chemotherapeutic agents. Exercise (Smuder et al. 2011a; Smuder et al. 2011b) and the inhibition of calpain activation (Min et al. 2015) have attenuated some of the detrimental effects of doxorubicin on muscle tissue.

In addition to doxorubicin, the effects of other chemotherapeutic agents, such as Folfiri, on muscle tissue have recently been investigated (e.g. Barreto et al. 2016). These studies have shown muscle wasting effects also with other chemotherapeutic agents in rodents (Barreto et al. 2016; Barreto et al. 2017). However, not all cancer treatments induce cachexia (Talbert et al. 2017). A comprehensive comparison of the muscle wasting effects of doxorubicin and other cancer therapies in rodents, and especially in patients, is lacking.

In tumour-bearing mice, chemotherapy with antitumour effect has been found to restore muscle protein synthesis (Samuels et al. 2001), but in some cases, the negative effect of chemotherapy on nitrogen balance has been exacerbated in tumour-bearing animals despite antitumour activity (Le Bricon et al. 1995), underlining the specificity of the effects of chemotherapeutic agents and the interaction of them with the tumour. However, despite multiple studies investigating the proteolytic pathways in skeletal muscle, the effect of doxorubicin as well as concomitant blocking of myostatin and activins on muscle protein synthesis in non-tumour-bearing animals was unknown at the time of planning this dissertation. In addition, the effects of blocking myostatin and activins in chemotherapy-associated cardiac atrophy had not been studied before.

In addition to the effects of the anticancer treatments on muscle tissue, the development of cachexia may cause some limitations to the anticancer therapies, thus potentially hindering the effectiveness of the treatment and the overall outcome toxicity (Fearon, Arends & Baracos 2013; Kazemi-Bajestani, Mazurak & Baracos 2016; Prado et al. 2009; Prado et al. 2007). These effects are reviewed in the next section.

### 2.1.5 Cachexia and survival

As mentioned earlier, development of cachexia syndrome is associated with impaired overall prognosis and survival in cancer patients (Arthur et al. 2014; Dewys et al. 1980; Fearon, Arends & Baracos 2013; Kazemi-Bajestani, Mazurak & Baracos 2016). It has been suggested that about 20% of cancer-related deaths may be attributable to cachexia and death usually occurs when weight loss approaches 30% (Argiles et al. 2014; Loberg et al. 2007; Tisdale 2009). Many studies have reported that sarcopenia, i.e. low muscle mass or area, at baseline independently predicts poorer survival in cancer patients (Camus et al. 2014; Harimoto et al. 2013; Iritani et al. 2015; Kazemi-Bajestani, Mazurak & Baracos 2016; Martin et al. 2013; Meza-Junco et al. 2013; Miyamoto et al. 2015; Peng et al. 2012;

Prado et al. 2008; Psutka et al. 2014; van Vledder et al. 2012; Veasey Rodrigues et al. 2013; Voron et al. 2015). Moreover, sarcopenia has been suggested to have an especially strong association with poor survival in overweight and obese patients as compared to non-sarcopenic obese patients (Cooper et al. 2015; Iritani et al. 2015; Kazemi-Bajestani, Mazurak & Baracos 2016; Prado et al. 2008; Rollins et al. 2016; Tan et al. 2009). In addition to directly assessed muscularity, low fat free mass has been found to predict increased one-year mortality in cancer patients receiving chemotherapy (Stobaus et al. 2013). However, not all studies have found association between sarcopenia at baseline and poor survival (Joglekar et al. 2015; Lodewick et al. 2015; Peng et al. 2011; Rollins et al. 2016; Stene et al. 2015; Tan et al. 2009). In addition to sarcopenia, relative loss of body weight as well as body mass index (BMI) have been shown to predict survival independently of cancer site, stage and performance status that are conventional prognostic factors (Bachmann et al. 2008; Dewys et al. 1980; Fouladiun et al. 2007; Martin et al. 2015; Martin et al. 2013). Moreover, low BMI associated with any degree of weight loss increased the risk of mortality when compared with high BMI (Martin et al. 2015).

There are very few studies reporting the effects of muscle wasting, instead of baseline measures of muscularity or changes in body mass, during cancer progression. However, Stene et al. found that skeletal muscle wasting in particular, and not sarcopenia at baseline, independently predicted survival in patients with advanced non-small cell lung cancer receiving chemotherapy (Stene et al. 2015). The importance of muscle maintenance is supported by studies in pancreatic cancer patients, where muscle loss was associated with poorer survival (Dalal et al. 2012; Fogelman et al. 2014). In addition, skeletal muscle loss has correlated with disease free survival (Cooper et al. 2015). However, the association between muscle loss and survival has not been found in all studies (Cooper et al. 2015; Tan et al. 2009). In addition to muscle mass and size, the quality and function of the muscle tissue is also important (Tardif, Grip & Rooyackers 2017). Indeed, for example the fat content and contractile function of muscle have been shown to be altered in cachexia and associated with survival in cancer and other muscle wasting conditions, and also in general (Cooper et al. 2010; Martin et al. 2013; Rantanen, Sakari-Rantala & Heikkinen 2002; Rollins et al. 2016; Tardif, Grip & Rooyackers 2017). Moreover, cachexia (Arthur et al. 2014; van Vugt et al. 2015) and decreased grip strength (Guo et al. 1996) have been associated with increased risk of different comorbidities, post-operative complications, major loss of function, as well as length and cost of hospital stay.

Many studies have reported that sarcopenia, low muscle size, or low lean body mass are associated with increased incidence of toxicity in patients receiving chemotherapy (Barret et al. 2014; Kazemi-Bajestani, Mazurak & Baracos 2016; Prado et al. 2007; Prado et al. 2009; Tan et al. 2015). The toxic effects of chemotherapy in patients with low muscularity may require dose limitations, delays in the treatment, or even termination of the treatment, and this obviously hinders the efficacy of the treatment (Fearon et al. 2011; Kazemi-Bajestani, Ma-

zurak & Baracos 2016; Prado et al. 2009). Indeed, weight loss and muscle wasting have been suggested to be associated with response to treatment (Cooper et al. 2015; Dewys et al. 1980). However, the association between lean body mass and chemotherapy toxicity has not been observed in all studies (Prado et al. 2014). The increased toxicity observed in many studies may be due to the conventional dosage of the drug based on body surface area rather than body composition: patients with low fat-free mass in relation to body surface area may have lower volume of distribution of the drug resulting in increased toxicity in this patient group, comprising especially women and obese patients (Prado et al. 2007; Prado et al. 2008; Prado et al. 2009; Stobaus et al. 2013). Thus, considering both the potentially harmful effect of chemotherapy on muscle tissue and the negative effect of low muscle mass on the outcome of the treatment, it would be of great importance to find effective therapies to counteract muscle wasting that would potentially provide more time to treat the underlying disease.

In addition to cancer, cachexia and muscle wasting have been associated with increased mortality also in other diseases such as in chronic heart failure (Anker et al. 1997), and in mechanically ventilated critically ill patients (Weijs et al. 2014), whereas greater muscle mass indicated by higher serum creatinine level was associated with greater survival rate even in the presence of weight loss in patients receiving haemodialysis (Kalantar-Zadeh et al. 2010). These findings support the independent role of muscle wasting in survival, and underline the importance of muscle tissue in disease states.

Despite the association between low muscle mass, wasting, and mortality risk, it is still debated whether this link is actually causal, and there is still no consensus on the mechanisms via which cachexia causes premature death (Kalantar-Zadeh et al. 2013). As cachexia never exists without the underlying disease, it is possible that cachexia is just an epiphenomenon that is secondary to the disease or its risk factors, and that the disease causes death independent of cachexia (Figure 2) (Kalantar-Zadeh et al. 2013). However, given the piling and consistent evidence, it is also possible that cachexia is a true cause of death (Kalantar-Zadeh et al. 2013), but this is practically impossible to prove with epidemiological studies in human patients where there are multiple confounding factors. This problem has been tackled through the use of pre-clinical animal models attempting to determine, whether there is a causal link between cachexia and mortality.

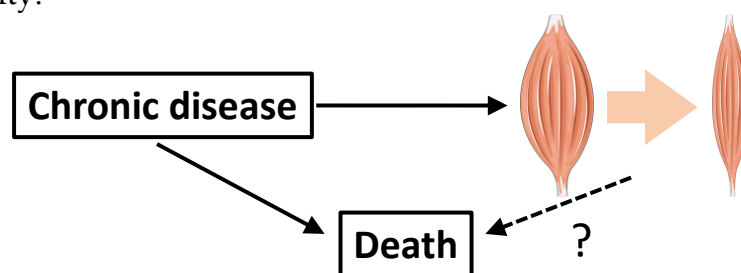


FIGURE 2 Causality hypothesis between cachexia and death. Images were obtained from <https://smart.servier.com>. (Adopted from Kalantar-Zadeth et al. 2013)

Supporting the existence of a causal link between cachexia and mortality, prevention of muscle wasting has been associated with improved survival in pre-clinical murine models of cancer cachexia (Cai et al. 2004; Gallot et al. 2014; Hatakeyama et al. 2016; Johnston et al. 2015; Lerner et al. 2016; Pretto et al. 2015; Toledo et al. 2016b; Tseng et al. 2015; Zhou et al. 2010). For example, inhibition of NF- $\kappa$ B signalling in muscle (Cai et al. 2004) or TWEAK/Fn14 signalling in the tumour (Johnston et al. 2015), blocking of GDF15 (Lerner et al. 2016), treatment with histone deacetylase inhibitor (Tseng et al. 2015), or blockade of myostatin and activins (Gallot et al. 2014; Hatakeyama et al. 2016; Li et al. 2007; Toledo et al. 2016b; Zhou et al. 2010) have resulted in prevention of muscle wasting and improved survival in different murine cancer cachexia models. Importantly, prevention of cancer associated muscle wasting by blocking myostatin and activins with a soluble receptor (sACVR2B) resulted in marked improvement in survival without an effect on tumour growth in C26 carcinoma model, and survival was improved even when the treatment was not started until severe cachexia had already developed (Zhou et al. 2010). Similar blockade of myostatin and activins or genetic myostatin deficiency also prevented muscle wasting and improved survival in LLC and *Apc<sup>min/+</sup>* models of cancer cachexia (Gallot et al. 2014) as well as in inhibin-deficient mice (Li et al. 2007; Zhou et al. 2010), but in those cases, tumour growth was also partially inhibited probably playing a role in the improved survival.

All in all, the evidence from the majority of human and animal studies supports the existence of an association between muscle size and survival, but more evidence is still needed to confirm the causality. In addition, the mechanisms of how preservation of muscle mass improves survival are poorly understood and warrant further studies. For example, considering the multitude of organs, tissues and systems involved in cachexia, the interaction between muscle tissue and other tissues in relation to survival needs further investigation. In addition, given the association between sarcopenia at baseline and shorter survival in human studies, it would be of interest to determine, if having a greater muscle mass before cancer development had beneficial effects on survival.

### 2.1.6 Cancer, chemotherapy and physical exercise

**Physical activity in cancer and chemotherapy.** Studies with human patients suggest that physical activity is decreased in cancer patients compared with healthy subjects (Crowgey et al. 2014; Dahele et al. 2007; Fouladiun et al. 2007; Moses et al. 2004) or compared with activity levels before cancer diagnosis (Irwin et al. 2003). Many studies reporting reduced activity levels in cancer patients have been conducted in cancer patients currently or previously treated with chemotherapy (Crowgey et al. 2014; Dahele et al. 2007; Irwin et al. 2003). It is possible that chemotherapy contributes to the decline in physical activity in these patients (Courneya & Friedenreich 1997; Courneya & Friedenreich 1998; Demark-Wahnefried et al. 1997; Irwin et al. 2003). However, it is difficult to distinguish between the effects of cancer and anticancer therapy in human patients, and thus, animal studies are needed to be able to study the independent effects

of cancer and chemotherapy. Indeed, in the limited number of studies available, home-cage physical activity or distance covered in voluntary wheel running have been found to decline in healthy rats treated with sorafenib (Toledo et al. 2016a) or doxorubicin (Marques-Aleixo et al. 2015), respectively. However, amelioration in physical activity has been observed in tumour-bearing mice treated with the same chemotherapeutic agent (Toledo et al. 2014), and thus, more studies on the effect of different chemotherapeutic agents on physical activity are needed. In addition, decreased physical activity has also been observed in untreated tumour-bearing animals compared with healthy counterparts in many different preclinical cancer cachexia models (Baltgalvis et al. 2010; Busquets et al. 2012; Murphy et al. 2012; Penna et al. 2011; Pigna et al. 2016; Toledo et al. 2011; Toledo et al. 2014; Toledo et al. 2016a; Toledo et al. 2016b; van Norren et al. 2009b). The lowered physical activity may contribute to muscle wasting in cancer (Fearon 2008), but the relevance and the underlying mechanisms need further investigation.

**Effects of cancer and chemotherapy on exercise capacity, muscle function and quality.** In addition to decreased physical activity, poor exercise capacity (Dimeo et al. 1997), impaired aerobic capacity (Op den Kamp et al. 2012; Weber et al. 2009) and impaired muscle strength and function of locomotor muscles (Busquets et al. 2012; Johnston et al. 2015; Murphy et al. 2011b; Murphy et al. 2012; Penna et al. 2011; Pigna et al. 2016; Pin et al. 2015; Toledo et al. 2011; Toledo et al. 2016a; Toledo et al. 2016b; van Norren et al. 2009b; Weber et al. 2009; Zhou et al. 2010), and also respiratory muscles (Murphy et al. 2011b; Murphy et al. 2012; Roberts et al. 2013), are typically associated with cancer and preclinical animal models of cancer cachexia. These impairments may be in part related to multiple metabolic and structural alterations in cachectic skeletal muscle that affect muscle quality and function (Hardee, Montalvo & Carson 2017; Penna et al. 2019), such as mitochondrial damage and dysfunction (Pin et al. 2015; Shum et al. 2012), decreased capacity for oxidative metabolism and ATP production (Fontes-Oliveira et al. 2013), oxidative (Mastrocola et al. 2008) and endoplasmic reticulum stress (Bohnert et al. 2016), altered fibre type distribution (Pin et al. 2015), disruption of the sarcomere structure (Aulino et al. 2010; Shum et al. 2012), and lipid accumulation (Stephens et al. 2011).

In breast cancer patients, functional capacity has been impaired after treatment with chemotherapy, including doxorubicin (Schwartz 2000). Moreover, chemotherapy administered to healthy animals has decreased muscle force or grip strength, and caused contractile and mitochondrial dysfunction (Ertunc et al. 2009; Gilliam et al. 2009; Gilliam et al. 2013; Gouspillou et al. 2015; Min et al. 2015; Toledo et al. 2016a). However, sorafenib chemotherapy has increased grip strength in tumour-bearing rats (Toledo et al. 2016a). In diaphragm, doxorubicin has been found to cause muscle damage, including alterations in the ultrastructure of sarcoplasmic reticulum and mitochondria and myofibrillar degeneration (Doroshov, Tallent & Schechter 1985), as well as decrease in force and contractile dysfunction (Gilliam et al. 2011a). However, the effects of chem-

otherapy, doxorubicin in particular, on maximal running capacity have not yet been studied.

**Effects of exercise in cancer and chemotherapy.** Physical exercise seems to be feasible and safe for cancer patients undergoing cancer treatment, and it may have multiple positive effects, such as improvement in physical fitness, functional capacity, body composition and quality of life of the patients, as well as alleviation of fatigue related to cancer and cancer therapy (Courneya et al. 2007; Courneya et al. 2009; Doyle et al. 2006; Knols et al. 2005; Schwartz 2000; Scott et al. 2018), without hindering the efficacy of the treatment (Courneya et al. 2009, Jones et al. 2005). In addition, resistance training has been effective in increasing muscle strength, lean body mass, and chemotherapy completion rate in breast cancer patients (Courneya et al. 2007), and in improving physical functioning and muscle strength in breast cancer survivors (Battaglini et al. 2014; Dos Santos et al. 2017). Exercise may help to counteract adverse systemic and muscle-specific effects associated with cancer cachexia (Argiles et al. 2012; Lira, Neto & Seelaender 2014). Depending on the type of exercise, it can have anti-inflammatory or anti-catabolic effects, preserve muscle mass, improve oxidative capacity, and consequently alleviate hyperlipidemia and insulin resistance in cancer patients (Argiles et al. 2012; Lira, Neto & Seelaender 2014). Furthermore, it has been suggested that adequate recreational physical activity after cancer diagnosis may be associated with decreased disease-specific mortality, improved overall survival, and reduced the risk of recurrence in colorectal and breast cancer patients (Holmes et al. 2005; Ibrahim & Al-Homaidh 2011; Meyerhardt, Heseltine et al. 2006; Meyerhardt, Giovannucci et al. 2006), and could slow the cancer progression and thus reduce the risk of mortality in prostate cancer (Giovannucci et al. 2005). However, an epidemiological study by Hardee et al. (2014) suggested that resistance training, but not physical activity, was associated with lower risk of all-cause mortality (Hardee et al. 2014). Despite the observed associations, the causality between physical activity and survival remains uncertain. In some animal models of cancer cachexia, exercise interventions have also been successful in improving muscle size and function (Penna et al. 2011; Pigna et al. 2016; Pin et al. 2015), reducing tumour growth and improving survival (Pigna et al. 2016) but the mechanisms underlying these positive effects are not fully understood. Exercise has also been protective against harmful effects of chemotherapy on the heart and skeletal muscle in animal studies (Kavazis et al. 2010; Marques-Aleixo et al. 2015; Smuder et al. 2011a; Smuder et al. 2011b; Smuder et al. 2013).

To conclude, an exercise intervention might be beneficial as a part of a multi-modal treatment at least in some cancers and in patients receiving chemotherapy, but the potential adverse effects and contraindications, such as anaemia and cardiac dysfunction, as well as patient-specific exercise capacity and tolerance need to be taken into consideration (Argiles et al. 2012).

## 2.2 Myostatin, activins and their receptors

### 2.2.1 Discovery and function

Transforming growth factor  $\beta$  (TGF- $\beta$ ) superfamily consists of more than 30 growth factors representing TGF- $\beta$ s, growth and differentiation factors (GDFs), bone morphogenetic proteins (BMPs), activins, and nodal (Wu & Hill 2009). The main and best known activin receptor type 2B ligands, myostatin and activins, are in the focus of this dissertation and will be reviewed more in detail below.

Myostatin (also known as GDF-8) is a member of TGF- $\beta$  superfamily. It was discovered in 1997, when its expression during embryonic development and in adult muscle were first described (McPherron, Lawler & Lee 1997). It was found that myostatin mRNA was expressed almost exclusively in skeletal muscle tissue. In addition, homozygous disruption of myostatin gene resulted in ~30% higher body mass as compared to wild-types and heterozygotes, which was due to increased muscle mass as masses of individual muscles were 2–3 times larger (McPherron, Lawler & Lee 1997). The histology of the hypertrophied muscles was normal and the increased mass resulted from the combination of fibre hypertrophy and hyperplasia (McPherron, Lawler & Lee 1997). In addition, mutations in myostatin gene have led to double muscled phenotype in cattle (Grobet et al. 1997; Kambadur et al. 1997; McPherron & Lee 1997). These results led to a conclusion that myostatin acts specifically as a negative regulator of muscle growth. Indeed, blockade of endogenous myostatin has resulted in muscle hypertrophy (Lee & McPherron 2001; Whittemore et al. 2003, Yang et al. 2001) and increased strength also in adult muscle (Whittemore et al. 2003), and overexpression of myostatin has caused muscle atrophy (Durieux et al. 2007; Zimmers et al. 2002), showing that myostatin is able to regulate muscle size also in adulthood. In addition to the regulation of mature muscle fibre size, myostatin plays a vital role in muscle development and embryonic myogenesis (Chen et al. 2016). Moreover, at least in some pathological conditions, myostatin may play a role also in other tissues, such as the heart (Sharma et al. 1999, Walker et al. 2016).

Like other TGF- $\beta$  members, myostatin is synthesized and secreted as a precursor protein and activated by proteolytic cleavage of the N-terminal prodomain from the C-terminal mature domain, providing an additional level of regulation for its biological activity (Chen et al. 2016; McPherron, Lawler & Lee 1997; Wolfman et al. 2003). The latent precursor form of myostatin is cleaved by BMP-1/tolloid family of metalloproteinases after the aspartate-76 residue within the prodomain, which releases the biologically active mature domain (Wolfman et al. 2003). The mature domain then binds to its receptor activin receptor type II (ACVR2) (Lee & McPherron 2001). This results in activation of the intracellular signaling cascades, that ultimately result in alterations promoting muscle atrophy, such as downregulation of Akt/mTORC1 signalling pathway (Amirouche et al. 2009; Trendelenburg et al. 2009).



GDF11 is a TGF- $\beta$  member closely related to myostatin, and it has been found to be expressed in many tissues and to play a role in many processes during development, e.g. in skeletal patterning and development of bone and nervous system, as well as in ageing and in different diseases (McPherron, Lawler & Lee 1999; Zhang et al. 2017). It also seems to have potency to induce muscle atrophy *in vitro* and *in vivo* (Hammers et al. 2017). For example, overexpression of GDF11 has caused atrophy in skeletal and cardiac muscles, whereas the effect of myostatin seems to be typically specific to skeletal muscle (Hammers et al. 2017). However, muscle-specific deletion of GDF11 gene has not affected skeletal muscle size, indicating that at least muscle-derived endogenous GDF11 may not be vital for regulation of skeletal muscle size (McPherron, Huynh & Lee 2009), although some controversy exists concerning the role of GDF11 in the regulation of skeletal muscle tissue during the whole life span (Walker et al. 2016). Thus, as specific blockade of either myostatin or GDF11 alone is difficult due to the high level of homology, the effects of GDF11 and its blocking in adult skeletal muscle require further investigation.

Activins are pleiotropic proteins that also belong to the TGF- $\beta$  superfamily (Bloise et al. 2019). The discovery of activin A was reported in 1986 by Vale and colleagues, when it was purified and characterized from porcine ovarian follicular fluid (Vale et al. 1986). Their name originates from their ability to stimulate the release of follicle-stimulating hormone from the pituitary gland, in contrast to inhibin, which inhibits the release of follicle-stimulating hormone (Bloise et al. 2019). Activins are composed of two  $\beta$ -subunits of inhibin linked by a disulfide bridge thus forming a dimeric polypeptide (whereas inhibins contain one  $\alpha$  and one  $\beta$  subunit), activin A being a homodimer of two inhibin  $\beta$ A subunits, while activin B consists of two inhibin  $\beta$ B subunits, for instance (Bloise et al. 2019). Activins are initially synthesized as large precursor polypeptides, and their activation requires the proteolytic cleavage of the N-terminal prodomain yielding a biologically active C-terminal mature domain. Activins play important roles in reproduction and embryonic development (Bloise et al. 2019). In addition, activins and their receptors are present in virtually all mammal body systems, and thus they have varying functions all over the body in normal physiology and in response to injury or disease (Bloise et al. 2019; Namwanje & Brown 2016). For example, activin A has been shown to have important effects on multiple extra-reproductive systems, including the brain, cardiac, renal, digestive, immune and respiratory systems, as well as the musculoskeletal system (Bloise et al. 2019). The effects on the muscular system are in the scope of this dissertation, and those are reviewed more in detail below.

Mice deficient in inhibin, a competitive antagonist for activin, have been shown to develop gonadal tumours and severe cachexia. This has been found to be associated with increased levels of activin A and B, secreted from the tumours, that potentially contributes to development of cachexia (Matzuk et al. 1994). Like myostatin, activin A acts as a negative regulator of muscle growth both during development and in adult muscle. This is supported by studies showing that overexpression of activin A leads to muscle atrophy (Chen et al.

2014; Gilson et al. 2009), while heterozygous loss-of-function mutation in the activin A gene (Lee et al. 2010) and activin A antagonism via overexpression of activin A prodomain (Chen et al. 2017) result in increased muscle mass. Both activin A and its receptor (reviewed more in detail below) are expressed in adult myocytes. Their effects on skeletal muscle cells include inhibition of protein synthesis and promotion of protein breakdown, thus negatively regulating muscle size (Bloise et al. 2019). Moreover, activin A has been suggested to affect muscle contractile function and force production (Chen et al. 2014), mitochondrial oxidative phosphorylation, and regeneration after injury (Bloise et al. 2019). Similarly to activin A, activin B overexpression has resulted in muscle atrophy (Chen et al. 2014), and inhibition via overexpression of activin B prodomain (Chen et al. 2017) has resulted in muscle hypertrophy, suggesting that activin B can act as a negative regulator of muscle size, but the contribution of endogenous levels of activin B to the regulation of muscle size requires further investigation.

Myostatin, activins and GDF11 exert their effects through binding to activin receptors (Chen et al. 2016; Zhang et al. 2017). Two types of activin receptors have been identified, and based on their molecular weight, named type I (low molecular weight) and type II (high molecular weight) receptors (Bloise et al. 2019). The ligand first binds to the activin receptor type II (ACVR2), which is a transmembrane protein consisting of an extracellular ligand-binding domain and an intracellular serine/threonine kinase domain (Bloise et al. 2019; Chen et al. 2016). It was first characterized by Mathews and Vale in 1991 (Mathews & Vale 1991), and two forms, i.e. ACVR2A and ACVR2B, have been identified (Bloise et al. 2019). The binding of the ligand to ACVR2 enables the interaction of the ligand with type I receptor, i.e. activin receptor-like kinase (ALK), further enabling the recruitment and phosphorylation of ALK by the activated kinase domain of ACVR2 (Bloise et al. 2019; Chen et al. 2016). This renders ALK active and results in phosphorylation of its downstream targets, such as Smad2 and Smad3. Smad2 and 3 then form a heterodimer that incorporates with Smad4 and this complex translocates to the nucleus and influences the transcription of target genes (Bloise et al. 2019; Chen et al. 2016). Ultimately, the activation of Smad signalling results in inhibition of protein synthesis via inhibition of Akt, which is an upstream activator of mTOR, and promotion of protein degradation via enhanced nuclear translocation of FoxO, and increased expression of ubiquitin ligases (Figure 3) (Chen et al. 2016). In addition to the so-called canonical Smad signalling, other non-canonical pathways may also be regulated by activin receptor signaling (Figure 3). These Smad-independent pathways include p38 mitogen-activated protein kinase (p38 MAPK), extracellular signal-regulated kinase 1 and 2 (ERK1/2), and c-Jun NH<sub>2</sub>-terminal kinase (JNK) signalling that have variable functions in muscle cells (Bloise et al. 2019; Chen et al. 2016).

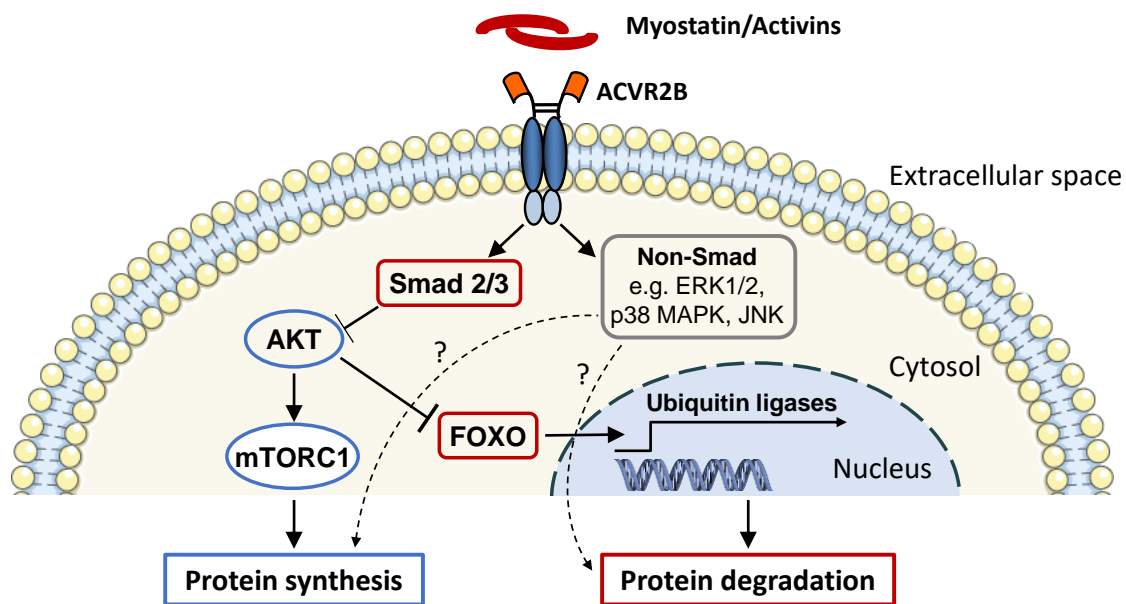


FIGURE 3 A simplified illustration of intracellular signalling induced by binding of myostatin or activins to their receptor ACVR2B. Cell membrane and DNA images were obtained from <https://smart.servier.com>. (Modified from Chen et al. 2016)

## 2.2.2 Blocking of myostatin and activins in muscle atrophy

Given their important role in the regulation of muscle size, ACVR2B ligands, such as myostatin and activin A, are attractive targets for development of therapies to counteract muscle wasting. Indeed, many different strategies to block myostatin and activin A have been developed and successfully used in animals, and some have also been tested in humans (Amthor & Hoogaars 2012). The strategies developed cover all the steps from the inhibition of synthesis to blockade of intracellular downstream signalling (Amthor & Hoogaars 2012). The synthesis of myostatin may be inhibited by RNA interference by antisense oligonucleotides that induce exon skipping on myostatin RNA, or with small interfering RNAs (siRNA) or short hairpin RNAs (shRNA) (Amthor & Hoogaars 2012). After synthesis and secretion, blockade can be achieved by different strategies, such as treatment with mutated myostatin propeptide that binds myostatin and is resistant to proteolytic cleavage by BMP-1/tolloid family of metalloproteinases, administration or expression of dominant negative form of myostatin, treatment with anti-myostatin antibody or peptibody, or administration or expression of a native protein that binds myostatin and/or activins (Amthor & Hoogaars 2012). An example of such protein is follistatin (FS), which is an endogenous inhibitor of myostatin, activins, GDF11 and some BMPs (Amthor & Hoogaars 2012; Chen et al. 2016; Lee et al. 2010). It exists in different isoforms, including a long soluble isoform FS315 and a short isoform FS288 that has a heparan sulphate binding domain and thus resides on the cell surface (Amthor & Hoogaars 2012; Chen et al. 2016). In addition, a very potent strategy to block myostatin and activins is a soluble form of the extracellular

domain of their endogenous receptor, sACVR2B (Lee et al. 2005). Both FS and sACVR2B sequester myostatin and activins thus preventing their binding to the endogenous receptor (Amthor & Hoogaars 2012). Finally, the effects of myostatin and activins on target cells can be prevented by over-expression of dominant negative ACVR2B (Lee & McPherron 2001), treatment with neutralizing anti-ACVR2B antibody, or inhibition of ACVR2B or Smad2/3 synthesis (Amthor & Hoogaars 2012). In addition to these therapeutic strategies, different genetic models, such as constitutive, conditional and inducible knockout models, or heterozygous loss-of-function mutations, have been used to study the lack of myostatin or activin A (Amthor & Hoogaars 2012).

Multiple different strategies to block the function of myostatin and/or activins have been shown to induce muscle hypertrophy in healthy animals (Amthor & Hoogaars 2012; Chen et al. 2017) and in various disease models associated with muscle atrophy (Chen et al. 2017; Han et al. 2013). For example, antagonism of myostatin (Chen et al. 2017; Lee & McPherron 2001), activin A, and activin B (Chen et al. 2017) via prodomain overexpression have all resulted in muscle hypertrophy in healthy mice, myostatin inhibition inducing the greatest increase in muscle mass and fibre size (Chen et al. 2017). It has also been suggested, that myostatin and activins have synergistic effects in the regulation of muscle mass, as the simultaneous blocking of myostatin and activin A, or myostatin and activin B has resulted in even greater hypertrophy than blocking any of them alone (Chen et al. 2017). The simultaneous blocking of myostatin and activins is in the scope of this dissertation and thus, the effects of sACVR2B and follistatin in healthy and wasting conditions are presented below.

In healthy animals, myostatin/activin blockade using sACVR2B has resulted in marked and rapid muscle hypertrophy shown by increased mass of individual muscles (Hulmi et al. 2013a; Lee et al. 2005; Rahimov et al. 2011) as well as increased muscle fibre size (Hulmi et al. 2013a; Lee et al. 2005). Increase in maximal force (Akpan et al. 2009; Relizani et al. 2014), and grip strength (Akpan et al. 2009; Hulmi et al. 2013a) has also been reported after treatment with sACVR2B, with no effects on specific force (force relative to muscle mass) suggesting that improvement in force is proportional to muscle hypertrophy (Relizani et al. 2014). Administration of sACVR2B also been shown to acutely stimulate muscle protein synthesis (Hulmi et al. 2013a). Moreover, in healthy human subjects, this strategy has increased lean mass and muscle size (Attie et al. 2013). Similar to the effects of sACVR2B, adeno-associated virus (AAV) mediated overexpression of circulating form of follistatin has been shown to increase the mass of individual muscles accompanied by increase in grip strength in mice (Haidet et al. 2008), and to increase thigh circumference accompanied by increased muscle force and muscle fibre size in non-human primates (Kota et al. 2009). In addition to these systemic effects, follistatin (FS288) transgene with muscle-specific promoter (Lee & McPherron 2001) and local AAV or plasmid mediated overexpression of FS288 in muscle (Gilson et al. 2009; Sepulveda et al. 2015; Winbanks et al. 2012) have also been shown to result in rapid and pronounced muscle hypertrophy, associated with increased fibre size (Gilson et al.

2009; Winbanks et al. 2012) and force producing capacity in rodents (Winbanks et al. 2012).

Blocking of myostatin and activins has been found to prevent or attenuate muscle wasting associated with different diseases, including cancer, renal failure, heart failure, metabolic diseases, immobilization, and sarcopenia, to name a few (Han et al. 2013). Improvement in muscle strength and function has also been reported (Han et al. 2013), although specific force may also decrease in part due to larger increase in muscle mass relative to muscle force (Relizani et al. 2014). Importantly, treatment with sACVR2B has been successful in prevention of cancer-induced muscle wasting (Benny Klimek et al. 2010; Busquets et al. 2012; Toledo et al. 2016b; Zhou et al. 2010) and decline in strength (Busquets et al. 2012; Toledo et al. 2016b; Zhou et al. 2010) in different pre-clinical models of cancer cachexia. In addition, anti-myostatin antibody has prevented the loss of muscle mass and function (Murphy et al. 2011b). However, mice genetically lacking myostatin have been shown to be more prone to cancer induced muscle wasting (Benny Klimek et al. 2010).

Interestingly, treatment with sACVR2B has improved survival and reversed cancer induced muscle wasting, even if the treatment was started at an advanced level of cachexia (Zhou et al. 2010). However, it is not known, what happens, if mice are pre-treated with sACVR2B to increase muscle mass before cancer and if the treatment is terminated before cachexia develops. In addition, the mechanisms underlying the positive effects of myostatin/activin blocking in cancer cachexia require further investigation, and potential effects beyond skeletal muscle tissue need to be studied. For example, some studies have not found effects for the blocking of myostatin (Murphy et al. 2010) or myostatin and activins (Haidet et al. 2008; Kota et al. 2009) on the heart in healthy animals, whereas prevention of cardiac cachexia by sACVR2B administration has been reported in tumour-bearing mice (Zhou et al. 2010). In addition, the effects of blocking myostatin and activins on the heart have not yet been studied in chemotherapy-induced cardiac atrophy. Thus, the effects of myostatin/activin blocking in the heart need further investigation in the cachectic conditions associated with cancer and chemotherapy. Moreover, the interaction of myostatin/activin blocking with protein synthesis and its regulation in cancer, chemotherapy and conditions of reduced activity and food intake is poorly understood.

### 3 AIMS AND HYPOTHESES

The aim of this dissertation was to study the effects of different wasting conditions, namely, chemotherapy and cancer cachexia as well as reduced physical activity and fasting, and the concomitant blocking of myostatin and activins on muscle size and its regulation, and the importance of maintaining adequate muscle mass in these wasting conditions. In addition, the effects of these wasting conditions on physical activity, exercise capacity and oxidative properties of skeletal muscle were also investigated.

The specific aims were to study:

1. The effects of doxorubicin chemotherapy on skeletal muscle and aerobic capacity, and the effects of blocking myostatin and activins in mice receiving chemotherapy. In addition, the study aimed to clarify the molecular mechanisms underlying the effects of chemotherapy and myostatin/activin blocking, and the potential health related outcomes. (I)

Hypothesis: Chemotherapy induces muscle toxicity accompanied by muscle atrophy and impaired aerobic capacity. These changes are associated with increased markers of protein degradation and decreased protein synthesis, and impaired mitochondrial function, and decreased capillarization, respectively, in skeletal muscle. The blocking of myostatin and activins prevents chemotherapy-induced muscle atrophy via enhanced protein synthesis, but does not ameliorate aerobic capacity, mitochondrial function, or capillary density.

2. The similarities and differences of cardiac and skeletal muscles in the transcriptomic responses to chemotherapy and myostatin/activin blocking. (II)

Hypothesis: Chemotherapy induces both similar and different changes in the heart and skeletal muscle transcriptomes, but the extent of the alterations is expected to be comparable between the tissues or slightly more extensive in the heart. Myostatin/activin blocking has more pronounced effects on skeletal muscle transcriptome compared with the heart.

3. The effects of increasing muscle mass via the blocking of myostatin and activins only before, or both before and after tumour formation on survival in cancer cachexia. In addition, the aim was to explore potential factors influencing survival, and thus, food intake, physical activity, and effects on muscle and several non-muscle tissues were studied. Moreover, the aim was to investigate the molecular mechanisms of muscle wasting associated with cachexia and the effects of blocking myostatin and activins. (III)

Hypothesis: Having larger muscles at baseline prolongs survival in cancer cachexia, and maintenance of the increased muscle size provides additional survival benefit. Worse survival is associated with muscle wasting and atrophy of respiratory muscles, inflammation, and haematological alterations. Habitual physical activity decreases in cancer and this is not restored by the blocking of myostatin and activins. Muscle wasting is associated with a combination of decreased protein synthesis and increased protein degradation, while the blocking of myostatin and activins induces hypertrophy via promotion protein synthesis. Differences in muscle protein synthesis are associated with altered mTOR localization and signalling activity.

4. The interaction between the blocking of myostatin and activins and decreased levels of physical activity and food intake in muscle protein synthesis and its regulation. (IV)

Hypothesis: Low levels of physical activity and food intake are associated with decreased levels of protein synthesis, and this effect is counteracted by myostatin/activin blocking. Blunted protein synthesis is associated with decreased colocalisation of mTOR with the lysosomes/late endosomes and/or translocation away from sarcolemma, resulting in decreased mTORC1 signalling, while the blocking of myostatin and activins promotes the colocalisation of mTOR with the lysosomes/late endosomes and increases mTORC1 signalling.

## 4 MATERIALS AND METHODS

### 4.1 Animals

Male mice from two different backgrounds were used in the experiments. In chemotherapy (I, II) and follistatin (IV) experiments, C57Bl/6J mice aged 9–10 weeks (Envigo, The Netherlands), or aged 10–12 weeks (Janvier, France), respectively, were used. The C26 cancer experiments (III) were conducted on the syngeneic BALB/c mice (BALB/cAnNCrI, Charles River Laboratories, Germany), aged 5–6 weeks. In all experiments, mice were housed under standard conditions (22°C, 12:12 h light/dark cycle) in an environmentally controlled facility with water and standard feed (R36; 4% fat, 55.7% carbohydrate, 18.5% protein, 3 kcal/g, Labfor, Stockholm Sweden) provided *ad libitum* with the exception of the short-term fasting in the follistatin experiment (IV). The mice were housed in individually ventilated cages (IVC) in chemotherapy experiments (I, II), and in open cages in a Scantainer ventilated cabinet (Scanbur, Karlslunde, Denmark) in C26 cancer and follistatin experiments (III, IV).

#### 4.1.1 Ethics statement

The treatment of the animals was in strict accordance with the European Legislation for the protection of animals used for scientific purposes (directive 2010/63/EU), and the experimental procedures described here were approved by the National Animal Experiment Board, Finland (permit numbers: ESAVI/10137/04.10.07/2014 (I–IV), and ESAVI/14457/2018 (IV)).

#### 4.1.2 Humane endpoint criteria (III)

In the survival experiment, mice were followed until the predetermined humane endpoint criteria were fulfilled, or until three weeks after C26 cell inoculation the latest, to investigate survival. The endpoint criteria combined the body mass loss, tumour mass and the overall condition of the mice. The mice



needed to be euthanized if the body mass loss exceeded 20% and was accompanied by any other marker of poor health status. In the evaluation of the overall health status of the mice, the following aspects were considered in addition to the body mass loss: appearance and posture (lack of grooming, piloerection, and hunched posture), natural and provoked behaviour (inactivity, impaired locomotion, and reduced reactivity to external stimuli), and food intake or the ability to eat and drink. Additional endpoint criteria included tumour ulceration and self-mutilation, and in those cases, the mice were excluded from the final analysis. The fulfillment of the endpoint criteria was confirmed by two researchers. During the experiment, seven mice were euthanized based on criteria unrelated to study purposes (i.e. tumour ulceration or self-mutilation), and thus excluded from final survival analyses. In addition, three mice were excluded from analysis due to delayed tumour growth. These exclusions did not have major effect on the results. No mice needed to be euthanized due to excessive tumour growth.

## **4.2 Experimental design**

### **4.2.1 Randomization of the mice (I-IV)**

Mice were randomly assigned into one of the experimental groups in all of the experiments. However, the groups were approximately matched by the mean and standard deviation of the body mass to minimize systematic difference in body and muscle mass and size in the beginning of the experiment, as those were some of the main variables of interest. The experimental designs are illustrated in Figure 4.

### **4.2.2 Chemotherapy experiments (I, II)**

Four chemotherapy experiments and one experiment combining chemotherapy and tumour (Lewis Lung Carcinoma, LLC) were conducted. In the chemotherapy experiments, mice were randomized into three groups: 1) vehicle (phosphate-buffered saline, PBS) treated control mice (CTRL), 2) doxorubicin hydrochloride treated mice (DOX), and 3) doxorubicin-treated mice administered with soluble ACVR2B-Fc (DOX+sACVR2B). A two-week experiment and two four-week experiments were conducted. In these longer-term experiments, the mice were given four intraperitoneal (i.p.) injections of doxorubicin (6 mg/kg in PBS) every third day during the first two weeks of the experiments, yielding a cumulative dose of 24 mg/kg. An equal volume of vehicle (PBS) was administered to the control mice. Treatment with sACVR2B was started prior to the first doxorubicin injection and it was administered (5 mg/kg in PBS) twice a week for the first two weeks and once a week after that (in the four-week experiments). The samples were collected two or four weeks after the first doxorubicin injection. The doxorubicin-treatment protocol was designed to mimic the

treatment of human patients (Vejjongsak & Yeh 2014). In addition, an acute experiment was conducted. In the acute experiment, mice were given a single i.p. injection of doxorubicin (15 mg/kg in PBS) or an equal volume of vehicle/PBS 20 hours before sample collection. Half of the doxorubicin-treated mice received additionally an i.p. injection of sACVR2B (10 mg/kg in PBS) 48 hours before doxorubicin administration as it has previously been shown that sACVR2B increases muscle protein synthesis 48 hours after its administration (Hulmi et al. 2013a).

In the tumour experiment, mice were randomly assigned into one of five groups: 1) healthy controls (CTRL), 2) LLC tumour-bearing (TB) mice (LLC+PBS), 3) LLC TB mice treated with doxorubicin (LLC+DOX), 4) LLC TB mice treated with sACVR2B-Fc (LLC+sACVR2B), and 5) LLC TB mice treated with doxorubicin and sACVR2B (LLC+DOX+sACVR2B). The mice were anaesthetized by i.p. administration of ketamine and xylazine and subsequently inoculated with  $5 \times 10^5$  LLC cells suspended in 100  $\mu$ l of PBS (TB mice), or with an equal volume of vehicle only (CTRL mice) into the subcutis of the right abdominal region. Two i.p. injections of doxorubicin (6 mg/kg in PBS), on the sixth and eleventh day after LLC cell inoculation, were given during the experiment (cumulative dose 12 mg/kg). Administration of sACVR2B-Fc (5 mg/kg in PBS) was started on the third day after LLC cell inoculation and continued twice a week until two days before sample collection (four injections in total). Samples were collected 14 days after LLC cell inoculation.

#### 4.2.3 C26 cancer experiments (III)

The mice were randomized into one of four groups: 1) healthy control mice (CTRL), 2) Colon-26 (C26) TB mice receiving vehicle treatment throughout the experiment (C26 + PBS), 3) C26 TB mice receiving sACVR2B treatment before tumour formation (until day one after C26 cell inoculation) followed by vehicle treatment until the end of the experiment (C26 + sACVR/b), and 4) C26 TB mice receiving continued sACVR2B treatment throughout the experiment (C26 + sACVR/c). The mice were followed either until the pre-determined humane endpoint criteria (described in the previous section) were fulfilled (survival experiment) or until a pre-determined time point at 11 days after C26 cell inoculation (short-term experiment). The short-term experiment was replicated with three groups (CTRL, C26 + PBS, and C26 + sACVR/c groups) and with endpoint at 13 days after C26 cell injection to replicate the findings of the first short-term experiment and to collect more samples and data for further analysis. In all experiments, mice were injected i.p. with sACVR2B (5 mg/kg) or PBS (100  $\mu$ l) twice a week, three times before and three times after C26 cell inoculation (on days -11, -7, -3, 1, 5, and 9). On day 0, mice were inoculated with  $5 \times 10^5$  C26 cells suspended in 100  $\mu$ l of PBS (TB mice) or with an equal volume of vehicle (CTRL mice) into the intrascapular subcutis under anaesthesia (60–70 mg/kg ketamine, and 9 mg/kg xylazine, i.p., Ketaminol® and Rompun®, respectively).

#### 4.2.4 Follistatin experiments (IV)

The mice were administered i.p. with ketamine and xylazine (50–60 mg/kg and 7–8 mg/kg, respectively) to induce short-term anaesthesia, and subsequently given an intramuscular (i.m.) injection of recombinant adeno-associated viral vector 9 (AAV9) encoding follistatin-288 (FS288, 30  $\mu$ l) into one tibialis anterior (TA) muscle, and non-protein coding AAV9-CTRL into the contralateral TA. The order of the experimental and control legs was randomized. In the first experiment (dose-response experiment), three different doses of AAVs,  $4 \times 10^9$ ,  $1.6 \times 10^{10}$ , and  $6.4 \times 10^{10}$  viral particles (vp)/muscle, were injected into different mice, and the samples were collected 20 days after the injection. In the following acute experiments, mice were given an i.m. injection of AAV9-FS288 or AAV9-CTRL in a dose of  $4 \times 10^9$  vp/muscle, as that was the lowest dose producing significant hypertrophy in TA and extensor digitorum longus (EDL) muscles without major effects on the mass of the other muscles in the same leg. The blood and muscle samples were collected seven days after the AAV injection. The mice were housed individually for the last two days of the experiments either in Promethion respirometry cages (time of day experiment, Sable Systems, North Las Vegas, NV, USA) or in normal cages (fasting experiment). In the time of day experiment, blood and muscle samples were collected either in the night-time at dark phase (on average at 12 AM, N = 8), or in the daytime at light phase (on average at 3 PM, N = 8). The time points were selected based on our pilot measurements to represent periods of high physical activity and feeding (night-time) in contrast to low levels physical activity and feeding (daytime). In the fasting experiment, blood and muscle samples were collected in the morning after overnight feeding *ad libitum* (AD, N = 8), overnight (12 h) fasting (F, N = 8), or overnight (11 h) fasting followed by one-hour refeeding (RF, N = 8). The food was withdrawn at 9 PM to allow feeding in the beginning of the dark phase and thus to avoid more prolonged fasting and to better standardize the fasting time.

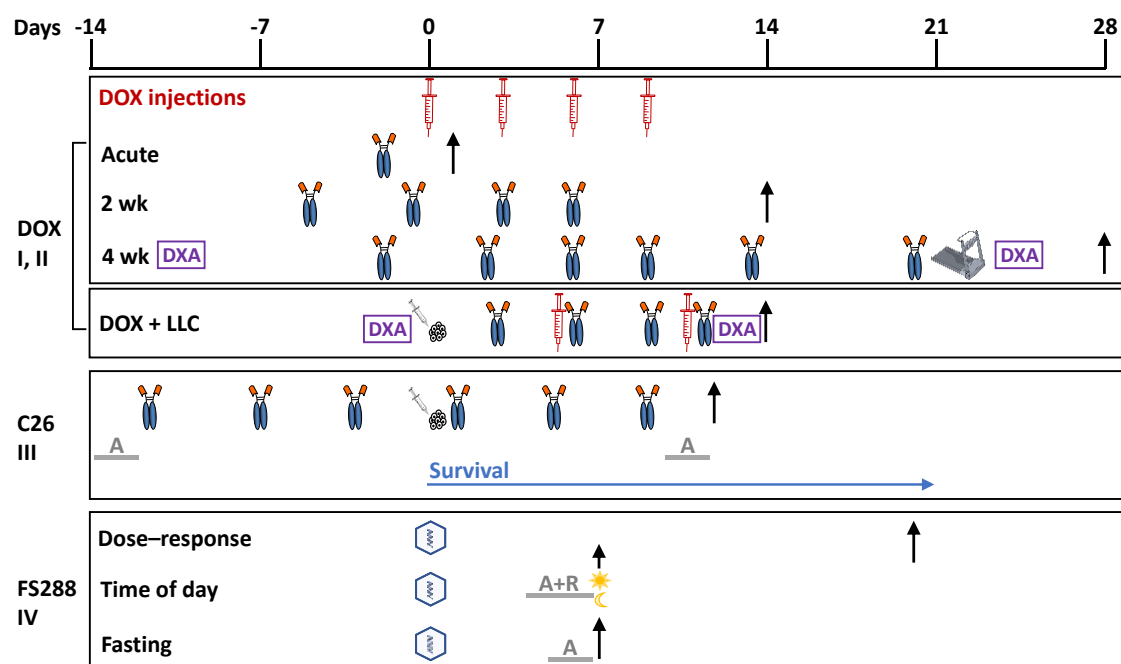


FIGURE 4 Schematic representation of the experimental designs for doxorubicin (DOX), C26 cancer (C26), and follistatin (FS288) experiments. Black arrows depict the timing of the sample collection. The red syringes depict DOX or vehicle injections. The receptor depicts administration of sACVR2B or vehicle. DXA indicates the timing of body composition analyses with dual-energy X-ray absorptiometry (DXA). The treadmill designates the timing of the maximal treadmill running test. The syringe accompanied by a cluster of cells depicts the timing of cancer cell (or vehicle) inoculation. The hexagon depicts the timing of the AAV injection. A, activity recording; R, respirometry; LLC, Lewis lung carcinoma. The treadmill image was obtained from <https://smart.servier.com>.

### 4.3 Blocking of myostatin and activins

#### 4.3.1 Production of the soluble Activin receptor type IIB (I-III)

The recombinant fusion protein was produced and purified in house at the University of Helsinki, Helsinki, Finland by Dr. Arja Pasternack and Dr. Olli Ritvos (Hoogaars et al. 2012; Hulmi et al. 2013a). The ectodomain of human ACVR2B was amplified via PCR (5'-GGACTAGTAACATGACGGCGCCCTGG-3' and 5'-CCAGATCTGCGGTGGG-GGCTGTCCG-3') from a pCR-Blunt II-TOPO plasmid containing the human ACVR2B sequence (pCR-Blunt II-TOPO AM2-G17 ActRIIB, IMAGE clone no. 40005760; The IMAGE Consortium). A human IgG1 Fc domain containing a hexa histidine (His6) tag in the C-terminus was amplified via PCR (5'-GCAGATCTAATCGAAGGTCGTGGTGATCCCAAATCTTGT-GAC-3' and 5'-TCCCTGTCTCCGGGTAACACCATCACCATCACCATTGAGCGGCCGCTT-

3') from the pIgPlus expression plasmid. These products were subcloned into the pGEM-T easy vectors (Promega, Madison, WI, USA), sequenced, and fused before cloning into the expression vector pEFIRES-P. For the protein production, chinese hamster ovary (CHO-S) cells were transfected with the pEFIRES-P-ACVR2Becc-FcHis6 expression vector via lipofection (Fugene 6; Roche, Basel, Switzerland) and selected with puromycin (Sigma-Aldrich, Darmstadt, Germany). During selection, cells were grown in F12 Ham medium (N4888, Sigma-Aldrich, Darmstadt, Germany) supplemented with 2 mmol/l L-alanyl-L-glutamine, 100 µg/ml streptomycin, 100 IU/ml penicillin, and 10% FBS. For large-scale production, cells were adapted to CD OptiCHO medium (12681029, Life Technologies, Carlsbad, CA, USA) supplemented with 2 mmol/l L-alanyl-L-glutamine and cultured in suspension in an orbital shaker. After 7-10 days, cell culture supernatants were filtrated through a 0.22-µm membrane (Steritop; Millipore, Burlington, MA, USA). Next, NaCl and imidazole were added, and the solution was pumped through a Ni<sup>2+</sup>-loaded Protino® Ni-NTA 5 mL Columns 5 (Macherey-Nagel, Düren, Germany) at 4°C. The column was washed with raising imidazole concentrations and eluted with 250 mM imidazole (5 × 10 ml). The eluate was then dialyzed against PBS and the concentration was measured with NanoDrop spectrophotometer, and finally concentrated with Amicon Ultra concentrator (30 000 MWCO; Millipore, Burlington, MA, USA). The purity of our sACVR2B-Fc preparation after IMAC purification was estimated to be > 90% based on silver-stained SDS-PAGE. The protein is similar, but not identical to that originally generated by Lee and colleagues (Lee et al. 2005).

#### **4.3.2 Production of the adeno-associated virus vectors (IV)**

The FS288+6His -insert was amplified from pOTB7 AU24-F5 Follistatin plasmid, I.M.A.G.E. clone #3688745 (Geneservice Ltd, Cambridge, UK) via PCR and cloned into pSupCAG vector for AAV production. pSubCAG plasmid containing the gene of interest was then transfected to CHO-S cells and transgene expression was confirmed by Western blotting using anti-tetra-histidine antibody (1:5000, #34670, Qiagen, Hilden, Germany). To produce recombinant adeno-associated viral vectors (serotype 9), HEK293T cells were transfected with the pSubCAG-FS288 or pSubCAG-Scramble (AAV9-CTRL) and helper plasmids. Media were collected after 2 and 3 days and the rAAV preparations were purified by ultracentrifugation using an iodixanol step gradient. The titers were determined by real-time qPCR. Finally, HEK293T cells were transduced with the AAVs encoding FS288 (AAV9-FS288) or a non-gene coding control AAV (AAV9-CTRL), and the transgene expression was confirmed by Western blotting using anti-tetra-histidine antibody. AAVs were manufactured by the AAV Gene Transfer and Cell Therapy Core Facility of Faculty of Medicine, University of Helsinki, Finland.

## **4.4 Tumour cell lines and cultures (I, III)**

### **4.4.1 Lewis lung carcinoma cells (I)**

Lewis lung carcinoma (LLC) cells were purchased from American Type Culture Collection (Manassas, VA, USA) and maintained in complete Dulbecco's Modified Eagle's Medium (DMEM) supplemented with 2 mmol/L L-glutamine, penicillin (100 U/mL), streptomycin (100 µg/mL), and 10% FBS.

### **4.4.2 Colon-26 adenocarcinoma cells (III)**

Colon-26 carcinoma (C26) cells (provided by Dr. Fabio Penna, obtained from Prof. Mario P. Colombo, and originally characterized by Corbett et al. (Corbett et al. 1975)) were maintained in complete DMEM (high glucose, GlutaMAX™ Supplement, pyruvate, Gibco™, Life Technologies) supplemented with penicillin (100 U/mL), streptomycin (100 µg/mL), and 10% FBS.

### **4.4.3 Cell harvesting for injection (I, III)**

After expansion of the cell line, cancer cells (LLC or C26) were seeded on the day before injection resulting in ~70% confluence on the day of harvest and injection. On the day of injection, the cells were washed with PBS, trypsinized for 5 minutes at +37°C, and collected in sterile plastic tubes after addition of complete growth medium. The cells were counted and subsequently centrifuged at 390 g for 5 minutes. The supernatant was removed and the cell pellet were suspended in sterile PBS. The cell suspension was then aliquoted for each mouse and stored on ice until the injection.

## **4.5 Analysis of running capacity, behavior and body composition**

### **4.5.1 Treadmill running test (I)**

All mice were familiarized with treadmill running on a separate day prior to the test. In the familiarization protocol, the mice ran first for five minutes at speeds of 9, 12, and 15 m/min, and then for one minute at 17 m/min, yielding a total of 16 minutes. In the actual test, the mice ran for five minutes at speeds of 9, 12, and 15 m/min after which the velocity was increased by 2 m/min every 2 minutes until exhaustion. The criterion for exhaustion was inability to keep up with the treadmill speed and continuous staying on the grid despite encouragement with compressed air. The treadmill running test was conducted during the last week of the four-week chemotherapy experiment.

#### 4.5.2 Physical activity (III, IV)

Home cage physical activity was analysed by measuring the vertical ground reaction forces by our validated custom-made force plate system as previously described (Kainulainen et al. 2015; Silvennoinen, Rantalainen & Kainulainen 2014). Forces were measured by strain gauge based sensors. Force signal was pre-amplified and then digitized using a 14-bit A/D converter (DI-710; DATAQ Instruments, Akron, OH, USA). As the outcome variable, the activity index of the mice housing the same cage (1–3 mice per cage) was calculated from the data as described previously with slight modifications (Silvennoinen, Rantalainen & Kainulainen 2014). The one-minute activity index values from the studied time period were then summed to yield a single value representing the total spontaneous activity of the mouse during that time period. To eliminate the contribution of the background activity (including measurement noise, and forces caused by an inactive animal, e.g. breathing and heartbeat) in the C26 cancer experiments, the lowest activity index value for a five-minute interval was analysed, and this value was then scaled to the whole measurement time and subtracted from the total activity index (III). For technical reasons, the lowest value for one-minute activity index was subtracted from each individual value to estimate the contribution of the background activity in the follistatin experiments (IV).

In C26 cancer experiments (III), a 22-hour activity recording was performed at baseline and on day 10 after C26 cell inoculation. The mice were housed in pairs and the activity index of each cage reflects the total locomotive activity in all directions (y, x and z axes) of the two mice housing the same cage. The cohoused mice represented the same experimental group. In follistatin experiments (IV), the mice were housed in individual cages for the last two days of the experiment. The first day was considered as an acclimatization period to individual housing and to the respirometry cages in the case of time-of-day experiment. The activity of the mice was recorded during the second day of individual housing, i.e. the last day of the experiment, and analysed from suitable time periods with respect to the purpose of the experiment (three-hour period preceding sample collection, or 10-hour fasting period).

#### 4.5.3 Dual-energy X-ray absorptiometry (DXA) (I)

For the analysis of body composition by DXA, mice were anaesthetized by administration of ketamine and xylazine, and subsequently imaged with Lunar PIXImus II densitometer (GE Healthcare, Boston, MA, USA). The mice were imaged prior to the beginning of any treatment and during the last week of the four-week chemotherapy experiment. The images were analysed using standard procedures.

#### **4.5.4 Food intake (I, III, IV)**

Food intake of the mice was monitored at different time points by repeatedly weighing the food of the mice. In the four-week chemotherapy experiment, the food intake was monitored twice in three-day periods, once during the administration of chemotherapy and one after cessation of chemotherapy (I). In C26 cancer experiments, the food intake was monitored daily by weighing the food every morning (III). In the time-of-day experiment, the timing and amount of food intake was mainly monitored by Promethion High-Definition Multiplexed Respirometry System and MetaScreen software (described more in detail below), but the total food intake was validated by weighing the food before and after the measurement (IV).

#### **4.5.5 Respirometry (IV)**

Respiratory gases and the amount and timing of food intake were monitored with Promethion High-Definition Multiplexed Respirometry System and MetaScreen software (Sable Systems, North Las Vegas, NV, USA) in the time-of-day experiment. The mice were measured for 48 hours, of which the first 24 hours was considered as an acclimatization period to the respirometry cages and the individual housing. Respirometry and food intake data acquired from Promethion system were analysed with ExpeData software (version 1.9.14, Sable Systems, North Las Vegas, NV, USA). The data from the last three hours of the measurement is reported to reflect the activity level and food intake of the mice just before the sample collection. The total food intake was validated by weighing the food before and after the two-day measurement.

### **4.6 Tissue collection and processing**

#### **4.6.1 Sample collection (I-IV)**

At the end of the experiments, the mice were anaesthetized by intraperitoneal injection of ketamine (110–120 mg/kg) and xylazine (15–16 mg/kg) (Ketaminol® and Rompun®, respectively, I-IV), or by isoflurane inhalation in the four-week chemotherapy experiment (I, II), and euthanized by cardiac puncture followed by cervical dislocation. A sample of the blood collected by cardiac puncture was collected in K3 EDTA tubes (I, III) for the analysis of basic haematology, and the rest was collected in serum collection tubes. The samples in serum collection tubes were centrifuged at 2000 g for 10 minutes, after which the serum was separated and stored at -80°C for further analyses (III, IV). Tissue samples were rapidly excised and weighed with an analytical balance (Table 1). For protein and messenger RNA analyses, tissue samples were snap-frozen in liquid nitrogen and stored at -80°C for further analyses. For histological analyses, tissue samples were embedded in Tissue-Tek® O.C.T. compound (Sakura



Finetek, Torrance, CA, USA) and snap-frozen in isopentane (-150°C) cooled with liquid nitrogen. Finally, the length of the tibia, to which tissue masses were normalized, was measured with a digital caliper.

TABLE 1 Collected tissue samples and analyses conducted on them in each study.

Tissue	Analysis	Study
M. Tibialis anterior (TA)	WB, IHC, histology, microarray, qPCR	I-IV
M. Gastrocnemius (GA)	DOX measurement, qPCR	II, III
Heart	WB, microarray, qPCR	II, III
Diaphragm	WB	III
Liver	WB	III
Spleen	IHC, pPCR	III
Epididymal white adipose tissue	-	I, III
Tumour	qPCR	I, III
Whole blood	Basic haematology	I, III
Serum	ELISA (cytokine assay)	III

WB, Western blotting; IHC, immunohistochemistry; qPCR, quantitative real-time polymerase chain reaction; ELISA, enzyme-linked immunosorbent assay; -, tissue was weighed but no further analyses were performed.

#### 4.6.2 Analysis of protein synthesis (I-IV)

The *in vivo* surface sensing of translation (SUnSET) method was applied to analyse protein synthesis from different tissues (Goodman et al. 2011; Schmidt et al. 2009). For this purpose, mice were anaesthetized by i.p. administration of ketamine and xylazine and subsequently injected i.p. with 0.040  $\mu\text{mol/g}$  puromycin (Calbiochem, Darmstadt, Germany) dissolved in 200  $\mu\text{l}$  of PBS. At 25 (I, II, III) or 22 (IV) minutes after puromycin administration, mice were euthanized by cardiac puncture followed by cervical dislocation. The tissue samples were then isolated, weighed and snap-frozen in liquid nitrogen at specific time points: the TA muscle (I, III, IV) and the heart (II, III) were frozen at exactly 30 minutes, and the diaphragm (III) and a sample of the median lobe of the liver (III) at exactly 35 and 40 minutes after puromycin administration, respectively. The puromycin incorporation was then analysed with Western blotting as described in section 4.9.3.

#### 4.6.3 Mitochondrial function (I)

A 5–10 mg sample from the belly of the left TA muscle was taken and stored temporarily in BIOPS buffer. The sample was then homogenized with a shredder and carbohydrate SUIIT protocol was used to analyse mitochondrial function with Oxygraph-2k high-resolution respirometer (Oroboros, Innsbruck, Tyrol, Austria) as previously described (Kivelä et al. 2014).

#### **4.6.4 Measurement of doxorubicin content (II)**

Doxorubicin concentration was analysed from gastrocnemius muscles with an Agilent 1100 HPLC system (Agilent Technologies, Waldbronn, Germany) combined with an AB Sciex API 2000 tandem mass spectrometer (Framingham, MA, USA) as previously described (Räsänen et al. 2016).

### **4.7 Blood analyses**

#### **4.7.1 Basic haematology (I, III)**

Basic haematology was analysed from whole blood collected in K3 EDTA-containing blood collection tubes. Samples were diluted 1:25 in saline solution and analysed with an automated haematology analyser (Sysmex XP-300™, Sysmex Inc, Kobe, Japan). For the analysis of the platelet count, whole blood was diluted 1:250 due to high platelet counts in the samples.

#### **4.7.2 Serum cytokine analysis (III)**

A multiplex cytokine assay (Q-Plex Array 16-plex ELISA, Quansys Biosciences, Logan, Utah, USA) was performed in accordance with manufacturer's instructions from 25 µl of serum collected at 11 days after cancer cell inoculation.

### **4.8 Messenger RNA analyses**

#### **4.8.1 RNA extraction (I, II, III)**

Total RNA was extracted from TA muscle (I, II), GA muscle (III), heart (II), tumour (III), and spleen (III) samples using TRIsure (I, II) or QIAzol (III) reagent and purified with NucleoSpin® RNA II columns (I, II) or RNeasy Universal Plus kit (Qiagen, Hilden, Germany) (III) according to manufacturer's instructions resulting in high quality RNA. The RNA concentration of the samples was analysed with NanoDrop spectrophotometer. The integrity and quality of the RNA samples was analysed with Agilent 20100 Bioanalyzer (Agilent, Santa Clara, CA, USA; I, II).

#### **4.8.2 Microarray analysis (I, II)**

RNA extracted from the TA and the heart samples collected after a single injection of doxorubicin was analysed with Illumina Sentrix MouseRef-6 v2 Expression BeadChip containing 45281 transcripts (Illumina Inc., San Diego, CA, USA) by the Functional Genomics Unit at Biomedicum Helsinki, University of Hel-

sinki, Finland, according to the manufacturer's instructions. Five samples from each tissue were analysed from CTRL and DOX groups, whereas five muscle and three heart samples from DOX+sACVR2B group were included in the analysis. The integrity and quality of the RNA samples was analysed with Agilent Bioanalyzer 2100. Initial data analysis and quality control were conducted using Illumina's GenomeStudio software. Chipster software (IT Center for Science, Espoo, Finland) was used for normalization of raw data with quantile normalization (including log<sub>2</sub>-transformation of the data), assessment of data quality, and statistical analyses (Kallio et al. 2011). The statistical significance of differences between the groups was analysed using Empirical Bayes statistics and the Benjamini-Hochberg algorithm controlling false discovery rate (FDR). FDR values < 0.05 with ≥ 1.2-fold difference were considered significant. Array data generation, preprocessing, and analysis were conducted according to MI-AME guidelines. The complete data sets are publicly available in the NCBI Gene Expression Omnibus (<http://www.ncbi.nlm.nih.gov/geo/>; accession no. GSE77745 and GSE97642).

#### **4.8.3 Pathway analysis (I, II)**

Enrichment of functionally related genes was analysed using Gene Set Enrichment Analysis software (GSEA; Version 2.0) (Subramanian et al. 2005) as previously described (Kainulainen et al. 2015). Four different gene set collections, the Canonical Pathways, Biocarta, KEGG and Reactome, were used (<http://www.broadinstitute.org/gsea/msigdb/collections.jsp>). The number of permutations by gene set was set to 1000 and gene sets with at least ten and no more than 500 genes were taken into account in each analysis. FDR was calculated to determine statistical significance and values of FDR < 0.05 were considered significant.

#### **4.8.4 Transcription factor analysis (II)**

To detect enriched transcription factor motifs and their optimal set of direct target genes, a genome-wide ranking-and-recovery approach was applied using iRegulon software (Janky et al. 2014). This approach can reveal regulatory relationships from gene expression profiling data by reverse-engineering a gene regulatory network starting from the expression data.

#### **4.8.5 Reverse transcription and quantitative real-time PCR (I-III)**

RNA extracted from the skeletal muscle [TA (I, II) and GA (III)], the heart (II), and the tumour (III) was reverse transcribed to complementary DNA (cDNA) with iScript™ Advanced cDNA Synthesis Kit (Bio-Rad Laboratories, Hercules, CA, USA) according to the manufacturer's instructions. Quantitative real-time PCR (qPCR) was then performed according to standard procedures using iQ SYBR Supermix (Bio-Rad Laboratories, Hercules, CA, USA) and CFX96 Real-Time PCR Detection System combined with CFX Manager software (Bio-Rad

Laboratories, Hercules, CA, USA). Data analysis was carried out by using the standard curve or the efficiency corrected  $\Delta\Delta C_t$  method. The relative mRNA expressions were normalised to a housekeeping gene. Multiple potential housekeeping genes were analysed (*Rn18S*, *Gapdh*, and *36b4*), and based on the lowest variation between and within the groups, *36b4* was chosen for the tumour (III), TA (I, II), GA (III), and the heart (II). The primers used are listed in Table 2.

TABLE 2 Primers used for quantitative real-time PCR.

Transcript	Sequence, 5'-3'	Bio-Rad PrimePCR™ Assay ID	Study
<i>36B4</i>	F: GGCCCTGCACTCTCGCTTTC R: TGCCAGGACGCGCTTGT		I-III
<i>Gapdh</i>	F: AACTTTGGCATTGTGGAAGG R: GGATGCAGGGATGATGTTCT		I-III
<i>Rn18s</i>	F: GCAATTATTCCCCATGAACG R: GGCCTCACTAAACCATCCAA		I-III
<i>Activin A</i>	F: GAACGGGTATGTGGAGATAG R: TGAAATAGACGGATGGTGAC		II, III
<i>Myostatin</i>	F: AAGATGGGCTGAATCCCTTT R: GCAGTCAAGCCCCAAAGTCTC		II, III
<i>Il-6</i>	F: CTGATGCTGGTGACAACCAC R: CAGAATTGCCACATTGCACAAC		III
<i>Murf1</i>	F: GCTCAGAGAGCAGGGACTAG R: AAAGCACCAAATTGGCATA		I-III
<i>p21/Cdkn1a</i>	F: CGGTGTGTCAGAGTCTAGGGGA R: AGGATTGGACATGGTGCCTG		II
<i>Redd1/Ddit4</i>	F: GCCTCTGGGATCGTTTCTCG R: GGTC AAGGCCCTCTTCTCTG		I, II
<i>Myod1</i>		qMmuCED0003826	II
<i>Atrogin1</i>		qMmuCID0011869	II, III

F, Forward sequence; R, Reverse sequence.

## 4.9 Protein analyses

### 4.9.1 Protein extraction and total protein content (I-IV)

Samples of the TA muscle (I-IV), the heart (II, III), the diaphragm (III), and the liver (III) were homogenized in ice-cold HEPES-buffer [20 mM Hepes, 1 mM EDTA, 5 mM EGTA, 10 mM MgCl<sub>2</sub>, 2 mM DTT, 1 mM Na<sub>3</sub>VO<sub>4</sub>, 100 mM  $\beta$ -glycerophosphate, 1% NP-40, 3% Halt™ Protease and Phosphatase Inhibitor Cocktail (Thermo Scientific)] followed by 30 minutes of agitation at 4°C. The samples were then centrifuged at 500 g for 5 minutes at 4°C, after which a sample of the supernatant was collected for the analysis of the protein synthesis, and subsequently at 10 000 g for 10 minutes at 4°C, after which the whole su-

pernatant was collected for other analyses. Total protein content was determined using the bicinchoninic acid (BCA) protein assay (Pierce Biotechnology, Thermo Scientific, Waltham, MA, USA) with an automated KoneLab device (Thermo Scientific, Vantaa, Finland).

#### 4.9.2 Citrate synthase activity (I, III)

Citrate synthase activity was measured from TA, diaphragm and heart homogenates using a citrate synthase assay kit (CS0720, Sigma-Aldrich, Darmstadt, Germany) with an automated KoneLab device (Thermo Scientific, Vantaa, Finland).

#### 4.9.3 Western blotting (I-IV)

Tissue homogenates containing 30  $\mu$ g of protein were solubilized in Laemmli sample buffer containing 5%  $\beta$ -mercaptoethanol and heated for 10 min at 95°C (except for the analysis of OXPHOS proteins, for which the samples were heated for 5 min at 50°C) to denature proteins. Proteins were separated by SDS-PAGE using Criterion TGX (I-III) or Criterion TGX Stain-Free (IV) precast 4–20% gradient gels on Criterion electrophoresis cell (Bio-Rad Laboratories, Hercules, California, USA) and then transferred to PVDF membrane using Criterion blotter on ice at 4°C (I-III) or Trans-Blot® Turbo™ Transfer System (IV) (Bio-Rad Laboratories, Hercules, California, USA). Membranes were then scanned with ChemiDoc MP device (Bio-Rad Laboratories, Hercules, California, USA) to obtain stain free images (IV), or stained with Ponceau S and imaged with ChemiDoc XRS device (Bio-Rad Laboratories, Hercules, California, USA; I-III). After that, the membranes were blocked with 5% non-fat dry milk in Tris-buffered saline with 0.1% Tween 20 (TBS-T), and subsequently probed overnight with primary antibodies diluted in TBS-T containing 2.5% non-fat dry milk or 2.5% BSA at 4°C. The antibodies used are listed in Table 3, except for the anti-puromycin antibody (clone 12D10), which was a generous gift from Dr Philippe Pierre, and was diluted 1:6000. After primary antibody incubation, the membranes were washed with TBS-T and incubated with horseradish peroxidase conjugated secondary antibodies (Jackson ImmunoResearch Europe) for 1 hour in room temperature. The proteins were then detected by enhanced chemiluminescence (SuperSignal West Femto Maximum Sensitivity Substrate; Pierce Biotechnology, Thermo Scientific, Waltham, MA, USA) and ChemiDoc XRS (I-III) or ChemiDoc MP device (IV) (Bio-Rad Laboratories) and quantified (band intensity  $\times$  volume) with Quantity One software version 4.6.3 (I– III) (Bio-Rad Laboratories, Hercules, California, USA) or Image Lab software version 6.0 (IV) (Bio-Rad Laboratories, Hercules, California, USA). In the case of the analysis of puromycin-incorporated proteins, ubiquitinated proteins, and total protein loading (stain-free), the intensity of the whole lane was quantified. All Western blot results were normalized to the total protein loading, i.e. the mean of Ponceau S staining and GAPDH quantification (I, II, III) or the quantification of the stain free image of the membrane (IV).

TABLE 3 Antibodies used in Western blot protein analyses.

Antigen	Dilution	Catalog #	Manufacturer	Study
GAPDH	1:10 000	ab9485	Abcam	I-IV
p-rpS6 (Ser240/244)	1:1500	#2215	Cell Signaling Technology	I, III, IV
rpS6	1:2000	#2217	Cell Signaling Technology	I, III, IV
p-p70 (Thr398)	1:1000	#9234	Cell Signaling Technology	I, III, IV
p70	1:1000	#2708	Cell Signaling Technology	I, III, IV
p-ERK1/2 (Thr202/Tyr204)	1:1000	#9101	Cell Signaling Technology	I
ERK1/2	1:1000	#9102	Cell Signaling Technology	I
p-Stat3 (Tyr705)	1:1000	#9145	Cell Signaling Technology	III
Stat3	1:3000	#9139	Cell Signaling Technology	III
FoxO1	1:1000	#2880	Cell Signaling Technology	I
p53	1:500- 1:1000	sc-263	Santa Cruz Biotechnology	II
Ubiquitin	1:700	sc-8017	Santa Cruz Biotechnology	I-III
Total OXPHOS	1:1000	ab110413	Abcam	I, III
Fibrinogen	1:10 000	ab27913	Abcam	III
Serpina3n	1:1000	AF4709-SP	R&D Systems	III

GAPDH, Glyceraldehyde 3-phosphate dehydrogenase; rpS6, Ribosomal protein S6; p70; p70 S6 Kinase; ERK, Extracellular signal-regulated protein kinases 1 and 2; Stat3, Signal transducer and activator of transcription 3; FoxO1, Forkhead box protein O1; p53, Cellular tumor antigen p53; OXPHOS, Oxidative phosphorylation; p, phosphorylated.

The samples were arranged to the gels according to the time and day of sample collection and in sets including one sample from each group. In chemotherapy experiments (I, II), the values of the CTRL and DOX+sACVR2B groups were normalized DOX sample of the same set. In C26 cancer experiments (III), the values of CTRL, C26+sACVR/b and C26+sACVR/b were normalized to the C26+PBS sample of the same set. These procedures were done in order to minimize between day and between time-of-day variation as well as to account for any variability of the signal and background within the membrane. In follistatin experiments (IV), when comparing the CTRL and FS288 legs, the value of the FS288 leg was normalized to the value of the CTRL leg of the same animal, and these samples were located next to each other on the gels. When doing comparisons between time-of-day or feeding status, the values were normalized to the mean of the CTRL leg of daytime or *ad libitum* feeding. The absolute FS288 effects were calculated from the values normalized to the mean of CTRL leg of

the daytime or *ad libitum* group, by subtracting the value of the CTRL leg from the value of the FS288 leg of the same animal.

## 4.10 Immunohistochemistry

### 4.10.1 Preparation of cryosections (I, III, IV)

For histological analyses, 10 µm thick frozen sections were cut from O.C.T.-embedded TA samples. The cross-sectional orientation of muscle fibres was verified with a light microscope. Before staining, the sections were air dried, fixed for 10 minutes with -20°C acetone, and washed with PBS.

### 4.10.2 Muscle immunohistochemistry (I, III, IV)

**Muscle fibre size and capillary density (I).** After fixation and washing, TA cross sections were permeabilized with 0.2% Triton-X in PBS, and blocked with 5% goat serum in PBS in room temperature. The sections were then incubated with overnight at +4°C with primary antibodies against dystrophin (1:500, ab15277, Abcam, Cambridge, UK) and PECAM-1/CD31 (1:500, #553370, BD Pharmingen, San Jose, CA, USA) diluted in 1% goat serum in PBS to visualize the sarcolemma and the capillaries, respectively. The next day, sections were washed and incubated with secondary antibodies (1:200, Goat anti-rabbit Alexa Fluor 555, and Donkey-anti rat Alexa Fluor 488, Invitrogen) for 1 hour at room temperature. After washing, sections were mounted with Mowiol-DABCO. The stained sections were scanned with Zeiss LSM 700 confocal microscope and ZEN software. The mean fibre cross-sectional area (CSA) was quantified from three random frames representing both the deep and the superficial regions of the muscle, and 1,065 ± 58 fibres were analysed from each sample. Fibre size distribution was analysed from 550 fibres that were randomly selected from each sample. Muscle fibre CSA, capillary density (capillaries/mm<sup>2</sup>) and capillary-to-fibre ratios were analysed with ImageJ software (NIH).

**mTOR-LAMP2 colocalisation (III, IV).** After fixation and washing, TA sections were blocked with a mixture containing 5% goat serum (III), or 4% sera mixture (IV), and 0.3% CHAPS in PBS. The sections were subsequently probed with primary antibodies against LAMP-2 (1:200, ab13524, Abcam, Cambridge, UK), mTOR (1:200, #2983, Cell Signaling Technology, Beverly, MA, USA), and dystrophin (1:200, NCL-DYS2, Novocastra, Newcastle upon Tyne, UK), followed by washing, and incubation with secondary antibodies (Alexa Fluor 488 donkey anti-rat, Alexa Fluor 555 goat anti-rabbit, and Alexa Fluor 405 (III) or Alexa Fluor 647 (IV) goat anti-mouse). The sections were then washed and mounted with Mowiol-DABCO. The sections were scanned using Zeiss LSM 700 confocal microscope and a Plan Apochromat 63x/1.4 NA Oil objective using ZEN black (2011 SP7). The colocalisation of mTOR with LAMP2 was analysed according to Costes et al. (Costes et al. 2004) from 10 images per section

(III), or from a stitched 4x4 tile scan (934  $\mu\text{m}^2$ ) consisting of 241 cells on average (IV) using the Colocalisation Threshold plugin in Image J (III) or Fiji (IV) (Schindelin et al. 2012). In IV, the data was first deconvoluted with a theoretical PSF before achieving cell segmentation with the Trainable Weka Segmentation plugin (Arganda-Carreras et al. 2017) in Fiji, and the intracellular marker classification and distance calculations were performed in Fiji and Matlab R2018b (MathWorks Inc), respectively (IV). All the steps were performed blinded to the sample identification.

#### 4.11 Statistical analyses

Statistical analyses, except for microarray results, were performed with IBM SPSS Statistics versions 22 or 24 for Windows (SPSS, Chicago, IL, USA). The data were checked for normality with Shapiro-Wilk test, and for the equality of variances with Levene's test. The statistical significance was set at  $P < 0.05$ . All data are presented as means  $\pm$  SEM, unless otherwise stated.

**Chemotherapy experiments (I, II).** Data from the two four-week experiments were pooled if there were no statistically significant differences between the experiments, and the experiment was included as a covariate in the analyses. The multiple group comparisons were performed with general linear model (GLM) analysis of variance (ANOVA), or by non-parametric Kruskal-Wallis test followed by the analysis of between-group differences by Bonferroni post hoc test, or Holm-Bonferroni corrected Mann-Whitney U test, respectively, when appropriate. For two-group comparisons a two-tailed unpaired Student's t-test or non-parametric Mann-Whitney U test were used. Correlations were analysed using Pearson's Product Moment Coefficient.

**C26 cancer experiments (III).** The Kaplan-Meier method (log-rank (Mantel-Cox) test) was used to analyse differences in survival time between groups, and the factors predicting survival time were determined using Cox regression analysis. The C26 cancer effect (CTRL vs. C26+PBS or CTRL vs. C26 groups pooled) was examined with Student's t-test or non-parametric Mann-Whitney U test. The differences between the TB groups were examined with one-way ANOVA followed by Holm-Bonferroni corrected LSD post hoc test, or non-parametric Kruskal-Wallis test followed by Holm-Bonferroni corrected Mann-Whitney U test, when appropriate. Correlations were analysed using Pearson's Product Moment Coefficient.

**Follistatin experiments (IV).** The main effects for FS288, time of day and feeding status were analysed with GLM ANOVA or Kruskal-Wallis test, when appropriate. Between-group (time of day or feeding status) comparisons were examined using Student's t-test or non-parametric Mann-Whitney U test, and Holm-Bonferroni correction was applied when more than two groups were compared, i.e. when effect of feeding status was analysed. A planned comparison approach was utilized when examining the between-group differences in the Western blot and mTOR-LAMP2 colocalisation results. Consequently, the



effects of time-of-day or feeding status were always examined within the leg (CTRL or FS288), and the differences between the CTRL and FS288 legs were analysed within time-of-day or feeding status. When examining differences between CTRL and FS288 legs, the (Western blot) results were analysed with non-parametric Mann-Whitney U -test, and the result of the FS288 leg was expressed relative to the CTRL leg of the same animal.

## 5 RESULTS

### 5.1 Cachexia and myostatin/activin blocking in chemotherapy and cancer

#### 5.1.1 Body mass, body composition and tissue masses (I-IV)

C26 tumour resulted in a significant progressive decline in body mass (Figure 5A). Mice treated with soluble activin receptor type IIB (sACVR2B) to block myostatin and activins before and after tumour formation first gained body mass and retained higher body mass compared with the vehicle-treated tumour-bearing (TB) mice until the endpoint at 11 days after cancer cell inoculation (Figure 5A). However, if sACVR2B administration was ceased before tumour formation, the mice were not protected from the cancer-induced loss of body mass (Figure 5A). At this 11-day time point, the significantly decreased body mass was accompanied by lower tibialis anterior (TA), diaphragm, and epididymal fat masses in the vehicle-treated TB mice compared with the healthy controls (Figure 5B-D). Administration of sACVR2B restored the TA and diaphragm masses, but not the adipose tissue mass (Figure 5B-D). However, the group in which sACVR2B treatment was discontinued showed the most prominent adipose tissue wasting (Figure 5D). Heart mass was unaffected by the tumour and the sACVR2B-Fc administration at this time point (Figure 5E). Tumour mass was unaffected by the sACVR2B administration (Figure 5F).

A two-week doxorubicin (DOX) chemotherapy protocol also induced a decrease in body mass that was sustained until the four-week time point despite the cessation of the DOX administration (Figure 6A). Treatment with sACVR2B prevented the DOX-induced decrease in body mass (Figure 6A). The decreased body mass in DOX-treated mice was accompanied by significantly decreased lean and fat mass analysed with dual-energy X-ray absorptiometry (DXA, Figure 6B and C). These results were supported by the individual tissue masses, as the masses of TA, gastrocnemius, epididymal fat and the heart were

significantly lower in the DOX-treated mice compared with the healthy controls (Figure 6D-G).

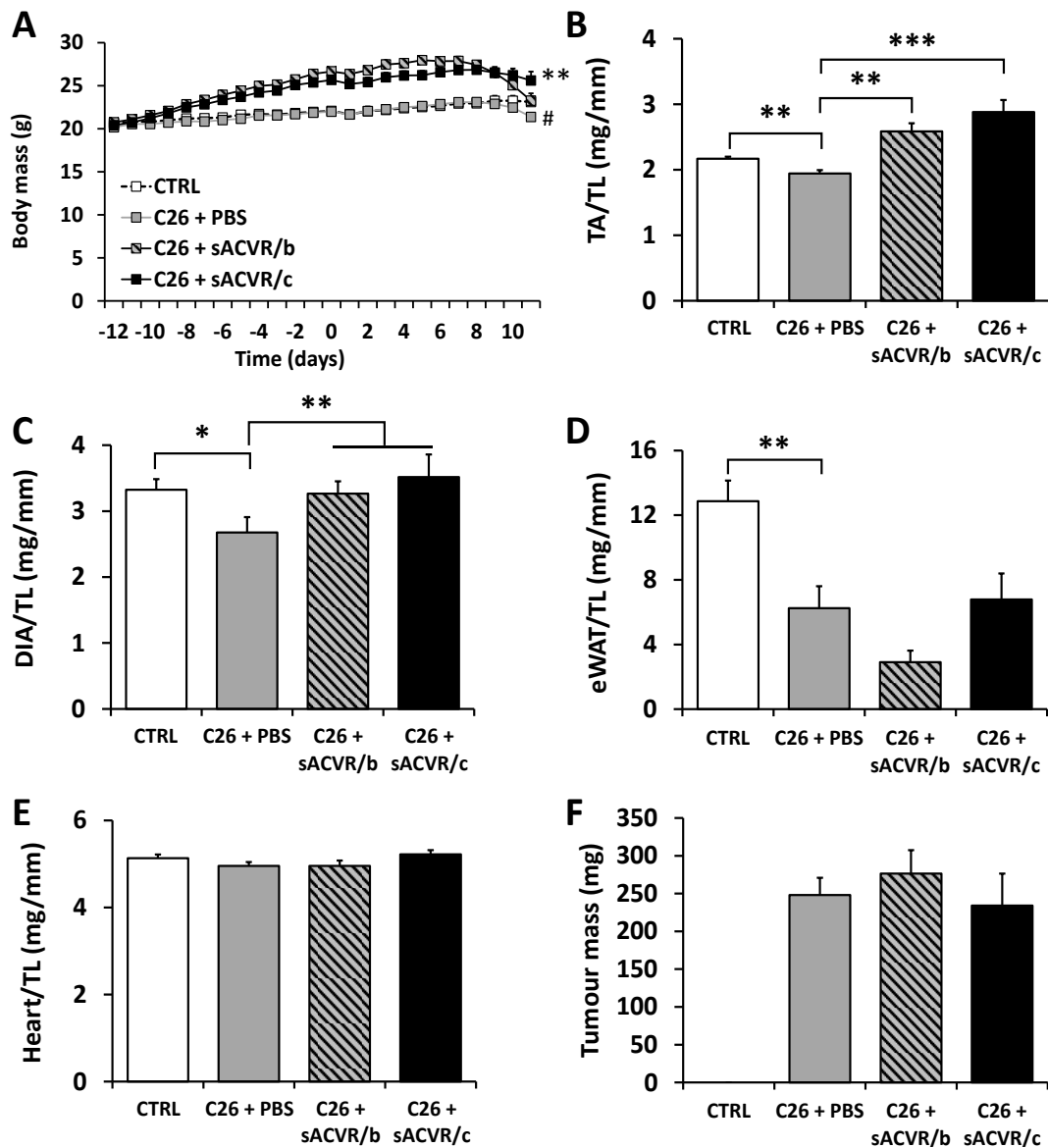


FIGURE 5 Body and tissue masses in experimental cancer (III). Body mass curve (A) and the masses of tibialis anterior (TA, B), diaphragm (C), epididymal white adipose tissue (eWAT, D), and the heart (E) normalized to the length of tibia (TL), and tumour mass (F) at 11 days after cancer cell inoculation. \*, \*\* and \*\*\* =  $P < 0.05$ ,  $0.01$  and  $0.001$ , respectively. In part A \*, different vs C26 + PBS; #, different vs CTRL. CTRL vs. C26 + PBS difference was analysed by Student's *t*-test (A-E), and differences between the C26-groups with one-way ANOVA with Holm-Bonferroni corrected LSD test (A-F). The line in part C designates a pooled effect of sACVR2B groups combined. N = 9, 7, 7, and 8 in CTRL, C26 + PBS, C26 + sACVR/b, and C26 + sACVR/c, respectively.

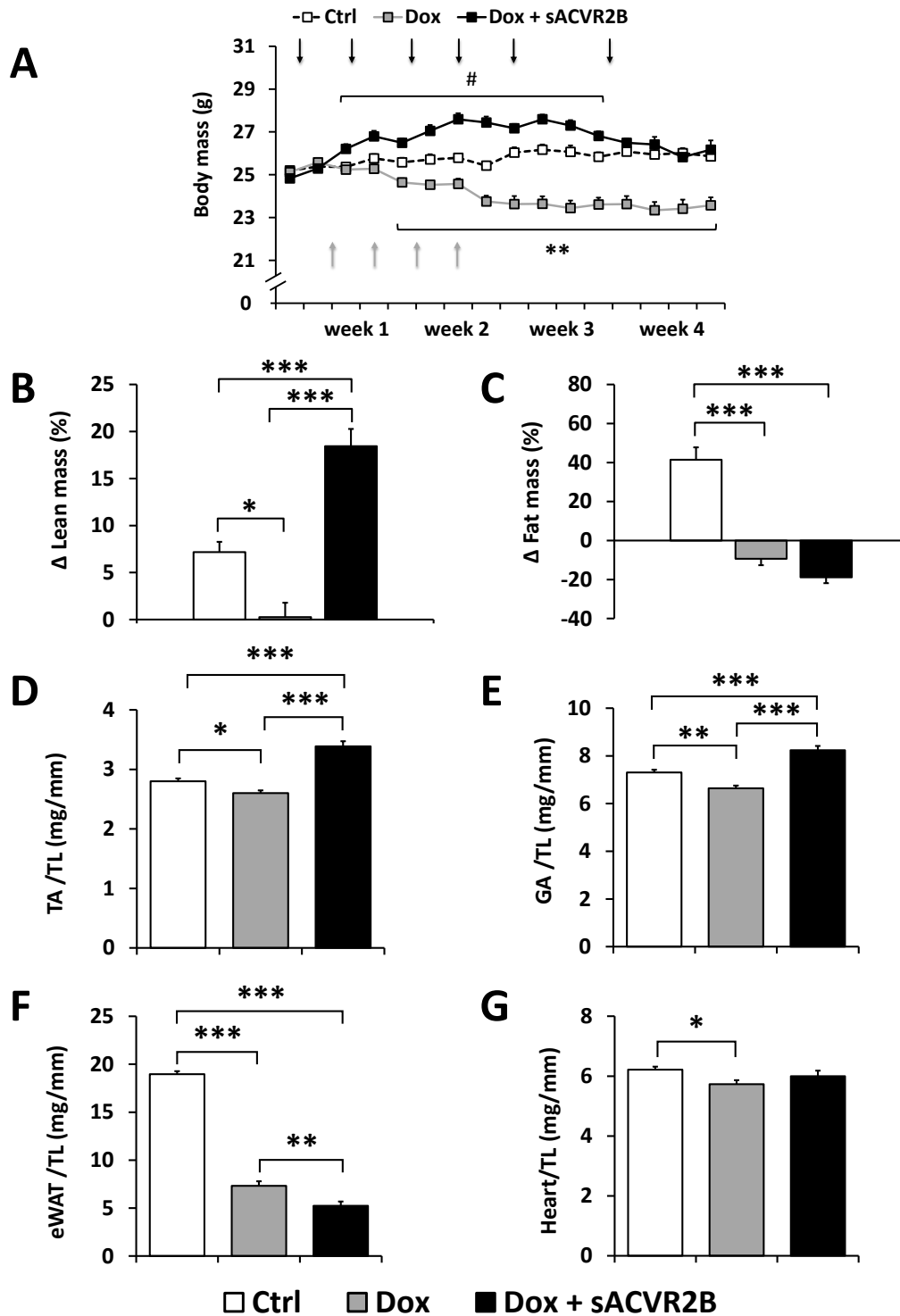


FIGURE 6 Body mass, body composition, and tissue masses in doxorubicin-treated mice (I). Body mass curve (A) and the changes in lean (B) and fat mass (C) in the four-week experiment. The masses of tibialis anterior (D), gastrocnemius (GA, E), epididymal white adipose tissue (F), and the heart (G) normalized to the length of tibia (TL) at four weeks. Arrows depict the timing of DOX (grey) and sACVR2B (black) injections. \*, \*\* and \*\*\* =  $P < 0.05$ ,  $0.01$  and  $0.001$ , respectively (Bonferroni). In part A #, different vs Ctrl; \*\*, different vs Ctrl and Dox + sACVR2B.  $N = 9, 10$ , and  $10$  (A-C),  $N = 15, 16$ , and  $17$  (D-F), and  $N = 14, 16$ , and  $16$  (G), in Ctrl, Dox, and Dox + sACVR2B, respectively.

In addition, the muscle fibre frequency curve shifted towards smaller fibres (Figure 7A). The treatment with sACVR2B again fully prevented the decrease in skeletal muscle and lean masses (Figure 6B, D and E), and restored the muscle fibre CSA (Figure 7A and B) at the four-week time point in the DOX-treated mice and even caused hypertrophy compared with the vehicle-treated control mice. However, sACVR2B treatment did not protect from the cardiac atrophy or the loss of fat mass (Figure 6F and G). In addition to the chemotherapy alone, the combination of LLC tumour and DOX decreased body and tissue masses, while treatment with sACVR2B prevented the loss of body and lean mass (I). Importantly, sACVR2B did not affect LLC tumour growth or tumour-response to DOX (I). sACVR2B had no effect on the DOX concentration in skeletal muscle (II).

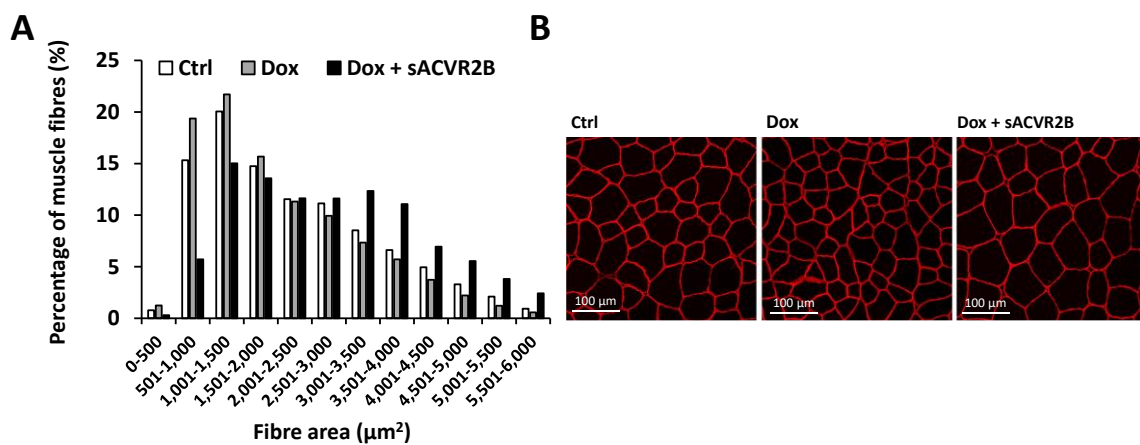


FIGURE 7 Muscle fibre size in doxorubicin-treated mice (I). TA muscle fibre size distribution (A) and a representative immunofluorescence image of dystrophin staining (B) at four weeks. N = 9/group.

When comparing the two different tumour models used in this dissertation, it was found that the injection of C26 cells resulted in a more marked cachexia with smaller tumour burden in comparison to the LLC tumour model (I, III). The C26 tumours had also considerably higher mRNA expression of *Activin A*, *Interleukin-6 (Il-6)* and *Myostatin* (III). These were not downregulated by sACVR2B despite the prevention of cachexia (III).

As in the cachectic conditions, the blocking of myostatin and activins induced marked skeletal muscle hypertrophy also in healthy animals, as shown by a substantial increase in the TA mass with local follistatin (FS288) gene delivery (IV). Different doses tested resulted in different levels of hypertrophy. In 20 days, TA mass increased by  $49.2 \pm 7.8\%$  (mean  $\pm$  SD),  $51.3 \pm 8.9\%$ , and  $72.8 \pm 7.0\%$ , with a dose of  $4 \times 10^9$ ,  $1.6 \times 10^{10}$ , and  $6.4 \times 10^{10}$  vp/leg, respectively, compared with the contralateral muscle injected with the control AAV ( $P < 0.001$ ). A small but significant increase ( $12.3 \pm 6.8\%$ ,  $P < 0.001$ ) in TA mass was noticed already after seven days with the lowest dose ( $4 \times 10^9$  vp/leg), which was selected for the actual experiments (see chapters 5.1.2 and 5.3.1).

### 5.1.2 Physical activity, running performance and food consumption (I, III, IV)

In the cancer experiments, home-cage physical activity was analysed at baseline and 10 days after the cancer cell injection (III). The TB mice were significantly less physically active compared with the healthy counterparts, sACVR2B administration having no effect on activity (Figure 8A). In the chemotherapy experiments, the aerobic running capacity of the mice was assessed in an incremental treadmill-running test (I). Chemotherapy impaired the running performance, and sACVR2B did not have any effect on the running performance of the DOX-treated mice (Figure 8B). Food intake was also decreased by the tumour and chemotherapy (Figure 8C and D). The administration of sACVR2B did not have any significant effect on food consumption in either condition (Figure 8C and D).

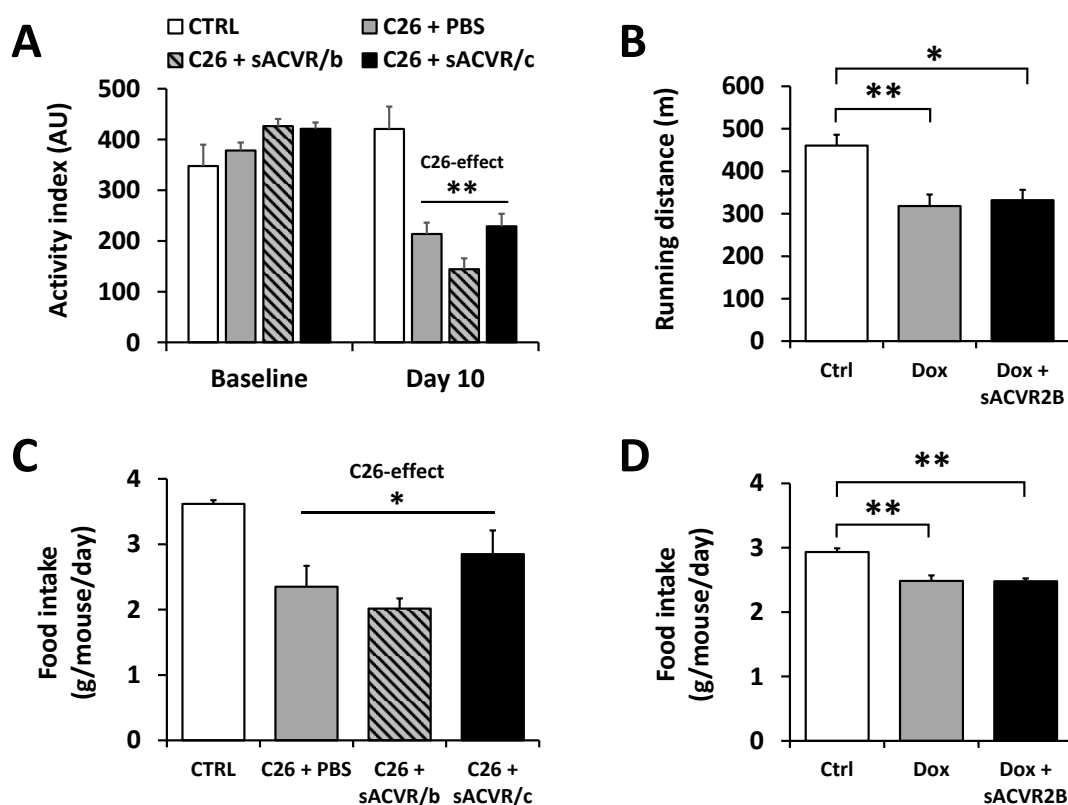


FIGURE 8 Physical activity, running performance and food intake in tumour-bearing (III) and doxorubicin-treated mice (I). (A) Activity index (AU) at baseline and at day 10 after cancer cell inoculation.  $N = 2-3$  cages/group, 2 mice/cage. (B) Distance covered in an incremental treadmill running test until exhaustion in DOX-treated mice in the four-week experiment.  $N = 15, 16,$  and  $17$  in Ctrl, Dox, and Dox + sACVR2B, respectively. Average food intake in tumour-bearing mice on days 8-10 after cancer cell inoculation (C), and DOX-treated mice in the four-week experiment (D).  $N = 3-4$  cages/group, 2-3 mice/cage in parts C and D. C26-effect indicates a significant difference between CTRL and the C26 groups pooled (A, C). \*, \*\* and \*\*\* =  $P < 0.05, 0.01$  and  $0.001$ , respectively [Student's  $t$ -test (A, C), Bonferroni (B, D)].

Due to the above-mentioned effects of cancer and chemotherapy on physical activity and food intake, further experiments targeting different levels of physical activity and food intake were conducted. In the first experiment, the natural fluctuation in physical activity and feeding due to the circadian rhythm was exploited, and mice were monitored and samples were collected either during the day or at night (IV). As hypothesized, the mice were significantly more active and ate more in the night-time and were more passive and ate less in the daytime (Figure 9A and B). The increased physical activity was associated with significantly increased oxygen consumption and energy expenditure in the night-time compared with the daytime (Figure 9C and D).

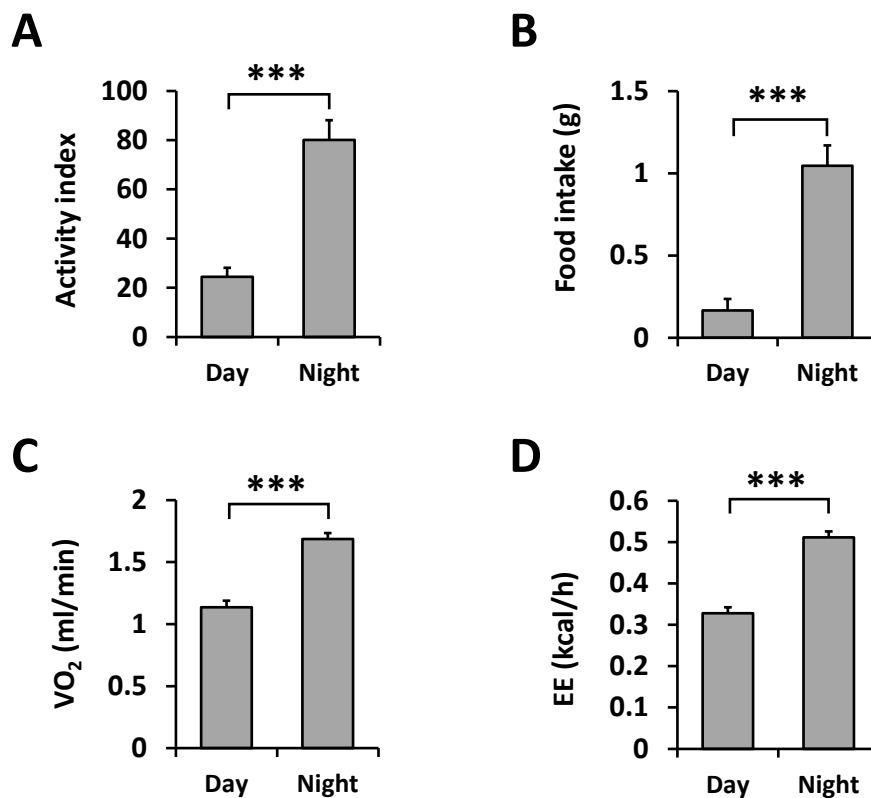


FIGURE 9 Physical activity and food intake at different times of the day (IV). Activity index (A), food intake (B), oxygen consumption (C), and energy expenditure (D) in the daytime and the night-time during a three-hour period before sample collection.  $N = 8/\text{group}$ . \*\*\* =  $P < 0.001$  [Mann-Whitney U test (A, C, D), Student's *t*-test (B)]. VO<sub>2</sub>, oxygen consumption; EE, energy expenditure.

### 5.1.3 Oxidative properties of skeletal muscle (I, III)

As the running capacity was impaired by chemotherapy and the habitual physical activity decreased in experimental cancer, oxidative properties of cardiac and skeletal muscle tissues were analysed. In the TB mice, the citrate synthase activity was slightly decreased in skeletal muscle and the heart and tended to be decreased in the diaphragm compared with the healthy controls (Figure 10A). The total content of mitochondrial respiratory chain subunits (OXPHOS

proteins) was unaltered by cancer and sACVR2B (Figure 10B), with only minor alterations in the individual subunits in skeletal muscle and the heart (III).

Despite the impaired maximal running capacity, DOX chemotherapy did not have any significant effects on mitochondrial respiratory function of the TA muscle analysed at the four-week timepoint, two weeks after the cessation of DOX administration (Figure 10C). Consistent with the mitochondrial respiratory function, chemotherapy had no effect on citrate synthase activity or the levels of OXPHOS proteins (Figure 10D and E). However, sACVR2B administration resulted in a significant increase in muscle citrate synthase activity, while the sum of OXPHOS proteins and mitochondrial respiratory function remained unaltered by sACVR2B (Figure 10C-E). Capillary density and the number of capillaries per muscle fibre were unaltered by chemotherapy and sACVR2B treatment at the four-week time point (Figure 11A-C).

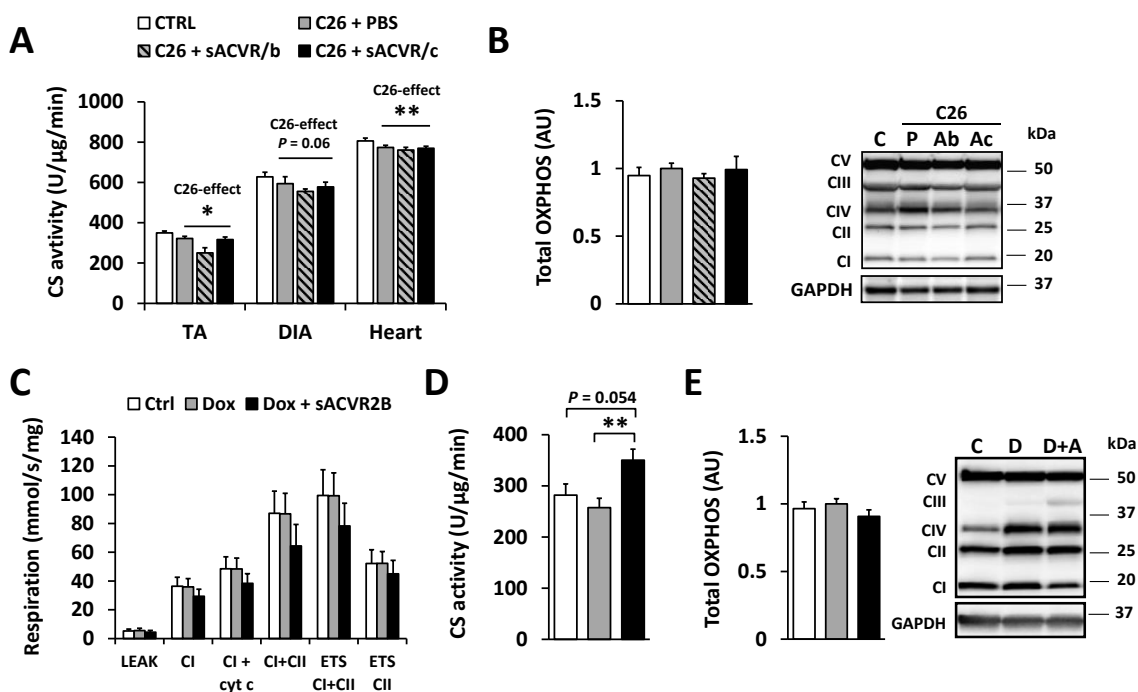


FIGURE 10 Mitochondrial function and markers in tumour-bearing (III) and doxorubicin-treated mice (I). Citrate synthase (CS) activity in tibialis anterior (TA), diaphragm (DIA) and the heart (A), and mitochondrial OXPHOS protein content in TA (B) in TB mice at 11 days after cancer cell inoculation. Mitochondrial respiration in TA muscle with carbohydrate substrates (C), citrate synthase activity (D), and mitochondrial OXPHOS protein content in DOX-treated mice (E) in the four-week experiment. C26-effect indicates a significant difference between CTRL and the C26 groups pooled. \* and \*\* =  $P < 0.05$  and  $0.01$ , respectively [Student's  $t$ -test (A), Bonferroni (D)]. Cyt c, cytochrome c; CI-IV = OXPHOS complex I-IV; ETS, electron transfer system; OXPHOS, oxidative phosphorylation; C, CTRL; P, C26 + PBS; Ab, C26 + sACVR/b; Ac, C26 + sACVR/c; D, Dox; D+A, Dox + sACVR2B.  $N = 7-9$ /group (A, B),  $N = 7-8$ /group (C),  $N = 15-17$ /group (D), and  $N = 8$ /group (E).



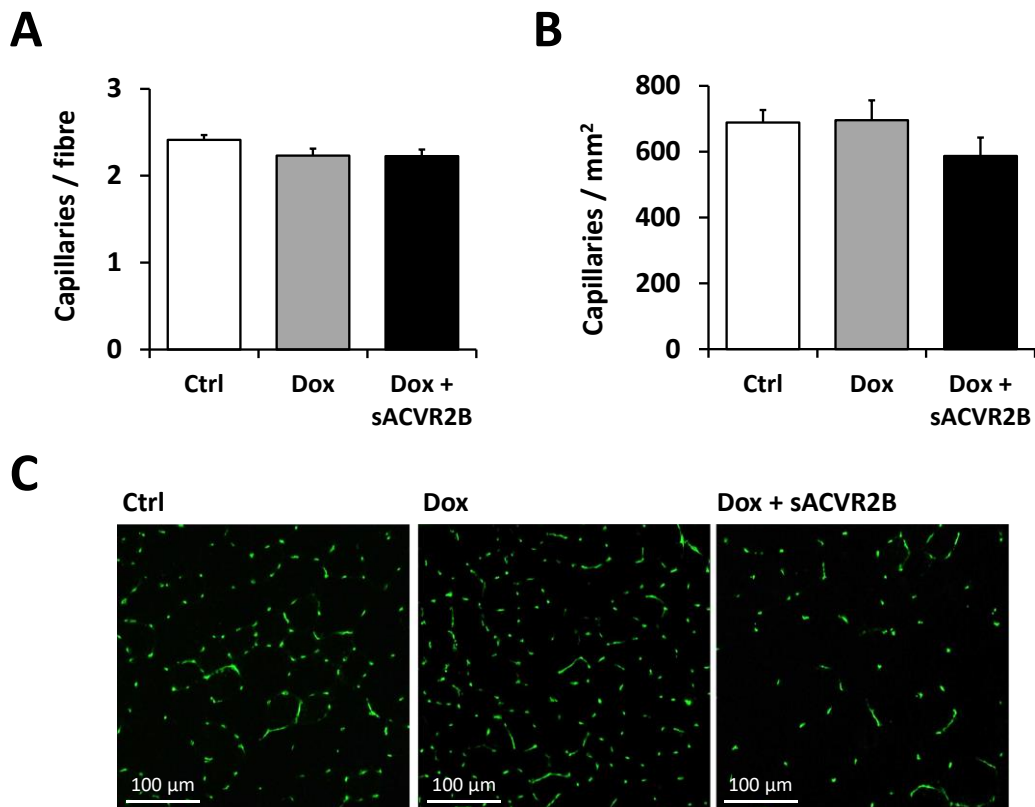


FIGURE 11 Capillary density in doxorubicin-treated mice (I). Quantification of the number of capillaries per muscle fibre (A) and per muscle area (B), and the representative immunofluorescence images of CD31/PECAM-1 staining for capillaries (C) in the four-week experiment. The representative capillary images are from exactly the same location as the dystrophin images in Figure 7B. PECAM-1, platelet endothelial cell adhesion molecule-1. N = 8, 10, and 9 in Ctrl, Dox, and Dox + sACVR2B, respectively.

#### 5.1.4 Comparison of the effects on the heart and skeletal muscle in chemotherapy (II)

Chemotherapy resulted in a similar relative, approximately 10%, decrease in both TA and heart masses (Figure 6D and G). However, only the loss of TA mass was prevented by sACVR2B treatment, while the heart mass was relatively unaffected by sACVR2B (Figure 6D and G). Despite the similar decreases in tissue masses, a single injection of DOX induced more extensive alterations in the skeletal muscle transcriptome compared with those observed in the heart (II). A whole-genome microarray analysis using FDR < 0.05 and fold change  $\geq 1.2$  criteria showed that 485 and 40 annotated transcripts were upregulated, and 473 and 24 were downregulated by DOX in skeletal muscle and the heart, respectively. Only 21 transcripts were commonly upregulated, and six commonly downregulated in skeletal muscle and the heart, showing a notable difference in the responses of these tissues. These results may reflect a larger regeneration potential of the skeletal muscle, as mRNA expression of *Myod1*, an important factor in skeletal muscle regeneration, and MyoD target genes were upregulat-

ed by DOX in skeletal muscle, but not in the heart (Table 4, II). In addition, the pre-treatment with sACVR2B induced more extensive changes in the skeletal muscle transcriptome than it did in the heart, with 118 annotated transcripts upregulated and 82 transcripts downregulated in skeletal muscle, and only one annotated transcript upregulated, and two transcripts downregulated in the heart in DOX+sACVR2B-treated mice compared with DOX alone (II).

The pathway analysis showed that the p53 pathway is upregulated in both skeletal muscle and the heart in response to DOX (Table 4, II). In addition, the transcription factor analysis showed enrichment of genes with p53 targeted motifs in both tissues (II). These genes included a well-known cell-cycle inhibitor *p21/Cdkn1a*, and a DNA-damage response indicator *Redd1/Ddit4* that were highly upregulated by DOX in skeletal muscle and the heart in both microarray and qPCR analyses (Table 4, I and II). These responses were partially blocked by sACVR2B, especially in the skeletal muscle (Table 4, I and II). Furthermore, the p53 protein level was increased by DOX in both tissues, and this increase was prevented by sACVR2B (Table 4, II). These results indicate that p53-p21-REDD1 is the main common pathway activated by DOX in both skeletal muscle and the heart. In addition, the activation of that pathway can be attenuated by the blocking of myostatin and activins, especially in skeletal muscle. The difference in the response to sACVR2B treatment between skeletal muscle and the heart may be explained by the different expression levels of activin receptor type IIB, its ligands, or their responses to DOX. The largest difference between the tissues was observed in myostatin (*Gdf8*) mRNA expression that was approximately 18-fold higher in skeletal muscle than in the heart ( $P < 0.001$ , II).

TABLE 4 Gene sets, pathways and individual genes or proteins involved in muscle atrophy and regeneration in tumour-bearing (III) and doxorubicin-treated mice (I, II), analysed from the short-term cancer experiment and the acute chemotherapy experiment, respectively. Arrows indicate the direction and the magnitude of the effect for the tumour, DOX and sACVR2B. C26 + sACVR2B and DOX + sACVR2B indicate the difference to C26 and DOX, respectively.

Gene set/ pathway	Skeletal muscle		Skeletal muscle		Heart	
	C26	C26 + sACVR2B	DOX	DOX + sACVR2B	DOX	DOX + sACVR2B
p53-REDD1-p21	NA	NA	↑↑	↔	↑↑	↔
Atrogenes	NA	NA	↑	↓	NA	NA
Proteasome	NA	NA	↑	↔	↑ (Räsänen et al. 2016)	NA
Apoptosis	NA	NA	↑	↔	↑ (Räsänen et al. 2016)	NA
Caspase	NA	NA	↑	↔	NA	NA
Autophagy	NA	NA	↔	↔	NA	NA
<b>mRNA/Protein</b>						
<i>Myod1</i>	NA	NA	↑	↔	NA	NA
<i>Redd1/Ddit4</i>	NA	NA	↑↑	↓	↑	↔
<i>p21/Cdkn1a</i>	NA	NA	↑↑	↓	↑↑	↔
p53	NA	NA	↑↑	↓↓	↑↑	↓↓
Ubiquitinated proteins	↑	↔	↔	↔	↔	↔
<i>MuRF1</i>	↑	↔	↔	↓	↓	↔
<i>Atrogin1</i>	↑	↔	↑	↓	↑	↔
FoxO1	NA	NA	↑	↔	NA	NA
LC3-II	↑ (Hentilä et al. 2018)	↔	↔	↔	NA	NA

NA, not analysed; Atrogin1, F-Box Protein 32 (FBXO32)/Muscle Atrophy F-Box Protein (MAFbx); p21/Cdkn1a, Cyclin Dependent Kinase Inhibitor 1A; Ddit4, DNA Damage Inducible Transcript 4; FoxO1, Forkhead box protein O1; LC3-II, lipidated form of Microtubule-associated protein 1A/1B-light chain 3; MuRF1, Muscle RING-finger protein-1; Myod1, Myogenic Differentiation 1/Myoblast Determination Protein 1; p53, Cellular tumor antigen p53; Redd1, Regulated in development and DNA damage responses 1.

## 5.2 Effects of cachexia and its treatment on survival and other tissues in cancer and after chemotherapy (I, III)

### 5.2.1 Survival time (III)

Survival in C26 cancer was investigated during a three-week period after the cancer cell inoculation (III). The survival was significantly improved in the group that was treated with sACVR2B both before and after tumour formation when compared with vehicle-treated TB mice and the TB mice treated with sACVR2B only before the tumour formation (Figure 12). The survival time did not differ significantly between the vehicle-treated TB mice and the TB mice treated with sACVR2B only before the tumour formation (Figure 12). To determine a suitable time point to study the mechanisms of cachexia and the potential factors explaining differences in the survival time, the associations between body mass change and survival time were analysed with Cox regression analysis. It was found that especially the body mass change from Day 10 to Day 11 after the cancer cell inoculation predicted survival ( $B = 1.82$ ,  $P < 0.001$ ). Thus, Day 11 was determined as the endpoint for the second experiment to target the early phase of cachexia.

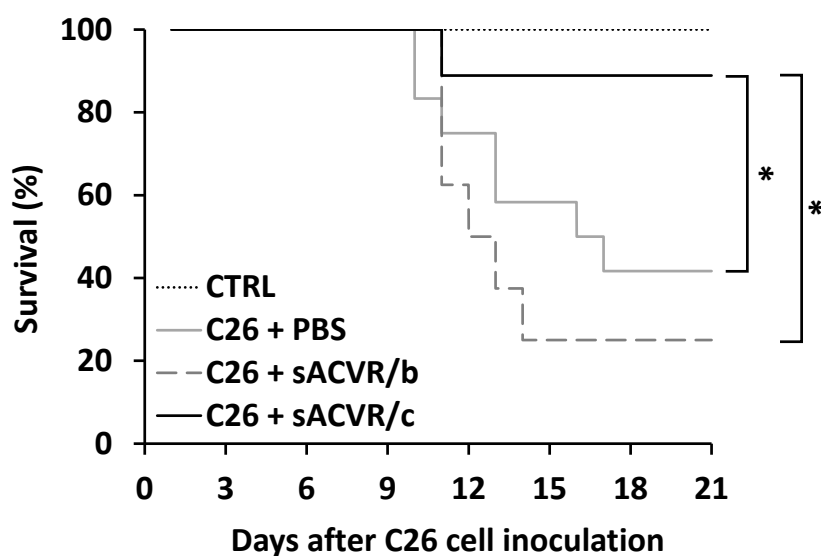


FIGURE 12 Survival in experimental cancer and the effect of myostatin/activin blocking (III). The figure represents a three-week Kaplan-Meier survival curve for CTRL and TB mice. \* =  $P < 0.05$  [log-rank (Mantel-Cox) test]. N = 6, 12, 8, and 9 in CTRL, C26 + PBS, C26 + sACVR/b, and C26 + sACVR/c, respectively.

### 5.2.2 Inflammation (III) and haematological parameters (I, III)

At the 11-day time point after the cancer cell inoculation, the TB mice had significantly elevated serum levels of proinflammatory cytokines IL-6 and MCP-1

(Table 5). Neither sACVR2B treatment protocol was able to attenuate any of the inflammatory cytokines (Table 5). The vehicle-treated TB mice had increased liver protein synthesis accompanied by activation of the acute phase response, indicated by increased Stat3 phosphorylation, and elevated levels of fibrinogen and serpin3N (Figure 13A-C). The increases in liver protein synthesis and phosphorylation of Stat3 were partially prevented by sACVR2B, but no significant effects on fibrinogen and serpin3N were observed (Figure 13A-C). The protein contents of fibrinogen and serpin3N correlated with the body mass loss during the last day in the TB mice ( $r = -0.659$ ,  $P = 0.001$ , and  $r = -0.845$ ,  $P < 0.001$ , respectively). As another marker of inflammation, the vehicle-treated TB mice had an over 2.5-fold increase in spleen mass when compared with the healthy controls (Figure 13D) and this was accompanied by increased abundance of markers of splenic myeloid-derived suppressor cells (MDSCs) in the TB mice (III). This increase in spleen mass, but not that observed in MDSC markers, was significantly attenuated by sACVR2B irrespective of the treatment protocol (Figure 13D, III).

TABLE 5 Serum cytokine levels (pg/ml) in tumour-bearing mice (III). The C26-effect was analysed by pooling all the tumour-bearing groups. The sACVR-effect shows the lowest  $P$ -value for the sACVR2B treated groups in comparison to C26 + PBS. N = 8, 7, 6 and 8 in CTRL, C26 + PBS, C26 + sACVR/b and C26 + sACVR/c groups, respectively.

Cytokine	CTRL	C26 + PBS	C26 + sACVR/b	C26 + sACVR/c	C26-effect	sACVR-effect
IL-6	N/A	2061.7 ± 695.7	2165.2 ± 433.9	1374 ± 524.6	$P < 0.001$	$P = 0.672$
MCP-1	N/A	156.2 ± 21.3	220.5 ± 47.9	622.1 ± 329.4*	$P < 0.001$	$P = 0.042$
RANTES	61.3 ± 2.5	20.7 ± 3.2	17.5 ± 1.8	21.6 ± 3.4	$P < 0.001$	$P = 0.890$
IL-1 $\beta$	N/A	N/A	18.6 ± 9.0	21.7 ± 5.0*	$P = 0.270$	$P = 0.012$
IL-12p70	12.2 ± 0.8	20.9 ± 6.8	25.9 ± 14.5	47.5 ± 10.9	$P = 0.170$	$P = 0.120$
IL-5	12.9 ± 2.9	14.8 ± 4.6	12.5 ± 9.7	23.3 ± 5.2	$P = 0.880$	$P = 0.730$

\* = the value that is significantly different compared with C26 + PBS; N/A, Concentration under detection limit; IL, Interleukin; MCP-1, Monocyte chemoattractant protein-1; RANTES, Regulated upon activation, normal T cell expressed and secreted (also known as CCL5); Values are presented as mean  $\pm$  SEM.

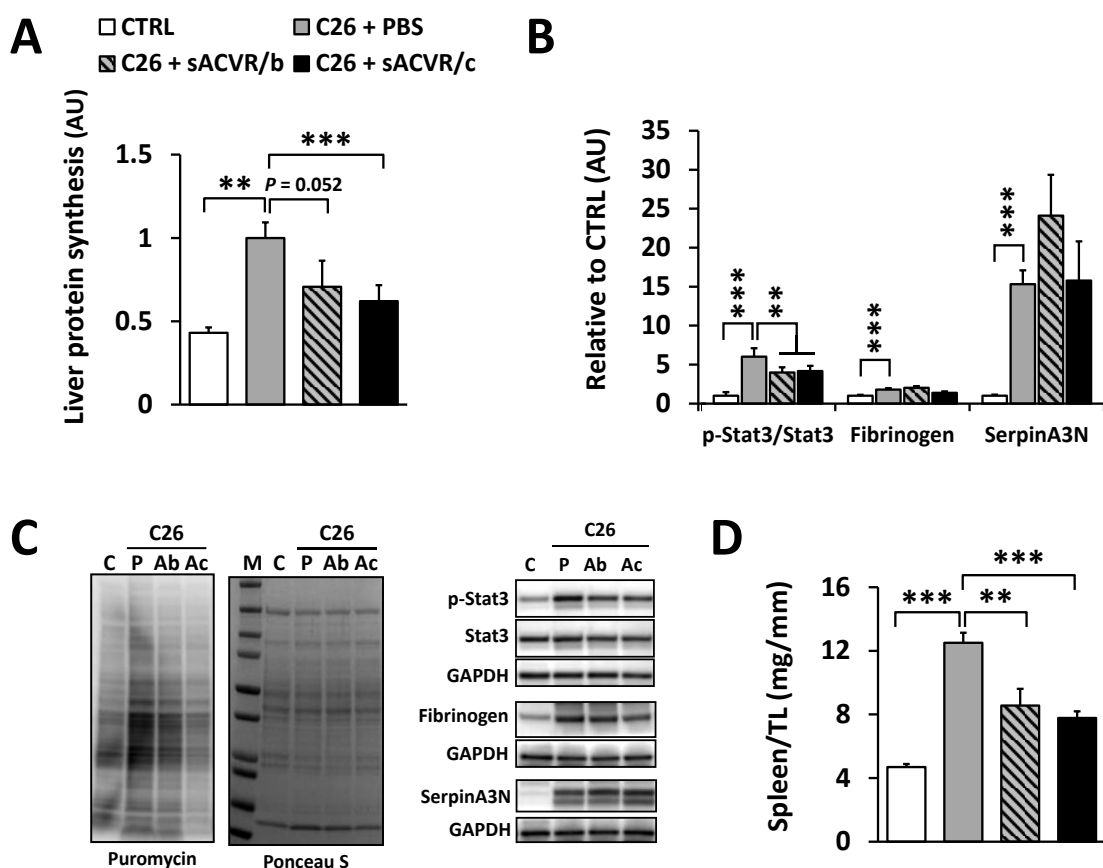


FIGURE 13 Liver protein synthesis, acute phase response markers and spleen mass in tumour-bearing mice (III). Liver protein synthesis relative to C26 + PBS (A), phosphorylation of Stat3 at Tyr705, and protein contents of fibrinogen and serpinA3N in liver (B), representative blots (C), and spleen mass normalized to the length of tibia (D) in TB mice at 11 days after cancer cell inoculation. C, CTRL; P, C26 + PBS; Ab, C26 + sACVR/b; Ac, C26 + sACVR/c; M = molecular weight marker. \*\* and \*\*\* =  $P < 0.01$  and  $0.001$ , respectively [Holm-Bonferroni corrected Mann-Whitney U test (A, B), Student's *t*-test and Holm-Bonferroni corrected LSD (D)].  $N = 6-9$ /group.

The C26 tumour caused mild anaemia, which was shown by small but significant decreases in haemoglobin and haematocrit in the TB mice compared with the healthy controls (Figure 14A and B). Both treatment protocols with sACVR2B at least partially prevented these decreases and thus alleviated the cancer-induced anaemia (Figure 14A and B). Platelet count was robustly increased in the TB mice, and was not altered by the sACVR2B treatment (III). Two weeks of DOX chemotherapy also caused a significant decline in haemoglobin and haematocrit (Figure 14C and D), which was not present anymore at the four-week time point (Figure 14E and F). Unlike in experimental cancer, the anaemia was not influenced by sACVR2B treatment in the DOX-treated mice (Figure 14C and D).

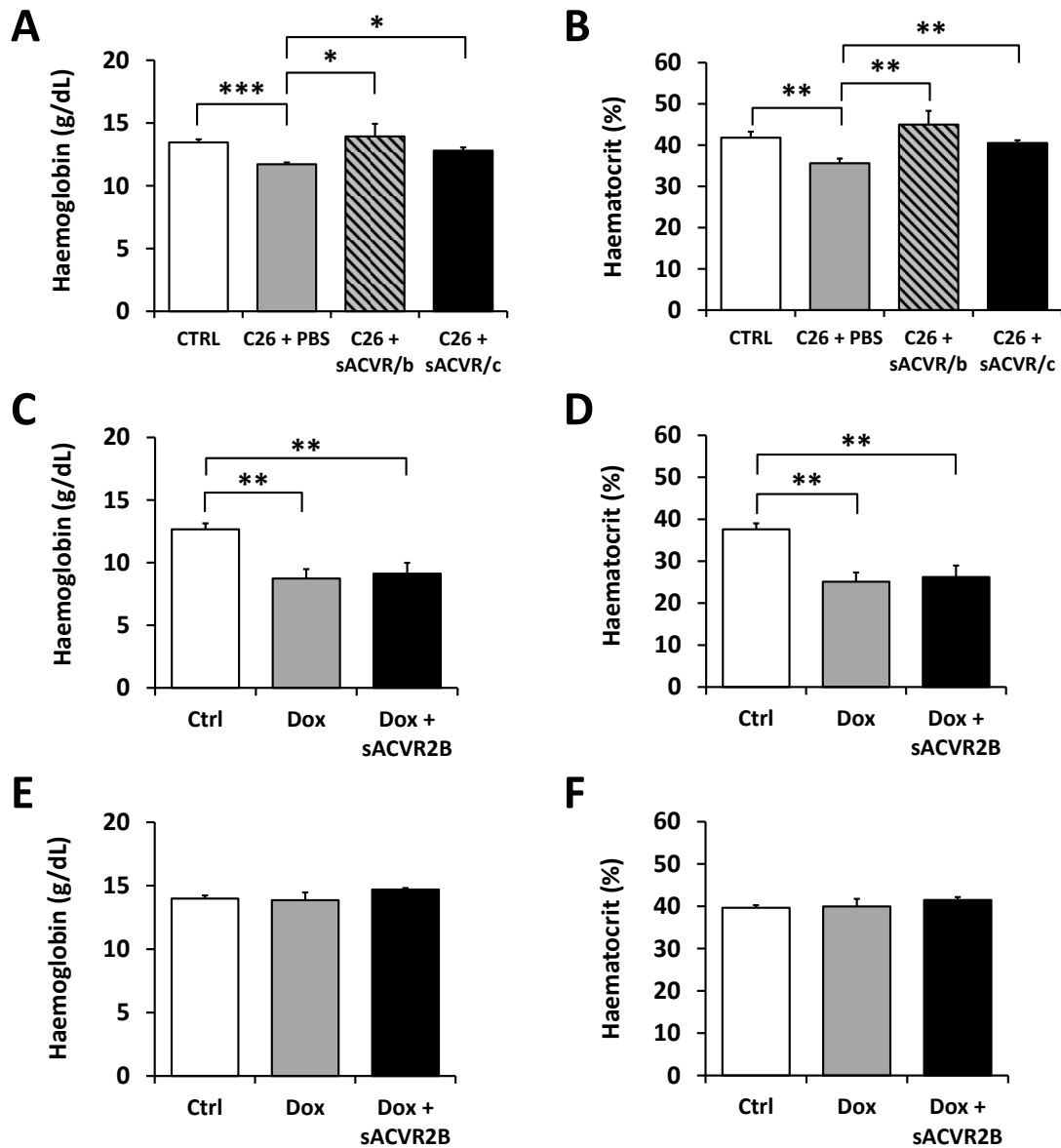


FIGURE 14 Haemoglobin and haematocrit in tumour-bearing (III) and doxorubicin-treated mice (I). Haemoglobin (A) and haematocrit (B) in TB mice at 11 days after cancer cell inoculation. Haemoglobin (C) and haematocrit (D) in DOX-treated mice in the two-week experiment and in the four-week experiment (E, F). \*, \*\* and \*\*\* =  $P < 0.05$ ,  $0.01$  and  $0.001$ , respectively [Holm-Bonferroni corrected Mann-Whitney U (A, B), Bonferroni (C-F)].  $N = 7-9$ /group (A, B),  $N = 6-7$ /group (C, D),  $N = 3-6$  (E, F).

### 5.2.3 Bone parameters (I)

Both bone mineral density (BMD) and bone mineral content (BMC) analysed by DXA were decreased by DOX chemotherapy at the four-week time point indicating chronic impairment in bone quality due to chemotherapy (Figure 15A and B). Both bone parameters were restored by sACVR2B treatment (Figure 15A and B). The changes in BMD ( $r = 0.70$ ;  $P < 0.001$ ) and BMC ( $r = 0.72$ ;  $P < 0.001$ ) correlated positively with the changes in lean mass. In addition, the

endpoint values of and the changes in BMD and BMC were highly associated with the endpoint measures of lean and muscle mass and muscle fibre CSA (I).

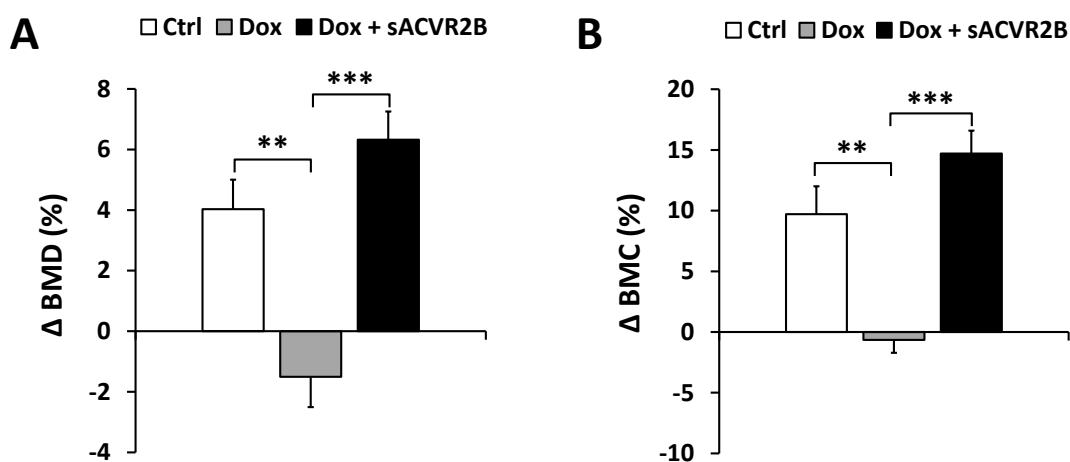


FIGURE 15 Changes in bone mineral density (A) and bone mineral content (B) in doxorubicin-treated mice in the four-week experiment (I). \*\* and \*\*\* =  $P < 0.01$  and  $0.001$ , respectively (Bonferroni). BMD, bone mineral density; BMC, bone mineral content.  $N = 9-10$ /group.

### 5.3 Regulation of muscle size in chemotherapy, cancer and reduced physical activity and fasting – effects of myostatin/activin blocking

#### 5.3.1 Muscle protein synthesis and its regulation (I-IV)

A single dose of DOX chemotherapy resulted in a significant decrease in muscle protein synthesis, as analysed from puromycin incorporation, while protein synthesis remained unaltered in the heart (Figure 16A). sACVR2B restored the muscle protein synthesis in mice treated with DOX without an effect on the heart protein synthesis (Figure 16A). Signalling through the master regulator of protein synthesis, mechanistic target of rapamycin complex 1 (mTORC1), was not affected by chemotherapy, as the levels of phosphorylated rpS6 (at Ser240/244) and p70 S6K (at Thr389) were not altered acutely in the DOX-treated mice (Figure 16B and C). However, sACVR2B acutely increased the phosphorylation of these proteins after a single dose of DOX, indicating increased mTORC1 signalling in response to sACVR2B administration (Figure 16B and C). Unlike mTORC1 signalling, the phosphorylation of ERK1/2 at Thr202/Tyr204 was decreased in the DOX-treated mice and restored by sACVR2B (Figure 16D).



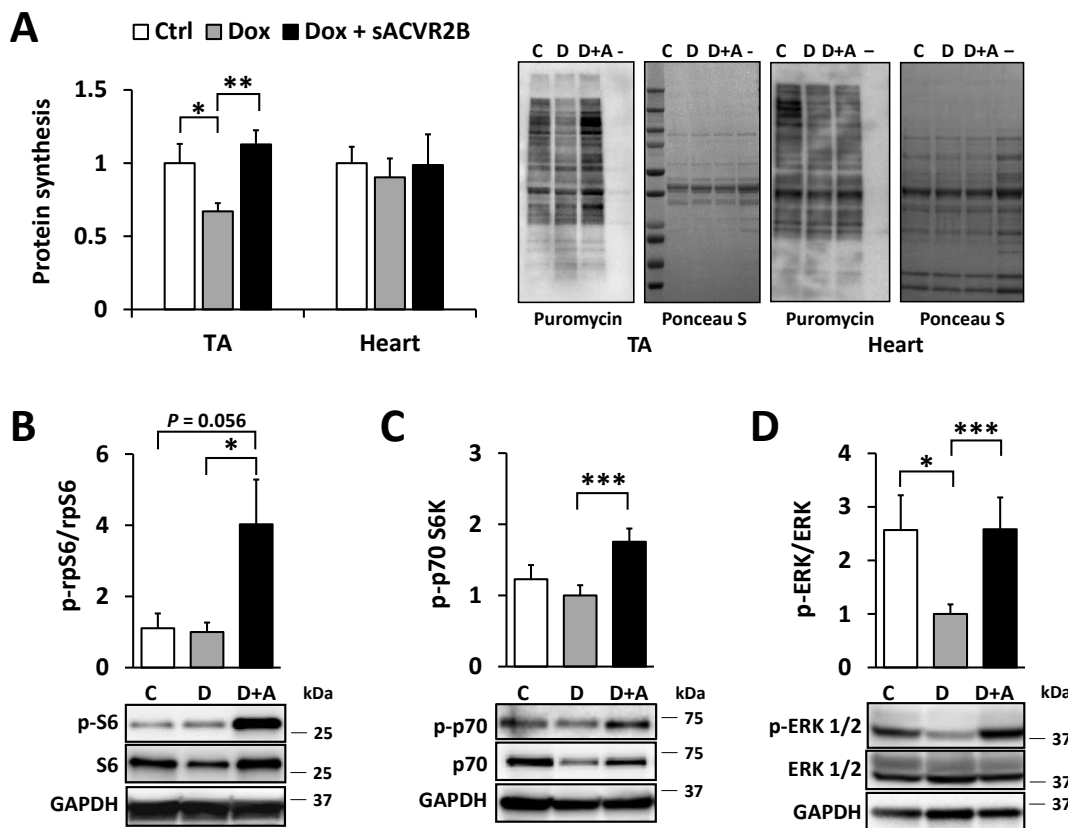


FIGURE 16 Protein synthesis in skeletal muscle and the heart and markers of mTORC1 and ERK1/2 signalling in skeletal muscle in doxorubicin-treated mice (I, II). Protein synthesis analysed with SUnSET and representative blots in TA and the heart (A), and phosphorylation of ribosomal protein (rp) S6 at Ser240/244 (B), p70 S6 kinase at Thr389 (C), and extracellular signal-regulated kinase (ERK) 1/2 at Thr202/Tyr204 (D) and representative blots in TA in the acute chemotherapy experiment. The results are presented as arbitrary units relative to Ctrl (A) or Dox (B-D. D, Dox; D+A, Dox + sACVR2B. \*, \*\* and \*\*\* =  $P < 0.05$ , 0.01 and 0.001, respectively [Bonferroni (A), Holm-Bonferroni corrected Mann-Whitney U test (B-D)]. N = 6-9/group.

Muscle protein synthesis was significantly decreased also by C26 cancer. More specifically, it was decreased in TA muscle and to a lesser extent in the diaphragm and the heart (Figure 17A). The administration of sACVR2B did not restore the decreased muscle protein synthesis at the investigated time point in the TB mice (Figure 17A). In the TB mice, the colocalisation of mTOR with the lysosomal/late endosomal marker LAMP2 was decreased, indicating attenuated mTORC1 activation (Figure 18). Accordingly, mTOR-LAMP2 colocalisation correlated positively with the TA protein synthesis ( $r = 0.751$ ;  $P < 0.01$ ), and also with the body mass change of the last day ( $r = 0.630$ ;  $P < 0.01$ ). In line with the mTOR localization results, the levels of phosphorylated rpS6 and p70 S6K were also markedly decreased in the TB mice compared with the healthy controls (Figure 17B-D). The continued treatment with sACVR2B restored the colocalisation of mTOR with LAMP2 (Figure 18) and the levels of phosphorylated rpS6 (Figure 17B and D).

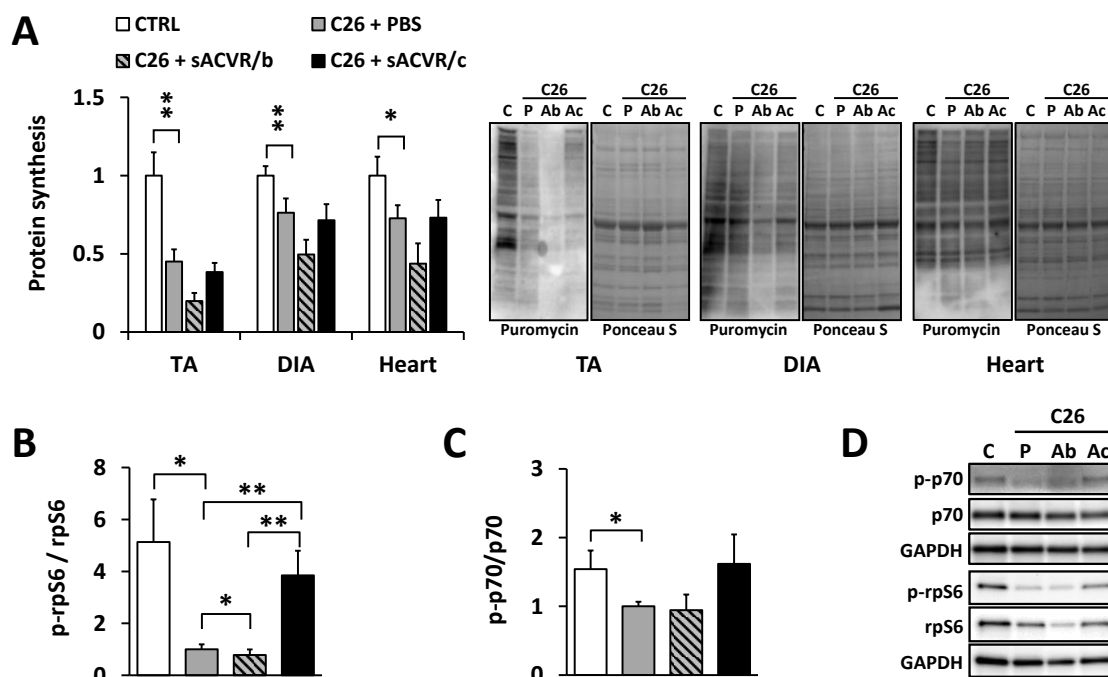


FIGURE 17 Muscle protein synthesis and markers of mTORC1 in tumour-bearing mice (III). Protein synthesis in TA, the diaphragm (DIA) and the heart and representative blots (A), and phosphorylation of ribosomal protein (rp) S6 at Ser240/244 (B) and p70 S6 kinase at Thr389 (C) in TA, and representative blots (D) at 11 days after cancer cell inoculation. The results are presented as arbitrary units relative to CTRL (A) or C26 + PBS (B, C). C, CTRL; P, C26 + PBS; Ab, C26 + sACVR/b; Ac, C26 + sACVR/c. \*, \*\* and \*\*\* =  $P < 0.05$ , 0.01 and 0.001, respectively (Holm-Bonferroni corrected Mann-Whitney U test). N = 6–8/group.

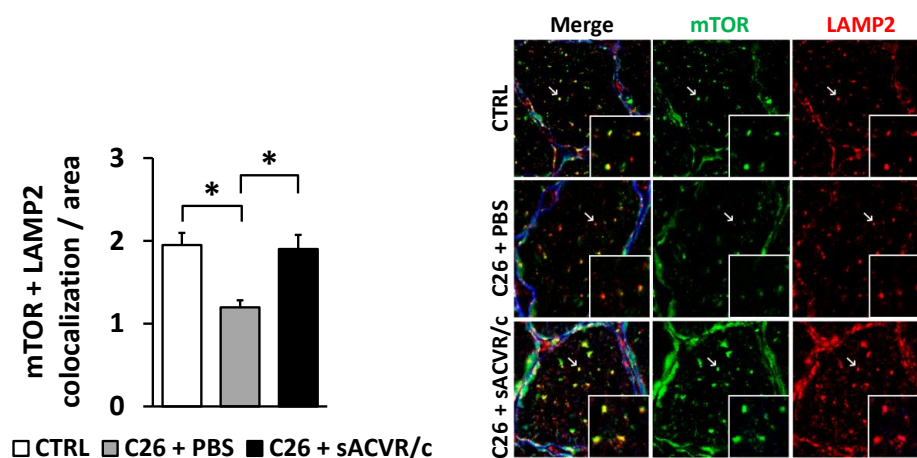


FIGURE 18 Colocalisation of mTOR with lysosomes/late endosomes in tumour-bearing mice (III). Quantification of the colocalisation of mTOR with LAMP2 (left) and a representative immunofluorescence image (right). Scale bar equals 10  $\mu\text{m}$ . \* =  $P < 0.05$  [Student's *t*-test (C26- and sACVR2B-effects)]. N = 7–9/group. LAMP2, Lysosomal Associated Membrane Protein 2; mTOR, mechanistic target of rapamycin.

As cancer and chemotherapy were associated with significantly decreased food intake and physical inactivity or impaired exercise capacity, respectively, muscle protein synthesis and its regulation, and the effects of blocking myostatin and activins were subsequently assessed in healthy mice in settings of altered levels of physical activity and food intake (IV). In healthy mice, time of day did not significantly alter muscle protein synthesis (Figure 19A), even though mice were more active and ate more at night compared with the daytime (Figure 9). The FS288 gene delivery significantly increased muscle protein synthesis irrespective of time of day (Figure 19A). The increased muscle protein synthesis by FS288 was accompanied by increased mTORC1 signalling (Figure 19B-D). However, the levels of phosphorylated rpS6 were significantly lower in the daytime compared with the night-time in both FS288- and control-treated muscles (Figure 19B and D).

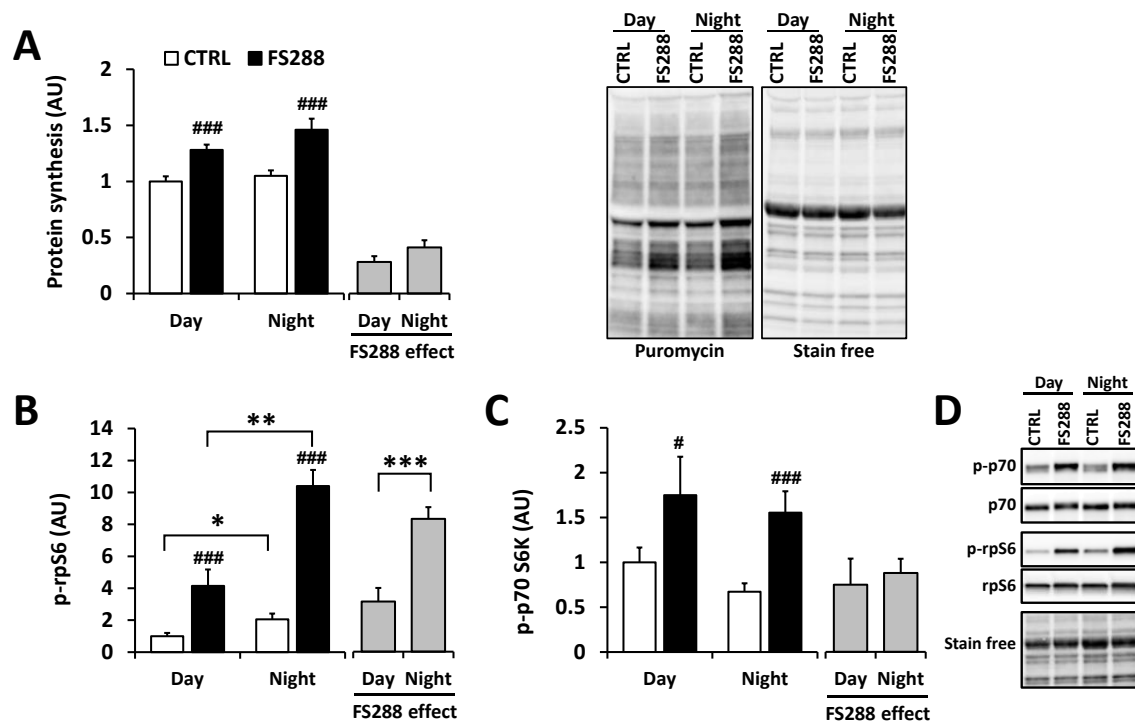


FIGURE 19 Effects of follistatin gene delivery on muscle protein synthesis and mTORC1 signalling at different times of the day (IV). Protein synthesis analysed by SUnSET and representative blots (A), and phosphorylation of rpS6 at Ser240/244 (B) and p70 S6 kinase at Thr389 (C) in TA, and representative blots (D). The results are presented as arbitrary units relative to the “Day CTRL”. Time of day comparisons: \* and \*\* =  $P < 0.05$  and  $0.01$ , respectively (Holm-Bonferroni corrected Student’s t-test). FS288 vs. CTRL comparisons: #, and ### =  $P < 0.05$ , and  $0.001$ , respectively (Mann-Whitney U test).  $N = 8$ /group.

Muscle protein synthesis was slightly blunted in fasted mice (Figure 20A). The FS288 gene delivery significantly increased muscle protein synthesis irrespective of the feeding status, and the increased protein synthesis was accompanied by increased markers of mTORC1 signalling in all feeding conditions (Figure 20A-C). However, despite the negligible effects on muscle protein synthesis, the



phosphorylation of rpS6 and p70 S6K when compared with the fasted group and both the *ad libitum* and the fasted group, respectively (Figure 20B and C).

As with the sACVR2B administration in the TB mice, the FS288 gene delivery resulted in increased amount of mTOR colocalised with the lysosomal marker LAMP2 independent of the feeding status (Figure 21A and C). The FS288 gene delivery did not cause translocation of the colocalised mTOR-LAMP2 towards the sarcolemma (Figure 21B), or their colocalisation with dystrophin (IV).

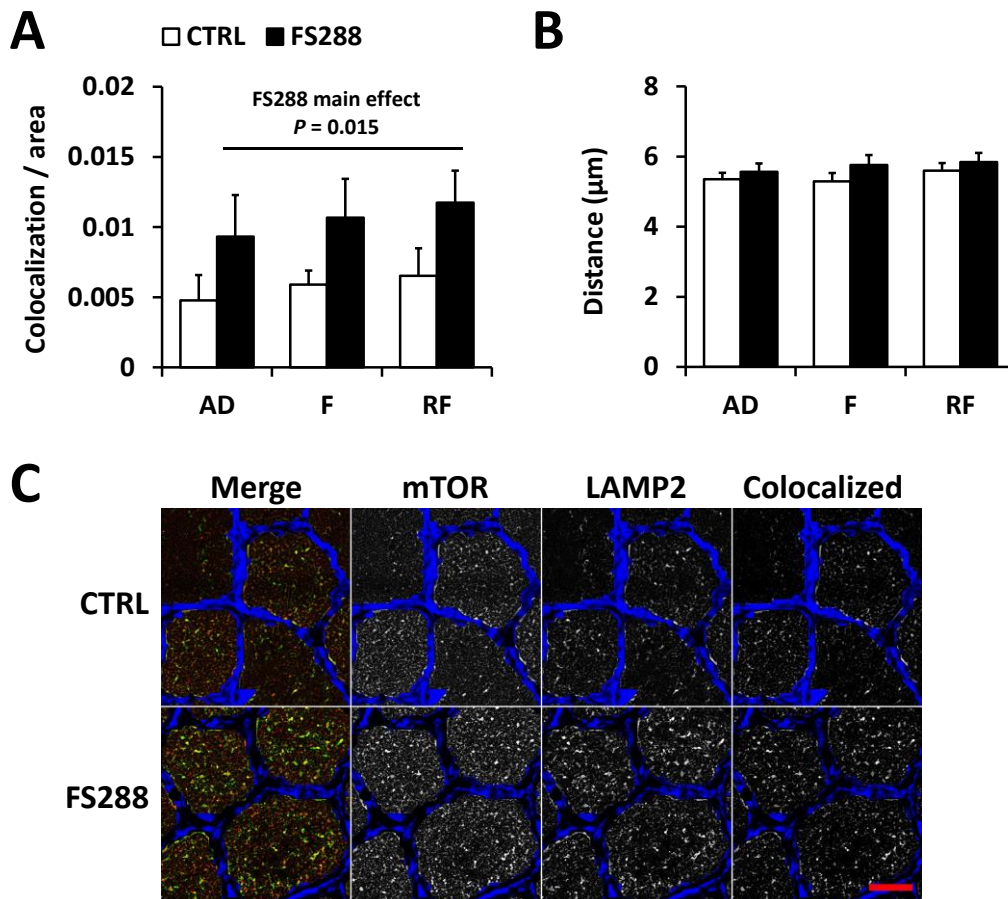


FIGURE 21 The effect of follistatin gene delivery on the colocalisation of mTOR with lysosomes/late endosomes in fasted and fed mice (IV). Quantification of the amount of colocalised mTOR and LAMP2 relative to area (A), and the average distance of the colocalised particles from the sarcolemma (B) in TA muscle. A representative immunofluorescence image of cytosolic mTOR (red), LAMP2 (green) and their colocalisation (yellow in merged image) in the CTRL and FS288 muscles of the AD group (C). Dystrophin represented in blue. Scale bar equals 20 µm. Main effect for FS288 was analysed with Kruskal Wallis test. AD, *ad libitum*; F, fasted; RF, refed. N = 7-8/group.

### 5.3.2 Protein degradation pathways in skeletal muscle (I-III)

As muscle size is regulated by the balance between protein synthesis and degradation, the effects of cancer and chemotherapy on typical markers of protein

degradation pathways were also analysed. A single dose of DOX chemotherapy did not increase the amount of ubiquitinated proteins or the mRNA expression of the muscle-specific E3 ubiquitin ligase MuRF1 in TA muscle at the investigated time point (Table 4, I). The MuRF1 mRNA was decreased by sACVR2B despite the lack of chemotherapy effect (Table 4, I). The mRNA expression of the ubiquitin ligase Atrogin1, contributing via the degradation of proteins related to protein synthesis (Attaix & Baracos 2010), was increased due to chemotherapy and this increase was prevented by sACVR2B (Table 4, II).

Gene set enrichment analysis (GSEA) revealed that chemotherapy resulted in a slight enrichment of the proteasome related genes, on which sACVR2B administration did not have any additional effect (Table 4, I). Based on the GSEA, chemotherapy caused a slight enrichment in the gene set of atrogenes, genes commonly found altered in different muscle atrophy conditions, and this enrichment was prevented by sACVR2B administration (Table 4, I). However, the only individual atroгене increased by chemotherapy was *FOXO1*, and this increase was also verified on the protein level (Table 4, I). Pre-treatment with sACVR2B did not affect the protein level of FoxO1 (Table 4, I). In addition, there was a small enrichment in genes related to apoptosis and caspase pathways by DOX without effects from sACVR2B (Table 4, I). The gene set related to autophagy was not significantly altered by DOX or pre-treatment with sACVR2B, with only minor increases in a couple of genes (Table 4, I).

Experimental cancer resulted in a slightly but significantly increased amount of ubiquitinated proteins in TA muscle and in the diaphragm (Table 4, III). In addition, the mRNA expression of the ubiquitin ligases MuRF1 and Atrogin1 was increased in the gastrocnemius muscles of the TB mice (Table 4, III). Administration of sACVR2B did not have any significant effect on the ubiquitinated proteins or the expression of MuRF1 and Atrogin1 (Table 4, III).

## 6 DISCUSSION

The purpose of this dissertation was to study the effects of different wasting conditions – chemotherapy and cancer cachexia – as well as reduced physical activity and fasting, and the concomitant blocking of myostatin and activins on muscle size and its regulation. In addition, this dissertation aimed to elucidate the importance of maintaining adequate muscle mass in these wasting conditions, and the potential underlying mechanisms. Furthermore, the effects of these wasting conditions on physical activity, exercise capacity and oxidative properties of skeletal muscle were also investigated.

The main findings of this dissertation were that

1. Prevention of muscle wasting via myostatin/activin blocking associates with improved survival in cancer cachexia without effects on tumour mass, but increasing muscle mass via myostatin/activin blocking only before the cachectic stimulus does not provide survival benefit and may result in exacerbated wasting in tumour-bearing mice. (III)
2. Muscle wasting in cancer cachexia is associated with decreased colocalisation of mTOR with lysosomes/late endosomes. On the other hand, myostatin/activin blocking increases the amount of mTOR colocalised with lysosomes/late endosomes in both healthy and cachectic muscles. (III, IV)
3. Doxorubicin chemotherapy associated muscle wasting is due to decreased muscle protein synthesis rather than increased degradation. Myostatin/activin blocking restores size and protein synthesis in skeletal muscle, but not in the heart, in chemotherapy-treated mice without effects on the antitumour action of chemotherapy. Prevention of muscle wasting is associated with restored bone mineral density and content in mice receiving chemotherapy. (I, II)
4. Physical activity and running capacity are impaired in cancer cachexia and after chemotherapy, respectively, with negligible effects on skeletal

muscle oxidative properties, and these effects are not alleviated by blocking myostatin and activins. (III)

5. Myostatin/activin blocking increases muscle protein synthesis and the amount of mTOR colocalised with lysosomes/late endosomes independent of alterations in physical activity and food intake. However, the mTORC1 signalling response to myostatin/activin blocking is attenuated by fasting and diurnal decreases in food intake and physical activity. (IV)

To the best of my knowledge, this is the first study showing (1) the effect of cancer cachexia and myostatin/activin blocking on mTOR localization, (2) the effect of increasing muscle mass via myostatin/activin blocking only before the cachectic stimulus on survival in experimental cancer cachexia, and (3) the effect of doxorubicin chemotherapy on maximal running capacity and capillary density. Moreover, this was the first study to investigate the transcriptomic changes in skeletal muscle after doxorubicin chemotherapy alone or combined with myostatin/activin blocking, and to compare these changes between skeletal muscle and the heart.

## **6.1 Muscle size and its regulation in different wasting conditions with myostatin/activin blocking**

The results of this dissertation show that doxorubicin chemotherapy and experimental cancer cause loss of body mass, which is comprised of muscle and adipose tissue wasting. This is in line with previous findings in tumour-bearing mice (Aulino et al. 2010; Benny Klimek et al. 2010; Bonetto et al. 2016; Murphy et al. 2012; Toledo et al. 2014; Zhou et al. 2010) and doxorubicin-treated mice (Gilliam et al. 2016; Hiensch et al. 2019). In chemotherapy, muscle wasting was associated with a decrease in lean mass, and muscle fibre size tended to be reduced. Decreased muscle mass and muscle fibre size after treatment with doxorubicin is in line with previous studies (de Lima Junior et al. 2016; Gouspillou et al. 2015; Hiensch et al. 2019; Min et al. 2015). A significantly decreased muscle fibre cross-sectional area has not been observed in all studies after doxorubicin administration, but those studies have been acute in nature, and samples have been collected three to four days after doxorubicin administration (Gilliam et al. 2009; Yu et al. 2014). Interestingly, these effects were observed two weeks after the last dose of chemotherapy, meaning that decreased body, lean and fat mass, and muscle atrophy persist despite cessation of chemotherapy administration. Previously, repeated cycles of doxorubicin and dexamethasone treatment have resulted in impairment in growth and in decreased muscle mass and fibre size that were sustained at least until three months after the last treatment cycle (Gouspillou et al. 2015). Even though the treatment protocol was different than in the present study, this indicates that doxorubicin chemotherapy may have irreversible, or at least very long-term, effects on growth and muscle tissue.



In the present study, the blocking of myostatin and activins fully prevented the decrease in body and muscle mass due to doxorubicin chemotherapy and was even able to cause muscle hypertrophy compared with healthy control mice. In addition, the blocking of myostatin and activins significantly increased muscle fibre size, thus counteracting doxorubicin-induced muscle atrophy. A recent study reported decreased body, lean and fat masses, as well as lower skeletal muscle masses and muscle fibre atrophy after five-week administration of Folfiri chemotherapy (Barreto et al. 2017). As in the present study, the decreases in body, lean and muscle masses, as well as muscle fibre cross-sectional area were completely prevented by the blocking of myostatin and activins (Barreto et al. 2017).

In the experimental cancer induced by C26 cancer cell inoculation, wasting was observed in locomotor muscles, such as the tibialis anterior (TA), but also in the major respiratory muscle, the diaphragm. This indicates that the whole-body skeletal muscle tissue is prone to wasting in cachexia. Thus, cachexia may result not only in decline in physical function but also in alterations in whole body metabolism and in impairment of vital functions, such as respiration (Murphy et al. 2012; Roberts et al. 2013). Indeed, diaphragm atrophy, weakness, and fatigability (Murphy et al. 2012; Roberts et al. 2013), as well as ventilatory dysfunction (Roberts et al. 2013) have been observed in previous studies in the C26 model of cancer cachexia. Moreover, weakness (Gilliam et al. 2011a) and severe damage of the diaphragm (Doroshov, Tallent & Schechter 1985; Gilliam et al. 2011a) have also been associated with doxorubicin chemotherapy in healthy animals. Thus, diaphragm wasting and potentially resulting respiratory dysfunction may play a role in the poor prognosis associated with cachexia and in treatment toxicity (Fearon, Arends & Baracos 2013). Importantly, the blocking of myostatin and activins was able to prevent muscle wasting, also that of the diaphragm, in experimental cancer. This happened independent of whether the treatment was continued or discontinued after tumour formation. The positive effects of myostatin/activin blocking on muscle wasting in cancer cachexia are in line with previous studies in different murine models of cancer cachexia (Benny Klimek et al. 2010; Busquets et al. 2012; Hatakeyama et al. 2016; Toledo et al. 2016b; Zhong et al. 2019; Zhou et al. 2010). In a hallmark study by Zhou et al. (2010), treatment with soluble ACVR2B (sACVR2B) ligand trap was able to increase and maintain body mass in C26 tumour-bearing mice, when treatment was initiated at the onset of cachexia. Moreover, sACVR2B treatment initiated at advanced cachexia was able to fully restore the body mass. These effects were accompanied by reversal of decreased lean and muscle mass (Zhou et al. 2010). The present study adds to the previous study by Zhou et al. (2010), by providing evidence on whether the blocking of myostatin and activins before the onset of cachexia has protective effects on muscle tissue during cachexia or whether continued treatment is required to maintain muscle size. As mentioned, at the time point after cancer cell inoculation, when change in body mass predicted survival, muscle masses were similar between the two treatment protocols, both having significantly higher TA and diaphragm masses compared with vehicle-

treated tumour-bearing mice. However, the body mass curve shows a dramatic decline in the group in which the sACVR2B treatment was discontinued, and combined with the non-significantly lower muscle and fat masses in that group this suggests that having larger muscle mass to begin with did not protect from muscle wasting as opposed to when the muscle mass was maintained by continued treatment. This assumption is supported by a previous study showing that myostatin deficient mice having larger muscle mass are more prone to experimental cancer-induced muscle wasting (Benny Klimek et al. 2010).

In addition to skeletal muscle wasting, chemotherapy resulted in atrophy of the heart, the level of which was comparable to that of the tibialis anterior muscle. Doxorubicin-induced cardiotoxicity has been widely reported previously (Doroshov, Tallent & Schechter 1985; Nitiss & Nitiss 2014; Ichikawa et al. 2014; Räsänen et al. 2016; Zhang et al. 2012). However, even though myostatin/activin blocking was able to prevent skeletal muscle wasting, it had no effect on heart mass. Similar results were obtained in a previous study, in which Folfiri chemotherapy resulted in decreased heart mass that was not restored by sACVR2B treatment (Barreto et al. 2017). This is also consistent with previous findings in healthy mice treated with sACVR2B (Hulmi et al. 2013a).

Interestingly, C26 cancer did not seem to cause cardiac atrophy in our hands at the 11-day time point, when the cachexia was not yet very severe in all animals. This is contrary to a previous study by Zhou et al. (2010), who reported a 20% decrease in heart mass at the later time point than in the present study, that is, two weeks after C26 cancer cell injection (Zhou et al. 2010). In addition, they found that weekly administration of soluble ACVR2B at a dose of 10 mg/kg was able to prevent cancer-induced cardiac wasting determined after two weeks of treatment (Zhou et al. 2010), whereas treatment with sACVR2B had no effect on heart mass in any of the conditions studied in this dissertation. Potential differences in the study setups may contribute to these different results. For example, the cachexia may have been more advanced in the study by Zhou et al. compared with our study, which might explain why we did not observe marked cachexia in the heart, as it has been demonstrated that the severity of cachexia has impact on the cardiac wasting (Murphy et al. 2012). A mild but significant approximately 10% decrease in heart mass was observed in our pilot study at two weeks after cancer cell inoculation, which supports the hypothesis that severe heart wasting does not occur until an advanced level of cachexia has been reached. In addition, a slightly different mouse strain (CD2F1) and potentially a slightly different tumour location were used in the study by Zhou et al. (2010), both of which might have affected the results (Matsumoto et al. 1999). The reason behind the differences in the effect of blocking myostatin and activins on heart mass is unknown, but it might be due to different treatment protocol, dose, or injection site used. However, even though a larger dose per injection was administered in the study by Zhou et al. (2010), the weekly dose was similar to the present study. The results of the present study are supported by a previous study, in which heart mass was unaffected by the tumour or myostatin/activin blocking in LLC tumour-bearing mice at 14 days after can-

cer cell inoculation (Toledo et al. 2016b). In the chemotherapy experiment, the blocking of myostatin and activins had a much more pronounced effect on the skeletal muscle than on the heart also at the transcriptomic level, suggesting that systemic myostatin/activin blocking usually has a smaller effect on the heart than it does on skeletal muscle. This finding is also supported by a recent study by Szabó et al. (Szabo et al. 2020), and it potentially explains why no effects were seen on heart mass either. This lack of an effect may in part be due to much lower myostatin expression in the heart that was observed in healthy mice. However, in some situations sACVR2B has been shown to have beneficial effects also on the heart (Magga et al. 2019), suggesting that more research is needed on this area.

Muscle mass is in general regulated by the balance between protein synthesis and degradation. Negative net protein balance resulting in muscle atrophy can thus result from either decreased protein synthesis, increased protein degradation, or the combination of both (Gordon, Kelleher & Kimball 2013). According to previous studies, muscle wasting in cancer cachexia can be attributed to decreased protein synthesis (Horstman et al. 2016; Penna et al. 2019; Samuels et al. 2001; Smith & Tisdale 1993; Toledo et al. 2016b; White et al. 2011), increased protein degradation (Penna et al. 2019; Samuels et al. 2001; Smith & Tisdale 1993; Toledo et al. 2016b; White et al. 2011), and/or impaired regeneration (Talbert & Guttridge 2016). Protein synthesis was significantly decreased in TA muscle in experimental cancer and acutely after a single dose of doxorubicin chemotherapy. The present study showed decreased muscle protein synthesis after doxorubicin administration. A recent study showed increased (free) amino acid concentrations in skeletal muscle and in circulation acutely (24–192 hours) after doxorubicin administration, which suggests that doxorubicin administration results in a net protein breakdown that probably results from a combination of repressed protein synthesis and increased protein degradation in skeletal muscle (Fabris & MacLean 2018). Doxorubicin has inhibited protein synthesis previously in cell free systems (Momparler et al. 1976), in cells (Sauter et al. 2011) and in the heart (Zahringer 1981), but the results are not consistent (Momparler et al. 1976; Zima et al. 2001). However, the effects of doxorubicin administration on skeletal muscle protein synthesis have not been directly studied previously. In the present study, it was found that the blocking of myostatin and activins was able to fully restore muscle protein synthesis in doxorubicin-treated mice. This is consistent with previous results from our laboratory showing increased muscle protein synthesis acutely after administration of sACVR2B in healthy wild-type mice (Hulmi et al. 2013a).

The present study showed that muscle protein synthesis was significantly decreased in TA muscle and the diaphragm in tumour-bearing mice compared with healthy control mice. The decrease in muscle protein synthesis in tumour-bearing mice is in accordance with a number of previous studies (Emery, Lovell & Rennie 1984; Lopes et al. 1989; Pain & Garlick 1980; Samuels et al. 2001; Smith & Tisdale 1993; Toledo et al. 2016b; White et al. 2011). The decrease in protein synthesis was more dramatic in the TA muscle compared with the diaphragm,

which might indicate either different effects or mechanisms of cachexia in different types of muscle, or difference between constantly active muscles (the diaphragm) and locomotor muscles that are less active during cachexia due to the decreased physical activity in cancer (discussed in more detail in the next section). Unlike in healthy (Hulmi et al. 2013a) and doxorubicin-treated mice, the blocking of myostatin and activins was unable to restore the decreased muscle protein synthesis in tumour-bearing mice with this administration protocol and at the time point investigated. This finding is in line with a previous study utilizing the LLC model in which tumour-bearing mice had significantly blunted protein synthesis in all skeletal muscles investigated at 14 days after cancer cell inoculation and the decreased protein synthesis was not restored by treatment with sACVR2B (Toledo et al. 2016b). In contrast to these results, in a subsequent study, the blocking of myostatin and activins increased protein synthesis in C26 tumour-bearing mice when sACVR2B administration was started after cancer cell inoculation (Hulmi et al. 2020). The lack of an increase in muscle protein synthesis in tumour-bearing mice in the present study may be due to the fact that the strongest effects of sACVR2B are plateaued within 1 to 2 weeks of administration (Hulmi et al. 2013a). It is thus probable that muscle protein synthesis had been increased by myostatin/activin blocking at an earlier time point, based on the larger muscle masses and combined with evidence that the blocking of myostatin and activins usually has only minor effects on protein degradation based on a previous study (Sepulveda et al. 2015) and the transcriptomic analysis of the chemotherapy experiment. The reason for the lack of a protein synthesis effect may also be due to the refractory nature of cachexia at this time point when wasting had started to accelerate, or other factors, such as decreased food intake. Muscle protein synthesis levels were non-significantly the lowest in the group in which sACVR2B administration was discontinued before the onset of cachexia, further supporting accelerated wasting in that group.

Although the experiments conducted do not allow the definite molecular mechanisms underlying the observed decrease in muscle mass and protein synthesis to be determined, the protein and mRNA level findings provide a basis for further speculation. In cancer, at least at the investigated time point, protein synthesis seems to be associated with a robust downregulation of mTORC1 signalling, as shown by markedly decreased phosphorylation of mTORC1 downstream target proteins. Moreover, as a novel finding, the colocalisation of mTOR with lysosomes/late endosomes was decreased in tumour-bearing mice. This may at least in part explain the cachexia and the decreased muscle protein synthesis in tumour-bearing mice, as mTOR-LAMP2 colocalisation correlated with muscle protein synthesis and the body mass change in the vehicle-treated tumour-bearing mice. Decreased colocalisation of mTOR with lysosomes/late endosomes may also be at least one of the mechanisms underlying decreased mTORC1 signalling, as previously the activity of mTORC1 has been shown to be regulated at least in part via its localization (Jacobs, Goodman & Hornberger 2014; Sancak et al. 2010). Interestingly, the continued blocking of myostatin and activins restored the markers of mTORC1 activation and the colocalisation of

mTOR with lysosomes/late endosomes. In addition to the attenuated mTORC1 signalling, the increase in atrogin1 mRNA expression in tumour-bearing mice may contribute to the blunted protein synthesis in cancer cachexia via degradation of proteins involved in translation (Attaix & Baracos 2010). Increased atrogin1 expression was not attenuated by the blocking of myostatin and activins, and thus it may in part contribute to the lack of protein synthesis response in mice treated with sACVR2B despite partial restoration of mTORC1 signalling.

Contrary to with experimental cancer, the chemotherapy-induced decrease in muscle protein synthesis was not associated with decreased markers of mTORC1 signalling. The potential mechanisms of decreased protein synthesis in chemotherapy may include increased REDD1 expression (Gordon, Kelleher & Kimball 2013; Gordon et al. 2015; Hulmi et al. 2012; Kelleher et al. 2013), which correlated with muscle protein synthesis when control and doxorubicin only administered mice were included, and increased atrogin1 expression, as in tumour-bearing mice. Both of these effects were attenuated by sACVR2B administration along with restored muscle protein synthesis, supporting their role in the regulation of muscle protein synthesis and/or muscle size. However, as REDD1 acts at least in part via inhibition of mTORC1 (Gordon et al. 2015; Sofer et al. 2005), it would have been expected that its increased expression would have been associated with downregulation of mTORC1 signalling, but this was not observed at least at the investigated time point. The reason for the discrepancy between REDD1 expression and mTORC1 signalling responses is unknown, and would require further and more mechanistic experimentation to be resolved. Finally, the level of phosphorylated ERK1/2 was decreased by chemotherapy and restored by sACVR2B treatment, and may thus contribute to regulation of muscle size and protein synthesis in mice receiving chemotherapy (Salto et al. 2014). However, as the physiological importance of ERK1/2 signalling seems to be dependent on time point and context (Hulmi et al. 2013a; Lou, Danelisen & Singal 2005; Penna et al. 2010; Salto et al. 2014), the relevance of this finding and its potential role in the regulation of muscle size and protein synthesis in mice receiving chemotherapy requires further investigation.

Based on the findings of this dissertation, it seems that, unlike in many other muscle wasting conditions, the protein degradation pathways are not robustly activated acutely after a single dose of chemotherapy, despite slight enrichment in the gene sets of the proteasome system, apoptosis, and atrogenes, and increased atrogin1 and FoxO1 expression. This potential small increase in protein degradation and apoptosis is modest compared with what is typically observed in different wasting conditions (Lecker et al. 2004; Satchek et al. 2007), or with the results from previous studies with doxorubicin chemotherapy (Gilliam et al. 2012; Min et al. 2015; Smuder et al. 2011a; Smuder et al. 2011b). There can be many reasons for why we did not observe a “typical” response in the atroгене signature or the activation of the proteolytic pathways. Firstly, when compared with most of the doxorubicin studies reporting activation of proteolytic pathways, the dosage used in our studies was lower. The dose that was used (15–24 mg/kg) is equivalent to approximately 45–72 mg/m<sup>2</sup> in hu-

mans, and was determined to mimic clinical doses used in humans to treat cancer (30–90 mg/m<sup>2</sup>) (Vejpongsa & Yeh 2014). However, a dose of 20 mg/kg has been used in many of the rat studies (Gilliam et al. 2013; Min et al. 2015; Smuder et al. 2011a; Smuder et al. 2011b), and that can be considered equivalent to approximately 40 mg/kg in mice and 120 mg/m<sup>2</sup> in humans (Freireich et al. 1966), thus exceeding the dose typically used in the clinic. Consequently, the inconsistent results may be due to different dosages used, and it is possible that a higher dose is required to induce marked activation of the proteolytic pathways. Secondly, the effects may be dependent on timing and duration of the treatment. Although the induction of proteolytic pathways has been observed acutely (24–48 h) after a single injection of doxorubicin with higher dosage (Min et al. 2015; Smuder et al. 2011a; Smuder et al. 2011b), it is possible that with lower dosage, the proteolytic pathways might be activated during the course of a more prolonged treatment protocol. It has been found that the contribution of different mechanisms to the regulation of muscle size and protein turnover might change during the progression of cancer cachexia (White et al. 2011) and cytotoxic chemotherapy (Samuels et al. 2001). However, in the present study, there were no significant alterations in the amount of ubiquitinated proteins or lipidated LC3 acutely, or at two or four weeks, indicating that neither the ubiquitin-proteasome system nor autophagy were markedly activated at the later time points either.

Blocking of myostatin and activins prevented the slight increase in the atrogene gene set, but had no effect on gene sets of the proteasome system, caspase cascade, apoptosis, or autophagy in the acute experiment. However, myostatin/activin blocking attenuated the increase in the expression of atrogin1 and decreased the expression of MuRF1, potentially contributing to the non-significant decline in the levels of ubiquitinated proteins that was observed in the acute experiment. Moreover, mice treated with sACVR2B had lower levels of lipidated LC3, a marker of autophagosome content, after two weeks of doxorubicin chemotherapy supporting the evidence from healthy mice (Hulmi et al. 2013b) and from mice with heart failure (Szabo et al. 2020). These findings suggest that the blocking of myostatin and activins may have some minor effects on ubiquitin proteasome system or autophagy, but these effects may be time point specific and their physiological importance in the chemotherapy setting is not known.

In cancer, the level of ubiquitinated proteins and the expression of ubiquitin ligases, as well as the markers of autophagy (Hentila et al. 2019) were more consistently elevated, suggesting increased muscle protein degradation in tumour-bearing mice. These findings are consistent with previous studies in tumour-bearing animals (Aulino et al. 2010; Busquets et al. 2012; Johnston et al. 2015; Llovera et al. 1998; Penna et al. 2013a; Toledo et al. 2016b; Tseng et al. 2015; White et al. 2011; Zhou et al. 2010). The blocking of myostatin and activins did not have any marked effect on the markers on the protein degradation pathways, and discontinuation of the sACVR2B treatment may have even exacerbated the tumour-induced activation of the protein degradation pathways. This

finding is consistent with a previous study by Toledo et al. (2016), which also showed increased markers of protein degradation via the ubiquitin-proteasome system in tumour-bearing mice which were not rescued by the blocking of ACVR2B ligands (Toledo et al. 2016b). In contrast, Zhou et al. (2010) demonstrated that the tumour-induced increase in markers of the ubiquitin-proteasome system was prevented by sACVR2B treatment. The reason for these contradictory findings is unknown, but may be due to differences in the treatment protocol, time point investigated or the levels of cachexia.

All in all, the findings of this dissertation indicate that both chemotherapy and cancer result in muscle wasting, which in chemotherapy is at least acutely mainly due to a decrease in muscle protein synthesis, whereas the combination of decreased protein synthesis and increased degradation probably contribute to the wasting in cancer. In addition, it seems that in both conditions, the blocking of myostatin and activins increases muscle mass and/or prevents muscle wasting at least in part through increased mTORC1 signalling resulting in promotion of protein synthesis, even though the protein synthesis effect was not observed in tumour-bearing mice at the investigated time point. Moreover, in chemotherapy, it seems that doxorubicin and myostatin/activin blocking alter protein synthesis via partially different mechanisms, suggesting that the increased muscle mass by myostatin/activin blocking arises at least in part from increased *de novo* protein synthesis rather than mere counteraction of the effects of chemotherapy. However, direct comparison between the findings from the short-term chemotherapy and cancer experiments is difficult, as the nature of the cachectic stimuli and the time points investigated were different.

Decreased protein synthesis seems to play a role in both cancer- and chemotherapy-induced muscle wasting. What is then the upstream signal for decreased protein synthesis in these conditions? It is probable that multiple factors play a role, including tumour- and host-derived circulating factors, such as inflammatory cytokines, activins, myostatin, and GDF11, for instance (Fearon, Glass & Guttridge 2012). In addition, even though cachexia cannot by definition be fully reversed by nutritional support (Fearon et al. 2011), decreased food intake, or other impairment in nutritional state due to, for example, gut dysfunction (Bindels et al. 2018) or malabsorption (Argiles et al. 2014), or anabolic resistance to nutrient intake (Deutz et al. 2011; Engelen, van der Meij & Deutz 2016; Penna et al. 2019; Williams et al. 2012) may still play a role in the regulation of muscle protein synthesis. Previously, it has been found that starvation, fasting and calorie restriction result in decreased muscle protein synthesis and downregulation of mTORC1 signalling (Areta et al. 2014; Collins-Hooper et al. 2015; Li & Goldberg 1976; Margolis et al. 2016; Ogata, Fong & Holliday 1978; Pasiakos et al. 2010; Reeds et al. 1986; Welle, Mehta & Burgess 2011). In addition, healthy pair fed mice may have similar muscle masses to mildly cachectic mice, even though not significantly different from control mice (Murphy et al. 2012), suggesting that altered levels of food intake may in part also contribute to cachexia. However, not all studies have reported decreased food intake in C26 cancer cachexia, but muscle wasting has been observed independent of altera-

tions in food intake (Acharyya et al. 2005), suggesting that food intake alone does probably not play a major role in the development of cachexia and muscle wasting in this model. In addition, it has been suggested that cancer patients have blunted anabolic response to nutrient intake, while having similar basal rates of protein synthesis compared with healthy subjects (Williams et al. 2012). In the present study, the tumour-bearing and chemotherapy-treated mice were fed *ad libitum*, and can thus be considered to be in a fed state. Consequently, it is possible, that the decrease in protein synthesis observed in the tumour-bearing and doxorubicin-treated mice may be at least in part due to either decreased food intake, attenuated response to feeding, or potential malabsorption. However, the contribution of these factors cannot be verified with the data available from these experiments. In the case of chemotherapy, the food intake was monitored only in the long-term experiment, in which decreased food intake was observed in doxorubicin-treated mice. This decrease in food intake might contribute to the decreased muscle protein synthesis, but this hypothesis cannot be confirmed, because it is not known whether a single injection of doxorubicin induced acute changes in food intake.

In addition to nutrient availability, muscle mass and protein synthesis may be modulated by the level of physical activity. Muscle basal protein synthesis and/or protein synthesis in response to nutrient stimulation have been blunted in different models of disuse or inactivity-induced atrophies, such as immobilization, bed rest, and step reduction (Breen et al. 2013; Glover et al. 2008; Gordon, Kelleher & Kimball 2013; Phillips & McGlory 2014; Rudrappa et al. 2016; Sepulveda et al. 2015; Oikawa, Holloway & Phillips 2019). Moreover, a recent study suggests that altered physical activity behaviour in experimental cancer cachexia is associated with disrupted skeletal muscle mTORC1 signalling and cachexia progression (Counts et al. 2020). Thus, it seems possible that the decreased physical activity observed in tumour-bearing mice may contribute to the reduction in protein synthesis either on the basal level or in response to feeding. In addition, the locomotor muscle studied, meaning TA muscle, had the most dramatic decline in protein synthesis in response to cancer when compared with the respiratory muscle diaphragm and the heart, which might indicate that the constantly active muscles – the diaphragm and the heart – are partially protected from the decline in protein synthesis.

To further elucidate the effects of altered levels of physical activity and food intake on protein synthesis and mTORC1 signalling, as well as the role of myostatin and activins in that regulation, unilateral follistatin overexpression was induced in the TA muscles of healthy mice and samples were collected after different levels of physical activity and/or food intake, that is, at night or during the day, or after overnight fasting, refeeding, or *ad libitum* feeding. Pronounced muscle hypertrophy was observed at 20 days after follistatin gene delivery, consistent with previous studies utilizing intramuscular follistatin gene delivery (Han et al. 2019; Sepulveda et al. 2015; Winbanks et al. 2012,). As with the blocking of myostatin and activins with a soluble ACVR2B ligand trap, follistatin-induced hypertrophy was at least in part due to increased muscle pro-



tein synthesis that was observed at seven days after follistatin gene delivery. This is consistent with previous studies (Han et al. 2019; Winbanks et al. 2012). The results in this dissertation further demonstrate that follistatin gene delivery increased muscle protein synthesis independent of diurnal fluctuations in physical activity and food intake, and irrespective of the feeding status. The ability of follistatin overexpression to induce anabolic effects on skeletal muscle tissue despite altered levels of physical activity and food intake is consistent with previous studies showing that blocking myostatin or myostatin and activins protects from atrophy resulting from, for example, disuse, mechanical unloading or deervation (MacDonald et al. 2014; Murphy et al. 2011a; Sepulveda et al. 2015), and the present results from cachectic and doxorubicin-treated mice.

In the present study, protein synthesis was not markedly altered by the diurnal fluctuation in physical activity and food intake, while overnight fasting resulted in a slight decrease in muscle protein synthesis. These results were perhaps surprising, as previously mild and severe models of inactivity or disuse (Breen et al. 2013; Glover et al. 2008; Gordon, Kelleher & Kimball 2013; Oikawa, Holloway & Phillips 2019; Phillips & McGlory 2014; Rudrappa et al. 2016; Sepulveda et al. 2015), as well as nutrient deprivation (Collins-Hooper et al. 2015; Li & Goldberg 1976; Ogata, Fong & Holliday 1978; Reeds et al. 1986; Welle, Mehta & Burgess 2011) have resulted in decreased muscle protein synthesis. It is possible that the alterations in physical activity or food intake were not dramatic enough to have more pronounced effects on muscle protein synthesis or on the effects of strong anabolic stimuli, such as follistatin. In the time-of-day experiment, circadian factors other than nutrition and physical activity may play a role in the regulation of muscle protein synthesis.

Increased muscle protein synthesis by follistatin gene delivery was associated with marked induction in mTORC1 signalling as shown by increased phosphorylation of p70 S6K and ribosomal protein S6 (rpS6), which is consistent with previous evidence (Winbanks et al. 2012). As with protein synthesis, mTORC1 signalling was also induced by follistatin despite altered levels of physical activity and food intake or fasting. When the potential mechanisms underlying increased mTORC1 signalling and protein synthesis were investigated further, it was found that the amount of mTOR colocalised with lysosomes/late endosomes was increased by follistatin, which may in part contribute to the anabolic effects of follistatin. This is consistent with the finding that the blocking of ACVR2B ligands restored the colocalisation of mTOR with lysosomes/late endosomes in cachectic mice. In addition to colocalisation, the translocation of mTOR-lysosome complexes towards the cell periphery has been found to regulate mTORC1 activation (Hodson & Philp 2019; Korolchuk et al. 2011). However, follistatin gene delivery did not influence the subcellular localization of colocalised mTOR and lysosomes, suggesting that mTOR-lysosome translocation towards sarcolemma is not essential for follistatin-induced mTORC1 activation.

Despite the lack of effects on protein synthesis, markers of mTORC1 signalling were significantly altered especially by feeding status and time of day.

Phosphorylation of mTORC1 downstream targets was decreased after fasting and during the daytime, when mice were passive and ate very little. Moreover, in those conditions the response to follistatin gene delivery was also attenuated, but not abolished. This suggests that even though follistatin is able to induce mTORC1 signalling and protein synthesis even in a fasted state, the magnitude of the response may be compromised. This further indicates that in a fasted state, some factors other than myostatin and activins, such as nutrient availability, downregulate mTORC1 signalling. However, the colocalisation of mTOR with lysosomes was not altered by fasting, even though nutrient availability has previously been suggested to alter mTORC1 activity through altered colocalisation of mTOR with lysosomes/late endosomes (Demetriades, Doumpas & Telemann 2014; Sancak et al. 2010,). It is possible that the fasting protocol was not severe enough to cause a decrease in mTOR-lysosome colocalisation. Indeed, it has previously been suggested that in physiological nutrient deprivation, the inactivation of mTORC1 signalling is mediated via translocation of mTOR-lysosome complexes away from the cell periphery and thus away from the upstream activators of mTORC1 (Hodson & Philp 2019; Korolchuk et al. 2011). However, fasting only slightly decreased the colocalisation of the mTOR-lysosome complexes with the sarcolemmal marker dystrophin, and the distance of these complexes from the sarcolemma was not altered in the present study (IV). The modest effects on the subcellular localization of the mTOR-lysosome complexes may also be due to the mild model of nutrient deprivation. As a majority of the research on mTOR localization has been conducted *in vitro*, future studies should aim to elucidate the effects of fasting and other catabolic (and anabolic) states on mTOR localization, and the mechanisms of mTORC1 activation/inactivation *in vivo*.

To conclude, both doxorubicin chemotherapy and experimental C26 cancer result in muscle wasting that can be prevented by blocking myostatin and activins. In both conditions, muscle wasting is associated with decreased muscle protein synthesis, which in chemotherapy is restored by blocking myostatin and activins. In cancer, decreased protein synthesis is associated with decreased mTORC1 signalling, potentially due to decreased colocalisation of mTOR with lysosomes. In chemotherapy, on the other hand, decreased muscle protein synthesis might be mediated through increased p53-p21-REDD1 signalling and atrogin-1 expression, and/or decreased ERK1/2 activation, rather than markedly altered mTORC1 signalling. In addition, muscle protein degradation pathways are activated in cancer, but chemotherapy is associated with only very modest acute alterations in proteolytic pathways, unlike many other wasting conditions. The blocking of myostatin and activins through pharmacological or genetic approaches promotes muscle hypertrophy in conditions associated with muscle wasting mainly through increased muscle proteins synthesis and mTORC1 signalling, which may be in part due to the increased amount of mTOR colocalised with lysosomes/late endosomes. In addition, the findings of the present study suggest that the genetic or pharmacologic blocking of activin receptor signalling overrides the physiological regulatory mechanism of muscle

protein synthesis, as its anabolic effects take place largely independent of alterations in physical activity or food intake.

## **6.2 Physical activity and exercise capacity in different wasting conditions and the effects of myostatin/activin blocking**

The present study showed that habitual physical activity and exercise capacity are impaired in experimental settings of cancer cachexia and chemotherapy, respectively. In addition, mere prevention of muscle wasting associated with these conditions seems unable to rescue these impairments, as the blocking of myostatin and activins had no effect on physical activity or running performance. Decreased physical activity in tumour-bearing animals has been demonstrated earlier (Busquets et al. 2012; Toledo et al. 2011; Toledo et al. 2014; Toledo et al. 2016b) and also more recently (Counts et al. 2020) in different models. In addition, the severity of cachexia has been shown to have impact on the alterations in physical activity and potentially its diurnal variation (Counts et al. 2020; Murphy et al. 2012). The observation that the blocking of myostatin and activins was unable to restore the levels of physical activity despite prevention of muscle wasting is in line with previous studies using different cancer cachexia models (Busquets et al. 2012; Toledo et al. 2016b). However, regardless of the lack of influence on physical activity, the grip strength has been shown to be improved in tumour-bearing mice by the blocking of myostatin and activins, implying that maintenance of muscle mass is also associated with maintenance of muscle function (Busquets et al. 2012; Toledo et al. 2016b; Zhou et al. 2010). These studies together indicate that the physical inactivity associated with cancer cachexia is at least not solely due to muscle wasting or impaired muscle function.

The assessment of physical activity is important in the context of cancer cachexia, as physical activity has been shown to be beneficial for overall health, for cancer incidence and potentially also for tumour host survival (Friedenreich et al. 2016; Moore et al. 2016). However, the present study suggests that physical activity is not an important factor determining survival in tumour-bearing mice treated with sACVR2B, as survival was prolonged even though no improvement was observed in the levels of physical activity. This is supported by a recent study showing no benefit of exercise on survival in severe experimental cancer, despite other beneficial effects of exercise (Ballaro et al. 2019). Interventions targeted to increase the levels of physical activity would be needed in the future to elucidate whether there is a causal link between physical activity and survival in different types of cancer.

Several previous studies have demonstrated muscle weakness, fatigue and contractile dysfunction after exposure to doxorubicin (Ertunc et al. 2009; Gilliam et al. 2009; Gilliam & St Clair 2011; Gilliam et al. 2011a; Min et al. 2015; van Norren et al. 2009a), but the effect of doxorubicin on aerobic running capac-

ity has not been studied before. The present study showed that treadmill running performance is impaired in doxorubicin-treated mice. As this observation was made two weeks after the cessation of the doxorubicin administration, it seems that the impairment in running capacity is sustained for at least a short period of time after the treatment protocol. Previously, repeated cycles of doxorubicin-containing chemotherapy have resulted in sustained impairment in muscle mitochondrial function (Gospillou et al. 2015), supporting the chronic impairment in running capacity. These are important observations, as if the same happens in human patients treated with chemotherapeutic agents, it may contribute to the overall decline in functional capacity and have long-term negative impact on the quality of life of these patients. Future studies should thus investigate the longer-term effects of doxorubicin treatment on running capacity and if the running capacity can be restored by, for example, exercise training.

As physical activity and running capacity were not restored by sACVR2B treatment, the decline in physical activity in cancer and running performance in doxorubicin-treated mice are unlikely due to mere muscle atrophy. Previous studies have shown mitochondrial damage and dysfunction as well as impaired oxidative metabolism and ATP production in muscle in response to cancer cachexia (Fontes-Oliveira et al. 2013; Pin et al. 2015; Shum et al. 2012) and doxorubicin administration (Gilliam et al. 2013; Gospillou et al. 2015; Yamada et al. 1995). These kinds of alterations might contribute to decreased physical activity and running capacity, so the oxidative properties of skeletal muscles were investigated in both wasting conditions. In tumour-bearing mice, the citrate synthase activity was slightly but consistently decreased in the different muscle tissues investigated – TA, the heart and the diaphragm – and the blocking of myostatin and activins had no further effect. This result was more recently corroborated by a proteomics analysis conducted on the same mice showing that the TCA cycle proteins were downregulated in gastrocnemius muscles of tumour-bearing mice and unaffected by myostatin/activin blocking (Hulmi et al. 2020). Moreover, the percentage of muscle fibres with high SDH activity was lower in the TA muscles of the tumour-bearing mice, further supporting a slight decrease in oxidative capacity (Hulmi et al. 2020). These results are also consistent with previous studies suggesting mitochondrial dysfunction and impaired oxidative energy metabolism in tumour-bearing and chemotherapy-treated mice (Barreto et al. 2016; Ballaro et al. 2019). However, the protein level markers of mitochondrial content remained relatively unaltered in skeletal and cardiac muscles of the tumour-bearing mice irrespective of the treatment modality in the present dissertation. Interestingly, a proteomics approach revealed a significant reduction also in proteins involved in oxidative phosphorylation in the tumour-bearing mice accompanied by dysregulated NAD<sup>+</sup> metabolism, and these were in part prevented by myostatin/activin blocking (Hulmi et al. 2020). The discrepancy between these results may be due to a different muscle analysed or the analytical methods used. Taken together, these results suggest that skeletal muscle aerobic capacity and mitochondrial content and function may be slightly impaired in tumour-bearing mice, which may in part contribute to

the decreased physical activity observed in tumour-bearing mice. Furthermore, the blocking of myostatin and activins does not cause any further damage to the oxidative properties of skeletal muscle. However, more specific measurements of mitochondrial function would be required for definite conclusions, given the slight discrepancy in the results.

Impaired mitochondrial function due to doxorubicin has been demonstrated in numerous previous studies in both the heart (Lebrecht et al. 2003; Yamada et al. 1995) and in skeletal muscle (Gilliam et al. 2013; Gouspillou et al. 2015; Yamada et al. 1995). However, in the present study, neither mitochondrial function, analysed by the high-resolution respirometry and citrate synthase activity, nor the markers of mitochondrial content were affected by doxorubicin, when analysed two weeks after the cessation of doxorubicin administration. Moreover, two weeks of doxorubicin administration did not cause any acute impairments in mitochondrial function or content in the heart either, even though ultrastructural damage was observed in the mitochondria (Räsänen et al. 2016). The discrepancy between the results of the present and the previous studies may be at least in part due to different doses or treatment regimens used. However, mitochondrial dysfunction in skeletal muscle has been observed in response to a single injection of doxorubicin (Gilliam et al. 2013) as well as in longer term treatment protocols (Gouspillou et al. 2015; Yamada et al. 1995), and both acute and sustained effects have been reported (Gilliam et al. 2013; Gouspillou et al. 2015), but not in all studies (Lebrecht et al. 2003). Supporting the importance of the dosage and timing, Gouspillou et al. (2015) demonstrated that two cycles of doxorubicin and dexamethasone treatment with a cumulative dose of 20 mg/kg did not cause chronic impairments in mitochondrial function. However, four cycles of treatment with a cumulative dose of 40 mg/kg resulted in impaired mitochondrial respiration that was sustained over a 12-week period after the last cycle (Gouspillou et al. 2015). Interestingly, in accordance with the present study, despite the decreased mitochondrial respiration, the markers of mitochondrial content, such as OXPHOS proteins and mitochondrial DNA, were not affected, while citrate synthase activity was slightly decreased (Gouspillou et al. 2015). However, the contribution of each drug to the overall outcome cannot be determined, which limits the comparison to the present study. Taken together, the present and these previous studies suggest that the dosage of doxorubicin used and the time points investigated may play important roles in doxorubicin-induced alterations in skeletal muscle mitochondrial function. Moreover, as no impairments in mitochondrial function or markers were observed in the present study, they probably do not play a central role in the decreased running capacity of the mice treated with doxorubicin.

As the mitochondrial markers and function in the skeletal muscle were relatively unaffected by both cancer cachexia and chemotherapy, the capacity to deliver oxygen to skeletal muscle tissue was also assessed, as oxygen delivery to skeletal muscle may limit exercise capacity (Bassett & Howley 2000). In addition to cardiopulmonary factors, oxygen delivery to active muscle tissue may be

modulated by blood oxygen carrying capacity (haemoglobin and haematocrit) as well as capillary density in the active muscles (Bassett & Howley 2000). Cancer cachexia was associated with mild anaemia, which might play a role in decreased physical activity. The observed anaemia is in line with previous studies using the same and different tumour models (Penna et al. 2013b; Pin et al. 2015; Toledo et al. 2016b; Toledo et al. 2014). Treatment with erythropoietin to improve blood oxygen carrying capacity has counteracted some negative effects associated with cancer cachexia (Penna et al. 2013b; Pin et al. 2015), but its effectiveness in increasing physical activity and/or exercise capacity is currently not known. However, even though anaemia can limit exercise capacity in cancer (Argiles et al. 2012), the anaemia was alleviated by sACVR2B administration without effects on physical activity, making it unlikely that anaemia was the only underlying cause of decreased physical activity in the present study.

In mice treated with doxorubicin, anaemia was observed after the two-week treatment protocol, but it was not sustained for the two-week period after cessation of the treatment. Thus, it seems unlikely that blood oxygen carrying capacity was a limiting factor for exercise capacity anymore at the time point when the running test was performed. Contrary to tumour-bearing mice, the blocking of myostatin and activins did not alleviate anaemia in mice treated with doxorubicin, suggesting that effects of myostatin/activin blocking on red blood cells and blood oxygen carrying capacity may be dependent on the context.

As blood oxygen carrying capacity does not seem to be the main factor behind the decreased exercise capacity, muscle capillarization was analysed from TA muscles to gain insight into the capacity to deliver oxygen and nutrients throughout the active muscle. Neither capillary density nor the number of capillaries per muscle fibre were affected by doxorubicin, when analysed two weeks after the cessation of the treatment, suggesting that decreased capillarization does not explain the impaired running capacity. Despite increased fibre size, neither capillary density nor the capillary-to-fibre ratio were affected by the blocking of myostatin and activins. Previously, the administration of sACVR2B has decreased capillary density probably due to fibre hypertrophy, as the number of capillaries per muscle fibre remained unaltered (Hulmi et al. 2013a). Decreased capillarization in response to doxorubicin has previously been shown in the heart and was also observed in the present experiments (Räsänen et al. 2016). However, this was the first study to show the effects of doxorubicin on skeletal muscle capillarization. A more recent study demonstrated that short-term doxorubicin administration results in decreased capillary density in some (soleus), but not all (extensor digitorum longus, EDL) rat skeletal muscles, thus in part contradicting the results of the present study (D'Lugos et al. 2019). It is thus possible that predominantly slow-twitch oxidative muscles, such as the soleus, are more prone to doxorubicin-induced decrease in capillarization than predominantly fast-twitch, more glycolytic muscles, such as EDL and TA (present dissertation). This hypothesis, however, requires further investigation.

As decreased physical activity in tumour-bearing mice and impaired exercise capacity in doxorubicin-treated mice do not seem to be fully explained by muscle atrophy, decreased mitochondrial content or function or the capacity to deliver oxygen to active muscles, some other factors potentially contributing to these impairments could be discussed. Firstly, the mass and function of the heart might play a role in reduced physical activity levels and the impaired exercise capacity. However, in tumour-bearing mice, cardiac function was not assessed and the mass of the heart was unaltered yet at this time point, even though cardiac cachexia and dysfunction have been previously observed in tumour-bearing animals (Springer et al. 2014; Tian et al. 2010). On the other hand, doxorubicin caused atrophy and decreased capillarization in the heart and induced endothelial damage and dysfunction as well as damage in cardiomyocytes that might potentially contribute to decreased running capacity. However, cardiac function was not significantly affected (Räsänen et al. 2016). As with running capacity, myostatin/activin blocking was unable to prevent the decrease in heart mass, but the other factors were not assessed in mice treated with sACVR2B.

Secondly, defects in the primary respiratory muscle (i.e. the diaphragm) could cause impairments in exercise capacity. Indeed, previous studies have demonstrated atrophy and weakness of the diaphragm (Murphy et al. 2012, Roberts et al. 2013) accompanied by ventilatory dysfunction (Roberts et al. 2013) in a murine model of cancer cachexia. Moreover, doxorubicin has been found to cause diaphragm damage (Doroshov, Tallent & Schechter 1985), as well as decrease in force and contractile dysfunction (Gilliam et al. 2011a), suggesting that diaphragm function may be impaired in mice treated with doxorubicin. In the present study, diaphragm atrophy was observed in the tumour-bearing mice, but as this effect was abolished by the blocking of myostatin and activins without restoration of physical activity, mere diaphragm atrophy does not explain decreased physical activity. The diaphragm was not investigated in the doxorubicin experiments, so its role in determining the exercise capacity in these mice remains at the level of speculation.

Importantly, in the present study, the blocking of myostatin and activins did not have further negative effects on physical activity, running capacity, mitochondrial function and markers, or capillarization. Previously, decreased physical activity has been observed in dystrophic *mdx* mice administered with sACVR2B (Hulmi et al. 2013b) and impaired running capacity has been demonstrated in healthy wild-type mice after treatment with sACVR2B (Relizani et al. 2014). Moreover, the blocking of myostatin and activins has previously been associated with diminished mitochondrial oxidative capacity (Hulmi et al. 2013b; Kainulainen et al. 2015; Rahimov et al. 2011), and reduced the expression of proteins related to oxidative metabolism (e.g. TCA cycle and OXPHOS) (Barbe et al. 2017). This shows that the effects of blocking myostatin and activins on physical activity, exercise capacity and oxidative properties of skeletal muscle can be context specific.

### 6.3 Importance of skeletal muscle tissue in the wasting conditions and the role of myostatin/activin blocking

It is widely accepted that skeletal muscle tissue plays an important role in health and disease, having important functions not only in locomotion and performing daily tasks, but also in vital functions, such as breathing and whole body metabolism (Wolfe 2006). Moreover, muscle size, quality and function have been strongly related to the risk of mortality in general and to the overall outcome in different diseases and wasting conditions (Anker et al. 1997; Cooper et al. 2010; Fearon, Arends & Baracos 2013; Kalantar-Zadeh et al. 2013; Martin et al. 2013; Rantanen, Sakari-Rantala & Heikkinen 2002; Rollins et al. 2016; Tardif, Grip & Rooyackers 2017; Weijs et al. 2014). In addition, preservation of muscle mass may help reduce the toxic effects of chemotherapy and thus improve survival in cancer patients (Pin, Couch & Bonetto 2018). The results of the present study support the importance of increasing and/or maintaining muscle mass in situations that cause muscle wasting, such as cancer and chemotherapy. The present study shows that increasing and maintaining muscle mass via the blocking of myostatin and activins improves survival in tumour-bearing mice, thus supporting the previous and more recent findings in different models of cancer cachexia (Hatakeyama et al. 2016; Toledo et al. 2016b; Zhong et al. 2019; Zhou et al. 2010). Moreover, this study demonstrates an important novel finding that increasing muscle mass only before the cachectic stimulus does not provide a similar survival benefit as treatments targeted to prevent muscle wasting, at least when muscle hypertrophy is achieved by myostatin/activin blocking that is terminated before the cachectic stimulus.

However, the blocking of myostatin and activins has not improved survival in all pre-clinical animal models of cancer cachexia despite the prevention of weight loss. A recent study in a pancreatic cancer model induced by cancer cells expressing high levels of Activin A demonstrated that even though both systemic and muscle-specific blockade of myostatin and activins were able to preserve body mass, survival was not improved (Zhong et al. 2019). However, survival was improved by systemic myostatin/activin blocking when pancreatic cancer cells expressing low levels of Activin A were used (Zhong et al. 2019). The reason for this discrepancy is not fully understood, but might be due to a more aggressive phenotype of activin<sup>high</sup> tumours, or effects on some tissues other than skeletal muscle, which are discussed later in more detail.

The potential mechanisms underlying the survival benefit in the present study were studied in a shorter experiment with a pre-determined endpoint at the time point in which body mass change most strongly predicted survival. At this time point, individual muscle weights were significantly higher in both groups treated with sACVR2B compared with vehicle-treated tumour-bearing mice. Thus, the preservation of muscle tissue in general may contribute to the improved survival. This is supported by a large body of evidence showing that a number of different strategies to prevent muscle wasting in different models



of cancer cachexia can result in improved survival (Cai et al. 2004; Chiappalupi et al. 2020; Gallot et al. 2014; Hatakeyama et al. 2016; Johnston et al. 2015; Lerner et al. 2016; Li et al. 2007; Parajuli et al. 2018; Potsch et al. 2020; Toledo et al. 2016b; Tseng et al. 2015; Zhong et al. 2019; Zhou et al. 2010). However, it is also possible that the preservation of some vital muscles, such as the major respiratory muscles, plays an important role in survival (Azoulay et al. 2004; Schapira et al. 1993). Interestingly, already at the 11-day time point, tumour-bearing mice demonstrated diaphragm atrophy that might ultimately result in ventilatory dysfunction at some point. Indeed, diaphragm atrophy and weakness accompanied by ventilatory dysfunction have been previously reported in C26 tumour-bearing mice (Murphy et al. 2012; Roberts et al. 2013). Importantly, myostatin/activin blocking restored diaphragm mass in the present study, which may at least in part have explained the prolonged survival of these mice, although the differences between the treatment protocols were marginal at the time point investigated. Thus, more studies are required to confirm the importance of maintaining diaphragm mass and function during cancer cachexia.

The evidence from human studies showing that baseline sarcopenia is associated with shorter survival might imply that having larger muscle mass to begin with might be beneficial in terms of survival in cancer cachexia (Camus et al. 2014; Harimoto et al. 2013; Iritani et al. 2015; Kazemi-Bajestani, Mazurak & Baracos 2016; Martin et al. 2013; Meza-Junco et al. 2013; Miyamoto et al. 2015; Orell-Kotikangas et al. 2017; Prado et al. 2008; Peng et al. 2012; Psutka et al. 2014; van Vledder et al. 2012; Veasey Rodrigues et al. 2013; Voron et al. 2015). However, this hypothesis is not supported by the present study, as only pre-treatment with sACVR2B to increase muscle mass before the induction of cachexia was not associated with any survival benefit and in many terms resulted in an even worse outcome than with the vehicle treatment. This finding was somewhat surprising, even though a previous study has shown that having a larger muscle mass at baseline due to myostatin deficiency does not protect from tumour-induced muscle wasting, but results in even larger absolute and proportional muscle loss (Benny Klimek et al. 2010). However, muscle mass was still larger at the end of the study in the myostatin deficient mice when compared with wild-type counterparts (Benny Klimek et al. 2010). Unfortunately, the survival was not investigated in that study. These results do not necessarily imply, however, that having a larger muscle mass at the baseline would be harmful or at least not beneficial in the case of cancer cachexia. It is possible that, in the case of our study, stopping the treatment resulted in a decline in muscle mass due to the lack of the external stimulus to increase muscle mass. This might have coincided with tumour-induced muscle wasting resulting in an exacerbated wasting condition with even more detrimental effects than mere tumour-induced muscle wasting. This is supported by the body mass curve, which showed a steep decline in the discontinued treatment group during the last few days of the experiment. Moreover, the masses of TA and the diaphragm, as well as epididymal fat mass and body mass, were non-significantly lower in the group in which sACVR2B treatment was discontinued. In addition,

this group of mice showed systematically the lowest levels of protein synthesis in TA, diaphragm and the heart, and the highest levels of ubiquitin-proteasome system markers in the TA, indicating that this particular group had the most aggressive induction of muscle wasting at the time point investigated. It is thus possible that the presumably higher rate of muscle loss may have, directly or indirectly via some potential negative effects on other tissues, affected survival.

The hypothesis that the rate of muscle loss might in some cases determine the severity instead of absolute muscle size is supported by the fact that at the time of euthanasia, the muscle masses were higher in the mice pre-treated with sACVR2B compared with PBS-treated tumour-bearing mice in the survival experiment (unpublished observation). Additional support is provided by the fact that the change in body mass predicted survival. Moreover, in a previous study in pancreatic cancer patients, the higher rates of adipose and skeletal muscle tissue losses were associated with poorer survival, but this association did not reach statistical significance for skeletal muscle, thus providing only partial support to the hypothesis (Di Sebastiano et al. 2013). However, a number of studies have found association between the loss of skeletal muscle (Brown et al. 2018; Dalal et al. 2012; Fogelman et al. 2014; Järvinen et al. 2018a, Järvinen et al. 2018b; Stene et al. 2015) or body mass (Bachmann et al. 2008; Dewys et al. 1980; Fouladiun et al. 2007; Martin et al. 2013; Martin et al. 2015) and survival, thus suggesting that the rate of wasting might also be important. However, more research is required to confirm the effect of the rate of muscle loss on survival.

Importantly, in the present study, muscle and body masses were significantly lower only in the vehicle-treated tumour-bearing mice and no significant differences between the two different sACVR2B treatment protocols were observed in muscle masses, muscle protein synthesis or the markers of protein degradation despite a significant difference in the survival time. Thus, the underlying mechanism for lack of survival benefit in the group, in which sACVR2B administration was ceased before tumour formation, remains at the level of speculation. However, it currently seems that having low muscle mass to begin with is associated with impaired prognosis, but having especially large muscles may not provide any further benefit (Fearon, Arends & Baracos 2013). In fact, it has even been suggested that larger muscle or body mass may result in faster drug clearance, which may impair the prognosis (Chu et al. 2017; Muller et al. 2012; Riihijarvi et al. 2011). The key might be to prevent a rapid decline in muscle and body mass and to maintain adequate muscle size throughout the life span. Furthermore, it seems that body composition needs to be taken into account in the dosage of anti-cancer treatments, especially if a therapy targeted to preserve muscle mass is also used.

In addition to muscle wasting, alterations in many other tissues and systems have been associated with cancer cachexia and the poor prognosis related to it (Argiles et al. 2014; Argiles et al. 2018). For example, inflammation associated with increased levels of pro-inflammatory cytokines and acute phase response (Stephens, Skipworth & Fearon 2008), increased spleen mass and expansion of myeloid-derived suppressor cells (MDSCs) (Fearon, Glass & Guttridge

2012; Liefvers et al. 2009), haematological changes, such as anaemia and thrombocytosis (Kalantar-Zadeh et al. 2013), cardiac cachexia (Murphy 2016), fat depletion and adipose tissue browning (Argiles et al. 2014; Argiles et al. 2018), as well as alterations in gut microbiota (Bindels et al. 2016; Genton et al. 2019; Herremans et al. 2019) have been linked to the development of cachexia and survival. Many of these alterations were also investigated and observed in the present study and are discussed in more detail in the following section. In addition, it is possible that the blocking of myostatin and activins also has beneficial effects on tissues other than skeletal muscle. It was recently shown that muscle-specific blockade of myostatin and activins did not improve survival despite the maintenance of body mass in a mouse model of pancreatic cancer, and this was speculated to be due to essential effects on tissues other than skeletal muscle (Zhong et al. 2019). However, the fact that the survival was not improved may not be entirely due to the absence of beneficial effects of myostatin/activin blocking on other tissues, as even systemic blockade of myostatin and activins did not improve survival in that particular tumour-model (Zhong et al. 2019). Regardless, the present study supports the hypothesis that either the blocking of myostatin and activins directly or via preservation of skeletal muscle tissue also has some effects on non-muscle tissues that may play a role in survival. These include at least the effects on spleen mass, liver protein synthesis, and anaemia that opposed the effects of the tumour.

In addition to skeletal muscle, atrophy of the heart has also been observed in cancer cachexia (Murphy et al. 2012; Murphy 2016; Zhou et al. 2010), but not in all cases (Murphy et al. 2011b, Toledo et al. 2016b). In addition, cardiovascular complications are common, and may be a major cause of death in cancer patients (Kalantar-Zadeh et al. 2013; Murphy 2016). However, in the present study, cardiac atrophy was not yet observed at the 11-day time point in which clear wasting was observed in skeletal muscle tissue. It is possible, that cardiac cachexia does not become apparent until a more severe stage of cachexia has been reached, as already discussed (see chapter 6.1). Moreover, as myostatin/activin blocking had no effects on the heart mass in both experimental cancer and chemotherapy settings, the findings of the present dissertation suggest that the beneficial effects on survival by the blocking of myostatin and activins happen independent of effects on the heart mass. However, as myostatin/activin blocking has previously shown some beneficial effects on the heart (Magga et al. 2019; Zhou et al. 2010), a later time point demonstrating a more advanced level of cachexia, or a combination of cancer and chemotherapy potentially showing more effects on the heart, should be investigated to confirm this hypothesis.

Skeletal muscle wasting is often accompanied by loss of adipose tissue in cachexia (Argiles et al. 2014; Fearon et al. 2011). This was also observed in the present study already at the 11-day time point, in which tumour-bearing mice had markedly lower epididymal fat mass compared with healthy controls. Neither protocol of myostatin/activin blocking had any effect on fat mass, which is in line with a previous study using the same tumour model (Zhou et al. 2010).

This finding suggests that the improved survival with continued myostatin/activin blocking was not due to preservation of fat mass. However, fat loss has recently been shown to play an important role in cachexia and the mortality of pancreatic cancer patients (Kays et al. 2018), and might thus contribute to the finding that myostatin/activin blocking did not improve survival in activin<sup>high</sup> tumour-bearing mice despite maintenance on body mass (Zhong et al. 2019). However, the association between fat wasting and survival has not been observed in all studies (Danai et al. 2018) and the fat masses were not reported for the activin<sup>high</sup> tumour-bearing mice (Zhong et al. 2019), and thus the contribution of fat wasting to survival remains at the level of speculation. In addition, white adipose tissue browning, which has been suggested to happen in cancer cachexia and to contribute to the progression of cachexia (Argiles et al. 2018), was not observed in these experiments and the blocking of myostatin and activins did not alter markers related to it (Lautaoja et al. 2019). This implies that, as with adipose tissue wasting, adipose tissue browning was not a major factor determining survival time in these cachectic mice or the improved survival in mice treated with sACVR2B.

Consistent with previous studies in cachectic tumour-bearing mice (Bonetto et al. 2011; Lerner et al. 2016; Zhou et al. 2010,) and in human cancer patients (Lewis et al. 2017; Martin et al. 1999; Sirniö et al. 2018; Talbert et al. 2018), tumour-bearing mice exhibited significantly increased levels of circulating pro-inflammatory cytokines. The levels of these cytokines were not affected by the blocking of myostatin and activins, and the levels of MCP-1 and IL-1 $\beta$  were even augmented by the continued treatment with sACVR2B, which supports and extends the findings from previous studies (Zhou et al. 2010). Thus, even though inflammation (Argiles et al. 2014; Fearon, Glass & Guttridge 2012; Stephens, Skipworth & Fearon 2008) and increased levels of IL-6 (Martin et al. 1999) and MCP-1 (Lewis et al. 2017; Talbert et al. 2018) have previously been associated with the development of cancer cachexia and survival in human cancer patients, the levels of pro-inflammatory cytokines do not seem to contribute to the differences in survival time in the present study.

Even though the blocking of myostatin and activins did not have major effects on the levels of pro-inflammatory cytokines, it exhibited some effects on other markers related to inflammation. In the present study, the tumour-bearing mice showed increased markers of hepatic acute phase response (APR), such as increased liver protein synthesis, increased phosphorylation of Stat3 and increased protein levels fibrinogen and Serpina3n in the liver. The increased liver protein synthesis may have reflected increased production of exported APR proteins, as no effect on liver mass was observed. Elevation of hepatic protein synthesis (Samuels et al. 2006) and induction of acute phase response in liver and skeletal muscle (Bonetto et al. 2011; Hulmi et al. 2020) are consistent with other studies in tumour-bearing mice, and are also supported by findings in weight-losing human cancer patients (Barber et al. 2000). Liver protein synthesis, along with the phosphorylation of Stat3, were markedly attenuated by sACVR2B treatment. As APR has been associated with impaired

survival (Stephens, Skipworth & Fearon 2008), this might be one potential mechanism via which sACVR2B directly or via preservation of muscle mass, improves survival. However, there were no significant differences between the two treatment protocols in these variables at the time point investigated despite a significant difference in the survival time in the survival experiment. In addition, the levels of the positive APR proteins, fibrinogen and serpinA3n, were not altered by sACVR2B treatment in the liver in this dissertation or in skeletal muscle (Hulmi et al. 2020). Interestingly, the level of these hepatic APR proteins correlated with body mass loss, indicating that APR may either play a role in the development of cachexia or that different factors related to cachexia just simply coincide during tumour growth. All in all, these data suggest that the APR plays a role in cachexia, but its relevance in terms of survival still needs further investigation. In addition, the mechanisms and importance of the attenuated liver protein synthesis and Stat3 activation by myostatin/activin blocking remain to be elucidated. However, most probably, sACVR2B does not improve survival through affecting inflammation or APR.

Considerable splenomegaly (i.e. increased spleen size) was observed in the tumour-bearing mice, and this is in line with previous studies (Aulino et al. 2010; Bonetto et al. 2016; Cuenca et al. 2014; Mundy-Bosse et al. 2011). Interestingly, this effect was significantly attenuated by the blocking of myostatin and activins, independent of the treatment protocol, in the present study. This adds to previous evidence showing that sACVR2B treatment alleviated splenomegaly in an animal model of  $\beta$ -thalassemia (Suragani et al. 2014). Because the expansion of the myeloid-derived suppressor cell (MDSC) pool has previously been associated with the development of cachexia and potentially also with survival (Cuenca et al. 2014), the markers of MDSCs were analysed from the spleen samples. Despite a marked effect on spleen size, the blocking of myostatin and activins did not consistently attenuate the mRNA expression of MDSC markers that were elevated in tumour-bearing mice. Thus, the mechanism for the attenuation of splenomegaly by myostatin/activin blocking in the present study and its importance with respect to survival still require further investigation. However, as splenomegaly was attenuated by sACVR2B treatment independent of the treatment protocol in the present study, it may be argued that spleen size may not play a major role in enhanced survival with the continued myostatin/activin blocking.

Vehicle-treated tumour-bearing mice had significantly lower levels of haemoglobin, haematocrit and red blood cell count compared with healthy mice. This indicates mild anaemia in tumour-bearing mice and is in line with previous studies in rodents (Toledo et al. 2014) and human patients (e.g. Väyrynen et al. 2018). Interestingly, the blocking of myostatin and activins was able to reverse the mild anaemia in tumour-bearing mice. Previously, myostatin gene inactivation has restored haematocrit in *Apc<sup>Min/+</sup>* model (Gallot et al. 2014). In addition, sACVR2B treatment has alleviated anaemia in inhibin-deficient mice (Li et al. 2007) and in an animal model of  $\beta$ -thalassemia (Suragani et al. 2014). In contrast, in another murine model for cancer cachexia, LLC, sACVR2B treatment was able

to only partially alleviate the decrease in haemoglobin but not in haematocrit (Toledo et al. 2016b). However, in that study, the anaemia was more severe than in the present study and the sACVR2B treatment regimen was also different (Toledo et al. 2016b). Even though anaemia may be an independent prognostic factor in cancer patients (Caro et al. 2001; Väyrynen et al. 2018), and the prevention of anaemia can be beneficial in C26 tumour-bearing mice (Penna et al. 2013b; Pin et al. 2015), it does not seem to be a major factor contributing to the differences in survival time, as anaemia was similarly alleviated in both groups treated with sACVR2B despite a significant difference in the survival time. In addition, the platelet count was increased in all tumour-bearing groups, independent of blocking myostatin and activins, and thus thrombocytosis is also unlikely to be the major factor determining survival time in the present study.

However, all of the abovementioned effects of myostatin/activin blocking on other tissues were similar between the two treatment protocols at the investigated time point. Thus, based on the present data, it is impossible to state which, if any, of these factors played any role in the improved survival seen in one of the groups treated with sACVR2B. In addition to the factors presented in this dissertation, other variables potentially contributing to the differences in survival time have been analysed from the same animals and reported by others. For example, alterations in gut microbiota have been associated with cancer cachexia and impaired survival (Bindels et al. 2016; Genton et al. 2019; Herremans et al. 2019), and while altered gut microbiota in tumour-bearing mice was demonstrated in the present experiment and was in part associated with body weight loss, it did not explain differences in the survival time, as continued treatment with sACVR2B prolonged survival but did not prevent the cancer-associated alterations in gut microbiota (Pekkala et al. 2019). As with the analysis of gut microbiota, analysis of muscle and serum metabolomes, while providing new insight into metabolic alterations in cancer cachexia and potential new biomarkers for cachexia progression, did not provide any clear, plausible candidates to explain differences in survival (Lautaoja et al. 2019). However, the blocking of myostatin and activins by sACVR2B has recently been shown to rescue some of the metabolic alterations induced by chemotherapy, suggesting that myostatin/activin blocking has beneficial effects on muscle and serum metabolomes in some cachectic conditions (O'Connell et al. 2019). Interestingly, a proteomics approach and further analyses revealed disturbed NAD<sup>+</sup> homeostasis in muscles of tumour-bearing mice, which was in part rescued only by the continued sACVR2B treatment (Hulmi et al. 2020). This result opens up new, interesting research questions and hypotheses for future research aiming to elaborate on the mechanisms of cancer cachexia and improved survival by interventions targeted at maintaining muscle size.

Even though the exact mechanisms underlying the prolonged survival in C26 cancer cachexia with continued sACVR2B treatment are still not completely understood, it seems that in the present study, the beneficial effects of myostatin/activin blocking happened independent of effects on tumour mass or tumoural gene expression related to cachexia. In the present study, treatment

with sACVR2B had no effects on either C26 or LLC tumour mass at the investigated time points, independent of doxorubicin chemotherapy. In some other studies reporting improved survival in myostatin deficient mice in *Apc*<sup>Min/+</sup> and LLC models (Gallot et al. 2014), or after the blocking of myostatin and activins in inhibin- $\alpha$  deficient mice developing gonadal tumours (Li et al. 2007, Zhou et al. 2010), or in a murine model of pancreatic ductal adenocarcinoma (Zhong et al. 2019), the tumour progression has been partially attenuated, which may have contributed to the alleviation of cachexia and prolonged survival. Attenuation of metastasis formation in the LLC model has also been demonstrated with sACVR2B administration (Toledo et al. 2016b) and other therapies ameliorating cachexia and improving survival (Chiappalupi et al. 2020). This is an important point to consider, as in some cases the positive effects of the treatment may be due to the antitumour effect of the treatment rather than preservation of skeletal muscle tissue. In fact, it is possible that in some cases muscle mass is preserved in part due the delay in tumour progression.

Tumoural expression of cachexia-inducing factors may play an important role in the development of cachexia and potentially also survival (Fearon, Glass & Guttridge 2012; Hoda et al. 2016; Loumaye et al. 2017; Zhong et al. 2019). In the present study, C26 tumours had markedly higher expression levels of potential cachexia-inducing factors Activin A, myostatin and Il-6 compared with LLC tumours, and C26 tumours also resulted in more pronounced cachexia at a similar time point with the same number of injected cells. In the present study, treatment with sACVR2B did not influence tumoural *Activin A (Inhibin  $\beta$ A)* mRNA expression, and even increased *Il-6* mRNA expression in the C26 tumours, suggesting that the prevention of cachexia, or the improved survival, are not mediated through altered tumoural expression of genes related to cachexia. All in all, the results of the present study demonstrate that survival benefit with the continued blocking of myostatin and activins happens independent of effects on tumour mass or tumoural expression of cachexia-related factors or their tumour-induced expression in skeletal muscle tissue (III). Future studies should address the question of whether there is a causal link between the levels of cachexia-inducing factors, such as Activin A, and survival, or whether these factors act as mere biomarkers of cachexia and disease progression, or the aggressiveness of the tumour.

Interestingly, it was found that increasing muscle and lean mass via blocking of myostatin and activins also improved bone parameters that were impaired by doxorubicin. It is possible that the alterations in bone mineral density and content were secondary to changes in skeletal muscle mass, as these bone parameters were strongly correlated with changes in lean mass as well as the end-measures of muscle mass and muscle fibre cross-sectional area. These findings are in line with previous and more recent studies, as doxorubicin administration has been previously found to affect bone quality (Hayward et al. 2013), and the blocking of myostatin and activins has been shown to improve bone quantity and/or quality in different models (Barreto et al. 2017; Bialek et al. 2014; Puolakkainen et al. 2017a; Puolakkainen et al. 2017b). Interestingly, as in

the present study, a more recent study demonstrated that Folfiri chemotherapy resulted in loss of both muscle and bone mass, which were both prevented by the blocking of myostatin and activins (Barreto et al. 2017). Together these studies show that the blocking of myostatin and activins is effective in counteracting bone and muscle loss induced by different types of chemotherapy.

As a strong interaction has been demonstrated between skeletal muscle mass and function and bone quantity and quality (Brotto & Bonewald 2015; Goodman, Hornberger & Robling 2015), it may be speculated that the changes in bone adaptation observed in the present study were secondary to changes in skeletal muscle tissue. This would support the importance of skeletal muscle tissue *per se* on different markers of health. However, the existence of other direct or indirect effects from blocking myostatin and activins on bone is possible and cannot be excluded. Indeed, previously the blocking of ACVR2B ligands, but not the blocking of myostatin only, improved bone mass despite a similar increase in muscle mass with both treatments (Bialek et al. 2014). On the other hand, increased bone mass, density and strength have been demonstrated in mice lacking myostatin and thus having greater muscle mass, which would support either a role for muscle mass or myostatin in the regulation of bone quantity and quality (Elkasrawy & Hamrick 2010). Thus, more profound mechanistic evidence is needed to determine whether the blocking of myostatin and activins has direct effects on bone, or whether the improvement in bone quantity and quality are secondary to increased muscle mass.

Taken together, the findings from both tumour-bearing and chemotherapy-treated mice demonstrate that the blocking of myostatin and activins results in a number of positive health-related effects that counteract the detrimental effects of tumour or chemotherapy. These include muscle hypertrophy or prevention of muscle loss, attenuation of hepatic protein synthesis, splenomegaly and anaemia, and ultimately improvement in survival in tumour-bearing mice and improved bone mineral density and content in chemotherapy-treated mice. These results corroborate and add to the previous and recent evidence showing the beneficial effects of this strategy in animal models of cancer and chemotherapy beyond mere improvement in muscle mass (Barreto et al. 2017 O'Connell et al. 2019; Toledo et al. 2016b; Zhou et al. 2010). Given the importance of inter-tissue crosstalk in cachexia (Argiles et al. 2018), it is possible that some of the beneficial effects of myostatin/activin blocking on other tissues are mediated via positive effects on skeletal muscle tissue. However, in many cases, it is impossible to separate the effects of muscle size *per se* and the effects from blocking myostatin and activins that might be independent of changes in muscle size. Thus, it is possible that at least some of the positive effects of the treatment, such as the improvement in bone quality in chemotherapy-treated mice and the attenuation of splenomegaly, liver protein synthesis, and anaemia in tumour-bearing mice might be due to the direct effects of myostatin/activin blocking on those (or some other) tissues, instead of being indirectly mediated through increased muscle size. However, the evidence from both human cancer patients (Kazemi-Bajestani, Mazurak & Baracos 2016; Martin et al. 2013; Martin et al.



2015) and from pre-clinical animal studies using different strategies to prevent muscle wasting (Cai et al. 2004; Chiappalupi et al. 2020; Gallot et al. 2014; Hatakeyama et al. 2016; Johnston et al. 2015; Lerner et al. 2016; Pretto et al. 2015; Toledo et al. 2016b; Tseng et al. 2015; Zhou et al. 2010) supports the hypothesis that muscle size plays a role in survival in cachectic conditions. The present study and the related studies by our group specify certain interesting factors that should be addressed in the future investigation of the mechanisms underlying the improved survival due to myostatin/activin blocking and maintenance of muscle mass. These include the roles of vital muscles, such as the diaphragm, hepatic protein synthesis and acute phase response, splenomegaly, anaemia, and muscle NAD<sup>+</sup> metabolism and mTOR localization in cachexia and survival. Finally, the importance of these factors should also be investigated in human cancer patients.

## 6.4 Strengths and limitations

The strengths of this dissertation include the use of different models of muscle wasting, specifically, chemotherapy and cancer cachexia, as well as reduced physical activity and fasting. Thus, the effectiveness of activin receptor ligand blocking to induce muscle growth could be verified in different wasting conditions that might be mediated through different molecular mechanisms. In addition, two different strategies, designed and produced “in house”, were used to block myostatin and activins. On the first hand, the administration of soluble activin receptor type IIB trap (sACVR2B) allowed the investigation of systemic effects of myostatin/activin blocking and the effects of whole-body muscle hypertrophy. On the other hand, the intramuscular AAV-mediated follistatin gene delivery allowed the investigation of muscle-specific effects of myostatin/activin blocking, which also enabled the reduction of both the number of experimental animals used and the variation in the results as the effects of follistatin could be investigated within the same animal by comparison of the contralateral muscles. In addition, broad phenotyping was conducted in combination with the assessment of the effects of physical activity and food intake.

In doxorubicin chemotherapy experiments, different time points were investigated, which provided an idea of both acute and longer-term effects of the treatments. Related to that, one of the strengths was the use of DXA analysis at baseline and at the end of the four-week experiment, which enabled the determination of changes in body composition, namely, lean and fat mass, as well as bone parameters instead of mere endpoint measures of tissue masses. Moreover, this was the first study to explore the combined effects of doxorubicin chemotherapy and the blocking of myostatin and activins, as well as to compare the transcriptomic effects of doxorubicin alone or in combination with myostatin/activin blocking between skeletal muscle and the heart.

In the cancer cachexia survival experiment, the strength was that in addition to the loss of body mass, the humane endpoint criteria included also other

factors describing the overall condition of the mice. If a certain degree of body mass loss is the only endpoint criterion, it is obvious that any treatment able to increase body mass and/or slow down the rate of body mass loss prolongs survival. Moreover, the increase in the mass of some organs, such as the spleen, and ascites observed in some tumour-bearing animals reduces the value of body mass as the only endpoint criterion. That said, the endpoint criteria used in the present study could be optimized further to suit the particular experimental model even better, and to improve the objectivity of the evaluation of the fulfillment of the criteria. To this end, a scoring system based on appearance, behavior and body condition was piloted, and could be used in the possible later survival studies. Additionally, the effect of increasing muscle mass only beforehand via the blocking of myostatin and activins on survival has not been studied before in non-genetic models, and this adds to the novelty of this dissertation.

In the short-term experiment targeting the time point at which loss of body mass predicted survival, many different tissues and factors were analysed in addition to skeletal muscle tissue, giving a broader understanding of the multiorgan effects of both cancer cachexia and the blocking of myostatin and activins, thus providing new insights into the potential mechanisms underlying the improved survival with this kind of therapy. This study also shows the novel result of the colocalisation of mTOR with lysosomes in experimental cancer cachexia and in response to the blocking of myostatin and activins via soluble ACVR2B ligand trap or follistatin gene delivery, shedding more light on the molecular mechanisms of muscle atrophy and hypertrophy, respectively, in those conditions.

One of the major limitations of the present study is that in chemotherapy and cancer cachexia experiments, a group of healthy mice treated only with sACVR2B was not included, except in the acute experiment comparing skeletal muscle and the heart. In some cases, the addition of this group would have helped to determine if sACVR2B counteracted the effects of chemotherapy and/or cancer, or if the effects of sACVR2B took place independent of the effects of chemotherapy and/or cancer. Moreover, in cancer experiments, the addition of a group treated with sACVR2B only after cancer cell injection would have been interesting and potentially provided further value to the study and enabled better comparison with previous studies. Indeed, this experiment has now been conducted after this dissertation, as explained in the discussion. In addition, despite careful determination of the endpoint for the second cancer cachexia experiment, and the clear difference in the survival time between the two sACVR2B treatment protocols, the mechanism underlying the differences in the survival time could not be unambiguously determined based on the findings at the chosen time point. As muscle-specific blockade of myostatin and activins was not possible in the cancer cachexia experiments of the present study, it cannot be known if the non-muscle and survival effects of sACVR2B were due to direct effects of sACVR2B on the non-muscle tissues investigated, or indirect effects via increased muscle size.

In addition, individual food intake and activity data are lacking from chemotherapy and cancer cachexia experiments because these variables were measured from cages that were occupied by 2 to 4 mice from the same experimental group. Thus, these factors could not be correlated with other factors and their contribution to, for example, muscle atrophy, remains more or less at the level of speculation. Given the decreased food intake in both conditions, the addition of a pair-fed control group might have provided more insight into the contribution of the decreased food intake on wasting and alterations in muscle protein synthesis. Moreover, data from grip strength measurements or other muscle function measurements is not included due to unsuccessful measurements and inconsistent results, which may have been affected by the motivation of the mice and the lack of experience in conducting the measurements. Finally, some of the findings related to the activation of different signalling pathways were explorative in nature, and further mechanistic experiments were not conducted based on these findings, apart from the blocking of myostatin and activins.

## 6.5 Future directions

Based on the findings of the present study as well as previous and more recent ones, future studies should aim to elucidate the importance of skeletal muscle tissue *per se* for survival in cancer cachexia via muscle-specific strategies to counteract muscle wasting, such as the muscle-specific blockade of myostatin and activins. Those studies would be able to distinguish between the effects of maintenance of skeletal muscle and the direct effects of, for example, systemic myostatin/activin blocking on non-muscle tissues. Those studies should then be replicated using different tumour models. Moreover, strategies aiming to preserve certain individual muscles or muscle groups, such as the heart or the respiratory muscles, should be developed to be able to assess the importance of these vital muscles with respect to survival.

As there is evidence that the preservation of skeletal muscle mass is beneficial in cancer cachexia, cachexia models better enabling exercise interventions, especially resistance training interventions, should be examined in the future. Furthermore, it would be interesting to investigate the effects of increasing muscle mass before the cachectic stimulus by means of resistance training as opposed to the blocking of myostatin and activins as in the present study.

As it was shown that the colocalisation of mTOR with lysosomes/late endosomes was decreased in cachectic muscle and restored by myostatin/activin blocking, the potential effectiveness of therapies targeting mTOR localization in the prevention of cancer-induced muscle wasting should be studied in the future. Future studies should also aim to further elucidate the mechanism through which the blocking of myostatin and activins increases the colocalisation of mTOR with lysosomes/late endosomes and whether this is required for sACVR2B and follistatin-induced increase in mTORC1 signalling and protein synthesis.

## 7 MAIN FINDINGS AND CONCLUSIONS

The main findings and conclusions of this dissertation are summarized as follows:

1. Doxorubicin chemotherapy causes muscle atrophy that is potentially due to decreased muscle protein synthesis rather than increased protein degradation. In addition, maximal running capacity is impaired by doxorubicin, without marked decreases in mitochondrial markers or capillary density. The blocking of myostatin and activins prevents the doxorubicin-induced muscle atrophy and restores the muscle protein synthesis and bone quality without further damage to skeletal muscle oxidative properties, running capacity, or the antitumour effect of doxorubicin. (I)
2. Despite the comparable levels of atrophy, doxorubicin chemotherapy induces more extensive transcriptomic alterations in skeletal muscle than it does in the heart. This may be due to the greater regenerative capacity of skeletal muscle compared with that of the heart, supported by the up-regulation of *Myod1* mRNA and its target genes in skeletal muscle. The main common pathway induced by chemotherapy in both tissues is the p53-p21-REDD1, indicating a response to DNA-damage, and potentially contributing to the wasting. This response may be attenuated by blocking myostatin and activins, especially in skeletal muscle. All in all, the blocking of myostatin and activins has more pronounced effects on skeletal muscle than it does on the heart, which may at least partially be due to the greater myostatin expression in skeletal muscle. (II)
3. Muscle atrophy associated with cancer cachexia results from the combination of decreased muscle protein synthesis and activation of protein degradation pathways. The decreased muscle protein synthesis in cancer may be due to decreased lysosomal localization of mTOR resulting in attenuated mTORC1 signalling. The blocking of myostatin and activins in-

creases muscle mass and restores the co-localization of mTOR with the lysosomes and mTORC1 signalling in cachectic mice. In addition, the blocking of myostatin and activins improves survival in experimental cancer cachexia but only when the treatment is continued after the induction of cachexia. The prolonged survival may be attributed at least in part to the maintenance of the limb and respiratory muscles, but the observed effects on tissues other than the skeletal muscle suggest that other factors may also play a role in the improved survival. (III)

4. Follistatin gene delivery induces muscle protein synthesis independent of the diurnal fluctuations in physical activity and food intake, or the feeding status. However, the mTORC1 signalling response to follistatin is attenuated by fasting and diurnal decreases in food intake and physical activity. In addition, the follistatin-induced increases in mTORC1 signalling and protein synthesis are accompanied by an increased amount of mTOR co-localized with lysosomes, but not by their translocation towards sarcolemma. (IV)

## YHTEENVETO (FINNISH SUMMARY)

Luurankolihaskudos muodostaa noin 40% kehon kokonaismassasta. Sillä on keskeinen rooli kehon liikkeiden tuottamisessa ja näin ollen päivittäisten askareiden suorittamisessa ja liikunnan harrastamisessa. Luurankolihasia tarvitaan myös hengittämiseen ja luuston ylläpitoon, ja lisäksi ne vaikuttavat keskeisesti koko kehon aineenvaihduntaan.

Lihasmassa vähenee monissa eri sairauksissa, ikääntyessä ja tilanteissa, joissa ravinnonsaanti tai fyysinen aktiivisuus ovat vähentyneet. Sairauksiin liittyvää kuihtumista kutsutaan kakeksiaksi. Kakeksialle tunnusomaista on lihas- ja usein myös rasvamassan menetys sekä elimistön tulehdustila. Kakeksiassa myös monien muiden kudosten toiminta ja elimistön aineenvaihdunta häiriintyvät. Kakeksian on havaittu olevan yhteydessä heikompaan selviytymisennusteeseen sekä fyysisen toimintakyvyn laskuun esimerkiksi syövässä. Lisäksi syöpähoitot, kuten kemoterapia, saattavat pahentaa syöpään liittyvää lihasten merkittävää surkastumista eli lihaskatoa, mikä puolestaan voi altistaa hoitojen haittavaikutuksille ja siten heikentää selviytymisennustetta entisestään. Vaikka kakeksia ja sen yhteys heikentyneeseen selviytymisennusteeseen on ilmiönä tunnettu jo kauan, vasta viime aikoina on alettu tutkia luurankolihaskudoksen ylläpitoon suunnattujen hoitojen vaikutusta kakeksiaan ja selviytymiseen. Tehokasta hoitoa kakeksiaan ei kuitenkaan vielä ole.

Lihasmassaa voidaan kasvattaa ja ylläpitää esimerkiksi estämällä lihas-kasvua hillitseviä tekijöitä, kuten myostatiinia ja aktiviineja. Myostatiinia ja aktiviineja estämällä on pystytty ehkäisemään ja hoitamaan lihaskatoa kokeellisilla syöpämalleilla. Tämän on ollut yhteydessä parempaan selviytymiseen, mikä yhdessä epidemiologisen näytön kanssa viittaa lihasmassan ylläpidon tärkeyteen syövästä selviytymisessä. Paremman selviytymisen taustalla olevia mekanismeja ei kuitenkaan vielä tunneta. Ei myöskään tiedetä, onko lihasmassan kasvatukselta ennen syöpää vastaavaa hyötyä selviytymisen kannalta kuin lihaskadon ehkäisystä. Lisäksi myostatiinin ja aktiviinien eston vaikutuksia kemoterapiaan liittyvässä lihaskadossa ei ole juurikaan tutkittu.

Tämän väitöskirjan tarkoituksena oli tutkia myostatiinin ja aktiviinien eston vaikutuksia luurankolihasien kokoon ja sen säätelyyn sekä lihasmassan ylläpidon tärkeyttä erilaisissa lihaskatotilanteissa, joita olivat syöpä, kemoterapia sekä vähentynyt ravinnonsaanti ja fyysinen aktiivisuus. Väitöskirjassa tarkasteltiin myös syövän ja kemoterapian sekä myostatiinin ja aktiviinien eston vaikutuksia fyysiseen aktiivisuuteen ja suorituskykyyn. Lisäksi tavoitteena oli selvittää myostatiinin ja aktiviinien eston vaikutuksia muihin kudoksiin kuin luurankolihaseseen syövässä ja kemoterapiassa.

Väitöskirjatyö koostui kolmesta erillisestä osatutkimuksesta, joissa myostatiinin ja aktiviinien eston vaikutuksia tutkittiin (1) kemoterapiaa saavilla hiirillä, (2) hiirillä, joille aiheutettiin kokeellinen syöpä ja (3) passiivisilla ja aktiivisilla sekä paastonneilla ja ei-paastonneilla hiirillä. Myostatiinin ja aktiviinien estoon käytettiin kemoterapia- ja syöpäkokeissa liukoista kasvutekijäreseptoria ja viimeisessä osatutkimuksessa follistatiini-geeniterapiaa.

Tutkimuksessa havaittiin, että myostatiinin ja aktiviinien esto ehkäisi sekä kemoterapian että kokeellisen syövän aiheuttaman lihaskadon. Kokeellisessa syövässä tämä oli yhteydessä parempaan selviytymiseen, mutta vain silloin, kun lihaskokoa lisäävää tai ylläpitävää hoitoa jatkettiin myös kasvaimen muodostumisen jälkeen. Selviytymishyötyä ei havaittu ryhmällä, joita hoidettiin myostatiinin ja aktiviinien estäjällä ainoastaan ennen kasvaimen muodostumista. Myostatiinin ja aktiviinien esto ehkäisi kemoterapian aiheuttaman luuntiheyden laskun ja lievensi syöpään liittyvää anemiaa, pernan kasvua sekä maksan proteiinisynteesin nousua, mutta ei vaikuttanut kemoterapian aiheuttamaan juoksukapasiteetin heikkenemiseen eikä fyysisen aktiivisuuden laskuun syövässä.

Luurankolihaksen proteiinisynteesi laski akuutisti kemoterapian vaikutuksesta, ja myostatiinin ja aktiviinien esto ehkäisi tämän laskun. Samoja vaikutuksia ei havaittu sydänlihaksessa. Kaiken kaikkiaan kemoterapian ja myostatiinin ja aktiviinien eston vaikutukset luurankolihaksen geenien ilmentymiseen olivat suurempia kuin vaikutukset sydänlihakseen. Myös syövässä havaittiin proteiinisynteesin lasku sekä luurankolihaksessa, palleassa että sydämessä.

Proteiinisynteesin tärkeän säätelyproteiinin, mTOR:n, solunsisäisen sijainnin on havaittu vaikuttavan sen aktiivisuuteen. Luurankolihaksen proteiinisynteesin lasku syövässä oli yhteydessä vähentyneeseen mTOR:n sijoittumiseen lysosomien läheisyyteen ja mTOR-signaloinnin laskuun. Myostatiinin ja aktiviinien esto palautti mTOR:n sijainnin ja signaloinnin lihassoluissa lähes terveeseen verrokkiryhmän tasolle. Myostatiinin ja aktiviinien esto lisäsi luurankolihaksen proteiinisynteesiä myös terveillä hiirillä riippumatta fyysisen aktiivisuuden ja syömisestä määrästään ja lisäsi mTOR:n sijoittumista lysosomien läheisyyteen paastonneilla ja ei-paastonneilla hiirillä.

Tämä väitöskirja osoittaa, että syöpään liittyvän lihaskadon hoito myostatiinia ja aktiviineja estämällä voi pidentää selviytymistä. Tulosten perusteella näyttäisi myös, että lihaskoon ylläpitäminen voi olla selviytymisen kannalta hyödyllisempää kuin lihassmassan kasvatus ennen syöpää. Lisäksi myostatiinin ja aktiviinien estolla ja sitä myötä lihassmassan ylläpidolla näyttää olevan edullisia vaikutuksia myös muihin kudoksiin kemoterapiaa saavilla ja syöpää sairastavilla hiirillä. Myostatiinin ja aktiviinien eston aikaansaama luurankolihaksen proteiinisynteesin ja mTOR-signaloinnin nousu saattavat osittain selittyä lisääntyneellä mTOR:n sijoittumisella lysosomien läheisyyteen sekä terveessä että kakektisessa lihaksessa. Nämä tulokset lisäävät ymmärrystä luurankolihaskudoksen tärkeydestä sairaustilanteissa, lihaskadon mekanismeista ja mahdollisista uusista lihaskadon hoitomuodoista. Tutkimuksessa käytettyjä hoitomuotoja tulisi tulevaisuudessa tutkia myös ihmispotilailla, jotta tulosten soveltaminen käytäntöön olisi mahdollista.

## REFERENCES

- Acharyya, S., Butchbach, M. E., Sahenk, Z., Wang, H., Saji, M., Carathers, M., Ringel, M. D., Skipworth, R. J. E. Fearon, K. C. H., Hollingsworth, M. A., Muscarella, P., Burghes, A. H. M., Rafael-Fortney, J. A. & Guttridge, D. C. 2005. Dystrophin glycoprotein complex dysfunction: a regulatory link between muscular dystrophy and cancer cachexia. *Cancer cell* 8 (5), 421-432.
- Akpan, I., Goncalves, M. D., Dhir, R., Yin, X., Pistilli, E. E., et al. 2009. The effects of a soluble activin type IIB receptor on obesity and insulin sensitivity. *International journal of obesity* 33 (11), 1265-1273.
- Amirouche, A., Durieux, A. C., Banzet, S., Koulmann, N., Bonnefoy, R., et al. 2009. Down-regulation of Akt/mammalian target of rapamycin signaling pathway in response to myostatin overexpression in skeletal muscle. *Endocrinology* 150 (1), 286-294.
- Amthor, H. & Hoogaars, W. M. 2012. Interference with myostatin/ActRIIB signaling as a therapeutic strategy for Duchenne muscular dystrophy. *Current gene therapy* 12 (3), 245-259.
- Anker, S. D., Ponikowski, P., Varney, S., Chua, T. P., Clark, A. L., et al. 1997. Wasting as independent risk factor for mortality in chronic heart failure. *Lancet* 349 (9058), 1050-1053.
- Areta, J. L., Burke, L. M., Camera, D. M., West, D. W., Crawshay, S., et al. 2014. Reduced resting skeletal muscle protein synthesis is rescued by resistance exercise and protein ingestion following short-term energy deficit. *American journal of physiology. Endocrinology and metabolism* 306 (8), 989-997.
- Arganda-Carreras, I., Kaynig, V., Rueden, C., Eliceiri, K. W., Schindelin, J., et al. 2017. Trainable Weka Segmentation: a machine learning tool for microscopy pixel classification. *Bioinformatics* 33 (15), 2424-2426.
- Argiles, J. M., Busquets, S., Lopez-Soriano, F. J., Costelli, P. & Penna, F. 2012. Are there any benefits of exercise training in cancer cachexia? *Journal of cachexia, sarcopenia and muscle* 3 (2), 73-76.
- Argiles, J. M., Busquets, S., Stemmler, B. & Lopez-Soriano, F. J. 2014. Cancer cachexia: understanding the molecular basis. *Nature reviews. Cancer* 14 (11), 754-762.
- Argiles, J. M., Lopez-Soriano, F. J. & Busquets, S. 2019. Mediators of cachexia in cancer patients. *Nutrition* 66, 11-15.
- Argiles, J. M., Lopez-Soriano, F. J., Stemmler, B. & Busquets, S. 2019. Therapeutic strategies against cancer cachexia. *European journal of translational myology* 29 (1), 7960.
- Argiles, J. M., Stemmler, B., Lopez-Soriano, F. J. & Busquets, S. 2018. Inter-tissue communication in cancer cachexia. *Nature reviews. Endocrinology* 15 (1), 9-20.
- Arthur, S. T., Noone, J. M., Van Doren, B. A., Roy, D. & Blanchette, C. M. 2014. One-year prevalence, comorbidities and cost of cachexia-related inpatient admissions in the USA. *Drugs in context* 3, 212265.



- Attaix, D. & Baracos, V. E. 2010. MAFbx/ Atrogin-1 expression is a poor index of muscle proteolysis. *Current opinion in clinical nutrition and metabolic care* 13 (3), 223-224.
- Attie, K. M., Borgstein, N. G., Yang, Y., Condon, C. H., Wilson, D. M., et al. 2013. A single ascending-dose study of muscle regulator ACE-031 in healthy volunteers. *Muscle & nerve* 47 (3), 416-423.
- Aulino, P., Berardi, E., Cardillo, V. M., Rizzuto, E., Perniconi, B., et al. 2010. Molecular, cellular and physiological characterization of the cancer cachexia-inducing C26 colon carcinoma in mouse. *BMC cancer* 10, 363-363.
- Aversa, Z., Pin, F., Lucia, S., Penna, F., Verzaro, R., et al. 2016. Autophagy is induced in the skeletal muscle of cachectic cancer patients. *Scientific reports* 6, 30340.
- Azoulay, E., Thiery, G., Chevret, S., Moreau, D., Darmon, M., et al. 2004. The prognosis of acute respiratory failure in critically ill cancer patients. *Medicine* 83 (6), 360-370.
- Bachmann, J., Heiligensetzer, M., Krakowski-Roosen, H., Buchler, M. W., Friess, H., et al. 2008. Cachexia worsens prognosis in patients with resectable pancreatic cancer. *Journal of gastrointestinal surgery* 12 (7), 1193-1201.
- Ballaro, R., Beltra, M., De Lucia, S., Pin, F., Ranjbar, K., et al. 2019. Moderate exercise in mice improves cancer plus chemotherapy-induced muscle wasting and mitochondrial alterations. *FASEB journal* 33 (4), 5482-5494.
- Ballaro, R., Costelli, P. & Penna, F. 2016. Animal models for cancer cachexia. *Current opinion in supportive and palliative care* 10 (4), 281-287.
- Baltgalvis, K. A., Berger, F. G., Pena, M. M., Mark Davis, J., White, J. P., et al. 2010. Activity level, apoptosis, and development of cachexia in *Apc*(Min/+) mice. *Journal of applied physiology* 109 (4), 1155-1161.
- Barbe, C., Bray, F., Gueugneau, M., Devassine, S., Lause, P., et al. 2017. Comparative Proteomic and Transcriptomic Analysis of Follistatin-Induced Skeletal Muscle Hypertrophy. *Journal of proteome research* 16 (10), 3477-3490.
- Barber, M. D., Fearon, K. C., McMillan, D. C., Slater, C., Ross, J. A., et al. 2000. Liver export protein synthetic rates are increased by oral meal feeding in weight-losing cancer patients. *American journal of physiology. Endocrinology and metabolism* 279 (3), 707-714.
- Barret, M., Antoun, S., Dalban, C., Malka, D., Mansourbakht, T., et al. 2014. Sarcopenia is linked to treatment toxicity in patients with metastatic colorectal cancer. *Nutrition and cancer* 66 (4), 583-589.
- Barreto, R., Kitase, Y., Matsumoto, T., Pin, F., Colston, K. C., et al. 2017. ACVR2B/Fc counteracts chemotherapy-induced loss of muscle and bone mass. *Scientific reports* 7 (1), 14470-1.
- Barreto, R., Mandili, G., Witzmann, F. A., Novelli, F., Zimmers, T. A., et al. 2016. Cancer and Chemotherapy Contribute to Muscle Loss by Activating Common Signaling Pathways. *Frontiers in physiology* 7, 472.

- Bassett, D. R. & Howley, E. T. 2000. Limiting factors for maximum oxygen uptake and determinants of endurance performance. *Medicine and science in sports and exercise* 32 (1), 70-84.
- Battaglini, C. L., Mills, R. C., Phillips, B. L., Lee, J. T., Story, C. E., et al. 2014. Twenty-five years of research on the effects of exercise training in breast cancer survivors: A systematic review of the literature. *World journal of clinical oncology* 5 (2), 177-190.
- Benny Klimek, M. E., Aydogdu, T., Link, M. J., Pons, M., Koniaris, L. G., et al. 2010. Acute inhibition of myostatin-family proteins preserves skeletal muscle in mouse models of cancer cachexia. *Biochemical and biophysical research communications* 391 (3), 1548-1554.
- Bialek, P., Parkington, J., Li, X., Gavin, D., Wallace, C., et al. 2014. A myostatin and activin decoy receptor enhances bone formation in mice. *Bone* 60, 162-171.
- Bindels, L. B., Neyrinck, A. M., Claus, S. P., Le Roy, C. I., Grangette, C., et al. 2016. Synbiotic approach restores intestinal homeostasis and prolongs survival in leukaemic mice with cachexia. *The ISME journal* 10 (6), 1456-1470.
- Bindels, L. B., Neyrinck, A. M., Loumaye, A., Catry, E., Walgrave, H., et al. 2018. Increased gut permeability in cancer cachexia: mechanisms and clinical relevance. *Oncotarget* 9 (26), 18224-18238.
- Bloise, E., Ciarmela, P., Dela Cruz, C., Luisi, S., Petraglia, F., et al. 2019. Activin A in Mammalian Physiology. *Physiological Reviews* 99 (1), 739-780.
- Bohnert, K. R., Gallot, Y. S., Sato, S., Xiong, G., Hindi, S. M., et al. 2016. Inhibition of ER stress and unfolding protein response pathways causes skeletal muscle wasting during cancer cachexia. *FASEB journal* 30 (9), 3053-3068.
- Bonetto, A., Aydogdu, T., Kunzevitzky, N., Guttridge, D. C., Khuri, S., et al. 2011. STAT3 activation in skeletal muscle links muscle wasting and the acute phase response in cancer cachexia. *PloS one* 6 (7), e22538.
- Bonetto, A., Rupert, J. E., Barreto, R. & Zimmers, T. A. 2016. The Colon-26 Carcinoma Tumor-bearing Mouse as a Model for the Study of Cancer Cachexia. *Journal of visualized experiments* (117), doi 10.3791/54893.
- Bossola, M., Muscaritoli, M., Costelli, P., Grieco, G., Bonelli, G., et al. 2003. Increased muscle proteasome activity correlates with disease severity in gastric cancer patients. *Annals of Surgery* 237 (3), 384-389.
- Braun, T. P., Szumowski, M., Levasseur, P. R., Grossberg, A. J., Zhu, X., et al. 2014. Muscle atrophy in response to cytotoxic chemotherapy is dependent on intact glucocorticoid signaling in skeletal muscle. *PloS one* 9 (9), e106489.
- Breen, L., Stokes, K. A., Churchward-Venne, T. A., Moore, D. R., Baker, S. K., et al. 2013. Two weeks of reduced activity decreases leg lean mass and induces "anabolic resistance" of myofibrillar protein synthesis in healthy elderly. *The Journal of clinical endocrinology and metabolism* 98 (6), 2604-2612.
- Brotto, M. & Bonewald, L. 2015. Bone and muscle: Interactions beyond mechanical. *Bone* 80, 109-114.

- Brown, J. C., Caan, B. J., Meyerhardt, J. A., Weltzien, E., Xiao, J., et al. 2018. The deterioration of muscle mass and radiodensity is prognostic of poor survival in stage I-III colorectal cancer: a population-based cohort study (C-SCANS). *Journal of cachexia, sarcopenia and muscle* 9 (4), 664-672.
- Bruera, E. & Sweeney, C. 2000. Cachexia and asthenia in cancer patients. *The Lancet Oncology* 1, 138-147.
- Busquets, S., Toledo, M., Orpi, M., Massa, D., Porta, M., et al. 2012. Myostatin blockage using actRIIB antagonism in mice bearing the Lewis lung carcinoma results in the improvement of muscle wasting and physical performance. *Journal of cachexia, sarcopenia and muscle* 3 (1), 37-43.
- Cai, D., Frantz, J. D., Tawa, N. E., Melendez, P. A., Oh, B. C., et al. 2004. IKKbeta/NF-kappaB activation causes severe muscle wasting in mice. *Cell* 119 (2), 285-298.
- Camus, V., Lanic, H., Kraut, J., Modzelewski, R., Clatot, F., et al. 2014. Prognostic impact of fat tissue loss and cachexia assessed by computed tomography scan in elderly patients with diffuse large B-cell lymphoma treated with immunochemotherapy. *European journal of haematology* 93 (1), 9-18.
- Caro, J. J., Salas, M., Ward, A. & Goss, G. 2001. Anemia as an independent prognostic factor for survival in patients with cancer: a systemic, quantitative review. *Cancer* 91 (12), 2214-2221.
- Chen, J. L., Colgan, T. D., Walton, K. L., Gregorevic, P. & Harrison, C. A. 2016. The TGF-beta Signalling Network in Muscle Development, Adaptation and Disease. *Advances in Experimental Medicine and Biology* 900, 97-131.
- Chen, J. L., Walton, K. L., Hagg, A., Colgan, T. D., Johnson, K., et al. 2017. Specific targeting of TGF-beta family ligands demonstrates distinct roles in the regulation of muscle mass in health and disease. *Proceedings of the National Academy of Sciences of the United States of America* 114 (26), E5266-E5275.
- Chen, J. L., Walton, K. L., Winbanks, C. E., Murphy, K. T., Thomson, R. E., et al. 2014. Elevated expression of activins promotes muscle wasting and cachexia. *FASEB journal* 28 (4), 1711-1723.
- Chen, M. C., Chen, Y. L., Lee, C. F., Hung, C. H. & Chou, T. C. 2015. Supplementation of Magnolol Attenuates Skeletal Muscle Atrophy in Bladder Cancer-Bearing Mice Undergoing Chemotherapy via Suppression of FoxO3 Activation and Induction of IGF-1. *PloS one* 10 (11), e0143594.
- Chiappalupi, S., Sorci, G., Vukasinovic, A., Salvadori, L., Sagheddu, R., et al. 2020. Targeting RAGE prevents muscle wasting and prolongs survival in cancer cachexia. *Journal of cachexia, sarcopenia and muscle* 11 (4), 929-946.
- Chu, M. P., Lieffers, J., Ghosh, S., Belch, A., Chua, N. S., et al. 2017. Skeletal muscle density is an independent predictor of diffuse large B-cell lymphoma outcomes treated with rituximab-based chemoimmunotherapy. *Journal of cachexia, sarcopenia and muscle* 8 (2), 298-304.
- Collins-Hooper, H., Sartori, R., Giallourou, N., Matsakas, A., Mitchell, R., et al. 2015. Symmorphosis through dietary regulation: a combinatorial role for

- proteolysis, autophagy and protein synthesis in normalising muscle metabolism and function of hypertrophic mice after acute starvation. *PloS one* 10 (3), e0120524.
- Cooper, A. B., Slack, R., Fogelman, D., Holmes, H. M., Petzel, M., et al. 2015. Characterization of Anthropometric Changes that Occur During Neoadjuvant Therapy for Potentially Resectable Pancreatic Cancer. *Annals of surgical oncology* 22 (7), 2416-2423.
- Cooper, R., Kuh, D., Hardy, R., Mortality Review Group & FALCon and HALCyon Study Teams 2010. Objectively measured physical capability levels and mortality: systematic review and meta-analysis. *British Medical Journal* 341, c4467.
- Corbett, T. H., Griswold, D. P., Roberts, B. J., Peckham, J. C. & Schabel, F. M. 1975. Tumor induction relationships in development of transplantable cancers of the colon in mice for chemotherapy assays, with a note on carcinogen structure. *Cancer research* 35 (9), 2434-2439.
- Costelli, P., Carbo, N., Tessitore, L., Bagby, G. J., Lopez-Soriano, F. J., et al. 1993. Tumor necrosis factor-alpha mediates changes in tissue protein turnover in a rat cancer cachexia model. *The Journal of clinical investigation* 92 (6), 2783-2789.
- Costes, S. V., Daelemans, D., Cho, E. H., Dobbin, Z., Pavlakis, G., et al. 2004. Automatic and quantitative measurement of protein-protein colocalization in live cells. *Biophysical journal* 86 (6), 3993-4003.
- Counts, B. R., Hardee, J. P., Fix, D. K., Vanderveen, B. N., Montalvo, R. N., et al. 2020. Cachexia Disrupts Diurnal Regulation of Activity, Feeding, and Muscle Mechanistic Target of Rapamycin Complex 1 in Mice. *Medicine and science in sports and exercise* 52 (3), 577-587.
- Courneya, K. S. & Friedenreich, C. M. 1997. Relationship between exercise pattern across the cancer experience and current quality of life in colorectal cancer survivors. *Journal of alternative and complementary medicine* 3 (3), 215-226.
- Courneya, K. S., Segal, R. J., Mackey, J. R., Gelmon, K., Reid, R. D., et al. 2007. Effects of aerobic and resistance exercise in breast cancer patients receiving adjuvant chemotherapy: a multicenter randomized controlled trial. *Journal of clinical oncology* 25 (28), 4396-4404.
- Courneya, K. S., Sellar, C. M., Stevinson, C., McNeely, M. L., Peddle, C. J., et al. 2009. Randomized controlled trial of the effects of aerobic exercise on physical functioning and quality of life in lymphoma patients. *Journal of clinical oncology* 27 (27), 4605-4612.
- Courneya, K. S. & Friedenreich, C. M. 1998. Relationship Between Exercise During Treatment and Current Quality of Life Among Survivors of Breast Cancer. *Journal of Psychosocial Oncology* 15 (3-4), 35-57.
- Crowgey, T., Peters, K. B., Hornsby, W. E., Lane, A., McSherry, F., et al. 2014. Relationship between exercise behavior, cardiorespiratory fitness, and cognitive function in early breast cancer patients treated with doxorubicin-

- containing chemotherapy: a pilot study. *Applied physiology, nutrition, and metabolism* 39 (6), 724-729.
- Cuenca, A. G., Cuenca, A. L., Winfield, R. D., Joiner, D. N., Gentile, L., et al. 2014. Novel role for tumor-induced expansion of myeloid-derived cells in cancer cachexia. *Journal of immunology* 192 (12), 6111-6119.
- Dahele, M., Skipworth, R. J., Wall, L., Voss, A., Preston, T., et al. 2007. Objective physical activity and self-reported quality of life in patients receiving palliative chemotherapy. *Journal of pain and symptom management* 33 (6), 676-685.
- Dalal, S., Hui, D., Bidaut, L., Lem, K., Del Fabbro, E., et al. 2012. Relationships among body mass index, longitudinal body composition alterations, and survival in patients with locally advanced pancreatic cancer receiving chemoradiation: a pilot study. *Journal of pain and symptom management* 44 (2), 181-191.
- Danai, L. V., Babic, A., Rosenthal, M. H., Dennstedt, E. A., Muir, A., et al. 2018. Altered exocrine function can drive adipose wasting in early pancreatic cancer. *Nature* 558 (7711), 600-604.
- Das, S. K., Eder, S., Schauer, S., Diwoky, C., Temmel, H., et al. 2011. Adipose triglyceride lipase contributes to cancer-associated cachexia. *Science* 333 (6039), 233-238.
- de Lima Junior, E. A., Yamashita, A. S., Pimentel, G. D., De Sousa, L. G., Santos, R. V., et al. 2016. Doxorubicin caused severe hyperglycaemia and insulin resistance, mediated by inhibition in AMPk signalling in skeletal muscle. *Journal of cachexia, sarcopenia and muscle* 7 (5), 615-625.
- Delitto, D., Judge, S. M., Delitto, A. E., Nosacka, R. L., Rocha, F. G., et al. 2017. Human pancreatic cancer xenografts recapitulate key aspects of cancer cachexia. *Oncotarget* 8 (1), 1177-1189.
- Demark-Wahnefried, W., Hars, V., Conaway, M. R., Havlin, K., Rimer, B. K., et al. 1997. Reduced rates of metabolism and decreased physical activity in breast cancer patients receiving adjuvant chemotherapy. *The American Journal of Clinical Nutrition* 65 (5), 1495-1501.
- Demetriades, C., Doumpas, N. & Teleman, A. A. 2014. Regulation of TORC1 in response to amino acid starvation via lysosomal recruitment of TSC2. *Cell* 156 (4), 786-799.
- Deutz, N. E., Safar, A., Schutzler, S., Memelink, R., Ferrando, A., et al. 2011. Muscle protein synthesis in cancer patients can be stimulated with a specially formulated medical food. *Clinical nutrition* 30 (6), 759-768.
- Dewys, W. D., Begg, C., Lavin, P. T., Band, P. R., Bennett, J. M., et al. 1980. Prognostic effect of weight loss prior to chemotherapy in cancer patients. Eastern Cooperative Oncology Group. *The American Journal of Medicine* 69 (4), 491-497.
- Di Sebastiano, K. M., Yang, L., Zbuk, K., Wong, R. K., Chow, T., et al. 2013. Accelerated muscle and adipose tissue loss may predict survival in pancreatic cancer patients: the relationship with diabetes and anaemia. *The British journal of nutrition* 109 (2), 302-312.

- Dimeo, F., Stieglitz, R. D., Novelli-Fischer, U., Fetscher, S., Mertelsmann, R., et al. 1997. Correlation between physical performance and fatigue in cancer patients. *Annals of oncology* 8 (12), 1251-1255.
- D'Lugos, A. C., Fry, C. S., Ormsby, J. C., Sweeney, K. R., Brightwell, C. R., et al. 2019. Chronic doxorubicin administration impacts satellite cell and capillary abundance in a muscle-specific manner. *Physiological reports* 7 (7), e14052.
- Doroshov, J. H., Tallent, C. & Schechter, J. E. 1985. Ultrastructural features of Adriamycin-induced skeletal and cardiac muscle toxicity. *The American journal of pathology* 118 (2), 288-297.
- Dos Santos, W D N, Gentil, P., de Moraes, R. F., Ferreira Junior, J. B., Campos, M. H., et al. 2017. Chronic Effects of Resistance Training in Breast Cancer Survivors. *BioMed research international* 2017, 8367803.
- Doyle, C., Kushi, L. H., Byers, T., Courneya, K. S., Demark-Wahnefried, W., et al. 2006. Nutrition and physical activity during and after cancer treatment: an American Cancer Society guide for informed choices. *CA: a cancer journal for clinicians* 56 (6), 323-353.
- Durieux, A. C., Amirouche, A., Banzet, S., Koulmann, N., Bonnefoy, R., et al. 2007. Ectopic expression of myostatin induces atrophy of adult skeletal muscle by decreasing muscle gene expression. *Endocrinology* 148 (7), 3140-3147.
- Dworzak, F., Ferrari, P., Gavazzi, C., Maiorana, C. & Bozzetti, F. 1998. Effects of cachexia due to cancer on whole body and skeletal muscle protein turnover. *Cancer* 82 (1), 42-48.
- Eley, H. L., Russell, S. T. & Tisdale, M. J. 2007. Effect of branched-chain amino acids on muscle atrophy in cancer cachexia. *The Biochemical journal* 407 (1), 113-120.
- Elkasrawy, M. N. & Hamrick, M. W. 2010. Myostatin (GDF-8) as a key factor linking muscle mass and bone structure. *Journal of Musculoskeletal & Neuronal Interactions* 10 (1), 56-63.
- Emery, P. W., Edwards, R. H., Rennie, M. J., Souhami, R. L. & Halliday, D. 1984. Protein synthesis in muscle measured in vivo in cachectic patients with cancer. *British medical journal* 289 (6445), 584-586.
- Emery, P. W., Lovell, L. & Rennie, M. J. 1984. Protein synthesis measured in vivo in muscle and liver of cachectic tumor-bearing mice. *Cancer research* 44 (7), 2779-2784.
- Engelen, M. P., van der Meij, B. S. & Deutz, N. E. 2016. Protein anabolic resistance in cancer: does it really exist? *Current opinion in clinical nutrition and metabolic care* 19 (1), 39-47.
- Ertunc, M., Sara, Y., Korkusuz, P. & Onur, R. 2009. Differential contractile impairment of fast- and slow-twitch skeletal muscles in a rat model of doxorubicin-induced congestive heart failure. *Pharmacology* 84 (4), 240-248.
- Fabris, S. & MacLean, D. A. 2018. Doxorubicin chemotherapy affects the intracellular and interstitial free amino acid pools in skeletal muscle. *PloS one* 13 (4), e0195330.

- Fanzani, A., Conraads, V. M., Penna, F. & Martinet, W. 2012. Molecular and cellular mechanisms of skeletal muscle atrophy: an update. *Journal of cachexia, sarcopenia and muscle* 3 (3), 163-179.
- Fearon, K. C. 2008. Cancer cachexia: developing multimodal therapy for a multidimensional problem. *European journal of cancer* 44 (8), 1124-1132.
- Fearon, K. C., Glass, D. J. & Guttridge, D. C. 2012. Cancer cachexia: mediators, signaling, and metabolic pathways. *Cell metabolism* 16 (2), 153-166.
- Fearon, K., Arends, J. & Baracos, V. 2013. Understanding the mechanisms and treatment options in cancer cachexia. *Nature reviews. Clinical oncology* 10 (2), 90-99.
- Fearon, K., Strasser, F., Anker, S. D., Bosaeus, I., Bruera, E., et al. 2011. Definition and classification of cancer cachexia: an international consensus. *The Lancet Oncology* 12 (5), 489-495.
- Fogelman, D. R., Holmes, H., Mohammed, K., Katz, M. H., Prado, C. M., et al. 2014. Does IGFR1 inhibition result in increased muscle mass loss in patients undergoing treatment for pancreatic cancer? *Journal of cachexia, sarcopenia and muscle* 5 (4), 307-313.
- Fontes-Oliveira, C. C., Busquets, S., Toledo, M., Penna, F., Paz Aylwin, M., et al. 2013. Mitochondrial and sarcoplasmic reticulum abnormalities in cancer cachexia: altered energetic efficiency? *Biochimica et biophysica acta* 1830 (3), 2770-2778.
- Fouladiun, M., Korner, U., Gunnebo, L., Sixt-Ammilon, P., Bosaeus, I., et al. 2007. Daily physical-rest activities in relation to nutritional state, metabolism, and quality of life in cancer patients with progressive cachexia. *Clinical cancer research* 13 (21), 6379-6385.
- Freireich, E. J., Gehan, E. A., Rall, D. P., Schmidt, L. H. & Skipper, H. E. 1966. Quantitative comparison of toxicity of anticancer agents in mouse, rat, hamster, dog, monkey, and man. *Cancer chemotherapy reports. Part 1* 50 (4), 219-244.
- Friedenreich, C. M., Neilson, H. K., Farris, M. S. & Courneya, K. S. 2016. Physical Activity and Cancer Outcomes: A Precision Medicine Approach. *Clinical cancer research* 22 (19), 4766-4775.
- Frontera, W. R. & Ochala, J. 2015. Skeletal muscle: a brief review of structure and function. *Calcified tissue international* 96 (3), 183-195.
- Gallagher, I. J., Jacobi, C., Tardif, N., Rooyackers, O. & Fearon, K. 2016. Omics/systems biology and cancer cachexia. *Seminars in cell & developmental biology* 54, 92-103.
- Gallot, Y. S., Durieux, A. C., Castells, J., Desgeorges, M. M., Vernus, B., et al. 2014. Myostatin gene inactivation prevents skeletal muscle wasting in cancer. *Cancer research* 74 (24), 7344-7356.
- Genton, L., Mareschal, J., Charretier, Y., Lazarevic, V., Bindels, L. B., et al. 2019. Targeting the Gut Microbiota to Treat Cachexia. *Frontiers in cellular and infection microbiology* 9, 305.
- Gilliam, L. A. A., Fisher-Wellman, K. H., Lin, C. T., Maples, J. M., Cathey, B. L., et al. 2013. The anticancer agent doxorubicin disrupts mitochondrial

- energy metabolism and redox balance in skeletal muscle. *Free radical biology & medicine* 65, 988-996.
- Gilliam, L. A., Ferreira, L. F., Bruton, J. D., Moylan, J. S., Westerblad, H., et al. 2009. Doxorubicin acts through tumor necrosis factor receptor subtype 1 to cause dysfunction of murine skeletal muscle. *Journal of applied physiology* 107 (6), 1935-1942.
- Gilliam, L. A., Lark, D. S., Reese, L. R., Torres, M. J., Ryan, T. E., et al. 2016. Targeted overexpression of mitochondrial catalase protects against cancer chemotherapy-induced skeletal muscle dysfunction. *American journal of physiology. Endocrinology and metabolism* 311 (2), 293-301.
- Gilliam, L. A., Moylan, J. S., Callahan, L. A., Sumandea, M. P. & Reid, M. B. 2011a. Doxorubicin causes diaphragm weakness in murine models of cancer chemotherapy. *Muscle & nerve* 43 (1), 94-102.
- Gilliam, L. A., Moylan, J. S., Ferreira, L. F. & Reid, M. B. 2011b. TNF/TNFR1 signaling mediates doxorubicin-induced diaphragm weakness. *American journal of physiology. Lung cellular and molecular physiology* 300 (2), 225-231.
- Gilliam, L. A., Moylan, J. S., Patterson, E. W., Smith, J. D., Wilson, A. S., et al. 2012. Doxorubicin acts via mitochondrial ROS to stimulate catabolism in C2C12 myotubes. *American journal of physiology. Cell physiology* 302 (1), 195-202.
- Gilliam, L. A. & St Clair, D. K. 2011. Chemotherapy-induced weakness and fatigue in skeletal muscle: the role of oxidative stress. *Antioxidants & redox signaling* 15 (9), 2543-2563.
- Gilson, H., Schakman, O., Kalista, S., Lause, P., Tsuchida, K., et al. 2009. Follistatin induces muscle hypertrophy through satellite cell proliferation and inhibition of both myostatin and activin. *American journal of physiology. Endocrinology and metabolism* 297 (1), 157-164.
- Giovannucci, E. L., Liu, Y., Leitzmann, M. F., Stampfer, M. J. & Willett, W. C. 2005. A prospective study of physical activity and incident and fatal prostate cancer. *Archives of Internal Medicine* 165 (9), 1005-1010.
- Glover, E. I., Phillips, S. M., Oates, B. R., Tang, J. E., Tarnopolsky, M. A., et al. 2008. Immobilization induces anabolic resistance in human myofibrillar protein synthesis with low and high dose amino acid infusion. *The Journal of physiology* 586 (24), 6049-6061.
- Go, K. L., Delitto, D., Judge, S. M., Gerber, M. H., George, T. J., et al. 2017. Orthotopic Patient-Derived Pancreatic Cancer Xenografts Engraft Into the Pancreatic Parenchyma, Metastasize, and Induce Muscle Wasting to Recapitulate the Human Disease. *Pancreas* 46 (6), 813-819.
- Goodman, C. A. 2019. Role of mTORC1 in mechanically induced increases in translation and skeletal muscle mass. *Journal of applied physiology* 127 (2), 581-590.
- Goodman, C. A., Hornberger, T. A. & Robling, A. G. 2015. Bone and skeletal muscle: Key players in mechanotransduction and potential overlapping mechanisms. *Bone* 80, 24-36.



- Goodman, C. A., Mabrey, D. M., Frey, J. W., Miu, M. H., Schmidt, E. K., et al. 2011. Novel insights into the regulation of skeletal muscle protein synthesis as revealed by a new nonradioactive in vivo technique. *FASEB journal* 25 (3), 1028-1039.
- Gordon, B. S., Kelleher, A. R. & Kimball, S. R. 2013. Regulation of muscle protein synthesis and the effects of catabolic states. *The international journal of biochemistry & cell biology* 45 (10), 2147-2157.
- Gordon, B. S., Williamson, D. L., Lang, C. H., Jefferson, L. S. & Kimball, S. R. 2015. Nutrient-induced stimulation of protein synthesis in mouse skeletal muscle is limited by the mTORC1 repressor REDD1. *The Journal of nutrition* 145 (4), 708-713.
- Gospillou, G., Scheede-Bergdahl, C., Spendiff, S., Vuda, M., Meehan, B., et al. 2015. Anthracycline-containing chemotherapy causes long-term impairment of mitochondrial respiration and increased reactive oxygen species release in skeletal muscle. *Scientific reports* 5, 8717.
- Grobet, L., Martin, L. J., Poncelet, D., Pirottin, D., Brouwers, B., et al. 1997. A deletion in the bovine myostatin gene causes the double-muscling phenotype in cattle. *Nature genetics* 17 (1), 71-74.
- Guo, C. B., Zhang, W., Ma, D. Q., Zhang, K. H. & Huang, J. Q. 1996. Hand grip strength: an indicator of nutritional state and the mix of postoperative complications in patients with oral and maxillofacial cancers. *The British journal of oral & maxillofacial surgery* 34 (4), 325-327.
- Haidet, A. M., Rizo, L., Handy, C., Umapathi, P., Eagle, A., et al. 2008. Long-term enhancement of skeletal muscle mass and strength by single gene administration of myostatin inhibitors. *Proceedings of the National Academy of Sciences of the United States of America* 105 (11), 4318-4322.
- Hammers, D. W., Merscham-Banda, M., Hsiao, J. Y., Engst, S., Hartman, J. J., et al. 2017. Supraphysiological levels of GDF11 induce striated muscle atrophy. *EMBO molecular medicine* 9 (4), 531-544.
- Han, H. Q., Zhou, X., Mitch, W. E. & Goldberg, A. L. 2013. Myostatin/activin pathway antagonism: molecular basis and therapeutic potential. *The international journal of biochemistry & cell biology* 45 (10), 2333-2347.
- Han, X., Moller, L. L. V., De Groote, E., Bojsen-Moller, K. N., Davey, J., et al. 2019. Mechanisms involved in follistatin-induced hypertrophy and increased insulin action in skeletal muscle. *Journal of cachexia, sarcopenia and muscle* 10 (6), 1241-1257.
- Han, Y. Q., Ming, S. L., Wu, H. T., Zeng, L., Ba, G., et al. 2018. Myostatin knockout induces apoptosis in human cervical cancer cells via elevated reactive oxygen species generation. *Redox biology* 19, 412-428.
- Hardee, J. P., Montalvo, R. N. & Carson, J. A. 2017. Linking Cancer Cachexia-Induced Anabolic Resistance to Skeletal Muscle Oxidative Metabolism. *Oxidative medicine and cellular longevity* 2017, 8018197.
- Hardee, J. P., Porter, R. R., Sui, X., Archer, E., Lee, I. M., et al. 2014. The effect of resistance exercise on all-cause mortality in cancer survivors. *Mayo Clinic proceedings* 89 (8), 1108-1115.

- Harimoto, N., Shirabe, K., Yamashita, Y. I., Ikegami, T., Yoshizumi, T., et al. 2013. Sarcopenia as a predictor of prognosis in patients following hepatectomy for hepatocellular carcinoma. *The British journal of surgery* 100 (11), 1523-1530.
- Hatakeyama, S., Summermatter, S., Jourdain, M., Melly, S., Minetti, G. C., et al. 2016. ActRII blockade protects mice from cancer cachexia and prolongs survival in the presence of anti-cancer treatments. *Skeletal muscle* 6, 26-2. eCollection 2016.
- Hayward, R., Iwaniec, U. T., Turner, R. T., Lien, C. Y., Jensen, B. T., et al. 2013. Voluntary wheel running in growing rats does not protect against doxorubicin-induced osteopenia. *Journal of pediatric hematology/oncology* 35 (4), 144.
- Hentila, J., Nissinen, T. A., Korkmaz, A., Lensu, S., Silvennoinen, M., et al. 2019. Activin Receptor Ligand Blocking and Cancer Have Distinct Effects on Protein and Redox Homeostasis in Skeletal Muscle and Liver. *Frontiers in physiology* 9, 1917.
- Herremans, K. M., Riner, A. N., Cameron, M. E. & Trevino, J. G. 2019. The Microbiota and Cancer Cachexia. *International journal of molecular sciences* 20 (24), 10.3390/ijms20246267.
- Hershey, J. W., Sonenberg, N. & Mathews, M. B. 2012. Principles of translational control: an overview. *Cold Spring Harbor perspectives in biology* 4 (12), doi 10.1101/cshperspect.a011528.
- Hiensch, A. E., Bolam, K. A., Mijwel, S., Jeneson, J. A. L., Huitema, A. D. R., et al. 2019. Doxorubicin-induced skeletal muscle atrophy: Elucidating the underlying molecular pathways. *Acta physiologica*, e13400.
- Hoda, M. A., Rozsas, A., Lang, E., Klikovits, T., Lohinai, Z., et al. 2016. High circulating activin A level is associated with tumor progression and predicts poor prognosis in lung adenocarcinoma. *Oncotarget* 7 (12), 13388-13399.
- Hodson, N. & Philp, A. 2019. The Importance of mTOR Trafficking for Human Skeletal Muscle Translational Control. *Exercise and sport sciences reviews* 47 (1), 46-53.
- Holmes, M. D., Chen, W. Y., Feskanich, D., Kroenke, C. H. & Colditz, G. A. 2005. Physical activity and survival after breast cancer diagnosis. *JAMA* 293 (20), 2479-2486.
- Hoogaars, W. M., Mouisel, E., Pasternack, A., Hulmi, J. J., Relizani, K., et al. 2012. Combined effect of AAV-U7-induced dystrophin exon skipping and soluble activin Type IIB receptor in mdx mice. *Human Gene Therapy* 23 (12), 1269-1279.
- Horstman, A. M., Olde Damink, S. W., Schols, A. M. & van Loon, L. J. 2016. Is Cancer Cachexia Attributed to Impairments in Basal or Postprandial Muscle Protein Metabolism? *Nutrients* 8 (8), 10.3390/nu8080499.
- Hulmi, J. J., Oliveira, B. M., Silvennoinen, M., Hoogaars, W. M., Ma, H., Pierre, P., Pasternack, A., Kainulainen, H. & Ritvos, O. 2013a. Muscle protein synthesis, mTORC1/MAPK/Hippo signaling, and capillary density are

- altered by blocking of myostatin and activins. *American journal of physiology. Endocrinology and metabolism* 304 (1), 41-50.
- Hulmi, J. J., Oliveira, B. M., Silvennoinen, M., Hoogaars, W. M., Pasternack, A., Kainulainen, H. & Ritvos, O. 2013b. Exercise restores decreased physical activity levels and increases markers of autophagy and oxidative capacity in myostatin/activin-blocked mdx mice. *American journal of physiology. Endocrinology and metabolism* 305 (2), 171-182.
- Hulmi, J. J., Penna, F., Pollanen, N., Nissinen, T. A., Hentila, J., Euro, L., Lautaoja, J. H., Ballaro, R., Soliymani, R., Baumann, M., Ritvos, O., Pirinen, E. & Lalowski, M. 2020. Muscle NAD(+) depletion and Serpina3n as molecular determinants of murine cancer cachexia-the effects of blocking myostatin and activins. *Molecular metabolism* 41, 101046.
- Hulmi, J. J., Silvennoinen, M., Lehti, M., Kivelä, R. & Kainulainen, H. 2012. Altered REDD1, myostatin, and Akt/mTOR/FoxO/MAPK signaling in streptozotocin-induced diabetic muscle atrophy. *American journal of physiology. Endocrinology and metabolism* 302 (3), 307-315.
- Hydock, D. S., Lien, C. Y., Jensen, B. T., Schneider, C. M. & Hayward, R. 2011. Characterization of the effect of in vivo doxorubicin treatment on skeletal muscle function in the rat. *Anticancer Research* 31 (6), 2023-2028.
- Ibrahim, E. M. & Al-Homaidh, A. 2011. Physical activity and survival after breast cancer diagnosis: meta-analysis of published studies. *Medical oncology* 28 (3), 753-765.
- Ichikawa, Y., Ghanefar, M., Bayeva, M., Wu, R., Khechaduri, A., et al. 2014. Cardiotoxicity of doxorubicin is mediated through mitochondrial iron accumulation. *The Journal of clinical investigation* 124 (2), 617-630.
- Iritani, S., Imai, K., Takai, K., Hanai, T., Ideta, T., et al. 2015. Skeletal muscle depletion is an independent prognostic factor for hepatocellular carcinoma. *Journal of gastroenterology* 50 (3), 323-332.
- Irwin, M. L., Crumley, D., McTiernan, A., Bernstein, L., Baumgartner, R., et al. 2003. Physical activity levels before and after a diagnosis of breast carcinoma: the Health, Eating, Activity, and Lifestyle (HEAL) study. *Cancer* 97 (7), 1746-1757.
- Jacobs, B. L., Goodman, C. A. & Hornberger, T. A. 2014. The mechanical activation of mTOR signaling: an emerging role for late endosome/lysosomal targeting. *Journal of muscle research and cell motility* 35 (1), 11-21.
- Jacobs, B. L., You, J. S., Frey, J. W., Goodman, C. A., Gundermann, D. M., et al. 2013. Eccentric contractions increase the phosphorylation of tuberous sclerosis complex-2 (TSC2) and alter the targeting of TSC2 and the mechanistic target of rapamycin to the lysosome. *The Journal of physiology* 591 (18), 4611-4620.
- Janky, R., Verfaillie, A., Imrichova, H., Van de Sande, B., Standaert, L., et al. 2014. iRegulon: from a gene list to a gene regulatory network using large motif and track collections. *PLoS computational biology* 10 (7), e1003731.

- Järvinen, T., Ilonen, I., Kauppi, J., Salo, J. & Räsänen, J. 2018. Loss of skeletal muscle mass during neoadjuvant treatments correlates with worse prognosis in esophageal cancer: a retrospective cohort study. *World journal of surgical oncology* 16 (1), 27-4.
- Järvinen, T., Ilonen, I., Kauppi, J., Volmonen, K., Salo, J., et al. 2018. Low skeletal muscle mass in stented esophageal cancer predicts poor survival: A retrospective observational study. *Thoracic cancer* 9 (11), 1429-1436.
- Jiang, Y., Guo, C., Zhang, D., Zhang, J., Wang, X., et al. 2014. The altered tight junctions: an important gateway of bacterial translocation in cachexia patients with advanced gastric cancer. *Journal of interferon & cytokine research* 34 (7), 518-525.
- Joglekar, S., Asghar, A., Mott, S. L., Johnson, B. E., Button, A. M., et al. 2015. Sarcopenia is an independent predictor of complications following pancreatectomy for adenocarcinoma. *Journal of surgical oncology* 111 (6), 771-775.
- Johnston, A. J., Murphy, K. T., Jenkinson, L., Laine, D., Emmrich, K., et al. 2015. Targeting of Fn14 Prevents Cancer-Induced Cachexia and Prolongs Survival. *Cell* 162 (6), 1365-1378.
- Jones, L. W., Eves, N. D., Courneya, K. S., Chiu, B. K., Baracos, V. E., et al. 2005. Effects of exercise training on antitumor efficacy of doxorubicin in MDA-MB-231 breast cancer xenografts. *Clinical cancer research* 11 (18), 6695-6698.
- Kainulainen, H., Papaioannou, K. G., Silvennoinen, M., Autio, R., Saarela, J., et al. 2015. Myostatin/activin blocking combined with exercise reconditions skeletal muscle expression profile of mdx mice. *Molecular and cellular endocrinology* 399, 131-142.
- Kalantar-Zadeh, K., Rhee, C., Sim, J. J., Stenvinkel, P., Anker, S. D., et al. 2013. Why cachexia kills: examining the causality of poor outcomes in wasting conditions. *Journal of cachexia, sarcopenia and muscle* 4 (2), 89-94.
- Kalantar-Zadeh, K., Streja, E., Kovesdy, C. P., Oreopoulos, A., Noori, N., et al. 2010. The obesity paradox and mortality associated with surrogates of body size and muscle mass in patients receiving hemodialysis. *Mayo Clinic proceedings* 85 (11), 991-1001.
- Kallio, M. A., Tuimala, J. T., Hupponen, T., Klemela, P., Gentile, M., et al. 2011. Chipster: user-friendly analysis software for microarray and other high-throughput data. *BMC genomics* 12, 507-507.
- Kambadur, R., Sharma, M., Smith, T. P. & Bass, J. J. 1997. Mutations in myostatin (GDF8) in double-musled Belgian Blue and Piedmontese cattle. *Genome research* 7 (9), 910-916.
- Kavazis, A. N., Smuder, A. J., Min, K., Tumer, N. & Powers, S. K. 2010. Short-term exercise training protects against doxorubicin-induced cardiac mitochondrial damage independent of HSP72. *American journal of physiology. Heart and circulatory physiology* 299 (5), 1515-1524.
- Kays, J. K., Shahda, S., Stanley, M., Bell, T. M., O'Neill, B. H., et al. 2018. Three cachexia phenotypes and the impact of fat-only loss on survival in

- FOLFIRINOX therapy for pancreatic cancer. *Journal of cachexia, sarcopenia and muscle* 9 (4), 673-684.
- Kazemi-Bajestani, S. M., Mazurak, V. C. & Baracos, V. 2016. Computed tomography-defined muscle and fat wasting are associated with cancer clinical outcomes. *Seminars in cell & developmental biology* 54, 2-10.
- Kelleher, A. R., Kimball, S. R., Dennis, M. D., Schilder, R. J. & Jefferson, L. S. 2013. The mTORC1 signaling repressors REDD1/2 are rapidly induced and activation of p70S6K1 by leucine is defective in skeletal muscle of an immobilized rat hindlimb. *American journal of physiology. Endocrinology and metabolism* 304 (2), 229-236.
- Kivelä, R., Bry, M., Robciuc, M. R., Räsänen, M., Taavitsainen, M., et al. 2014. VEGF-B-induced vascular growth leads to metabolic reprogramming and ischemia resistance in the heart. *EMBO molecular medicine* 6 (3), 307-321.
- Klionsky, D. J., Abdelmohsen, K., Abe, A., Abedin, M. J., Abeliovich, H., et al. 2016. Guidelines for the use and interpretation of assays for monitoring autophagy (3rd edition). *Autophagy* 12 (1), 1-222.
- Knols, R., Aaronson, N. K., Uebelhart, D., Fransen, J. & Aufdemkampe, G. 2005. Physical exercise in cancer patients during and after medical treatment: a systematic review of randomized and controlled clinical trials. *Journal of clinical oncology* 23 (16), 3830-3842.
- Korolchuk, V. I., Saiki, S., Lichtenberg, M., Siddiqi, F. H., Roberts, E. A., et al. 2011. Lysosomal positioning coordinates cellular nutrient responses. *Nature cell biology* 13 (4), 453-460.
- Kota, J., Handy, C. R., Haidet, A. M., Montgomery, C. L., Eagle, A., et al. 2009. Follistatin gene delivery enhances muscle growth and strength in nonhuman primates. *Science translational medicine* 1 (6), 6ra15.
- Krawiec, B. J., Frost, R. A., Vary, T. C., Jefferson, L. S. & Lang, C. H. 2005. Hindlimb casting decreases muscle mass in part by proteasome-dependent proteolysis but independent of protein synthesis. *American journal of physiology. Endocrinology and metabolism* 289 (6), 969-980.
- Laplante, M. & Sabatini, D. M. 2009. mTOR signaling at a glance. *Journal of cell science* 122 (Pt 20), 3589-3594.
- Lautaoja, J. H., Lalowski, M., Nissinen, T. A., Hentila, J., Shi, Y., et al. 2019. Muscle and serum metabolomes are dysregulated in colon-26 tumor-bearing mice despite amelioration of cachexia with activin receptor type 2B ligand blockade. *American journal of physiology. Endocrinology and metabolism* 316 (5), E852-E865.
- Le Bricon, T., Gugins, S., Cynober, L. & Baracos, V. E. 1995. Negative impact of cancer chemotherapy on protein metabolism in healthy and tumor-bearing rats. *Metabolism: clinical and experimental* 44 (10), 1340-1348.
- Lebrecht, D., Setzer, B., Ketelsen, U. P., Haberstroh, J. & Walker, U. A. 2003. Time-dependent and tissue-specific accumulation of mtDNA and respiratory chain defects in chronic doxorubicin cardiomyopathy. *Circulation* 108 (19), 2423-2429.

- Lecker, S. H., Jagoe, R. T., Gilbert, A., Gomes, M., Baracos, V., et al. 2004. Multiple types of skeletal muscle atrophy involve a common program of changes in gene expression. *FASEB journal* 18 (1), 39-51.
- Lee, S. J., Lee, Y. S., Zimmers, T. A., Soleimani, A., Matzuk, M. M., et al. 2010. Regulation of muscle mass by follistatin and activins. *Molecular endocrinology* 24 (10), 1998-2008.
- Lee, S. J. & McPherron, A. C. 2001. Regulation of myostatin activity and muscle growth. *Proceedings of the National Academy of Sciences of the United States of America* 98 (16), 9306-9311.
- Lee, S. J., Reed, L. A., Davies, M. V., Girgenrath, S., Goad, M. E., et al. 2005. Regulation of muscle growth by multiple ligands signaling through activin type II receptors. *Proceedings of the National Academy of Sciences of the United States of America* 102 (50), 18117-18122.
- Lerner, L., Tao, J., Liu, Q., Nicoletti, R., Feng, B., et al. 2016. MAP3K11/GDF15 axis is a critical driver of cancer cachexia. *Journal of cachexia, sarcopenia and muscle* 7 (4), 467-482.
- Lewis, H. L., Chakedis, J. M., Talbert, E., Haverick, E., Rajasekera, P., et al. 2017. Perioperative cytokine levels portend early death after pancreatectomy for ductal adenocarcinoma. *Journal of surgical oncology* 117(6):1260-1266.
- Li, J. B. & Goldberg, A. L. 1976. Effects of food deprivation on protein synthesis and degradation in rat skeletal muscles. *The American Journal of Physiology* 231 (2), 441-448.
- Li, Q., Kumar, R., Underwood, K., O'Connor, A. E., Loveland, K. L., et al. 2007. Prevention of cachexia-like syndrome development and reduction of tumor progression in inhibin-deficient mice following administration of a chimeric activin receptor type II-murine Fc protein. *Molecular human reproduction* 13 (9), 675-683.
- Lieffers, J. R., Mourtzakis, M., Hall, K. D., McCargar, L. J., Prado, C. M., et al. 2009. A viscerally driven cachexia syndrome in patients with advanced colorectal cancer: contributions of organ and tumor mass to whole-body energy demands. *The American Journal of Clinical Nutrition* 89 (4), 1173-1179.
- Lira, F. S., Neto, J. C. & Seelaender, M. 2014. Exercise training as treatment in cancer cachexia. *Applied physiology, nutrition, and metabolism* 39 (6), 679-686.
- Liu, X., Zhang, Q., Fan, C., Tian, J., Liu, X., et al. 2019. GDF11 upregulation independently predicts shorter overall-survival of uveal melanoma. *PloS one* 14 (3), e0214073.
- Llovera, M., Garcia-Martinez, C., Lopez-Soriano, J., Agell, N., Lopez-Soriano, F. J., et al. 1998. Protein turnover in skeletal muscle of tumour-bearing transgenic mice overexpressing the soluble TNF receptor-1. *Cancer letters* 130 (1-2), 19-27.
- Loberg, R. D., Bradley, D. A., Tomlins, S. A., Chinnaiyan, A. M. & Pienta, K. J. 2007. The lethal phenotype of cancer: the molecular basis of death due to malignancy. *CA: a cancer journal for clinicians* 57 (4), 225-241.

- Lodewick, T. M., van Nijnatten, T. J., van Dam, R. M., van Mierlo, K., Dello, S. A., et al. 2015. Are sarcopenia, obesity and sarcopenic obesity predictive of outcome in patients with colorectal liver metastases? *HPB* 17 (5), 438-446.
- Lopes, M. N., Black, P., Ashford, A. J. & Pain, V. M. 1989. Protein metabolism in the tumour-bearing mouse. Rates of protein synthesis in host tissues and in an Ehrlich ascites tumour at different stages in tumour growth. *The Biochemical journal* 264 (3), 713-719.
- Lou, H., Danelisen, I. & Singal, P. K. 2005. Involvement of mitogen-activated protein kinases in adriamycin-induced cardiomyopathy. *American journal of physiology. Heart and circulatory physiology* 288 (4), 1925-1930.
- Loumaye, A., de Barsey, M., Nachit, M., Lause, P., van Maanen, A., et al. 2017. Circulating Activin A predicts survival in cancer patients. *Journal of cachexia, sarcopenia and muscle* 8 (5), 768-777.
- Loumaye, A. & Thissen, J. P. 2017. Biomarkers of cancer cachexia. *Clinical biochemistry* 50 (18), 1281-1288.
- MacDonald, E. M., Andres-Mateos, E., Mejias, R., Simmers, J. L., Mi, R., et al. 2014. Denervation atrophy is independent from Akt and mTOR activation and is not rescued by myostatin inhibition. *Disease models & mechanisms* 7 (4), 471-481.
- Magga, J., Vainio, L., Kilpio, T., Hulmi, J. J., Taponen, S., et al. 2019. Systemic Blockade of ACVR2B Ligands Protects Myocardium from Acute Ischemia-Reperfusion Injury. *Molecular therapy* 27 (3), 600-610.
- Margolis, L. M., Rivas, D. A., Berrone, M., Ezzyat, Y., Young, A. J., et al. 2016. Prolonged Calorie Restriction Downregulates Skeletal Muscle mTORC1 Signaling Independent of Dietary Protein Intake and Associated microRNA Expression. *Frontiers in physiology* 7, 445.
- Marques-Aleixo, I., Santos-Alves, E., Mariani, D., Rizo-Roca, D., Padrao, A. I., et al. 2015. Physical exercise prior and during treatment reduces sub-chronic doxorubicin-induced mitochondrial toxicity and oxidative stress. *Mitochondrion* 20, 22-33.
- Martin, F., Santolaria, F., Batista, N., Milena, A., Gonzalez-Reimers, E., et al. 1999. Cytokine levels (IL-6 and IFN-gamma), acute phase response and nutritional status as prognostic factors in lung cancer. *Cytokine* 11 (1), 80-86.
- Martin, L., Birdsell, L., Macdonald, N., Reiman, T., Clandinin, M. T., et al. 2013. Cancer cachexia in the age of obesity: skeletal muscle depletion is a powerful prognostic factor, independent of body mass index. *Journal of clinical oncology* 31 (12), 1539-1547.
- Martin, L., Senesse, P., Gioulbasanis, I., Antoun, S., Bozzetti, F., et al. 2015. Diagnostic criteria for the classification of cancer-associated weight loss. *Journal of clinical oncology* 33 (1), 90-99.
- Mastrocola, R., Reffo, P., Penna, F., Tomasinelli, C. E., Boccuzzi, G., et al. 2008. Muscle wasting in diabetic and in tumor-bearing rats: role of oxidative stress. *Free radical biology & medicine* 44 (4), 584-593.
- Mathews, L. S. & Vale, W. W. 1991. Expression cloning of an activin receptor, a predicted transmembrane serine kinase. *Cell* 65 (6), 973-982.

- Matsumoto, T., Fujimoto-Ouchi, K., Tamura, S., Tanaka, Y. & Ishitsuka, H. 1999. Tumour inoculation site-dependent induction of cachexia in mice bearing colon 26 carcinoma. *British journal of cancer* 79 (5-6), 764-769.
- Matzuk, M. M., Finegold, M. J., Mather, J. P., Krummen, L., Lu, H., et al. 1994. Development of cancer cachexia-like syndrome and adrenal tumors in inhibin-deficient mice. *Proceedings of the National Academy of Sciences of the United States of America* 91 (19), 8817-8821.
- McCarthy, J. J. & Esser, K. A. 2010. Anabolic and catabolic pathways regulating skeletal muscle mass. *Current opinion in clinical nutrition and metabolic care* 13 (3), 230-235.
- McPherron, A. C., Huynh, T. V. & Lee, S. J. 2009. Redundancy of myostatin and growth/differentiation factor 11 function. *BMC developmental biology* 9, 24-24.
- McPherron, A. C., Lawler, A. M. & Lee, S. J. 1999. Regulation of anterior/posterior patterning of the axial skeleton by growth/differentiation factor 11. *Nature genetics* 22 (3), 260-264.
- McPherron, A. C., Lawler, A. M. & Lee, S. J. 1997. Regulation of skeletal muscle mass in mice by a new TGF-beta superfamily member. *Nature* 387 (6628), 83-90.
- McPherron, A. C. & Lee, S. J. 1997. Double muscling in cattle due to mutations in the myostatin gene. *Proceedings of the National Academy of Sciences of the United States of America* 94 (23), 12457-12461.
- Mehl, K. A., Davis, J. M., Berger, F. G. & Carson, J. A. 2005. Myofiber degeneration/regeneration is induced in the cachectic ApcMin/+ mouse. *Journal of applied physiology* 99 (6), 2379-2387.
- Melvin, A. T., Woss, G. S., Park, J. H., Waters, M. L. & Allbritton, N. L. 2013. Measuring activity in the ubiquitin-proteasome system: from large scale discoveries to single cells analysis. *Cell biochemistry and biophysics* 67 (1), 75-89.
- Meyerhardt, J. A., Giovannucci, E. L., Holmes, M. D., Chan, A. T., Chan, J. A., et al. 2006. Physical activity and survival after colorectal cancer diagnosis. *Journal of clinical oncology* 24 (22), 3527-3534.
- Meyerhardt, J. A., Heseltine, D., Niedzwiecki, D., Hollis, D., Saltz, L. B., et al. 2006. Impact of physical activity on cancer recurrence and survival in patients with stage III colon cancer: findings from CALGB 89803. *Journal of clinical oncology* 24 (22), 3535-3541.
- Meza-Junco, J., Montano-Loza, A. J., Baracos, V. E., Prado, C. M., Bain, V. G., et al. 2013. Sarcopenia as a prognostic index of nutritional status in concurrent cirrhosis and hepatocellular carcinoma. *Journal of clinical gastroenterology* 47 (10), 861-870.
- Mimeault, M. & Batra, S. K. 2010. Divergent molecular mechanisms underlying the pleiotropic functions of macrophage inhibitory cytokine-1 in cancer. *Journal of cellular physiology* 224 (3), 626-635.
- Min, K., Kwon, O. S., Smuder, A. J., Wiggs, M. P., Sollanek, K. J., et al. 2015. Increased mitochondrial emission of reactive oxygen species and calpain



- activation are required for doxorubicin-induced cardiac and skeletal muscle myopathy. *The Journal of physiology* 593 (8), 2017-2036.
- Miyamoto, Y., Baba, Y., Sakamoto, Y., Ohuchi, M., Tokunaga, R., et al. 2015. Sarcopenia is a Negative Prognostic Factor After Curative Resection of Colorectal Cancer. *Annals of surgical oncology* 22 (8), 2663-2668.
- Momparler, R. L., Karon, M., Siegel, S. E. & Avila, F. 1976. Effect of adriamycin on DNA, RNA, and protein synthesis in cell-free systems and intact cells. *Cancer research* 36 (8), 2891-2895.
- Moore, S. C., Lee, I. M., Weiderpass, E., Campbell, P. T., Sampson, J. N., et al. 2016. Association of Leisure-Time Physical Activity With Risk of 26 Types of Cancer in 1.44 Million Adults. *JAMA internal medicine* 176 (6), 816-825.
- Moses, A. W., Slater, C., Preston, T., Barber, M. D. & Fearon, K. C. 2004. Reduced total energy expenditure and physical activity in cachectic patients with pancreatic cancer can be modulated by an energy and protein dense oral supplement enriched with n-3 fatty acids. *British journal of cancer* 90 (5), 996-1002.
- Muller, C., Murawski, N., Wiesen, M. H., Held, G., Poeschel, V., et al. 2012. The role of sex and weight on rituximab clearance and serum elimination half-life in elderly patients with DLBCL. *Blood* 119 (14), 3276-3284.
- Mundy-Bosse, B. L., Lesinski, G. B., Jaime-Ramirez, A. C., Benninger, K., Khan, M., et al. 2011. Myeloid-derived suppressor cell inhibition of the IFN response in tumor-bearing mice. *Cancer research* 71 (15), 5101-5110.
- Murphy, K. T. 2016. The pathogenesis and treatment of cardiac atrophy in cancer cachexia. *American journal of physiology. Heart and circulatory physiology* 310 (4), 466-477.
- Murphy, K. T., Chee, A., Gleeson, B. G., Naim, T., Swiderski, K., et al. 2011b. Antibody-directed myostatin inhibition enhances muscle mass and function in tumor-bearing mice. *American journal of physiology. Regulatory, integrative and comparative physiology* 301 (3), 716-726.
- Murphy, K. T., Chee, A., Trieu, J., Naim, T. & Lynch, G. S. 2012. Importance of functional and metabolic impairments in the characterization of the C-26 murine model of cancer cachexia. *Disease models & mechanisms* 5 (4), 533-545.
- Murphy, K. T., Cobani, V., Ryall, J. G., Ibebunjo, C. & Lynch, G. S. 2011a. Acute antibody-directed myostatin inhibition attenuates disuse muscle atrophy and weakness in mice. *Journal of applied physiology* 110 (4), 1065-1072.
- Murphy, K. T., Ryall, J. G., Snell, S. M., Nair, L., Koopman, R., et al. 2010. Antibody-directed myostatin inhibition improves diaphragm pathology in young but not adult dystrophic mdx mice. *The American journal of pathology* 176 (5), 2425-2434.
- Namwanje, M. & Brown, C. W. 2016. Activins and Inhibins: Roles in Development, Physiology, and Disease. *Cold Spring Harbor perspectives in biology* 8 (7), doi 10.1101/cshperspect.a021881.

- Nitiss, K. C. & Nitiss, J. L. 2014. Twisting and ironing: doxorubicin cardiotoxicity by mitochondrial DNA damage. *Clinical cancer research* 20 (18), 4737-4739.
- O'Connell, T. M., Pin, F., Couch, M. E. & Bonetto, A. 2019. Treatment with Soluble Activin Receptor Type IIB Alters Metabolic Response in Chemotherapy-Induced Cachexia. *Cancers* 11 (9), doi 10.3390/cancers11091222.
- Ogata, E. S., Fong, S. K. & Holliday, M. A. 1978. The effects of starvation and refeeding on muscle protein synthesis and catabolism in the young rat. *The Journal of nutrition* 108 (5), 759-765.
- Oikawa, S. Y., Holloway, T. M. & Phillips, S. M. 2019. The Impact of Step Reduction on Muscle Health in Aging: Protein and Exercise as Countermeasures. *Frontiers in nutrition* 6, 75.
- Op den Kamp, C. M., Langen, R. C., Minnaard, R., Kelders, M. C., Snepvangers, F. J., et al. 2012. Pre-cachexia in patients with stages I-III non-small cell lung cancer: systemic inflammation and functional impairment without activation of skeletal muscle ubiquitin proteasome system. *Lung cancer* 76 (1), 112-117.
- Orell-Kotikangas, H., Osterlund, P., Makitie, O., Saarilahti, K., Ravasco, P., et al. 2017. Cachexia at diagnosis is associated with poor survival in head and neck cancer patients. *Acta Oto-Laryngologica* 137 (7), 778-785.
- Pain, V. M. & Garlick, P. J. 1980. The effect of an Ehrlich ascites tumour on the rate of protein synthesis in muscle and liver of the host [proceedings]. *Biochemical Society transactions* 8 (3), 354.
- Parajuli, P., Kumar, S., Loumaye, A., Singh, P., Eragamreddy, S., et al. 2018. Twist1 Activation in Muscle Progenitor Cells Causes Muscle Loss Akin to Cancer Cachexia. *Developmental cell* 45 (6), 712-725.e6.
- Pasiakos, S. M., Vislocky, L. M., Carbone, J. W., Altieri, N., Konopelski, K., et al. 2010. Acute energy deprivation affects skeletal muscle protein synthesis and associated intracellular signaling proteins in physically active adults. *The Journal of nutrition* 140 (4), 745-751.
- Pekkala, S., Keskitalo, A., Kettunen, E., Lensu, S., Nykanen, N., et al. 2019. Blocking Activin Receptor Ligands Is Not Sufficient to Rescue Cancer-Associated Gut Microbiota-A Role for Gut Microbial Flagellin in Colorectal Cancer and Cachexia? *Cancers* 11 (11), doi 10.3390/cancers11111799.
- Peng, P. D., van Vledder, M. G., Tsai, S., de Jong, M. C., Makary, M., et al. 2011. Sarcopenia negatively impacts short-term outcomes in patients undergoing hepatic resection for colorectal liver metastasis. *HPB* 13 (7), 439-446.
- Peng, P., Hyder, O., Firoozmand, A., Kneuert, P., Schulick, R. D., et al. 2012. Impact of sarcopenia on outcomes following resection of pancreatic adenocarcinoma. *Journal of gastrointestinal surgery* 16 (8), 1478-1486.

- Penna, F., Baccino, F. M. & Costelli, P. 2014. Coming back: autophagy in cachexia. *Current opinion in clinical nutrition and metabolic care* 17 (3), 241-246.
- Penna, F., Ballaro, R., Beltra, M., De Lucia, S., Garcia Castillo, L., et al. 2019. The Skeletal Muscle as an Active Player Against Cancer Cachexia. *Frontiers in physiology* 10, 41.
- Penna, F., Bonetto, A., Aversa, Z., Minero, V. G., Rossi Fanelli, F., et al. 2016. Effect of the specific proteasome inhibitor bortezomib on cancer-related muscle wasting. *Journal of cachexia, sarcopenia and muscle* 7 (3), 345-354.
- Penna, F., Busquets, S. & Argiles, J. M. 2016. Experimental cancer cachexia: Evolving strategies for getting closer to the human scenario. *Seminars in cell & developmental biology* 54, 20-27.
- Penna, F., Busquets, S., Pin, F., Toledo, M., Baccino, F. M., et al. 2011. Combined approach to counteract experimental cancer cachexia: eicosapentaenoic acid and training exercise. *Journal of cachexia, sarcopenia and muscle* 2 (2), 95-104.
- Penna, F., Busquets, S., Toledo, M., Pin, F., Massa, D., et al. 2013b. Erythropoietin administration partially prevents adipose tissue loss in experimental cancer cachexia models. *Journal of lipid research* 54 (11), 3045-3051.
- Penna, F., Costamagna, D., Fanzani, A., Bonelli, G., Baccino, F. M., et al. 2010. Muscle wasting and impaired myogenesis in tumor bearing mice are prevented by ERK inhibition. *PloS one* 5 (10), e13604.
- Penna, F., Costamagna, D., Pin, F., Camperi, A., Fanzani, A., et al. 2013a. Autophagic degradation contributes to muscle wasting in cancer cachexia. *The American journal of pathology* 182 (4), 1367-1378.
- Phillips, S. M. & McGlory, C. 2014. CrossTalk proposal: The dominant mechanism causing disuse muscle atrophy is decreased protein synthesis. *The Journal of physiology* 592 (24), 5341-5343.
- Pichard, C., Baracos, V. & Attaix, D. 2011. Would you buy a new tool to improve your practice? *Current opinion in clinical nutrition and metabolic care* 14 (3), 221-222.
- Pigna, E., Berardi, E., Aulino, P., Rizzuto, E., Zampieri, S., et al. 2016. Aerobic Exercise and Pharmacological Treatments Counteract Cachexia by Modulating Autophagy in Colon Cancer. *Scientific reports* 6, 26991.
- Pin, F., Busquets, S., Toledo, M., Camperi, A., Lopez-Soriano, F. J., et al. 2015. Combination of exercise training and erythropoietin prevents cancer-induced muscle alterations. *Oncotarget* 6 (41), 43202-43215.
- Pin, F., Couch, M. E. & Bonetto, A. 2018. Preservation of muscle mass as a strategy to reduce the toxic effects of cancer chemotherapy on body composition. *Current opinion in supportive and palliative care* 12 (4), 420-426.
- Potsch, M. S., Ishida, J., Palus, S., Tschirner, A., von Haehling, S., et al. 2020. MT-102 prevents tissue wasting and improves survival in a rat model of severe cancer cachexia. *Journal of cachexia, sarcopenia and muscle* 11 (2), 594-605.

- Prado, C. M., Baracos, V. E., McCargar, L. J., Mourtzakis, M., Mulder, K. E., et al. 2007. Body composition as an independent determinant of 5-fluorouracil-based chemotherapy toxicity. *Clinical cancer research* 13 (11), 3264-3268.
- Prado, C. M., Baracos, V. E., McCargar, L. J., Reiman, T., Mourtzakis, M., et al. 2009. Sarcopenia as a determinant of chemotherapy toxicity and time to tumor progression in metastatic breast cancer patients receiving capecitabine treatment. *Clinical cancer research* 15 (8), 2920-2926.
- Prado, C. M., Baracos, V. E., Xiao, J., Birdsell, L., Stuyckens, K., et al. 2014. The association between body composition and toxicities from the combination of Doxil and trabectedin in patients with advanced relapsed ovarian cancer. *Applied physiology, nutrition, and metabolism* 39 (6), 693-698.
- Prado, C. M., Lieffers, J. R., McCargar, L. J., Reiman, T., Sawyer, M. B., et al. 2008. Prevalence and clinical implications of sarcopenic obesity in patients with solid tumours of the respiratory and gastrointestinal tracts: a population-based study. *The Lancet Oncology* 9 (7), 629-635.
- Pretto, F., Ghilardi, C., Moschetta, M., Bassi, A., Rovida, A., et al. 2015. Sunitinib prevents cachexia and prolongs survival of mice bearing renal cancer by restraining STAT3 and MuRF-1 activation in muscle. *Oncotarget* 6 (5), 3043-3054.
- Psutka, S. P., Carrasco, A., Schmit, G. D., Moynagh, M. R., Boorjian, S. A., et al. 2014. Sarcopenia in patients with bladder cancer undergoing radical cystectomy: impact on cancer-specific and all-cause mortality. *Cancer* 120 (18), 2910-2918.
- Puolakkainen, T., Ma, H., Kainulainen, H., Pasternack, A., Rantalainen, T., et al. 2017a. Treatment with soluble activin type IIB-receptor improves bone mass and strength in a mouse model of Duchenne muscular dystrophy. *BMC musculoskeletal disorders* 18 (1), 20-3.
- Puolakkainen, T., Rummukainen, P., Lehto, J., Ritvos, O., Hiltunen, A., et al. 2017b. Soluble activin type IIB receptor improves fracture healing in a closed tibial fracture mouse model. *PloS one* 12 (7), e0180593.
- Puppa, M. J., White, J. P., Sato, S., Cairns, M., Baynes, J. W., et al. 2011. Gut barrier dysfunction in the Apc(Min/+) mouse model of colon cancer cachexia. *Biochimica et biophysica acta* 1812 (12), 1601-1606.
- Rahimov, F., King, O. D., Warsing, L. C., Powell, R. E., Emerson, C. P., et al. 2011. Gene expression profiling of skeletal muscles treated with a soluble activin type IIB receptor. *Physiological genomics* 43 (8), 398-407.
- Rantanen, T., Sakari-Rantala, R. & Heikkinen, E. 2002. Muscle strength before and mortality after a bone fracture in older people. *Scandinavian Journal of Medicine & Science in Sports* 12 (5), 296-300.
- Räsänen, M., Degerman, J., Nissinen, T. A., Miinalainen, I., Kerkela, R., et al. 2016. VEGF-B gene therapy inhibits doxorubicin-induced cardiotoxicity by endothelial protection. *Proceedings of the National Academy of Sciences of the United States of America* 113 (46), 13144-13149.

- Reeds, P. J., Palmer, R. M., Hay, S. M. & McMillan, D. N. 1986. Protein synthesis in skeletal muscle measured at different times during a 24 hour period. *Bioscience reports* 6 (2), 209-213.
- Relizani, K., Mouisel, E., Giannesini, B., Hourde, C., Patel, K., et al. 2014. Blockade of ActRIIB signaling triggers muscle fatigability and metabolic myopathy. *Molecular therapy* 22 (8), 1423-1433.
- Rennie, M. J., Edwards, R. H., Emery, P. W., Halliday, D., Lundholm, K., et al. 1983. Depressed protein synthesis is the dominant characteristic of muscle wasting and cachexia. *Clinical physiology* 3 (5), 387-398.
- Riihijarvi, S., Taskinen, M., Jerkeman, M. & Leppa, S. 2011. Male gender is an adverse prognostic factor in B-cell lymphoma patients treated with immunochemotherapy. *European journal of haematology* 86 (2), 124-128.
- Roberts, B. M., Ahn, B., Smuder, A. J., Al-Rajhi, M., Gill, L. C., et al. 2013. Diaphragm and ventilatory dysfunction during cancer cachexia. *FASEB journal* 27 (7), 2600-2610.
- Rollins, K. E., Tewari, N., Ackner, A., Awwad, A., Madhusudan, S., et al. 2016. The impact of sarcopenia and myosteatorsis on outcomes of unresectable pancreatic cancer or distal cholangiocarcinoma. *Clinical nutrition* 35 (5), 1103-1109.
- Rudrappa, S. S., Wilkinson, D. J., Greenhaff, P. L., Smith, K., Idris, I., et al. 2016. Human Skeletal Muscle Disuse Atrophy: Effects on Muscle Protein Synthesis, Breakdown, and Insulin Resistance-A Qualitative Review. *Frontiers in physiology* 7, 361.
- Sacheck, J. M., Hyatt, J. P., Raffaello, A., Jagoe, R. T., Roy, R. R., et al. 2007. Rapid disuse and denervation atrophy involve transcriptional changes similar to those of muscle wasting during systemic diseases. *FASEB journal* 21 (1), 140-155.
- Salto, R., Vilchez, J. D., Cabrera, E., Guinovart, J. J. & Giron, M. D. 2014. Activation of ERK by sodium tungstate induces protein synthesis and prevents protein degradation in rat L6 myotubes. *FEBS letters* 588 (14), 2246-2254.
- Samuels, S. E., Knowles, A. L., Tilignac, T., Debiton, E., Madelmont, J. C., et al. 2001. Higher skeletal muscle protein synthesis and lower breakdown after chemotherapy in cachectic mice. *American journal of physiology. Regulatory, integrative and comparative physiology* 281 (1), 133-139.
- Samuels, S. E., McLaren, T. A., Knowles, A. L., Stewart, S. A., Madelmont, J. C., et al. 2006. Liver protein synthesis stays elevated after chemotherapy in tumour-bearing mice. *Cancer letters* 239 (1), 78-83.
- Sancak, Y., Bar-Peled, L., Zoncu, R., Markhard, A. L., Nada, S., et al. 2010. Ragulator-Rag complex targets mTORC1 to the lysosomal surface and is necessary for its activation by amino acids. *Cell* 141 (2), 290-303.
- Sandri, M. 2016. Protein breakdown in cancer cachexia. *Seminars in cell & developmental biology* 54, 11-19.
- Sandri, M. 2008. Signaling in muscle atrophy and hypertrophy. *Physiology* 23, 160-170.

- Sato, N., Michaelides, M. C. & Wallack, M. K. 1981. Characterization of tumorigenicity, mortality, metastasis, and splenomegaly of two cultured murine colon lines. *Cancer research* 41 (6), 2267-2272.
- Sauter, K. A., Wood, L. J., Wong, J., Iordanov, M. & Magun, B. E. 2011. Doxorubicin and daunorubicin induce processing and release of interleukin-1beta through activation of the NLRP3 inflammasome. *Cancer biology & therapy* 11 (12), 1008-1016.
- Saxton, R. A. & Sabatini, D. M. 2017. mTOR Signaling in Growth, Metabolism, and Disease. *Cell* 168 (6), 960-976.
- Schapira, D. V., Studnicki, J., Bradham, D. D., Wolff, P. & Jarrett, A. 1993. Intensive care, survival, and expense of treating critically ill cancer patients. *Jama* 269 (6), 783-786.
- Schindelin, J., Arganda-Carreras, I., Frise, E., Kaynig, V., Longair, M., et al. 2012. Fiji: an open-source platform for biological-image analysis. *Nature methods* 9 (7), 676-682.
- Schmidt, E. K., Clavarino, G., Ceppi, M. & Pierre, P. 2009. SUnSET, a nonradioactive method to monitor protein synthesis. *Nature methods* 6 (4), 275-277.
- Schwartz, A. L. 2000. Daily fatigue patterns and effect of exercise in women with breast cancer. *Cancer practice* 8 (1), 16-24.
- Scott, J. M., Zabor, E. C., Schwitzer, E., Koelwyn, G. J., Adams, S. C., et al. 2018. Efficacy of Exercise Therapy on Cardiorespiratory Fitness in Patients With Cancer: A Systematic Review and Meta-Analysis. *Journal of clinical oncology* 36 (22), 2297-2305.
- Sengupta, S., Peterson, T. R. & Sabatini, D. M. 2010. Regulation of the mTOR complex 1 pathway by nutrients, growth factors, and stress. *Molecular cell* 40 (2), 310-322.
- Sepulveda, P. V., Lamon, S., Hagg, A., Thomson, R. E., Winbanks, C. E., et al. 2015. Evaluation of follistatin as a therapeutic in models of skeletal muscle atrophy associated with denervation and tenotomy. *Scientific reports* 5, 17535.
- Sharma, M., Kambadur, R., Matthews, K. G., Somers, W. G., Devlin, G. P., et al. 1999. Myostatin, a transforming growth factor-beta superfamily member, is expressed in heart muscle and is upregulated in cardiomyocytes after infarct. *Journal of cellular physiology* 180 (1), 1-9.
- Shaw, J. H., Humberstone, D. A., Douglas, R. G. & Koea, J. 1991. Leucine kinetics in patients with benign disease, non-weight-losing cancer, and cancer cachexia: studies at the whole-body and tissue level and the response to nutritional support. *Surgery* 109 (1), 37-50.
- Shukla, S. K., Dasgupta, A., Mehla, K., Gunda, V., Vernucci, E., et al. 2015. Silibinin-mediated metabolic reprogramming attenuates pancreatic cancer-induced cachexia and tumor growth. *Oncotarget* 6 (38), 41146-41161.
- Shum, A. M., Mahendradatta, T., Taylor, R. J., Painter, A. B., Moore, M. M., et al. 2012. Disruption of MEF2C signaling and loss of sarcomeric and

- mitochondrial integrity in cancer-induced skeletal muscle wasting. *Aging* 4 (2), 133-143.
- Silvennoinen, M., Rantalainen, T. & Kainulainen, H. 2014. Validation of a method to measure total spontaneous physical activity of sedentary and voluntary running mice. *Journal of neuroscience methods* 235, 51-58.
- Sirnio, P., Tuomisto, A., Tervahartiala, T., Sorsa, T., Klintrup, K., Karhu, T., Herzig, K. H., Makela, J., Karttunen, T. J., Salo, T., Makinen, M. J. & Väyrynen, J. P. 2018. High-serum MMP-8 levels are associated with decreased survival and systemic inflammation in colorectal cancer. *British journal of cancer* 119 (2), 213-219.
- Smith, K. L. & Tisdale, M. J. 1993. Increased protein degradation and decreased protein synthesis in skeletal muscle during cancer cachexia. *British journal of cancer* 67 (4), 680-685.
- Smuder, A. J., Kavazis, A. N., Min, K. & Powers, S. K. 2013. Doxorubicin-induced markers of myocardial autophagic signaling in sedentary and exercise trained animals. *Journal of applied physiology* 115 (2), 176-185.
- Smuder, A. J., Kavazis, A. N., Min, K. & Powers, S. K. 2011a. Exercise protects against doxorubicin-induced markers of autophagy signaling in skeletal muscle. *Journal of applied physiology* 111 (4), 1190-1198.
- Smuder, A. J., Kavazis, A. N., Min, K. & Powers, S. K. 2011b. Exercise protects against doxorubicin-induced oxidative stress and proteolysis in skeletal muscle. *Journal of applied physiology* 110 (4), 935-942.
- Sofer, A., Lei, K., Johannessen, C. M. & Ellisen, L. W. 2005. Regulation of mTOR and cell growth in response to energy stress by REDD1. *Molecular and cellular biology* 25 (14), 5834-5845.
- Springer, J., Tschirner, A., Haghikia, A., von Haehling, S., Lal, H., et al. 2014. Prevention of liver cancer cachexia-induced cardiac wasting and heart failure. *European heart journal* 35 (14), 932-941.
- Stene, G. B., Helbostad, J. L., Amundsen, T., Sorhaug, S., Hjelde, H., et al. 2015. Changes in skeletal muscle mass during palliative chemotherapy in patients with advanced lung cancer. *Acta Oncologica* 54 (3), 340-348.
- Stephens, N. A., Skipworth, R. J. & Fearon, K. C. 2008. Cachexia, survival and the acute phase response. *Current opinion in supportive and palliative care* 2 (4), 267-274.
- Stephens, N. A., Skipworth, R. J., Macdonald, A. J., Greig, C. A., Ross, J. A., et al. 2011. Intramyocellular lipid droplets increase with progression of cachexia in cancer patients. *Journal of cachexia, sarcopenia and muscle* 2 (2), 111-117.
- Stobaus, N., Kupferling, S., Lorenz, M. L. & Norman, K. 2013. Discrepancy between body surface area and body composition in cancer. *Nutrition and cancer* 65 (8), 1151-1156.
- Subramanian, A., Tamayo, P., Mootha, V. K., Mukherjee, S., Ebert, B. L., et al. 2005. Gene set enrichment analysis: a knowledge-based approach for interpreting genome-wide expression profiles. *Proceedings of the National Academy of Sciences of the United States of America* 102 (43), 15545-15550.

- Suragani, R. N., Cawley, S. M., Li, R., Wallner, S., Alexander, M. J., et al. 2014. Modified activin receptor IIB ligand trap mitigates ineffective erythropoiesis and disease complications in murine beta-thalassemia. *Blood* 123 (25), 3864-3872.
- Szabo, Z., Vainio, L., Lin, R., Swan, J., Hulmi, J. J., et al. 2020. Systemic blockade of ACVR2B ligands attenuates muscle wasting in ischemic heart failure without compromising cardiac function. *FASEB journal* 34 (8), 9911-9924.
- Talbert, E. E. & Guttridge, D. C. 2016. Impaired regeneration: A role for the muscle microenvironment in cancer cachexia. *Seminars in cell & developmental biology* 54, 82-91.
- Talbert, E. E., Lewis, H. L., Farren, M. R., Ramsey, M. L., Chakedis, J. M., et al. 2018. Circulating monocyte chemoattractant protein-1 (MCP-1) is associated with cachexia in treatment-naive pancreatic cancer patients. *Journal of cachexia, sarcopenia and muscle* 9 (2), 358-368.
- Talbert, E. E., Yang, J., Mace, T. A., Farren, M. R., Farris, A. B., Young, G. S., Elnaggar, O., Che, Z., Timmers, C. D., Rajasekera, P., Maskarinec, J. M., Bloomston, M., Bekaii-Saab, T., Guttridge, D. C. & Lesinski, G. B. 2017. Dual Inhibition of MEK and PI3K/Akt Rescues Cancer Cachexia through both Tumor-Extrinsic and -Intrinsic Activities. *Molecular cancer therapeutics* 16 (2), 344-356.
- Tan, B. H., Birdsell, L. A., Martin, L., Baracos, V. E. & Fearon, K. C. 2009. Sarcopenia in an overweight or obese patient is an adverse prognostic factor in pancreatic cancer. *Clinical cancer research* 15 (22), 6973-6979.
- Tan, B. H., Brammer, K., Randhawa, N., Welch, N. T., Parsons, S. L., et al. 2015. Sarcopenia is associated with toxicity in patients undergoing neo-adjuvant chemotherapy for oesophago-gastric cancer. *European journal of surgical oncology* 41 (3), 333-338.
- Tanaka, Y., Eda, H., Tanaka, T., Udagawa, T., Ishikawa, T., et al. 1990. Experimental cancer cachexia induced by transplantable colon 26 adenocarcinoma in mice. *Cancer research* 50 (8), 2290-2295.
- Tardif, N., Grip, J. & Rooyackers, O. 2017. Muscle metabolism. *Current opinion in critical care* 23 (4), 264-268.
- Tardif, N., Klaude, M., Lundell, L., Thorell, A. & Rooyackers, O. 2013. Autophagic-lysosomal pathway is the main proteolytic system modified in the skeletal muscle of esophageal cancer patients. *The American Journal of Clinical Nutrition* 98 (6), 1485-1492.
- Tessitore, L., Costelli, P., Bonetti, G. & Baccino, F. M. 1993. Cancer cachexia, malnutrition, and tissue protein turnover in experimental animals. *Archives of Biochemistry and Biophysics* 306 (1), 52-58.
- Thomas, D. R. 2007. Loss of skeletal muscle mass in aging: examining the relationship of starvation, sarcopenia and cachexia. *Clinical nutrition* 26 (4), 389-399.
- Tian, M., Nishijima, Y., Asp, M. L., Stout, M. B., Reiser, P. J., et al. 2010. Cardiac alterations in cancer-induced cachexia in mice. *International journal of oncology* 37 (2), 347-353.



- Tilignac, T., Temparis, S., Combaret, L., Taillandier, D., Pouch, M. N., et al. 2002. Chemotherapy inhibits skeletal muscle ubiquitin-proteasome-dependent proteolysis. *Cancer research* 62 (10), 2771-2777.
- Tipton, K. D., Hamilton, D. L. & Gallagher, I. J. 2018. Assessing the Role of Muscle Protein Breakdown in Response to Nutrition and Exercise in Humans. *Sports medicine* 48 (Suppl 1), 53-64.
- Tisdale, M. J. 2009. Mechanisms of cancer cachexia. *Physiological Reviews* 89 (2), 381-410.
- Toledo, M., Busquets, S., Penna, F., Zhou, X., Marmonti, E., et al. 2016b. Complete reversal of muscle wasting in experimental cancer cachexia: Additive effects of activin type II receptor inhibition and beta-2 agonist. *International journal of cancer* 138 (8), 2021-2029.
- Toledo, M., Busquets, S., Sirisi, S., Serpe, R., Orpi, M., et al. 2011. Cancer cachexia: physical activity and muscle force in tumour-bearing rats. *Oncology reports* 25 (1), 189-193.
- Toledo, M., Penna, F., Busquets, S., Lopez-Soriano, F. J. & Argiles, J. M. 2014. Distinct behaviour of sorafenib in experimental cachexia-inducing tumours: the role of STAT3. *PloS one* 9 (12), e113931.
- Toledo, M., Penna, F., Oliva, F., Luque, M., Betancourt, A., et al. 2016a. A multifactorial anti-cachectic approach for cancer cachexia in a rat model undergoing chemotherapy. *Journal of cachexia, sarcopenia and muscle* 7 (1), 48-59.
- Trendelenburg, A. U., Meyer, A., Rohner, D., Boyle, J., Hatakeyama, S., et al. 2009. Myostatin reduces Akt/TORC1/p70S6K signaling, inhibiting myoblast differentiation and myotube size. *American journal of physiology. Cell physiology* 296 (6), 1258-1270.
- Tseng, Y. C., Kulp, S. K., Lai, I. L., Hsu, E. C., He, W. A., et al. 2015. Preclinical Investigation of the Novel Histone Deacetylase Inhibitor AR-42 in the Treatment of Cancer-Induced Cachexia. *Journal of the National Cancer Institute* 107 (12), djv274.
- Twelkmeyer, B., Tardif, N. & Rooyackers, O. 2017. Omics and cachexia. *Current opinion in clinical nutrition and metabolic care* 20 (3), 181-185.
- Vale, W., Rivier, J., Vaughan, J., McClintock, R., Corrigan, A., et al. 1986. Purification and characterization of an FSH releasing protein from porcine ovarian follicular fluid. *Nature* 321 (6072), 776-779.
- van Norren, K., Kegler, D., Argiles, J. M., Luiking, Y., Gorselink, M., et al. 2009b. Dietary supplementation with a specific combination of high protein, leucine, and fish oil improves muscle function and daily activity in tumour-bearing cachectic mice. *British journal of cancer* 100 (5), 713-722.
- van Norren, K., van Helvoort, A., Argiles, J. M., van Tuijl, S., Arts, K., et al. 2009a. Direct effects of doxorubicin on skeletal muscle contribute to fatigue. *British journal of cancer* 100 (2), 311-314.
- van Vledder, M. G., Levolger, S., Ayez, N., Verhoef, C., Tran, T. C., et al. 2012. Body composition and outcome in patients undergoing resection of colorectal liver metastases. *The British journal of surgery* 99 (4), 550-557.

- van Vugt, J. L., Braam, H. J., van Oudheusden, T. R., Vestering, A., Bollen, T. L., et al. 2015. Skeletal Muscle Depletion is Associated with Severe Postoperative Complications in Patients Undergoing Cytoreductive Surgery with Hyperthermic Intraperitoneal Chemotherapy for Peritoneal Carcinomatosis of Colorectal Cancer. *Annals of surgical oncology* 22 (11), 3625-3631.
- Veasey Rodrigues, H., Baracos, V. E., Wheler, J. J., Parsons, H. A., Hong, D. S., et al. 2013. Body composition and survival in the early clinical trials setting. *European journal of cancer* 49 (15), 3068-3075.
- Vejjongsas, P. & Yeh, E. T. 2014. Prevention of anthracycline-induced cardiotoxicity: challenges and opportunities. *Journal of the American College of Cardiology* 64 (9), 938-945.
- Voron, T., Tselikas, L., Pietrasz, D., Pigneur, F., Laurent, A., et al. 2015. Sarcopenia Impacts on Short- and Long-term Results of Hepatectomy for Hepatocellular Carcinoma. *Annals of Surgery* 261 (6), 1173-1183.
- Väyrynen, J. P., Tuomisto, A., Väyrynen, S. A., Klintrup, K., Karhu, T., Makela, J., Herzig, K. H., Karttunen, T. J. & Makinen, M. J. 2018. Preoperative anemia in colorectal cancer: relationships with tumor characteristics, systemic inflammation, and survival. *Scientific reports* 8 (1), 1126-y.
- Walker, R. G., Poggioli, T., Katsimpardi, L., Buchanan, S. M., Oh, J., et al. 2016. Biochemistry and Biology of GDF11 and Myostatin: Similarities, Differences, and Questions for Future Investigation. *Circulation research* 118 (7), 1125-1142.
- Warren, S. 1932. The immediate causes of death in cancer. *The American Journal of the Medical Sciences* 184 (5), 610-615.
- Weber, M. A., Krakowski-Roosen, H., Schroder, L., Kinscherf, R., Krix, M., et al. 2009. Morphology, metabolism, microcirculation, and strength of skeletal muscles in cancer-related cachexia. *Acta Oncologica* 48 (1), 116-124.
- Weijs, P. J., Looijaard, W. G., Dekker, I. M., Stapel, S. N., Girbes, A. R., et al. 2014. Low skeletal muscle area is a risk factor for mortality in mechanically ventilated critically ill patients. *Critical Care* 18 (2), R12.
- Welle, S., Mehta, S. & Burgess, K. 2011. Effect of postdevelopmental myostatin depletion on myofibrillar protein metabolism. *American journal of physiology. Endocrinology and metabolism* 300 (6), E993-E1001.
- White, J. P., Baynes, J. W., Welle, S. L., Kostek, M. C., Matesic, L. E., et al. 2011. The regulation of skeletal muscle protein turnover during the progression of cancer cachexia in the Apc(Min/+) mouse. *PloS one* 6 (9), e24650.
- Whittemore, L. A., Song, K., Li, X., Aghajanian, J., Davies, M., et al. 2003. Inhibition of myostatin in adult mice increases skeletal muscle mass and strength. *Biochemical and biophysical research communications* 300 (4), 965-971.
- Williams, J. P., Phillips, B. E., Smith, K., Atherton, P. J., Rankin, D., et al. 2012. Effect of tumor burden and subsequent surgical resection on skeletal muscle mass and protein turnover in colorectal cancer patients. *The American Journal of Clinical Nutrition* 96 (5), 1064-1070.

- Winbanks, C. E., Weeks, K. L., Thomson, R. E., Sepulveda, P. V., Beyer, C., et al. 2012. Follistatin-mediated skeletal muscle hypertrophy is regulated by Smad3 and mTOR independently of myostatin. *The Journal of cell biology* 197 (7), 997-1008.
- Winfield, R. D., Delano, M. J., Pande, K., Scumpia, P. O., Laface, D., et al. 2008. Myeloid-derived suppressor cells in cancer cachexia syndrome: a new explanation for an old problem. *Journal of parenteral and enteral nutrition* 32 (6), 651-655.
- Wolfe, R. R. 2006. The underappreciated role of muscle in health and disease. *The American Journal of Clinical Nutrition* 84 (3), 475-482.
- Wolfman, N. M., McPherron, A. C., Pappano, W. N., Davies, M. V., Song, K., et al. 2003. Activation of latent myostatin by the BMP-1/tolloid family of metalloproteinases. *Proceedings of the National Academy of Sciences of the United States of America* 100 (26), 15842-15846.
- Wu, M. Y. & Hill, C. S. 2009. Tgf-beta superfamily signaling in embryonic development and homeostasis. *Developmental cell* 16 (3), 329-343.
- Yamada, K., Sugiyama, S., Kosaka, K., Hayakawa, M. & Ozawa, T. 1995. Early appearance of age-associated deterioration in mitochondrial function of diaphragm and heart in rats treated with doxorubicin. *Experimental gerontology* 30 (6), 581-593.
- Yanagihara, K., Kubo, T., Iino, Y., Mihara, K., Morimoto, C., et al. 2019. Development and characterization of a cancer cachexia model employing a rare human duodenal neuroendocrine carcinoma-originating cell line. *Oncotarget* 10 (25), 2435-2450.
- Yang, J., Ratovitski, T., Brady, J. P., Solomon, M. B., Wells, K. D., et al. 2001. Expression of myostatin pro domain results in muscular transgenic mice. *Molecular reproduction and development* 60 (3), 351-361.
- Yu, A. P., Pei, X. M., Sin, T. K., Yip, S. P., Yung, B. Y., et al. 2014. Acylated and unacylated ghrelin inhibit doxorubicin-induced apoptosis in skeletal muscle. *Acta physiologica* 211 (1), 201-213.
- Zahringer, J. 1981. The regulation of protein synthesis in heart muscle under normal conditions and in the adriamycin-cardiomyopathy. *Klinische Wochenschrift* 59 (23), 1273-1287.
- Zhang, S., Liu, X., Bawa-Khalife, T., Lu, L. S., Lyu, Y. L., et al. 2012. Identification of the molecular basis of doxorubicin-induced cardiotoxicity. *Nature medicine* 18 (11), 1639-1642.
- Zhang, Y., Wei, Y., Liu, D., Liu, F., Li, X., et al. 2017. Role of growth differentiation factor 11 in development, physiology and disease. *Oncotarget* 8 (46), 81604-81616.
- Zhong, X., Pons, M., Poirier, C., Jiang, Y., Liu, J., et al. 2019. The systemic activin response to pancreatic cancer: implications for effective cancer cachexia therapy. *Journal of cachexia, sarcopenia and muscle* 10 (5), 1083-1101.
- Zhou, X., Wang, J. L., Lu, J., Song, Y., Kwak, K. S., et al. 2010. Reversal of cancer cachexia and muscle wasting by ActRIIB antagonism leads to prolonged survival. *Cell* 142 (4), 531-543.

- Zima, T., Tesar, V., Mantle, D., Koll, M., Patel, V., et al. 2001. Acute doxorubicin (adriamycin) dosage does not reduce cardiac protein synthesis in vivo, but decreases diaminopeptidase I and proline endopeptidase activities. *Experimental and molecular pathology* 70 (2), 154-161.
- Zimmers, T. A., Davies, M. V., Koniaris, L. G., Haynes, P., Esquela, A. F., et al. 2002. Induction of cachexia in mice by systemically administered myostatin. *Science* 296 (5572), 1486-1488.
- Zimmers, T. A., Fishel, M. L. & Bonetto, A. 2016. STAT3 in the systemic inflammation of cancer cachexia. *Seminars in cell & developmental biology* 54, 28-41.





## ORIGINAL PAPERS

### I

#### **SYSTEMIC BLOCKADE OF ACVR2B LIGANDS PREVENTS CHEMOTHERAPY-INDUCED MUSCLE WASTING BY RESTORING MUSCLE PROTEIN SYNTHESIS WITHOUT AFFECTING OXIDATIVE CAPACITY OR ATROGENES**

by

Nissinen, T.A., Degerman, J., Räsänen, M., Poikonen, A.R., Koskinen, S.,  
Mervaala, E., Pasternack, A., Ritvos, O., Kivelä, R. & Hulmi, J.J. 2016

Scientific reports 6, 32695

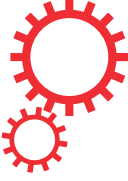
<https://doi.org/10.1038/srep32695>

Reproduced with kind permission by Springer Nature Limited.

Published under CC BY-NC 4.0 license.



# SCIENTIFIC REPORTS



OPEN

## Systemic blockade of ACVR2B ligands prevents chemotherapy-induced muscle wasting by restoring muscle protein synthesis without affecting oxidative capacity or atrogenes

T. A. Nissinen<sup>1</sup>, J. Degerman<sup>2</sup>, M. Räsänen<sup>2</sup>, A. R. Poikonen<sup>1</sup>, S. Koskinen<sup>3</sup>, E. Mervaala<sup>4</sup>, A. Pasternack<sup>5</sup>, O. Ritvos<sup>5,6</sup>, R. Kivelä<sup>2</sup> & J. J. Hulmi<sup>1,6</sup>

Doxorubicin is a widely used and effective chemotherapy drug. However, cardiac and skeletal muscle toxicity of doxorubicin limits its use. Inhibiting myostatin/activin signalling can prevent muscle atrophy, but its effects in chemotherapy-induced muscle wasting are unknown. In the present study we investigated the effects of doxorubicin administration alone or combined with activin receptor ligand pathway blockade by soluble activin receptor IIB (sACVR2B-Fc). Doxorubicin administration decreased body mass, muscle size and bone mineral density/content in mice. However, these effects were prevented by sACVR2B-Fc administration. Unlike in many other wasting situations, doxorubicin induced muscle atrophy without markedly increasing typical atrogenes or protein degradation pathways. Instead, doxorubicin decreased muscle protein synthesis which was completely restored by sACVR2B-Fc. Doxorubicin administration also resulted in impaired running performance without effects on skeletal muscle mitochondrial capacity/function or capillary density. Running performance and mitochondrial function were unaltered by sACVR2B-Fc administration. Tumour experiment using Lewis lung carcinoma cells demonstrated that sACVR2B-Fc decreased the cachectic effects of chemotherapy without affecting tumour growth. These results demonstrate that blocking ACVR2B signalling may be a promising strategy to counteract chemotherapy-induced muscle wasting without damage to skeletal muscle oxidative capacity or cancer treatment.

Cancer-related cachexia has been suggested to account for up to 20–30% of all cancer deaths<sup>1</sup>. In addition, decreased skeletal muscle mass is associated with increased toxicity of chemotherapy and impaired prognosis<sup>2</sup>. In contrast, maintenance of skeletal muscle mass predicts better response to treatment and survival<sup>2,3</sup>. Therefore, it is crucial to discover and develop effective strategies to counteract chemotherapy-induced muscle loss.

Doxorubicin is a widely used and effective anthracycline chemotherapeutic agent. Some of its most important antineoplastic effects are suggested to include prevention of DNA replication via DNA Topoisomerase II inhibition, DNA damage via formation of reactive oxygen species (ROS) and apoptosis (programmed cell death)<sup>4</sup>. However, doxorubicin has deleterious effects on several tissues other than tumour, which limits its clinical use. Particularly well-known side-effect is doxorubicin-induced cardiotoxicity<sup>4,5</sup>. Doxorubicin has also been shown

<sup>1</sup>Department of Biology of Physical Activity, Neuromuscular Research Center, University of Jyväskylä, Jyväskylä, Finland. <sup>2</sup>Wihuri Research Institute and Translational Cancer Biology Program, University of Helsinki, Helsinki, Finland. <sup>3</sup>LIKES Research Center for Sport and Health Sciences, Jyväskylä, Finland. <sup>4</sup>Department of Pharmacology, Faculty of Medicine, University of Helsinki, Helsinki, Finland. <sup>5</sup>Department of Bacteriology and Immunology, Haartman Institute, University of Helsinki, Helsinki, Finland. <sup>6</sup>Department of Physiology, Faculty of Medicine, University of Helsinki, Helsinki, Finland. Correspondence and requests for materials should be addressed to J.J.H. (email: juha.hulmi@jyu.fi)



to have adverse effects on skeletal muscle tissue: muscle weakness, fatigue, dysfunction and atrophy have been reported in both humans<sup>4,6</sup> and animals<sup>4,7–11</sup> after chemotherapy. The proposed cellular and molecular mechanisms for skeletal muscle toxicity, at least with high doses, include oxidative stress induced by doxorubicin accumulating into skeletal muscle, which may lead to contractile and mitochondrial dysfunction associated with activation of proteolytic and apoptotic signalling pathways<sup>4,8,9,12</sup>. Protein degradation pathways have been extensively studied in different muscle atrophy models and in human diseases<sup>13</sup>. In adults, muscle size is, however, regulated by the balance between protein synthesis and degradation<sup>14</sup>. Currently, the effect of doxorubicin on muscle protein synthesis is unknown.

Muscle size is negatively regulated by myostatin and activins that belong to the TGF- $\beta$  superfamily of proteins<sup>15,16</sup>. They exert their effect through binding to their receptor activin receptor type IIb (ACVR2B)<sup>17</sup>. An often used strategy to prevent muscle loss in animal models is to block these ACVR2B ligands by administration of a soluble ligand binding domain of ACVR2B fused to the Fc region of IgG (sACVR2B-Fc). This strategy has been shown to increase muscle mass effectively in mice<sup>17–19</sup>. In addition, sACVR2B-Fc treatment has been found to reverse cancer cachexia and prolong survival in different mouse models of cancer cachexia<sup>20,21</sup>. However, blocking ACVR2B ligands can also, depending on the context, have adverse effects<sup>22–24</sup>. It is not known whether sACVR2B-Fc administration could prevent doxorubicin-induced muscle atrophy without negatively altering muscle oxidative capacity.

The effects of blocking ACVR2B signalling on muscle growth in healthy mice have been shown earlier by us and others<sup>19,25</sup>. In the present study we investigated the effects of systemic doxorubicin administration alone or combined with sACVR2B-Fc treatment on skeletal muscle size and function and the underlying molecular mechanisms. For this purpose, five doxorubicin experiments were performed: 1–2) two four-week experiments, 3) a two-week experiment, 4) an acute 20 h experiment, and 5) a tumour experiment with doxorubicin treatment. The dose of doxorubicin was selected to mimic clinical doses used in humans. These studies demonstrate that doxorubicin induces muscle atrophy that is, at least in part, due to blunted skeletal muscle protein synthesis. We also showed that blocking ACVR2B signalling can counteract chemotherapy-induced muscle loss without further damage to skeletal muscle oxidative capacity or mitochondria. Importantly, sACVR2B-Fc administration did not affect tumour growth or the effect of doxorubicin on tumour growth.

## Results

### sACVR2B treatment prevents doxorubicin-induced skeletal muscle atrophy but not loss of fat.

In the first experiments, mice were given a total cumulative dose of 24 mg/kg of doxorubicin (comparable to clinical dose<sup>5,26</sup>), or PBS, during the first two weeks of the experiment. In the four-week experiment, doxorubicin was not administered during the latter two weeks and thus the results represent more chronic effects of doxorubicin treatment. This doxorubicin administration resulted in marked decrease in body weight (Fig. 1a). The weight loss was most dramatic during the second week of doxorubicin administration and the reduced body weight was sustained after the cessation of doxorubicin administration (Fig. 1a). This was accompanied by a significant reduction in tissue masses of tibialis anterior (TA) and gastrocnemius muscles and epididymal fat pads determined upon euthanasia (Fig. 1b–e and Supplementary Fig. S1a–d). These findings were substantiated by dual-energy X-ray absorptiometry (DXA) analysis, which showed a significant decrease in lean mass and fat mass (Fig. 1f,g). sACVR2B-Fc treatment fully prevented the doxorubicin-induced decrease in body mass, lean mass and skeletal muscle weights and could even induce hypertrophy when compared to untreated healthy mice. However, sACVR2B-Fc treatment was unable to prevent the decrease in fat mass, which was even slightly exacerbated. Doxorubicin treated mice ate significantly less compared with the vehicle treated counterparts. sACVR2B-Fc treatment did not have any additional effect on feed consumption (Fig. 1h).

In line with skeletal muscle weights, doxorubicin treated mice tended ( $P = 0.075$ ) to have decreased average muscle fibre cross-sectional area (CSA) in TA muscle (Fig. 2a,c) and fibre frequency curve shifted towards smaller fibres (Fig. 2b). This decrement was completely prevented by sACVR2B-Fc administration which resulted in significantly increased fibre size compared with both controls and doxorubicin treated mice (Fig. 2a–c).

**Blocking of the muscle loss prevents decrease in bone quality.** To further investigate the potential positive effects of maintaining muscle mass during chemotherapy, bones were analysed as a downstream outcome of the treatments. DXA-analysis showed a decrement in bone mineral density (BMD) and in bone mineral content (BMC) in doxorubicin-treated mice when compared to controls, whereas sACVR2B-Fc prevented these adverse effects (Fig. 3a,b). Our association analysis using a computationally determined network<sup>27</sup> showed that BMD and BMC at the end and the change in BMD and BMC are highly correlated to changes in lean mass as well as the end-measures of muscle mass and muscle fibre CSA (Fig. 3c–f).

### Doxorubicin administration resulted in chronic impairment of treadmill running capacity.

Doxorubicin treated mice had significantly impaired maximal running performance in an incremental treadmill running test (Fig. 4). sACVR2B-Fc treatment did not have any effect on running performance.

### Doxorubicin induces muscle atrophy with only small alterations in proteolytic pathways.

To investigate the factors that might contribute to doxorubicin-induced muscle atrophy and its reversal by sACVR2B-Fc, an acute experiment was conducted. Non-tumour bearing mice received a single intraperitoneal injection of doxorubicin (15 mg/kg in PBS) and were euthanized 20 hours post injection. Half of the doxorubicin treated mice were administered with sACVR2B-Fc (10 mg/kg in PBS) 48 hours before doxorubicin administration, as it has previously been reported that sACVR2B-Fc increases muscle protein synthesis 48 hours after its administration<sup>19</sup>. Microarray analysis was conducted from TA muscle to study gene expression responses to the treatments. To find out whether doxorubicin-induced muscle atrophy was

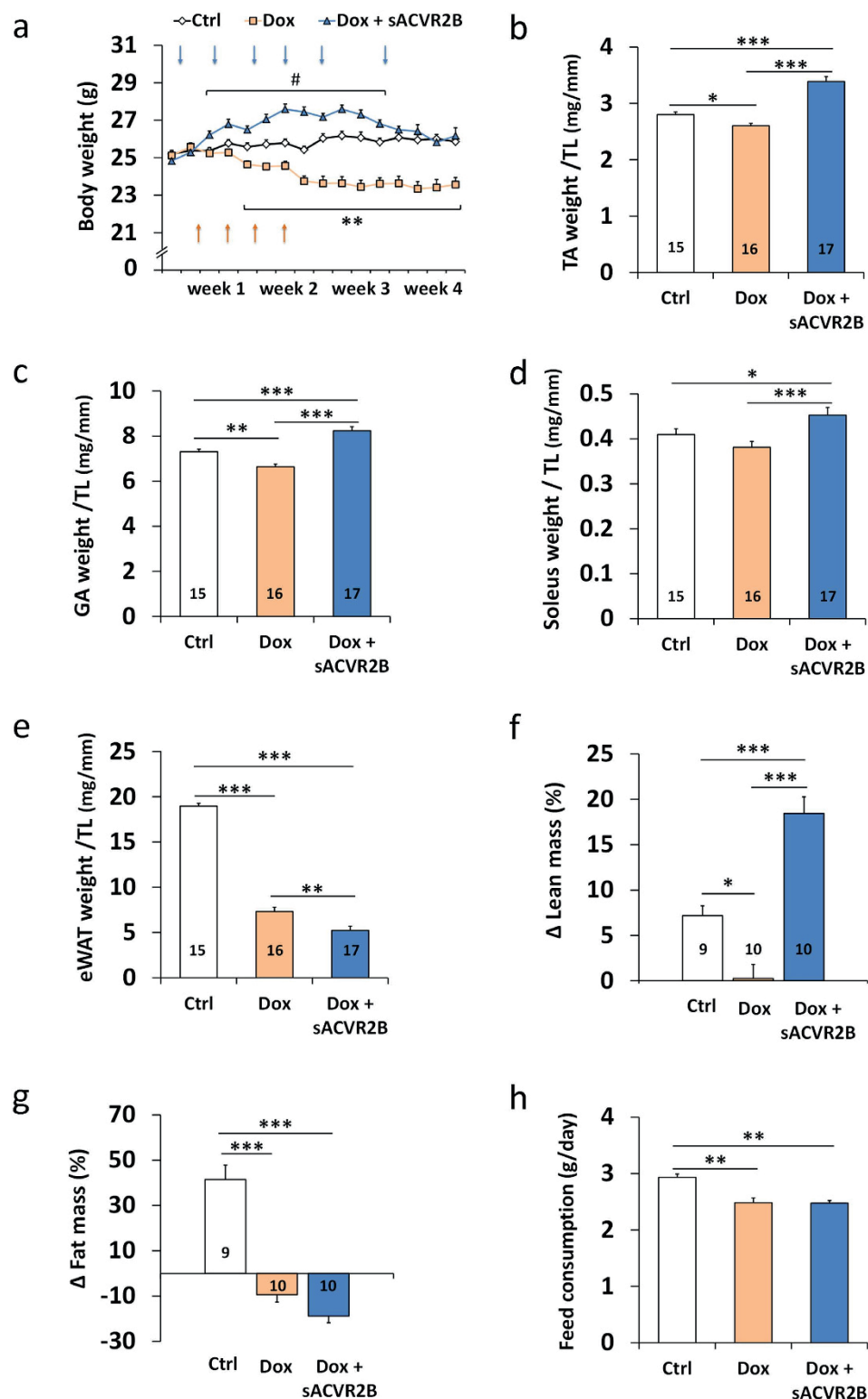


**Figure 1. Doxorubicin administration resulted in decreased body and muscle weights that were restored by sACVR2B-Fc treatment.** (a) Body weights during the four-week experiment. Arrows indicate the timing of doxorubicin (orange) and sACVR2B-Fc (blue) injections. Repeated measures ANOVA revealed time x group interaction effect ( $P < 0.001$ ). Tissue weights of TA (b), gastrocnemius (GA) (c) and soleus (d) muscles and epididymal fat pads (e) relative to tibial length (Supplementary Fig. S1e). Percentage changes in lean (f) and fat (g) mass analysed with DXA. (h) Average feed consumption during and after the treatment with doxorubicin and sACVR2B-Fc. Average feed consumption per mouse was calculated from the pooled feed intake of the whole cage (2–3 mice/cage;  $N = 3–4$  cages/group).  $N$  sizes are depicted in the bar graphs. Data are presented as mean  $\pm$  SEM. In Fig. a:  $^{\#}P < 0.05$  compared to Ctrl;  $^{**}P < 0.01$  compared to Ctrl and Dox + sACVR2B (Bonferroni). In Figs. b–h:  $^{*}P < 0.05$ ;  $^{**}P < 0.01$ ;  $^{***}P < 0.001$  (Bonferroni).

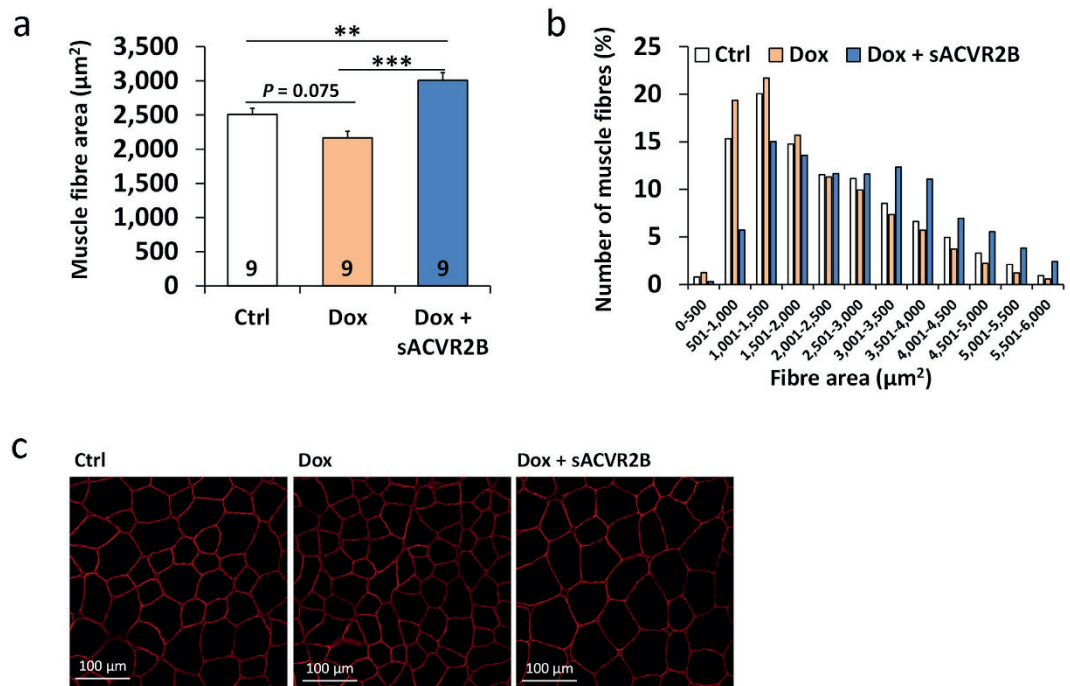


**Figure 2. sACVR2B-Fc administration increased muscle fibre cross-sectional area in doxorubicin-treated mice.** Average fibre CSA (a) and fibre size distribution (b) of the TA muscle at the end of the four-week experiment. (c) Representative immunofluorescence images of dystrophin-stained muscle cryosections. Data are presented as mean  $\pm$  SEM. \*\* $P < 0.01$ ; \*\*\* $P < 0.001$  (Bonferroni).

due to increased protein catabolism, a common atrogene signature for genes that has previously been shown to be commonly down- or upregulated in fasting, cancer cachexia, renal failure, diabetes, and in loss of contractile activity<sup>28</sup> was investigated (listed in Table 1). There were no systematic changes by doxorubicin or by sACVR2B-Fc on these transcripts (Table 1). There was however a minor trend that the atrogenes tended to follow the same trend in doxorubicin-administered mice as earlier<sup>28</sup>, although with a much smaller magnitude than with the other muscle wasting situations. Therefore, a gene set enrichment analysis (GSEA), able to detect small changes in several genes<sup>29</sup>, was conducted. Indeed, a custom-made gene set for these atrogenes showed a small increased enrichment (normalized enrichment score (NES) 1.44, FDR = 0.05) in doxorubicin administered mice when compared to vehicle treated control mice (Supplementary Fig. S2a) and this was blocked by sACVR2B-Fc administration (Supplementary Fig. S2b). GSEA analysis also revealed a small, but significant increase due to doxorubicin in the proteasome pathway (FDR = 0.041, Supplementary Fig. S2c,d) and also a trend in the caspase cascade (NES 1.75, FDR = 0.051) without any effect of sACVR2B-Fc. Of the individual atrogenes, *FOXO1* was the only one that was significantly (adjusted  $P < 0.05$ ) induced by doxorubicin (Table 1, Supplementary Fig. S2a). Thus, FoxO1 protein level and its phosphorylation were analysed. Similarly as in the microarray analysis, total FoxO1 protein expression was increased significantly ( $P < 0.05$ ) by doxorubicin, whereas phosphorylated FoxO1 remained at similar level between the groups (Supplementary Fig. S3a,e). In addition, mRNA expression of a well-known atrogene, MuRF1, was confirmed with qPCR, which, in accordance with the microarray result, showed no effect of doxorubicin treatment (Supplementary Fig. S3b). However, sACVR2B-Fc decreased MuRF1 mRNA (Supplementary Fig. S3b).

To study protein degradation pathways further, common markers of ubiquitin-proteasome system, autophagy and calpain content were analysed by western blotting. Doxorubicin administration did not result in any acute or chronic alterations in ubiquitinated proteins, lipidated LC3, or calpain1 protein content (Fig. 5a–d). No changes were noticed acutely or at 4 weeks, but at two weeks, sACVR2B-Fc treatment resulted in decreased lipidated LC3 (Fig. 5b). As LC3 lipidation alone is not sufficient marker for autophagy<sup>30</sup>, we also checked gene expression changes related to autophagy. Supporting the results above, autophagy gene set (KEGG) was not regulated by doxorubicin (FDR = 0.48, Supplementary Fig. S4a). Also after adjustment, the only significantly increased genes in this pathway were slightly increased *Ulk1* (1.41 fold,  $P = 0.02$ ) and *Becn1* (1.31 fold,  $P = 0.01$ ) in doxorubicin-administered mice, without marked effects of sACVR2B-Fc (Supplementary Fig. S4a,b). Doxorubicin has previously been shown to increase apoptosis, also in skeletal muscle<sup>31</sup>. Indeed, GSEA analysis revealed small increase in the gene set of apoptosis (NES 1.9, FDR = 0.01) without any effect of sACVR2B-Fc (Supplementary Fig. S4c,d).

To examine the possible delayed effects on muscle regeneration, TA muscles from mice from the four-week experiment were analysed for centrally nucleated fibres. Doxorubicin administration did not result in markedly and consistently increased number of centrally nucleated fibres (data not shown).

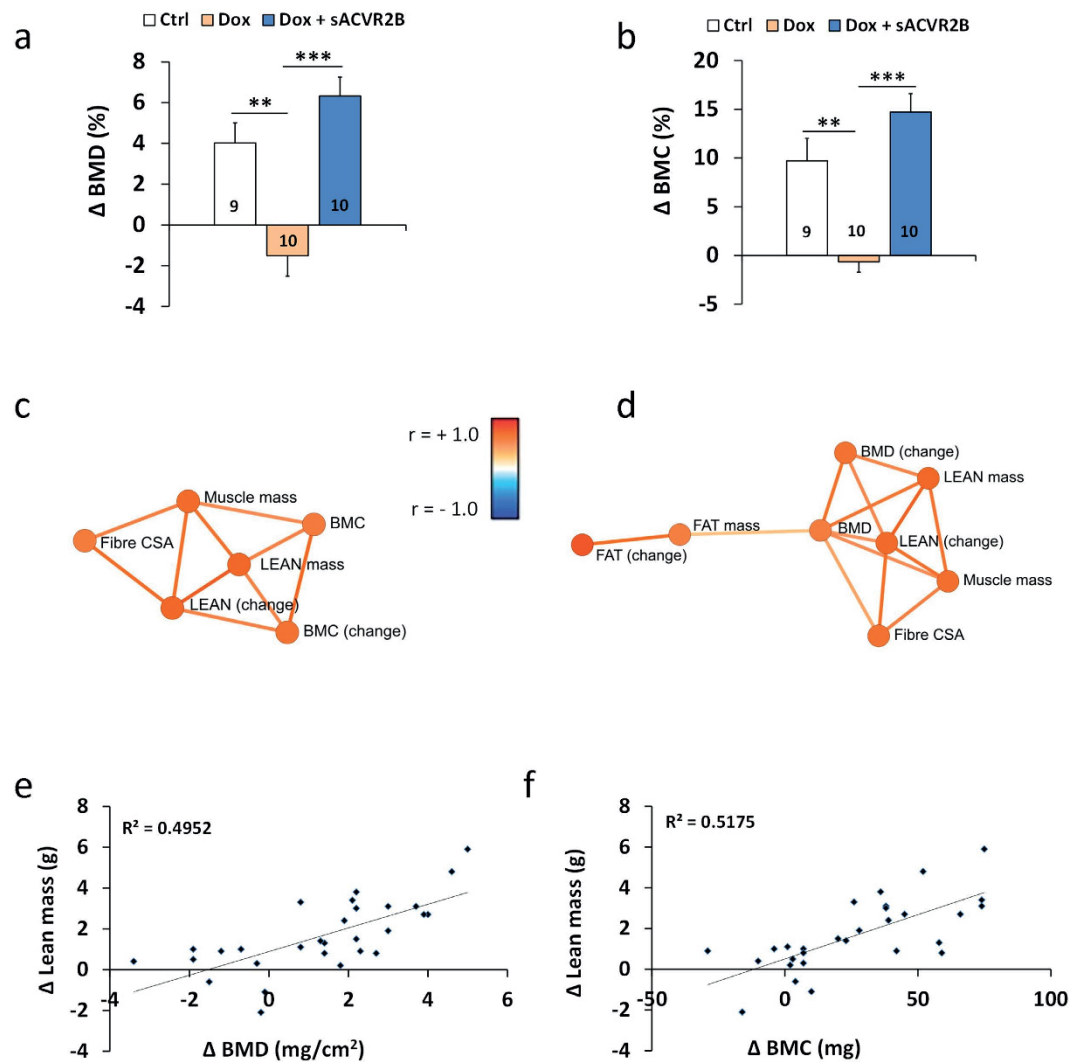


**Figure 3.** sACVR2B-Fc treatment improved bone quality in doxorubicin treated mice. Changes in bone mineral density (a) and content (b) in the four-week experiment. (c) Associations between muscle and lean mass and bone parameters. (d) Associations between muscle size, fat mass and BMD. Correlations between change in lean mass and change in BMD (e,  $r = 0.70$ ,  $P < 0.001$ ) and BMC (f,  $r = 0.72$ ,  $P < 0.001$ ). Data are presented as mean  $\pm$  SEM. \*\* $P < 0.01$ ; \*\*\* $P < 0.001$  (Bonferroni).

**Doxorubicin administration results in blunted skeletal muscle protein synthesis which is restored by sACVR2B-Fc treatment.** As only small effects were seen in the expression of negative regulators of muscle size, the effects of doxorubicin and sACVR2B-Fc administration on positive regulators of muscle mass and protein synthesis were investigated. To study protein synthesis, a previously published method of surface sensing of translation (SUnSET)<sup>32,33</sup> was applied as earlier in our laboratory<sup>19</sup>. This analysis revealed that muscle protein synthesis was significantly blunted 20 hours after doxorubicin administration compared with the controls (Fig. 6a,b). This decrease in protein synthesis was completely inhibited in mice treated with sACVR2B-Fc 48 hours prior to the exposure to doxorubicin (Fig. 6a,b). This was accompanied by increased mTORC1 signalling illustrated by elevated phosphorylation of its downstream targets rpS6 and p70S6K1 in sACVR2B-Fc treated mice acutely, but less so in the later time-points (Fig. 6c,d,g). However, at all the time-points investigated, no change in the activation of mTORC1 signalling was observed by doxorubicin, which suggests that doxorubicin and sACVR2B-Fc are affecting different pathways regulating muscle mass. Additionally, no changes due to the treatments were observed in the phosphorylation of Akt (at Ser473) or the phosphorylation of 4EBP1 (at Thr37/46) (Supplementary Fig. S3c–e).

Increased phosphorylation of eIF2 $\alpha$  on Ser51 inhibits translation initiation and it has been associated with decreased muscle protein synthesis<sup>34</sup> and cachexia<sup>14</sup>. However, the western immunoblot analysis did not show any significant doxorubicin-induced changes in eIF2 $\alpha$  phosphorylation (Fig. 6e,g). Interestingly, sACVR2B-Fc decreased the phosphorylation of eIF2 $\alpha$  compared to control (Fig. 6e,g). Another pathway regulating muscle size, partially parallel to mTORC1 signalling, is MAPK signalling. The phosphorylation of ERK 1/2 was acutely downregulated in doxorubicin treated mice, while sACVR2B-Fc treatment prevented this decrease (Fig. 6f,g). At

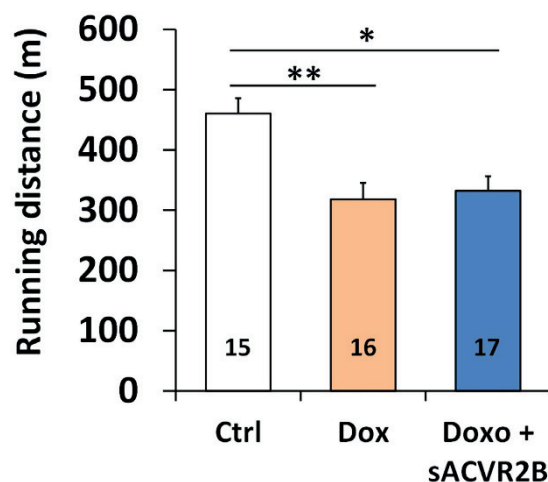


**Figure 4. Doxorubicin-treated mice had significantly impaired running capacity with no effect of sACVR2B-Fc.** Distance covered in an incremental treadmill running test until exhaustion. Data are presented as mean  $\pm$  SEM. \* $P < 0.05$ ; \*\* $P < 0.01$  (Bonferroni).

two and four weeks, the phosphorylation level of ERK 1/2 was similar between doxorubicin only treated mice and control mice.

**REDD1 is highly upregulated in doxorubicin-induced muscle loss.** To unravel the factors potentially underlying doxorubicin-induced decrease in protein synthesis and muscle size, microarray data was analysed for genes most induced by doxorubicin known to regulate muscle protein synthesis and size. Doxorubicin treated mice showed a significant 2-fold (adjusted  $P = 0.02$ ) increase in mRNA expression of *REDD1*, a protein previously connected to muscle wasting<sup>14,35</sup>. This increase was confirmed by qPCR, which showed a 3-fold increase in *REDD1* expression in doxorubicin treated mice (Fig. 6h). The effect of doxorubicin on *REDD1* expression was partially blocked by sACVR2B-Fc treatment.

**Skeletal muscle mitochondrial function and content are not chronically altered in response to doxorubicin administration.** To explore potential factors explaining impaired running capacity of the doxorubicin treated mice, skeletal muscle mitochondrial function was analysed with OROBOROS Oxygraph-2k high-resolution respirometer. At the four-week time-point, two weeks after cessation of doxorubicin administration, the analysis showed no differences in mitochondrial respiratory function of TA muscle between the three groups (Fig. 7a). This occurred independent of whether the results were presented as oxygen flux per wet weight of tissue or normalized to total TA weight or to an index of mitochondrial content. To study skeletal muscle mitochondrial function and content further, citrate synthase activity and expression of several mitochondrial proteins were analysed. Doxorubicin did not seem to alter citrate synthase activity, while increased activity was seen in mice treated with sACVR2B-Fc (Fig. 7b). Similarly as mitochondrial function, the total content of mitochondrial respiratory chain subunits (total OXPHOS) and cytochrome *c* (*cyt c*) protein remained unchanged in TA muscle irrespective of the treatment (Fig. 7c–e). However, an ion channel protein between cytosol and mitochondrial matrix, porin/VDAC1<sup>36</sup>, was significantly elevated in sACVR2B-Fc treated mice (Supplementary Fig. S5a,h). Of individual OXPHOS proteins, mitochondrial respiratory chain CI-NDUFB8 and CV-ATP5A were decreased in sACVR2B-Fc treated mice compared with doxorubicin only treated mice (Supplementary Fig. S5b–f). No differences were detected in the PGC-1 $\alpha$  protein (Supplementary Fig. S5g,h) or different PGC-1 $\alpha$  isoforms by either doxorubicin alone or combined with sACVR2B-Fc (Supplementary Fig. S6a–d).

**Skeletal muscle oxygen carrying capacity, but not capillary density, is altered in response to doxorubicin administration.** To study if blood oxygen carrying capacity was altered due to the treatments, haematological parameters were investigated at two and four weeks. Doxorubicin administration independently of sACVR2B-Fc administration resulted in decline in blood haemoglobin and haematocrit at two weeks (immediately after treatment), but this effect disappeared at four weeks (Supplementary Fig. S7a–d).

As no major differences were found in skeletal muscle mitochondrial function or content, capillary count was analysed from TA. There were no significant effects of doxorubicin or sACVR2B-Fc treatment on capillary-to-fibre ratio or capillary density (Fig. 8a–c).

**sACVR2B administration did not have any effect on tumour growth or on the antineoplastic effect of doxorubicin.** To investigate whether the sACVR2B-Fc treatment has effect on the antineoplastic effect of chemotherapy or tumour growth, a two-week tumour experiment using the Lewis lung carcinoma (LLC) model was conducted. LLC-cancer did not induce muscle atrophy yet at this time-point (Supplementary Fig. S8a–d). Similarly as with doxorubicin treated non-tumour bearing mice, doxorubicin treatment seemed to be associated with increased loss of lean and fat mass also in tumour bearing mice (Supplementary Fig. S8c–e,g,h) despite relatively low cumulative dose (12 mg/kg) of doxorubicin used. sACVR2B-Fc increased skeletal muscle and lean

Accession no.	Gene	Dox vs. Ctrl		Dox + sACVR2B vs. Dox	
		FC	P adj.	FC	P adj.
Protein degradation					
NM_001039048.2	MuRF1	1.01	0.979	0.72	0.322
NM_026346.1	Fbxo32	1.81	0.200	0.46	0.196
NM_009984.2	Ctsl	0.99	0.976	0.97	0.931
NM_011971.4	Psmb3	1.04	0.564	1.03	0.841
NM_026545.2	Psmd8	0.89	0.134	1.27	0.041*
NM_178616.2	Psmd11	1.02	0.859	0.95	0.882
NM_008945.2	Psmb4	1.07	0.439	0.97	0.884
XM_001479832.1	UBC	1.07	0.469	0.95	0.848
NM_021522.2	Usp14	1.06	0.797	1.09	0.898
NM_134013.3	Psme4	1.12	0.434	0.87	0.367
NM_011664.3	Ubb	1.14	0.133	0.96	0.737
XM_284425.1	Uba52	1.00	0.986	1.02	0.955
NM_011965.2	Psm1	1.02	0.911	1.00	0.989
NM_001033865.1	Rps27a	1.02	0.924	1.09	0.805
Glycolysis					
NM_145614.3	DLAT	0.99	0.966	1.04	0.914
NM_010699.1	Ldha	1.03	0.789	1.04	0.783
NM_011079.2	Phkg1	0.93	0.561	0.94	0.881
NM_009415.1	Tpi1	0.93	0.613	1.09	0.724
NM_023418.2	Pgam1	0.98	0.877	1.02	0.959
NM_018870.2	Pgam2	0.87	0.297	1.03	0.942
ATP synthesis					
NM_007505.2	Atp5a1	1.02	0.953	1.00	1.000
NM_198415.2	Ckmt2	1.10	0.404	0.95	0.805
NM_028388.1	Ndufv2	0.99	0.960	0.98	0.967
NM_026255.4	Slc25a6/Slc25a26	1.00	1.000	0.95	0.800
NM_145518.1	Ndufs1	0.99	0.955	1.04	0.817
NM_008618.2	Mdh1	1.01	0.970	0.94	0.825
Other					
NM_011830	IMPDH2	0.99	0.983	1.03	0.968
NM_024188.5	Oxct1	1.17	0.163	0.81	0.043*
Transcription					
NM_009372.2	Tgif1	1.22	0.285	0.69	0.151
NM_019739	Foxo1	1.73	0.021*	0.76	0.567
XM_001478948.1	Ezh1	1.06	0.585	0.96	0.884
NM_009716.2	Atf4	1.00	0.995	0.95	0.931
NM_008416.1	Junb	0.98	0.979	1.08	0.941
Translation					
XR_033381.1	Sat	1.11	0.518	0.95	0.903
NM_007918.3	Eif4ebp1	1.14	0.601	1.11	0.844
NM_013506	Eif4a2	0.98	0.908	1.01	0.984
AK019693	Eif4g3	1.00	0.987	0.96	0.850
NM_027204.2	Mrpl12	0.87	0.171	1.16	0.125
Extracellular matrix					
NM_008495.1	Lgals1	0.95	0.888	1.06	0.924
NM_015784.2	OSF-2/Postn	1.01	0.953	0.97	0.868
NM_007742.2	Col1a1	0.85	0.401	0.76	0.792
NM_007737.2	Col5a2	0.98	0.795	1.03	0.884
NM_007993	Fbn1	0.79	0.491	1.05	0.964
NM_010233.1	Fn1	0.96	0.872	0.82	0.326
Miscellaneous					
NM_013602.2	Mt1	1.11	0.774	1.15	0.696
NM_019930.1	RANBP9	1.19	0.213	0.95	0.857
NM_009974.2	Csnk2a2	0.91	0.461	1.03	0.940
Continued					

Accession no.	Gene	Dox vs. Ctrl		Dox + sACVR2B vs. Dox	
		FC	<i>P</i> adj.	FC	<i>P</i> adj.
NM_016792	TXNL	1.01	0.969	1.00	0.993
NM_013494.2	CPE	1.02	0.937	0.90	0.449
NM_013645.3	Pvalb	0.87	0.208	1.02	0.948
NM_008409.2	Itm2a	0.92	0.736	1.26	0.192
NM_053078.3	Nrep/P311	0.88	0.672	0.73	0.199

**Table 1. Atrogenes previously altered by systemic diseases in mice (fasting, tumor, uremia, diabetes mellitus) as well as disuse<sup>28</sup>.** No common changes in muscle were observed due to doxorubicin or sACVR2B-Fc on atrogenes involved in protein degradation, energy production, growth transcription/translation, genes coding extracellular matrix proteins or other genes. FC = fold change and *P* adj. = adjusted *p*-value using the Benjamini and Hochberg (false discovery rate, FDR) method. \**P* < 0.05.

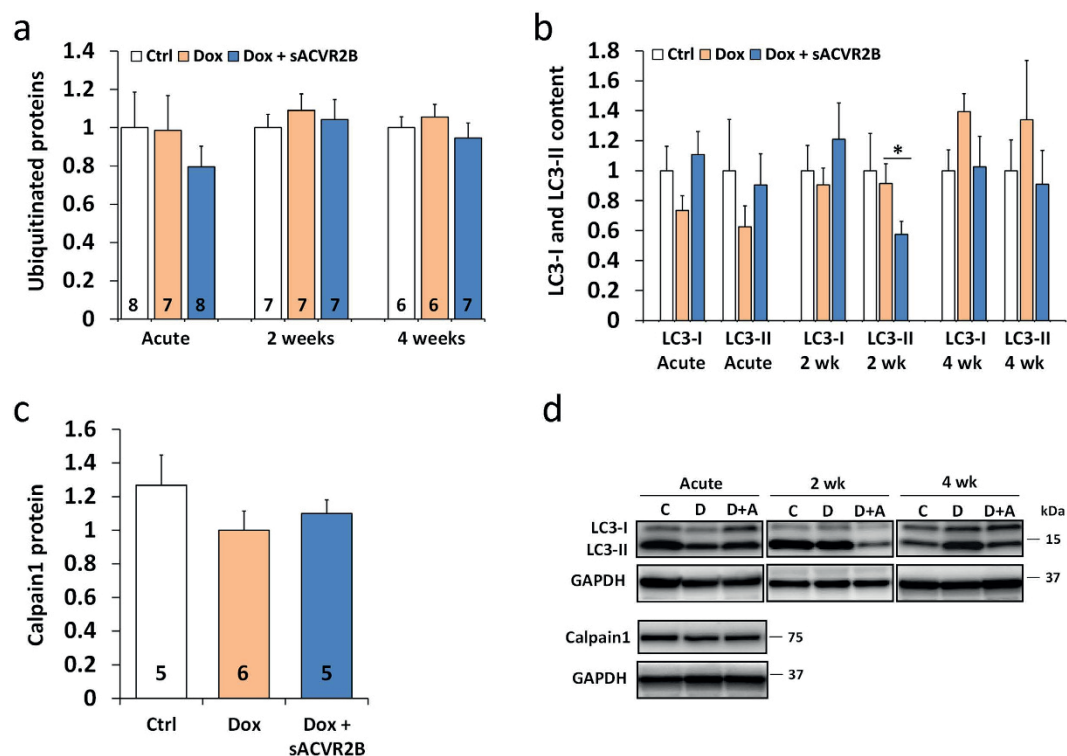


**Figure 5. Doxorubicin administration did not cause marked alterations in the markers of ubiquitin-proteasome system, autophagy or calpain1 content.** Time-course of protein ubiquitination (a) and LC3-I and -II content (N = 5–9/group) (b) relative to Ctrl and calpain1 content at 20 h relative to Dox (c) in TA muscles. (d) Representative blots of LC3 and calpain1. Data are presented as mean ± SEM. \**P* < 0.05 (Mann-Whitney U). C = Ctrl; D = Dox; D+A = Dox+sACVR2B.

mass similarly in tumour bearing mice irrespective of doxorubicin administration (Supplementary Fig. S8c,d,g). Interestingly, in contrast to the results from doxorubicin experiments in non-tumour bearing mice, in this setting, sACVR2B-Fc treatment also protected from the excessive loss of epididymal fat by doxorubicin, but not from the loss of total fat mass (DXA) (Supplementary Fig. S8e,h). The tumours of the sACVR2B-Fc treated mice had similar response to doxorubicin treatment compared to mice not treated with sACVR2B (Supplementary Fig. S8f). These results suggest that inhibiting ACVR2B ligands can decrease the cachectic effects of chemotherapy without adversely affecting tumour growth or compromising the antineoplastic effect of chemotherapy on the tumour.

## Discussion

Cancer-therapy aiming to treat malignancies can be associated with toxicities in various tissues, such as skeletal muscle, and also with shorter life span<sup>2,3</sup>. In the present study we show that prevention of doxorubicin chemotherapy-induced muscle atrophy can be achieved by preventing decreased muscle protein synthesis using a blocker for ACVR2B ligands without negative side-effects on aerobic capacity or tumour growth.

Doxorubicin administration resulted in marked decrease in body weight, comprised of loss of both lean and fat mass. Skeletal muscle atrophy was observed as a decrease in muscle masses and in TA fibre size. These results

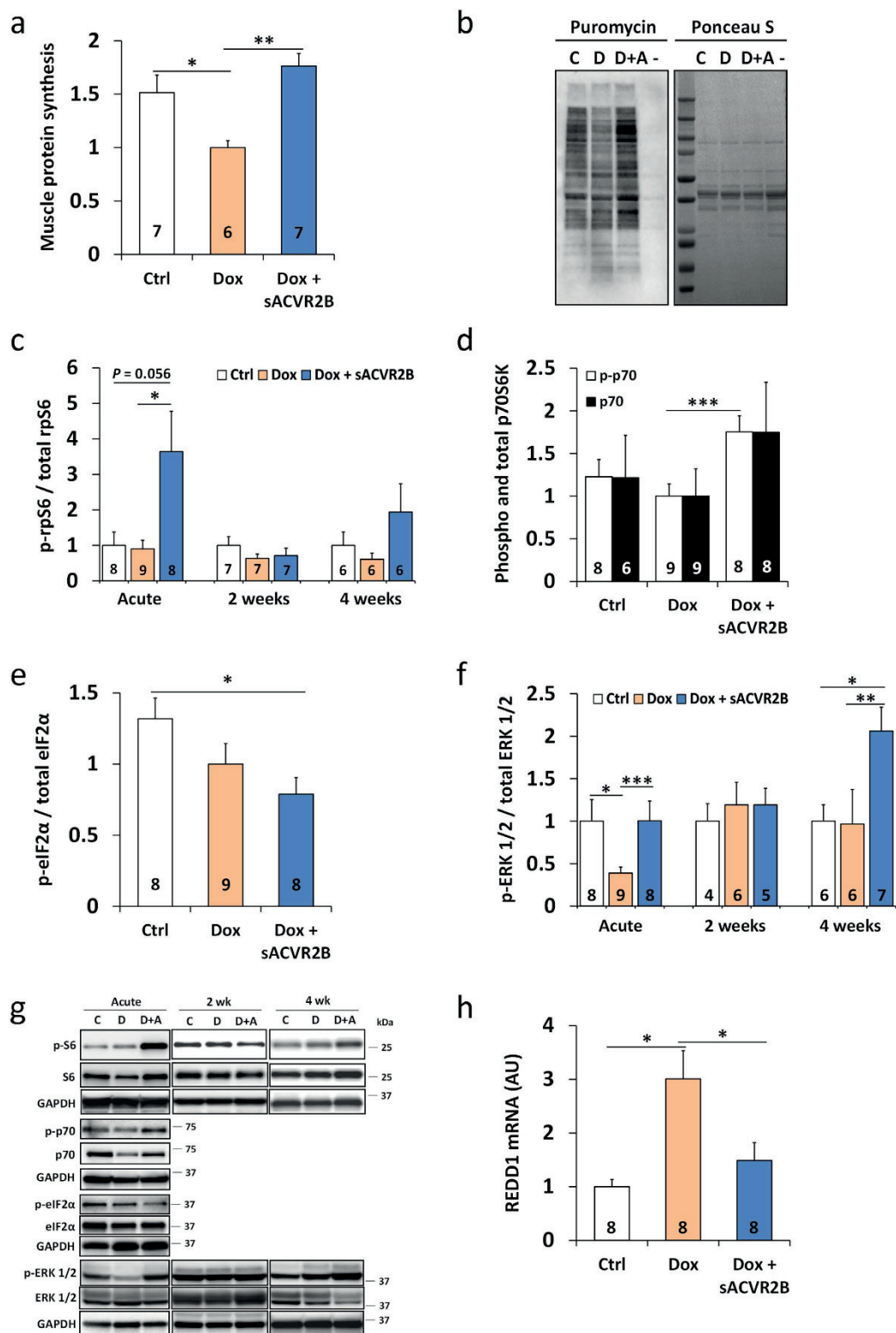


**Figure 6. Doxorubicin administration resulted in decreased muscle protein synthesis that was restored by sACVR2B-Fc.** (a) Muscle protein synthesis relative to Dox analysed with puromycin incorporation method and (b) representative blot (left) with Ponceau S staining (right). (– = negative control for puromycin). (c) Time-course of rpS6 phosphorylation at Ser240/244 relative to Ctrl in TA muscle. p70S6K (Thr389) (d) and eIF2α (Ser51) (e) phosphorylation response 20 hours after a single dose of doxorubicin relative to Dox. (f) Time-course of ERK 1/2 phosphorylation at Thr202/Tyr204 relative to Dox in TA muscle. (g) Representative blots of rpS6, p70S6K, eIF2α and ERK 1/2. (h) REDD1 mRNA expression normalized to 36b4 expression relative to Ctrl in TA muscle 20 hours after a single dose of doxorubicin. Data are presented as mean ± SEM. \* $P < 0.05$ ; \*\* $P < 0.01$ ; \*\*\* $P < 0.001$  (Bonferroni (a,h), Mann-Whitney U -test (c–f)).



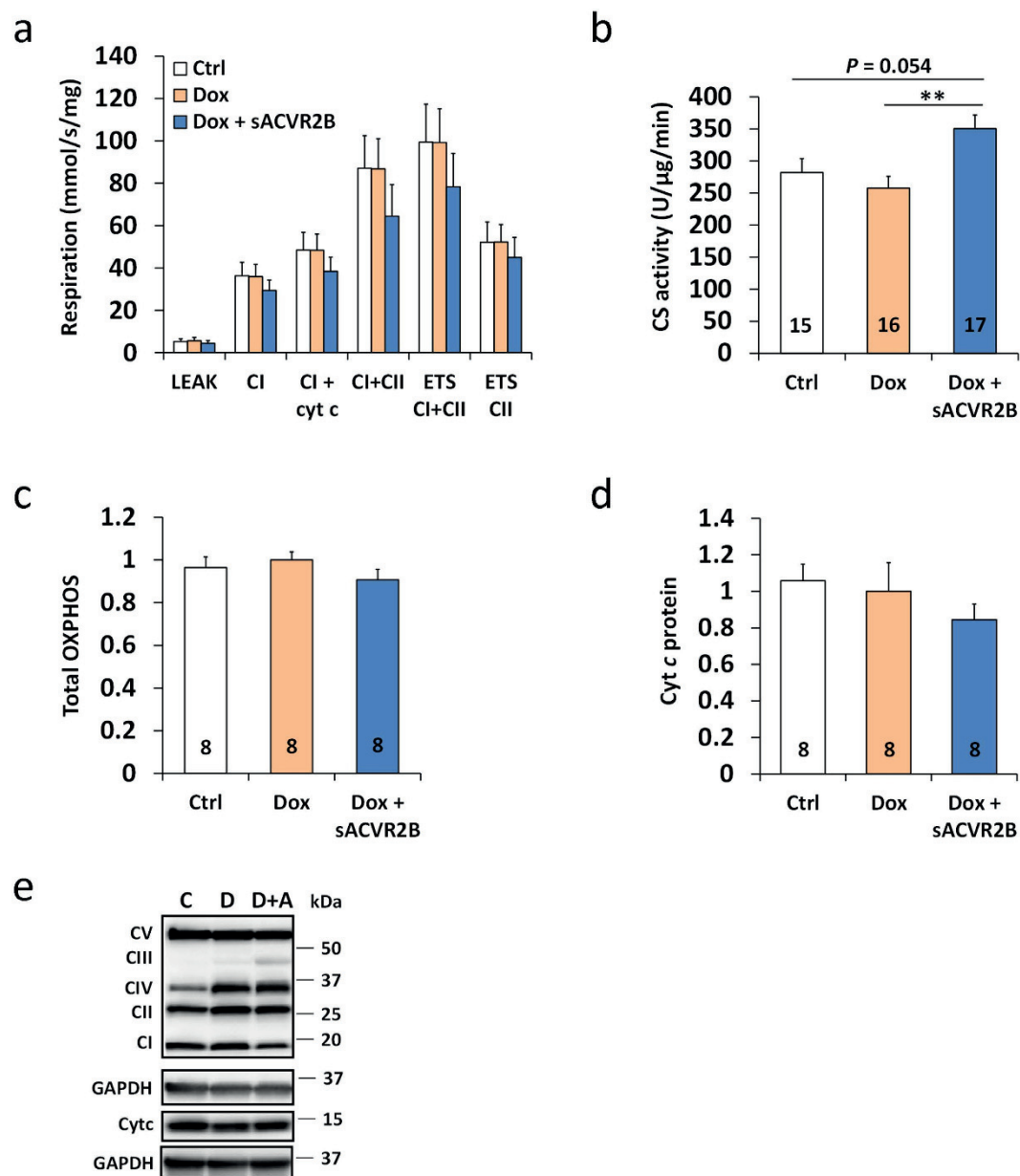


**Figure 7. Doxorubicin administration did not affect mitochondrial function or markers of mitochondrial content in skeletal muscle.** (a) Mitochondrial respiration in homogenized TA muscle with carbohydrate substrates ( $N = 7-8/\text{group}$ ). Cyt *c* = cytochrome *c*; CI/II = complex I/II; ETS = electron transfer system. (b) Citrate synthase (CS) activity measured from TA muscle. Quantification of total content of mitochondrial respiratory chain subunits (c) and cytochrome *c* (Cyt *c*) relative to Dox (d) and representative blots (e). Data are presented as mean  $\pm$  SEM. \*\* $P < 0.01$  (Bonferroni (a–b), Mann-Whitney U (c–d)).

are consistent with previous studies<sup>10,11,37</sup>. The reduced fat mass and muscle size by doxorubicin might be at least partially explained by reduced feed intake. However, as doxorubicin has been shown to accumulate in skeletal muscle tissue<sup>38</sup>, it is possible that doxorubicin also had a direct effect on skeletal muscle. Indeed, doxorubicin accumulation was detected in skeletal muscles, and it acutely led to a typical p53 and DNA-damage response (unpublished observations) in line with previous reports in cardiac muscle<sup>5,39</sup>. Importantly, treatment of muscle atrophy by blocking ACVR2B ligands was accomplished without any adverse effects on tumour, as shown earlier with several other tumour models<sup>20,21</sup>, or on the effect of doxorubicin on tumour.

Muscle atrophy is a result of a situation in which the rate of protein synthesis is, over a period of time, repressed relative to that of degradation. Protein synthesis responses in muscle atrophy have been overall less investigated than protein degradation pathways<sup>13,14</sup>. The present results show, for the first time, that doxorubicin administration acutely results in blunted protein synthesis in skeletal muscle. Previous studies have reported either repressed<sup>40</sup> or unchanged<sup>41</sup> protein synthesis in cardiac muscle or cardiomyocytes after acute doxorubicin administration. Importantly, the decreased muscle protein synthesis by doxorubicin was completely prevented by

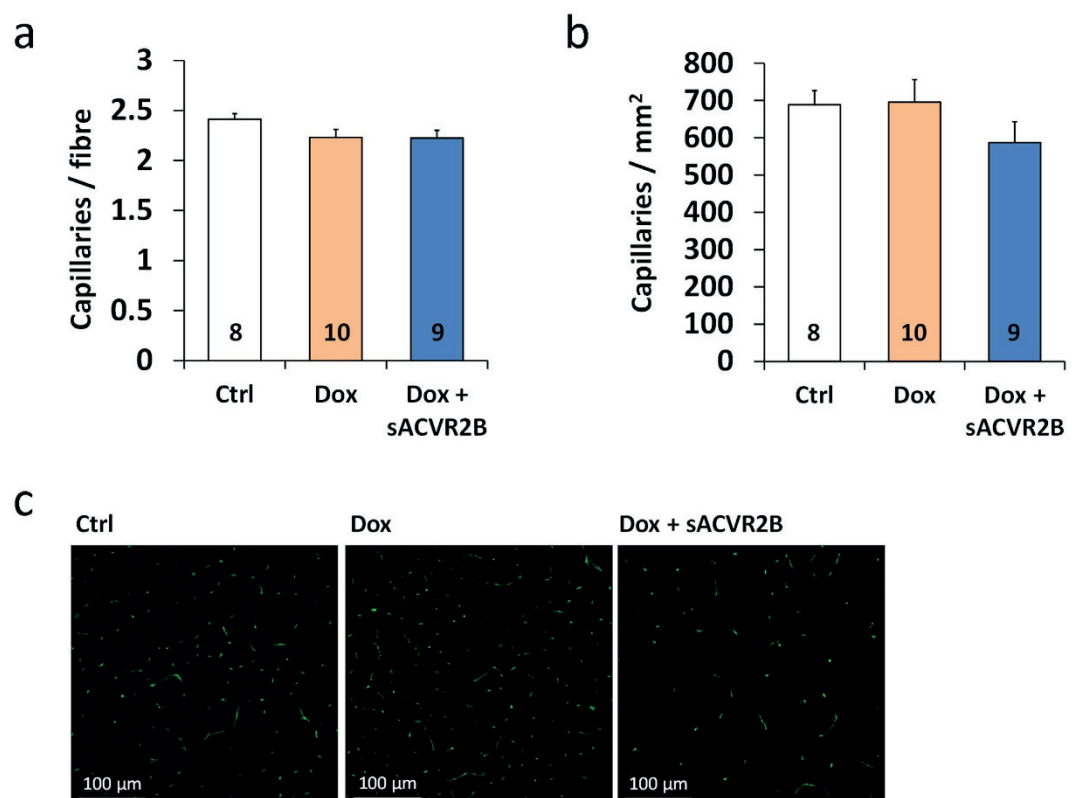


**Figure 8. Doxorubicin administration did not affect skeletal muscle capillary density.** Quantification of the capillary-to-fibre ratio (a) and the number of capillaries per muscle area (b) in TA muscle. (c) Representative immunofluorescence images of CD31/PECAM-1 staining for capillaries. Notice that the representative capillary images are from exactly the same location as the dystrophin staining in Fig. 2c. Data are presented as mean  $\pm$  SEM. \* $P < 0.05$  (Bonferroni).

sACVR2B-Fc administration. The increased protein synthesis by sACVR2B-Fc is likely due to increased mTORC1 signalling manifested by increased phosphorylation of p70S6K and rpS6. These markers of mTORC1 signalling also positively correlated with protein synthesis (Supplementary Fig. S9a). This is consistent with previous results from our laboratory, which showed that sACVR2B-Fc treatment in healthy wildtype mice increased muscle size, protein synthesis and mTORC1 signalling<sup>19</sup>. However, doxorubicin did not seem to affect this pathway at least at 20 h time-point as phosphorylation levels of p70S6K and rpS6 were similar to control group. This does not exclude the possibility that decrease in mTORC1 signalling would have preceded the decreased protein synthesis.

In the present study, no major changes were observed in protein degradation markers such as ubiquitinated proteins, atrogene expression<sup>28</sup>, or markers of autophagy. However, the slight enrichment of the atrogene, proteasome and apoptosis gene sets in response to doxorubicin administration might indicate at least a small increase in protein degradation and apoptosis. The previous available evidence on protein degradation and apoptosis pathways suggests activated calpain-caspase-3-apoptosis pathway<sup>9,11,42</sup>, and increased markers of ubiquitin-proteasome system<sup>9</sup>, and autophagy<sup>43</sup> as contributors to doxorubicin-induced muscle atrophy, but the evidence is inconsistent<sup>31,44</sup>. The reason why we observed only very small upregulation in the protein degradation and apoptosis pathways can be speculated to be the dosage of doxorubicin used in our study, i.e. 24 mg/kg cumulative dose or 15 mg/kg single dose in the acute experiment. The 15–24 mg/kg in mice is equivalent to ~45–72 mg/m<sup>2</sup> in humans and thus very close to the clinical doses used in cancers (30–90 mg/m<sup>2</sup>)<sup>5</sup>. These doses are relatively small compared to the ones typically used in the rat studies, i.e. 20 mg/kg in rats<sup>11,37,42</sup> that can be estimated to be equivalent to ~40 mg/kg in mice and ~120 mg/m<sup>2</sup> in humans<sup>26</sup>. Nevertheless, although the mechanisms behind doxorubicin-induced muscle atrophy can be dose-dependent<sup>9</sup>, the blockade of decreased protein synthesis without major alterations in the protein degradation, apoptosis or autophagy pathways seems to be the mechanism by which sACVR2B-Fc prevents doxorubicin-induced muscle loss. However, part of the increased protein synthesis may also be due to larger *de novo* protein synthesis, as we have shown earlier that sACVR2B-Fc increases muscle protein synthesis also in healthy mice<sup>19</sup>. Moreover, a decrease in the ubiquitin ligase MuRF1 mRNA by sACVR2B-Fc was noticed supporting previous studies by Rahimov *et al.* in wildtype mice and Zhou *et al.* in cachectic mice<sup>20,25</sup>. This shows a potential for sACVR2B-Fc in preventing atrophy also in situations where protein degradation pathways are more strongly activated.

A transcriptome analysis was conducted to investigate if genes previously shown to have a role in muscle atrophy were regulated by doxorubicin. Interestingly, REDD1, a DNA damage marker protein that has previously been connected to muscle wasting and decreased protein synthesis<sup>14</sup> also in other models, e.g.

streptozotocin-induced experimental type 1 diabetes<sup>35</sup>, was one of the most highly upregulated genes. A negative correlation between REDD1 expression and protein synthesis was observed (Supplementary Fig. S9b). This suggests that doxorubicin-induced REDD1 expression could, in part, contribute to decreased protein synthesis, but more mechanistic evidence is needed to verify this connection. Another candidate associated with the regulation of muscle size is MAPK-signalling<sup>45,46</sup>. Doxorubicin administration resulted in marked decrease in ERK 1/2 phosphorylation. Similar decrease in ERK phosphorylation has been previously reported five days after doxorubicin dose identical to our acute experiment (15 mg/kg) in mouse skeletal muscle<sup>31</sup>. The physiological importance of altered ERK 1/2 MAPK-signalling is unknown, and may be dependent on time-point and context<sup>19,45–47</sup>. Interestingly, in our setting, sACVR2B-Fc administration restored ERK 1/2 phosphorylation to the level of control mice. We have shown earlier that sACVR2B-Fc treatment decreased the phosphorylation of ERK 1/2 at early, but not at later time-points in healthy mice<sup>19</sup>. This shows that, in addition to the many other pathways, such as mTORC1 signalling, the regulation of MAPK signalling by blocking ACVR2B receptor ligands can also be dependent on timing and context. More research is needed to determine the consequences and importance of the doxorubicin-induced decrease in ERK 1/2 phosphorylation and prevention of this response by blocking sACVR2B ligands.

Several studies have investigated the effects of exercise training on the effects of doxorubicin. Majority<sup>42,43,48</sup>, but not all<sup>49</sup> of these studies suggest that exercise training protects against the adverse effects of doxorubicin on cardiac and skeletal muscle without compromising<sup>50</sup> or even enhancing its antitumor efficacy<sup>49</sup>. On the other hand, maximal aerobic capacity on a whole-body level has been associated with longevity and health<sup>51</sup>. Muscle weakness and fatigue as well as skeletal muscle contractile dysfunction have been reported after exposure to doxorubicin in patients<sup>4</sup> and in animal models *ex vivo*<sup>4,8,12</sup>. However, to the knowledge of the authors, the present study is the first one to show direct negative effects of doxorubicin administration on maximal aerobic running capacity *in vivo*. As this effect was observed two weeks after the cessation of doxorubicin administration, it seems that the impairment in aerobic capacity is sustained.

Impaired running performance by doxorubicin could have been expected to be accompanied by decreased mitochondrial respiratory capacity, but this was not the case in the present study. According to the previous literature, doxorubicin can cause impaired mitochondrial function in cardiac<sup>52,53</sup> and in skeletal muscle<sup>10,37,53</sup>. However, the evidence concerning skeletal muscle is inconsistent: not all studies report significant impairments in the markers of mitochondrial function in response to doxorubicin treatment<sup>52</sup>. In addition, Gouspillou and colleagues<sup>10</sup> did not observe any significant or sustained impairment in skeletal muscle mitochondrial respiratory function after two cycles of doxorubicin treatment (cumulative dose 20 mg/kg) in mice. However, four cycles of treatment (cumulative dose 40 mg/kg) resulted in impaired mitochondrial respiration that was sustained over a 12-week period after the last cycle<sup>10</sup>. In that study mice were also treated with dexamethasone, so the contribution of each drug to the effects cannot be confirmed<sup>10</sup>. Furthermore, impaired mitochondrial respiration has been reported 2–72 hours after a single high dose of doxorubicin (20 mg/kg) in rats<sup>37</sup>. According to the present and these previous studies, the dosage of doxorubicin used and the time-points investigated may play important roles in doxorubicin-induced alterations in skeletal muscle mitochondrial function.

As a novel finding of the present study, doxorubicin treatment did not alter muscle capillary density and thus, decreased capillarization cannot explain the impaired running capacity. Also limb muscle independent factors can lie behind the persistently impaired running performance. Systemic doxorubicin administration has previously been shown to cause weakness and contractile dysfunction in diaphragm<sup>11,12</sup>, the principal respiratory muscle. Doxorubicin-induced cardiotoxicity can also have an effect on whole body exercise capacity. Interestingly, sACVR2B-Fc could not prevent doxorubicin-induced cardiac atrophy (data not shown). This was, however, achieved by vascular endothelial growth factor-B (VEGF-B<sup>54</sup>) gene therapy in the same experimental setting (Räsänen *et al.* unpublished observations). The present study also showed that doxorubicin administration can reduce blood oxygen carrying capacity consistent with earlier reports<sup>55</sup>. However, this did not persist anymore two weeks after the cessation of doxorubicin administration. Thus, this effect probably does not play a major role in the persistently impaired running performance. It is likely that multiple factors, rather than just one, contribute to impaired exercise capacity by doxorubicin.

Contrary to previous results in wild type and dystrophic mice<sup>18,23</sup>, systemic sACVR2B-Fc administration did not cause any further impairment in running performance or mitochondrial content or function. Some more specific effects were, however, noticed. Unlike in wildtype or mice with muscular dystrophy<sup>18,23</sup>, citrate synthase activity and the content of a mitochondrial channel protein porin/VDAC1<sup>36</sup> were increased in doxorubicin treated mice administered with sACVR2B-Fc compared with doxorubicin alone. However, sACVR2B-Fc administration decreased mitochondrial respiratory chain subunit proteins CI-NDUFB8 and CV-ATP5A. This suggests that blocking ACVR2B ligands may have specific effects on mitochondrial proteins even though overall mitochondrial capacity or function may be unaltered. Previously, sACVR2B-Fc administration has decreased electron transport chain and oxidative phosphorylation gene sets in mdx mice<sup>22</sup>. As no effects on mitochondrial function or further decrease in running capacity were detected, these specific effects of blocking ACVR2B ligands have probably only minor physiological significance. Our laboratory has previously published evidence of interaction effects of exercise and sACVR2B-Fc in muscles<sup>18,22</sup>. Future studies should investigate the effects of blocking activin receptor ligands also in active mice.

Musculoskeletal system plays an important role in e.g. enabling locomotion. Bone can serve as an ion reserve to maintain serum ion concentrations of e.g. calcium and magnesium. Mechanical and molecular interaction between muscles and bone has got lots of attention during the last few years<sup>56</sup>. Many studies have shown that improving muscle size and strength can improve bone quantity or quality<sup>57</sup>. For instance, blocking myostatin/activins has improved bone mass, quality and strength<sup>58</sup>. On the other hand, bone parameters have been reported to be decreased in rodents after doxorubicin administration<sup>59</sup>. The present study showed that the decrease in BMD and BMC by doxorubicin was prevented by sACVR2B-Fc and that the bone results are strongly related to

muscle mass. Therefore, it is speculated that changes in bone adaptation were secondary to muscle showing the importance of muscle *per se* on certain markers of health. However, the possible existence of other direct or indirect effects of sACVR2B-Fc on bone cannot be excluded<sup>58</sup>.

In conclusion, unlike in many other cachexia-inducing diseases, our findings show that doxorubicin chemotherapy induces skeletal muscle atrophy without markedly increasing typical atrogenes or protein degradation pathways. In contrast, muscle atrophy induced by doxorubicin is probably mainly mediated by decreased protein synthesis, and this effect is prevented by blocking ACVR2B signalling. In addition, the current results suggest that blocking ACVR2B signalling may be a promising strategy to counteract chemotherapy-induced muscle and bone loss without further damage to skeletal muscle oxidative capacity or mitochondria or the actual treatment of malignancies.

## Methods

**Animals.** C57BL/6J male mice (Envigo), aged 9–10 weeks, were used in all experiments. Mice were maintained under standard conditions (temperature 22 °C, 12:12 h light/dark cycle) with free access to food and water. The protocols were approved by the National Animal Experiment Board, and all the experiments were carried out in accordance with the guidelines of that committee.

**Experimental design.** Five experiments were conducted: 1–2) two four-week experiments, 3) a two-week experiment, 4) an acute experiment, and 5) a tumour experiment. In experiments 1–4, the mice were randomly assigned into one of three groups: 1) vehicle (PBS) treated controls (Ctrl), 2) doxorubicin hydrochloride treated mice (Dox), and 3) doxorubicin treated mice administered intraperitoneally with sACVR2B-Fc (Dox + sACVR2B). In the tumour experiment (exp 5), the mice were randomized into five groups: 1) healthy controls (Ctrl), 2) LLC-tumour bearing mice (LLC + PBS), 3) LLC-mice treated with doxorubicin (LLC + Dox), 4) LLC-mice treated with sACVR2B-Fc (LLC + sACVR2B), and 5) LLC-mice treated with doxorubicin and sACVR2B-Fc (LLC + Dox + sACVR2B).

**Experimental treatments.** In experiments 1–3, all doxorubicin administered mice received a total of four intraperitoneal injections of doxorubicin (6 mg/kg in PBS), administered every third day during the first two weeks of the experiment. Control mice were administered with an equal volume of PBS. In the four-week experiments (1 and 2), the mice were euthanized four weeks after the first and 19 days after the last doxorubicin injection. In the two-week experiment (3), the mice were euthanized two weeks after the first and 4 days after the last doxorubicin injection. In these experiments, sACVR2B-Fc (5 mg/kg in PBS) was administered intraperitoneally for half of the doxorubicin treated mice twice a week during the first two weeks of the experiment and once a week after that (in the 4-week experiments). sACVR2B-Fc administration was started before the first doxorubicin injection and the last dose was administered seven days before euthanasia.

In the acute experiment, doxorubicin treated mice received a single intraperitoneal injection of doxorubicin (15 mg/kg in PBS) and controls an equal volume of PBS. sACVR2B-Fc treated mice received a single intraperitoneal injection of sACVR2B-Fc (10 mg/kg in PBS) 48 hours before doxorubicin administration, a time-point when sACVR2B-Fc shows increased muscle protein synthesis<sup>19</sup>. The mice were euthanized 20 hours after doxorubicin/PBS administration.

In the tumour experiment, mice were subcutaneously inoculated with  $0.5 \times 10^6$  LLC cells (a kind gift from Dr. Alitalo) in 100  $\mu$ l of PBS or with an equal volume of vehicle only (controls) into the right abdominal region. Doxorubicin was administered intraperitoneally twice during the experiment on the sixth and eleventh day after tumour inoculation (cumulative dose 12 mg/kg). sACVR2B-Fc (5 mg/kg in PBS) was administered intraperitoneally twice a week starting from third day after tumour inoculation and the last injection being two days before euthanasia. The mice were euthanized 14 days after tumour inoculation.

**Tissue collection.** At the end of all experiments, the mice were anaesthetized and then euthanized by heart puncture followed by cervical dislocation. Hindlimb muscles TA, gastrocnemius and soleus as well as epididymal fat pads were immediately excised and weighed. The left TA was snap-frozen in liquid nitrogen and the right TA muscle was mounted in O.C.T. embedding medium (Tissue Tek) and snap-frozen in isopentane cooled with liquid nitrogen. All tissue weights were normalized to the length of the tibia (mm).

**sACVR2B-Fc production.** The recombinant fusion protein was produced and purified *in house* as described earlier in detail<sup>19</sup>. Briefly, the ectodomain of human ACVR2B was fused with a human IgG1 Fc domain and the fusion protein was expressed in Chinese hamster ovary cells grown in a suspension culture. The protein is similar, but not identical to that originally generated by Lee and colleagues<sup>17</sup>.

**Tumour cell line and cell culture.** LLC cells were originally purchased from American Type Culture Collection (Manassas, VA) and maintained in complete Dulbecco's Modified Eagle's Medium (DMEM) supplemented with 2 mmol/L L-glutamine, penicillin (100 U/mL), streptomycin (100  $\mu$ g/mL), and 10% FBS.

**Dual-energy X-ray absorptiometry (DXA).** For the DXA analysis, mice were anaesthetized with a combination of ketamine and xylazine and imaged with Lunar PIXImus II densitometer (GE Healthcare). The images were analysed using standard procedures.

**Treadmill running protocol.** The mice ran first at 9, 12 and 15 m/min for 5 minutes each, after which the velocity was increased by 2 m/min every 2 minutes until exhaustion. All mice were familiarized with treadmill running on a separate day prior to the test.

**Muscle protein synthesis: *in vivo* surface sensing of translation.** Muscle protein synthesis was analysed using surface sensing of translation (SUnSET) method<sup>32,33</sup> as earlier in our laboratory<sup>19</sup>. At exactly 25 min after puromycin (Calbiochem) administration, mice were euthanized by heart puncture followed by cervical dislocation. Left TA muscle was isolated, weighed and snap-frozen in liquid nitrogen exactly 30 minutes after puromycin administration.

**Mitochondrial function analysis.** Skeletal muscle mitochondrial function was analysed with OROBOROS Oxygraph-2k high-resolution respirometer with similar procedures as earlier<sup>54</sup>. Briefly, a thin cross-section of 5–10 mg from the middle of the left TA muscle was removed and temporarily stored in Biops buffer. The sample was then homogenized with a shredder and carbohydrate SUIT protocol was used to analyse mitochondrial function as previously described<sup>54</sup>.

**RNA analysis.** Total RNA was extracted from the TA muscle with TRIreagent (Bioline) and further purified with NucleoSpin<sup>®</sup> RNA II columns. For qPCR RNA was reverse transcribed to cDNA using iScript<sup>™</sup> Advanced cDNA Synthesis Kit for RT-qPCR (Bio-Rad Laboratories) according to the manufacturer's instructions. Real-time qPCR was performed according to standard procedures using iQ SYBR Supermix (Bio-Rad Laboratories) and CFX96 Real-Time PCR Detection System (Bio-Rad Laboratories). Data analysis was carried out by using efficiency corrected  $\Delta\Delta C_t$  method. More information on qPCR is given in Supplementary methods.

RNA samples of five mice from each group were analysed with Illumina Sentrix MouseRef-6 v2 Expression BeadChip containing 45281 transcripts (Illumina Inc.) by the Functional Genomics Unit at Biomedicum Helsinki, University of Helsinki, Finland. Before the analysis, sample RNA was analysed for integrity and quality with Agilent Bioanalyzer 2100. Raw data were normalized with quantile normalization and data quality was assessed using Chipster software (IT Center for Science, Espoo, Finland)<sup>60</sup>. The complete data set is publicly available in the NCBI Gene Expression Omnibus (<http://www.ncbi.nlm.nih.gov/geo/>; accession no. GSE77745). More detailed description is provided in Supplementary methods.

**Protein extraction and content.** TA muscle samples were homogenized in ice-cold buffer with proper inhibitors and further treated as earlier<sup>19,35</sup> with slight modifications. Total protein content was determined using the bicinchoninic acid (BCA) protein assay (Pierce, Thermo Scientific) with an automated KoneLab device (Thermo Scientific).

**Citrate synthase activity.** Citrate synthase activity was measured from TA muscle homogenates using a kit (Sigma-Aldrich) with an automated KoneLab device (Thermo Scientific).

**Western blotting.** Western immunoblot analyses were performed as previously reported<sup>19,35</sup>, with slight modifications in the quantification of ubiquitinated proteins and puromycin incorporation: In the case of the analysis of puromycin-incorporated proteins and ubiquitinated proteins, the intensity of the whole lane was quantified. Ponceau S staining and GAPDH were used as loading controls and all the protein level results were normalized to the mean of Ponceau S and GAPDH, except for the puromycin-incorporated proteins that were normalized only to Ponceau S. The antibodies used are listed in the supplementary methods online.

**Muscle immunohistochemistry.** Cross-sections (10  $\mu$ m) were cut from TA muscle with a cryomicrotome. To analyse muscle fibre cross-sectional area (CSA), the sarcolemmas were visualized using antibodies against Dystrophin (Abcam) with Alexa Fluor 555 secondary antibody (Molecular Probes). This was combined with PECAM-1/CD31 (BD Pharmingen) staining with Alexa Fluor 488 secondary antibody (Molecular Probes) to visualize capillaries and DAPI for the nuclei. The stained sections were imaged with a confocal microscope (Zeiss) and ZEN software. The mean fibre CSA was quantified from 1,065  $\pm$  58 fibres representing both the deep and the superficial regions of the muscle. For the analysis of fibre size distribution, 550 fibres were randomly picked from each muscle sample. Muscle fibre CSA, capillary density (capillaries/mm<sup>2</sup>) and capillary-to-fibre ratios were analysed with ImageJ software (NIH).

**Statistical analyses.** Values are presented as means  $\pm$  SEM. The data from experiments 1 and 2 was pooled when there were no differences between the experiments. Data was checked for normality and differences between groups were analysed with general linear model ANOVA with Bonferroni post-hoc test, when appropriate. Western blot results were analysed with general linear model ANOVA with Bonferroni post-hoc test or with non-parametric Kruskal-Wallis test with Holm-Bonferroni corrected Mann-Whitney U as post-hoc when appropriate. Correlations were analysed using Pearson's Product Moment Coefficient. Differences were considered statistically significant at  $P \leq 0.05$ . Statistical analyses were performed with IBM SPSS Statistics version 22 for Windows (SPSS, Chicago, IL).

## References

1. Tisdale, M. J. Mechanisms of cancer cachexia. *Physiol. Rev.* **89**, 381–410 (2009).
2. Kazemi-Bajestani, S. M., Mazurak, V. C. & Baracos, V. Computed tomography-defined muscle and fat wasting are associated with cancer clinical outcomes. *Semin. Cell Dev. Biol.* (2015).
3. Cooper, A. B. *et al.* Characterization of Anthropometric Changes that Occur During Neoadjuvant Therapy for Potentially Resectable Pancreatic Cancer. *Ann. Surg. Oncol.* **22**, 2416–2423 (2015).
4. Gilliam, L. A. & St Clair, D. K. Chemotherapy-induced weakness and fatigue in skeletal muscle: the role of oxidative stress. *Antioxid. Redox Signal.* **15**, 2543–2563 (2011).
5. Vejpongsa, P. & Yeh, E. T. Prevention of anthracycline-induced cardiotoxicity: challenges and opportunities. *J. Am. Coll. Cardiol.* **64**, 938–945 (2014).
6. Bonifati, D. M. *et al.* Neuromuscular damage after hyperthermic isolated limb perfusion in patients with melanoma or sarcoma treated with chemotherapeutic agents. *Cancer Chemother. Pharmacol.* **46**, 517–522 (2000).

7. Braun, T. P. *et al.* Muscle atrophy in response to cytotoxic chemotherapy is dependent on intact glucocorticoid signaling in skeletal muscle. *PLoS One* **9**, e106489 (2014).
8. Gilliam, L. A. *et al.* Doxorubicin acts through tumor necrosis factor receptor subtype 1 to cause dysfunction of murine skeletal muscle. *J. Appl. Physiol.* (1985) **107**, 1935–1942 (2009).
9. Gilliam, L. A. *et al.* Doxorubicin acts via mitochondrial ROS to stimulate catabolism in C2C12 myotubes. *Am. J. Physiol. Cell. Physiol.* **302**, C195–202 (2012).
10. Gouspillou, G. *et al.* Anthracycline-containing chemotherapy causes long-term impairment of mitochondrial respiration and increased reactive oxygen species release in skeletal muscle. *Sci. Rep.* **5**, 8717 (2015).
11. Min, K. *et al.* Increased mitochondrial emission of reactive oxygen species and calpain activation are required for doxorubicin-induced cardiac and skeletal muscle myopathy. *J. Physiol.* **593**, 2017–2036 (2015).
12. Gilliam, L. A., Moylan, J. S., Ferreira, L. F. & Reid, M. B. TNF/TNFR1 signaling mediates doxorubicin-induced diaphragm weakness. *Am. J. Physiol. Lung Cell. Mol. Physiol.* **300**, L225–31 (2011).
13. Cohen, S., Nathan, J. A. & Goldberg, A. L. Muscle wasting in disease: molecular mechanisms and promising therapies. *Nat. Rev. Drug Discov.* **14**, 58–74 (2015).
14. Gordon, B. S., Kelleher, A. R. & Kimball, S. R. Regulation of muscle protein synthesis and the effects of catabolic states. *Int. J. Biochem. Cell Biol.* **45**, 2147–2157 (2013).
15. McPherron, A. C., Lawler, A. M. & Lee, S. J. Regulation of skeletal muscle mass in mice by a new TGF-beta superfamily member. *Nature* **387**, 83–90 (1997).
16. Chen, J. L. *et al.* Elevated expression of activins promotes muscle wasting and cachexia. *FASEB J.* **28**, 1711–1723 (2014).
17. Lee, S. J. *et al.* Regulation of muscle growth by multiple ligands signaling through activin type II receptors. *Proc. Natl. Acad. Sci. USA.* **102**, 18117–18122 (2005).
18. Hulmi, J. J. *et al.* Exercise restores decreased physical activity levels and increases markers of autophagy and oxidative capacity in myostatin/activin-blocked mdx mice. *Am. J. Physiol. Endocrinol. Metab.* **305**, E171–82 (2013).
19. Hulmi, J. J. *et al.* Muscle protein synthesis, mTORC1/MAPK/Hippo signaling, and capillary density are altered by blocking of myostatin and activins. *Am. J. Physiol. Endocrinol. Metab.* **304**, E41–50 (2013).
20. Zhou, X. *et al.* Reversal of cancer cachexia and muscle wasting by ActRIIB antagonism leads to prolonged survival. *Cell* **142**, 531–543 (2010).
21. Toledo, M. *et al.* Complete reversal of muscle wasting in experimental cancer cachexia: Additive effects of activin type II receptor inhibition and beta-2 agonist. *Int. J. Cancer* **138**, 2021–2029 (2016).
22. Kainulainen, H. *et al.* Myostatin/activin blocking combined with exercise reconditions skeletal muscle expression profile of mdx mice. *Mol. Cell. Endocrinol.* **399**, 131–142 (2015).
23. Relizani, K. *et al.* Blockade of ActRIIB signaling triggers muscle fatigability and metabolic myopathy. *Mol. Ther.* **22**, 1423–1433 (2014).
24. Lee, Y. S. *et al.* Muscle hypertrophy induced by myostatin inhibition accelerates degeneration in dysferlinopathy. *Hum. Mol. Genet.* **24**, 5711–5719 (2015).
25. Rahimov, F. *et al.* Gene expression profiling of skeletal muscles treated with a soluble activin type IIB receptor. *Physiol. Genomics* **43**, 398–407 (2011).
26. Freireich, E. J., Gehan, E. A., Rall, D. P., Schmidt, L. H. & Skipper, H. E. Quantitative comparison of toxicity of anticancer agents in mouse, rat, hamster, dog, monkey, and man. *Cancer Chemother. Rep.* **50**, 219–244 (1966).
27. Makinen, V. P. *et al.* Network of vascular diseases, death and biochemical characteristics in a set of 4,197 patients with type 1 diabetes (the FinnDiane Study). *Cardiovasc. Diabetol.* **8**, 54–2840–8–54 (2009).
28. Sackeck, J. M. *et al.* Rapid disuse and denervation atrophy involve transcriptional changes similar to those of muscle wasting during systemic diseases. *FASEB J.* **21**, 140–155 (2007).
29. Subramanian, A. *et al.* Gene set enrichment analysis: a knowledge-based approach for interpreting genome-wide expression profiles. *Proc. Natl. Acad. Sci. USA.* **102**, 15545–15550 (2005).
30. Klionsky, D. J. *et al.* Guidelines for the use and interpretation of assays for monitoring autophagy (3rd edition). *Autophagy* **12**, 1–222 (2016).
31. Yu, A. P. *et al.* Acylated and unacylated ghrelin inhibit doxorubicin-induced apoptosis in skeletal muscle. *Acta Physiol. (Oxf)* **211**, 201–213 (2014).
32. Schmidt, E. K., Clavarino, G., Ceppi, M. & Pierre, P. SUNSET, a nonradioactive method to monitor protein synthesis. *Nat. Methods* **6**, 275–277 (2009).
33. Goodman, C. A. *et al.* Novel insights into the regulation of skeletal muscle protein synthesis as revealed by a new nonradioactive *in vivo* technique. *FASEB J.* **25**, 1028–1039 (2011).
34. So, J. S., Cho, S., Min, S. H., Kimball, S. R. & Lee, A. H. IRE1alpha-Dependent Decay of CREP/Ppp1r15b mRNA Increases Eukaryotic Initiation Factor 2alpha Phosphorylation and Suppresses Protein Synthesis. *Mol. Cell. Biol.* **35**, 2761–2770 (2015).
35. Hulmi, J. J., Silvennoinen, M., Lehti, M., Kivela, R. & Kainulainen, H. Altered REDD1, myostatin, and Akt/mTOR/FoxO/MAPK signaling in streptozotocin-induced diabetic muscle atrophy. *Am. J. Physiol. Endocrinol. Metab.* **302**, E307–15 (2012).
36. Lawen, A. *et al.* Voltage-dependent anion-selective channel 1 (VDAC1)—a mitochondrial protein, rediscovered as a novel enzyme in the plasma membrane. *Int. J. Biochem. Cell Biol.* **37**, 277–282 (2005).
37. Gilliam, L. A. *et al.* The anticancer agent doxorubicin disrupts mitochondrial energy metabolism and redox balance in skeletal muscle. *Free Radic. Biol. Med.* **65**, 988–996 (2013).
38. Doroshov, J. H., Tallent, C. & Schechter, J. E. Ultrastructural features of Adriamycin-induced skeletal and cardiac muscle toxicity. *Am. J. Pathol.* **118**, 288–297 (1985).
39. Zhu, W. *et al.* Acute doxorubicin cardiotoxicity is associated with p53-induced inhibition of the mammalian target of rapamycin pathway. *Circulation* **119**, 99–106 (2009).
40. Zahringer, J. The regulation of protein synthesis in heart muscle under normal conditions and in the adriamycin-cardiomyopathy. *Klin. Wochenschr.* **59**, 1273–1287 (1981).
41. Zima, T. *et al.* Acute doxorubicin (adriamycin) dosage does not reduce cardiac protein synthesis *in vivo*, but decreases diaminopeptidase I and proline endopeptidase activities. *Exp. Mol. Pathol.* **70**, 154–161 (2001).
42. Smuder, A. J., Kavazis, A. N., Min, K. & Powers, S. K. Exercise protects against doxorubicin-induced oxidative stress and proteolysis in skeletal muscle. *J. Appl. Physiol.* (1985) **110**, 935–942 (2011).
43. Smuder, A. J., Kavazis, A. N., Min, K. & Powers, S. K. Exercise protects against doxorubicin-induced markers of autophagy signaling in skeletal muscle. *J. Appl. Physiol.* (1985) **111**, 1190–1198 (2011).
44. Dirks-Naylor, A. J., Tran, N. T., Yang, S., Mabolo, R. & Kouzi, S. A. The effects of acute doxorubicin treatment on proteome lysine acetylation status and apical caspases in skeletal muscle of fasted animals. *J. Cachexia Sarcopenia Muscle* **4**, 239–243 (2013).
45. Penna, F. *et al.* Muscle wasting and impaired myogenesis in tumor bearing mice are prevented by ERK inhibition. *PLoS One* **5**, e13604 (2010).
46. Salto, R., Vilchez, J. D., Cabrera, E., Guinovart, J. J. & Giron, M. D. Activation of ERK by sodium tungstate induces protein synthesis and prevents protein degradation in rat L6 myotubes. *FEBS Lett.* **588**, 2246–2254 (2014).
47. Lou, H., Danelisen, I. & Singal, P. K. Involvement of mitogen-activated protein kinases in adriamycin-induced cardiomyopathy. *Am. J. Physiol. Heart Circ. Physiol.* **288**, H1925–30 (2005).

48. Chicco, A. J., Schneider, C. M. & Hayward, R. Voluntary exercise protects against acute doxorubicin cardiotoxicity in the isolated perfused rat heart. *Am. J. Physiol. Regul. Integr. Comp. Physiol.* **289**, R424–R431 (2005).
49. Sturgeon, K. *et al.* Concomitant low-dose doxorubicin treatment and exercise. *Am. J. Physiol. Regul. Integr. Comp. Physiol.* **307**, R685–92 (2014).
50. Jones, L. W. *et al.* Effects of exercise training on antitumor efficacy of doxorubicin in MDA-MB-231 breast cancer xenografts. *Clin. Cancer Res.* **11**, 6695–6698 (2005).
51. Blair, S. N. *et al.* Influences of cardiorespiratory fitness and other precursors on cardiovascular disease and all-cause mortality in men and women. *JAMA* **276**, 205–210 (1996).
52. Lebrecht, D., Setzer, B., Ketelsen, U. P., Haberstroh, J. & Walker, U. A. Time-dependent and tissue-specific accumulation of mtDNA and respiratory chain defects in chronic doxorubicin cardiomyopathy. *Circulation* **108**, 2423–2429 (2003).
53. Yamada, K., Sugiyama, S., Kosaka, K., Hayakawa, M. & Ozawa, T. Early appearance of age-associated deterioration in mitochondrial function of diaphragm and heart in rats treated with doxorubicin. *Exp. Gerontol.* **30**, 581–593 (1995).
54. Kivela, R. *et al.* VEGF-B-induced vascular growth leads to metabolic reprogramming and ischemia resistance in the heart. *EMBO Mol. Med.* **6**, 307–321 (2014).
55. Desai, V. G. *et al.* Development of doxorubicin-induced chronic cardiotoxicity in the B6C3F1 mouse model. *Toxicol. Appl. Pharmacol.* **266**, 109–121 (2013).
56. Brotto, M. & Bonewald, L. Bone and muscle: Interactions beyond mechanical. *Bone* **80**, 109–114 (2015).
57. Goodman, C. A., Hornberger, T. A. & Robling, A. G. Bone and skeletal muscle: Key players in mechanotransduction and potential overlapping mechanisms. *Bone* **80**, 24–36 (2015).
58. Bialek, P. *et al.* A myostatin and activin decoy receptor enhances bone formation in mice. *Bone* **60**, 162–171 (2014).
59. Hayward, R. *et al.* Voluntary wheel running in growing rats does not protect against doxorubicin-induced osteopenia. *J. Pediatr. Hematol. Oncol.* **35**, e144–8 (2013).
60. Kallio, M. A. *et al.* Chipster: user-friendly analysis software for microarray and other high-throughput data. *BMC Genomics* **12**, 507–2164–12–507 (2011).

## Acknowledgements

This work was supported by the Academy of Finland (grant No. 275922) and Jenny and Antti Wihuri Foundation. Director of the Wihuri Research Institute Kari Alitalo is thanked for providing resources. We thank Doctor Philippe Pierre for kindly providing the anti-puromycin antibody. We also acknowledge Mika Silvennoinen, Tanja Holopainen, Maria Arrano de Kivikko, Kirsi Lintula, Nada Bechara-Hirvonen, Risto Puurtinen, Mervi Matero, Vasco Fachada, Juho Hyödynmaa, and Hongqiang Ma for their valuable help and technical assistance. Biomedicum Functional Genomics Unit for core services and technical support is thanked for the microarray-analysis and Reeta Huhtala for cryosectioning muscle samples at Tissue preparation and histochemistry unit at the Faculty of Medicine, University of Helsinki.

## Author Contributions

J.J.H., R.K., T.A.N., J.D. and M.R. designed the experiments. T.A.N., J.D. and M.R. performed the animal experiments and collected the tissues. E.M. led the mitochondrial function analyses. sACVR2B-Fc was produced by A.P. and O.R. T.A.N. performed the histological analyses and microscopy with the help of S.K. qPCR analyses were performed by A.R.P. and protein expression analyses by T.A.N. and A.R.P. T.A.N. and J.J.H. wrote the manuscript the help from R.K. The figures were prepared by T.A.N. with the help from J.J.H. and A.R.P. All authors reviewed the manuscript.

## Additional Information

**Supplementary information** accompanies this paper at <http://www.nature.com/srep>

**Competing financial interests:** The authors declare no competing financial interests.

**How to cite this article:** Nissinen, T.A. *et al.* Systemic blockade of ACVR2B ligands prevents chemotherapy-induced muscle wasting by restoring muscle protein synthesis without affecting oxidative capacity or atrogenes. *Sci. Rep.* **6**, 32695; doi: 10.1038/srep32695 (2016).



This work is licensed under a Creative Commons Attribution 4.0 International License. The images or other third party material in this article are included in the article's Creative Commons license, unless indicated otherwise in the credit line; if the material is not included under the Creative Commons license, users will need to obtain permission from the license holder to reproduce the material. To view a copy of this license, visit <http://creativecommons.org/licenses/by/4.0/>

© The Author(s) 2016



## II

# PREVENTION OF CHEMOTHERAPY-INDUCED CACHEXIA BY ACVR2B LIGAND BLOCKING HAS DIFFERENT EFFECTS ON HEART AND SKELETAL MUSCLE

by

Hulmi, J.J.\*, Nissinen, T.A.\*, Räsänen, M., Degerman, J., Lautaoja, J.H.,  
Hemanthakumar, K.A., Backman, J.T., Ritvos, O., Silvennoinen, M. & Kivelä,  
R. 2018.

\*Equal contribution

Journal of Cachexia, Sarcopenia and Muscle vol 9, 417–432.

<https://doi.org/10.1002/jcsm.12265>

Reproduced with kind permission by John Wiley & Sons Ltd.

Published under CC BY-NC 4.0 license.





# Prevention of chemotherapy-induced cachexia by ACVR2B ligand blocking has different effects on heart and skeletal muscle

Juha J. Hulmi<sup>1,2,\*†</sup>, Tuuli A. Nissinen<sup>1†</sup>, Markus Räsänen<sup>3</sup>, Joni Degerman<sup>3</sup>, Juulia H. Lautaoja<sup>1</sup>, Karthik Amudhala Hemanthakumar<sup>3</sup>, Janne T. Backman<sup>4</sup>, Olli Ritvos<sup>2</sup>, Mika Silvennoinen<sup>1</sup> & Riikka Kivelä<sup>3\*</sup>

<sup>1</sup>Biology of Physical Activity, Neuromuscular Research Center, Faculty of Sport and Health Sciences, University of Jyväskylä, Jyväskylä, Finland; <sup>2</sup>Department of Physiology, Faculty of Medicine, University of Helsinki, Helsinki, Finland; <sup>3</sup>Wihuri Research Institute, Helsinki, Finland and Translational Cancer Biology Program, Research Programs Unit, Faculty of Medicine, University of Helsinki, Helsinki, Finland; <sup>4</sup>Department of Clinical Pharmacology, Faculty of Medicine, University of Helsinki and Helsinki University Hospital, Helsinki, Finland

## Abstract

**Background** Toxicity of chemotherapy on skeletal muscles and the heart may significantly contribute to cancer cachexia, mortality, and decreased quality of life. Doxorubicin (DOX) is an effective cytostatic agent, which unfortunately has toxic effects on many healthy tissues. Blocking of activin receptor type IIB (ACVR2B) ligands is an often used strategy to prevent skeletal muscle loss, but its effects on the heart are relatively unknown.

**Methods** The effects of DOX treatment with or without pre-treatment with soluble ACVR2B-Fc (sACVR2B-Fc) were investigated. The mice were randomly assigned into one of the three groups: (1) vehicle (PBS)-treated controls, (2) DOX-treated mice (DOX), and (3) DOX-treated mice administered with sACVR2B-Fc during the experiment (DOX + sACVR2B-Fc). DOX was administered with a cumulative dose of 24 mg/kg during 2 weeks to investigate cachexia outcome in the heart and skeletal muscle. To understand similarities and differences between skeletal and cardiac muscles in their responses to chemotherapy, the tissues were collected 20 h after a single DOX (15 mg/kg) injection and analysed with genome-wide transcriptomics and mRNA and protein analyses. The combination group was pre-treated with sACVR2B-Fc 48 h before DOX administration. Major findings were also studied in mice receiving only sACVR2B-Fc.

**Results** The DOX treatment induced similar (~10%) wasting in skeletal muscle and the heart. However, transcriptional changes in response to DOX were much greater in skeletal muscle. Pathway analysis and unbiased transcription factor analysis showed that p53-p21-REDD1 is the main common pathway activated by DOX in both skeletal and cardiac muscles. These changes were attenuated by blocking ACVR2B ligands especially in skeletal muscle. Tceal7 (3-fold to 5-fold increase), transferrin receptor (1.5-fold increase), and Ccl21 (0.6-fold to 0.9-fold decrease) were identified as novel genes responsive to blocking ACVR2B ligands. Overall, at the transcriptome level, ACVR2B ligand blocking had only minor influence in the heart while it had marked effects in skeletal muscle. The same was also true for the effects on tissue wasting. This may be explained in part by about 18-fold higher gene expression of myostatin in skeletal muscle compared with the heart.

**Conclusions** Cardiac and skeletal muscles display similar atrophy after DOX treatment, but the mechanisms for this may differ between the tissues. The present results suggest that p53-p21-REDD1 signalling is the main common DOX-activated pathway in these tissues and that blocking activin receptor ligands attenuates this response, especially in skeletal muscle supporting the overall stronger effects of this treatment in skeletal muscles.

**Keywords** Myostatin; Activins; Transcriptome; p53; Doxorubicin; Ccl21

Received: 4 August 2017; Revised: 15 September 2017; Accepted: 12 October 2017

\*Correspondence to: Juha Hulmi, Neuromuscular Research Center, Faculty of Sport and Health Sciences, University of Jyväskylä, Jyväskylä, Finland. Email: juha.hulmi@jyu.fi  
Riikka Kivelä, Translational Cancer Biology Program, Faculty of Medicine, University of Helsinki, Helsinki, Finland. Email: riikka.kivela@helsinki.fi

†These authors contributed equally to the work.

## Introduction

Cancer cachexia is associated with increased mortality.<sup>1</sup> This may, in part, be related to increased toxicity of chemotherapy on skeletal muscles and the heart.<sup>1–5</sup> The maintenance of skeletal<sup>1</sup> and cardiac<sup>6</sup> muscle mass and function predicts better response to treatment and survival in diseases. Therefore, it is crucial to discover and develop effective strategies to counteract pathological skeletal and cardiac muscle loss.

Doxorubicin (DOX, Adriamycin®) is an anthracycline cytostatic agent, which acts through arresting cell cycle, and thus blocks proliferation of malignant cells.<sup>7</sup> Unfortunately, DOX has deleterious effects also on many healthy tissues. Large doses of DOX have been shown for decades to induce cardiotoxicity through various mechanisms.<sup>5,8,9</sup> In addition, DOX induces adverse effects on skeletal muscle tissue including muscle weakness, fatigue, dysfunction, and atrophy.<sup>10</sup> Some studies have suggested that the heart may be more sensitive to DOX than skeletal muscle,<sup>2,3</sup> but the degree of skeletal muscle dysfunction can be comparable to or even higher than that of heart.<sup>11,12</sup>

Skeletal and cardiac muscles are very similar in several aspects; both are striated and composed of myofibrils. However, cardiac cells are smaller, more circular, branched, and have junctions between cells called intercalated discs connecting cardiomyocytes (CMCs) together. This complexity in the heart may be an advantage, but also a disadvantage regarding regeneration, which has been thought to be among the weakest in the adult mammalian body.<sup>13,14</sup> In comparison to the heart, skeletal muscles have a remarkable regeneration capacity even after very severe injury.<sup>15</sup>

Skeletal muscle size is negatively regulated by myostatin, GDF11, and activins, which belong to the TGF- $\beta$  superfamily of proteins.<sup>16–18</sup> They exert their effects through binding to activin receptor type IIB (ACVR2B). An often used strategy to increase muscle size and to prevent muscle loss is to block these ACVR2B ligands by administration of a soluble ligand binding domain of ACVR2B (sACVR2B-Fc).<sup>4,19–21</sup> In addition, sACVR2B-Fc treatment has been found to prolong survival and to reverse cancer cachexia in mice.<sup>22,23</sup> Activin receptor signalling is important for heart growth regulation and homeostasis as well,<sup>18,22,24–29</sup> but the effects of blocking activin receptor ligands in the heart have not been investigated in chemotherapy-induced cardiac atrophy.

Previous studies have evaluated the effects of DOX and ACVR2B blocking either on the heart or skeletal muscle. In the present study, we compared the effects of DOX-treatment with or without pre-treatment with sACVR2B-Fc on cardiac and skeletal muscles. We show here that cardiac and skeletal muscle masses were similarly decreased by DOX chemotherapy treatment. However, transcriptional changes in response to DOX were much greater in skeletal muscle. Furthermore, we show that blocking of activin receptor ligands had more pronounced effect on skeletal muscle than cardiac wasting.

## Materials and methods

### Animals

C57BL/6J male mice (Envigo), aged 6–10 weeks were maintained under standard conditions (temperature 22°C, 12:12 h light/dark cycle) with free access to food and water. The protocols were approved by the National Animal Experiment Board, and all the experiments were carried out in accordance with the guidelines of the committee and the ethical standards of the Declaration of Helsinki.

### Experimental design

The mice were randomly assigned into three groups: (1) vehicle (PBS)-treated controls (CTRL), (2) DOX hydrochloride treated mice (DOX), and (3) DOX-treated mice administered with sACVR2B-Fc intraperitoneally (DOX + sACVR2B) (*Figure 1A*).

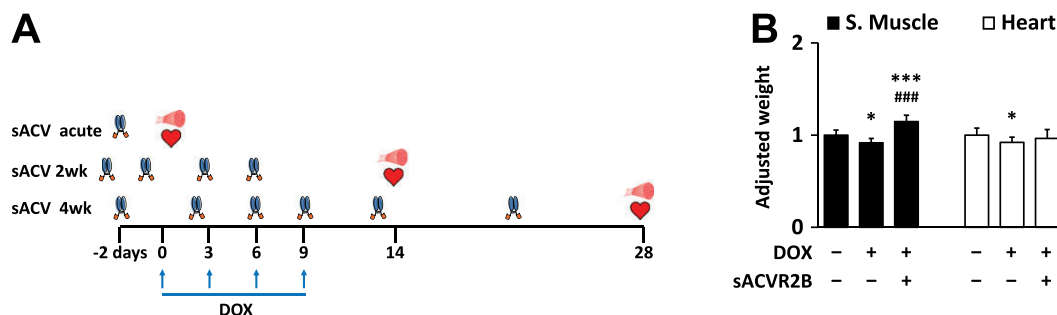
In the long-term treatment experiments, both DOX groups received four intraperitoneal injections of DOX (each 6 mg/kg in PBS), administered every third day during the first 2 weeks of the experiment.<sup>4,5</sup> Control mice were administered with an equal volume of PBS. The mice were euthanized at 2 weeks and at 4 weeks after the first DOX injection. Half of the DOX mice were injected with sACVR2B-Fc (5 mg/kg in PBS) twice a week during the first 2 weeks of the experiment and once a week after that. The DOX treatment protocol was designed to mimic the treatment of human patients with low DOX doses to induce cardiotoxicity but no treatment-related deaths.<sup>30</sup>

In the acute experiment, a single intraperitoneal injection of DOX (15 mg/kg in PBS) or an equal volume of PBS was administered. sACVR2B-Fc-treated mice received a single intraperitoneal injection of sACVR2B-Fc (10 mg/kg in PBS) 48 h before DOX administration, as we have previously shown that sACVR2B-Fc increases muscle protein synthesis 48 h after its administration.<sup>20</sup> The mice were euthanized 20 h after DOX/PBS administration. To analyse the effects of sACVR2B-Fc alone, another experiment was conducted in which sACVR2B-Fc (10 mg/kg in PBS) or PBS were administered 48 h before sample collection into wild-type mice.<sup>20</sup>

### Tissue collection

At the end of the experiment, the mice were anaesthetized with ketamine and xylazine and then euthanized by cardiac puncture followed by cervical dislocation. Hindlimb muscle tibialis anterior (TA), gastrocnemius, soleus, and the heart were immediately excised and weighed. The left TA and gastrocnemius muscles and part of the heart (apex) were snap-frozen in liquid nitrogen. Blood was fully drained from hearts prior to tissue weighing. All tissue weights were normalized to the length of the tibia (mm). TA muscle was used in

**Figure 1** (A) Experimental design. The study included acute as well as 2 and 4 week experiments. (B) Adjusted mass (control = 1, adjusted to tibial length) of skeletal muscle and the heart after 4 weeks of cumulative 24 mg/kg doxorubicin administration (mean  $\pm$  SD). Skeletal muscle mass is a sum of tibialis anterior, gastrocnemius, and soleus masses.  $n = 15, 16,$  and  $17$  in skeletal muscle and  $n = 14, 16,$  and  $16$  in heart in CTRL, DOX, and in DOX + sACVR2B, respectively. General linear model analysis of variance with Bonferroni post hoc test was used. \* or \*\*\* = significant ( $P < 0.05$  or  $P < 0.001$ , respectively) difference to respective CTRL. ### = significant ( $P < 0.001$ ) difference to respective DOX.



subsequent analyses, except when analysing the effects of sACVR2B-Fc alone<sup>20</sup> and DOX-measurements, in which gastrocnemius was used.

#### Puromycin injection for protein synthesis measurement

Puromycin incorporation assay<sup>31</sup> was conducted as earlier<sup>4,20,32</sup> with small modifications. In brief, mice were intraperitoneally injected with 0.040  $\mu\text{mol/g}$  (21.78 mg/kg) puromycin (Calbiochem, Darmstadt, Germany) dissolved in 200  $\mu\text{L}$  of PBS. At exactly 25 min after the injection of puromycin, mice were euthanized by cervical dislocation and heart was collected and snap-frozen at exactly 30 min after puromycin injection.

#### sACVR2B-Fc production

The recombinant fusion protein was produced and purified as described earlier in detail.<sup>20</sup> The ectodomain of human ACVR2B was fused with a human IgG1 Fc domain and expressed in Chinese hamster ovary cells grown in a suspension culture. The protein is similar but not identical to that originally generated by Lee and colleagues.<sup>19</sup>

#### RNA analysis

Total RNA was extracted from muscle and the heart with TRIreagent (Bioline) and further purified with NucleoSpin<sup>®</sup> RNA II columns. For quantitative polymerase chain reaction (qPCR), RNA was reverse transcribed to cDNA by using iScript<sup>™</sup> Advanced cDNA Synthesis Kit for real-time qPCR (Bio-Rad Laboratories) according to the manufacturer's instructions. Real-time qPCR was performed according to standard procedures by using iQ SYBR Supermix (Bio-Rad

Laboratories) and CFX96 Real-Time PCR Detection System (Bio-Rad Laboratories). Quantification was carried out by using standard curve or efficiency corrected  $\Delta\Delta\text{Ct}$  method. The relative mRNA expressions were normalized by using *36b4* as a reference gene, as it was the most stable (lowest intergroup and intragroup variances) from three candidate reference genes (*36b4*, *Gapdh*, and *Rn18S*). Primer sequences are listed in *Online Resource 1: Supplementary Methods*.

#### Microarray analysis

RNA from the TA and the heart samples of the acute experiment were analysed with Illumina Sentrix MouseRef-6 v2 Expression BeadChip containing 45 281 transcripts (Illumina Inc., San Diego, CA, USA) by the Functional Genomics Unit at Biomedicum Helsinki, University of Helsinki, Finland according to the manufacturer's instructions. Five muscle and three heart samples from control and DOX groups and five muscle and three heart samples from DOX + sACVR2B-Fc group were analysed. RNA was analysed for integrity and quality on Agilent Bioanalyser 2100. Illumina's GenomeStudio software was used for initial data analysis and quality control. Raw data were normalized with quantile normalization (including log<sub>2</sub>-transformation of the data), data quality was assessed, and statistical analyses were performed by using Chipster software (IT Center for Science, Espoo, Finland).<sup>33</sup> Statistically significant differences in individual genes between the groups were tested by using Empirical Bayes statistics and the Benjamini-Hochberg algorithm controlling false discovery rate (FDR). FDR values of  $<0.05$  with  $\geq 1.2$ -fold change difference were considered significant. MIAME guidelines were followed during array data generation, pre-processing, and analysis. The complete data set is publicly available in the NCBI Gene Expression Omnibus (<http://www.ncbi.nlm.nih.gov/geo/>; accession no. GSE77745 and GSE97642). Heatmap

illustrations were performed with GENE-E software (Broad Institute, Cambridge, USA).

### Transcription factor analysis

Transcription factor (TF) analysis is usually conducted in cultured cells rather than actual tissue samples, and it focuses on a single a priori chosen TF at a time. When the TF is not known in advance, or when only gene expression profiling is available, regulatory relationships can be uncovered by reverse-engineering a gene regulatory network starting from the expression data. A-genome-wide ranking-and-recovery approach using iRegulon software<sup>34</sup> was used to detect enriched TF motifs and their optimal set of direct target genes. This analysis also links these candidate motifs to TFs by using motif2TF procedure.

### Pathway analysis

Enrichment of functionally related genes in four different gene set collections was first performed by using a non-biased method by gene set enrichment analysis software (GSEA; Version 2.0)<sup>35</sup> as previously done in our laboratory.<sup>4,36,37</sup> The collections used were the Canonical Pathways, Biocarta, KEGG, and Reactome (<http://www.broadinstitute.org/gsea/msigdb/collections.jsp>). The number of permutations by gene set was set to 1000 and gene sets with at least 10, and no more than 500 genes were taken into account in each analysis. The statistical significance was calculated by using FDR, and the level of significance was set at  $FDR < 0.05$ .

### Doxorubicin measurement

The DOX concentration from gastrocnemius muscle was measured with an Agilent 1100 HPLC system (Agilent Technologies, Waldbronn, Germany) coupled to an AB Sciex API 2000 tandem mass spectrometer (Framingham, MA), as previously described.<sup>5</sup>

### Tissue processing for the protein analysis

Muscle and heart samples were homogenized and treated with proper inhibitors as previously reported.<sup>4,5</sup> One part of the heart homogenate was taken for the puromycin incorporation examination. For that purpose, the sample was centrifuged at 500 *g* for 5 min to remove cell debris. For the analysis of individual proteins, the rest of the homogenate was centrifuged at 10 000 *g* for 10 min. Total protein content was determined by using the bicinchonic acid protein assay (Pierce Biotechnology, Rockford, USA) with an automated KoneLab analyser (Thermo Scientific, Vantaa, Finland).

### Western immunoblot analyses

Western immunoblot analyses were performed as previously reported.<sup>4,5</sup> Ponceau S staining and GAPDH were used as loading controls, and all the results are normalized to the mean of Ponceau S and GAPDH. The quantification of GAPDH normalized to Ponceau S was similar among the groups, indicating that GAPDH protein content remained stable under the experimental conditions. The antibodies used are listed in the *Online Resource 1: Supplementary Methods*.

### Immunohistochemistry

Cardiac and skeletal muscle (TA) tissue sections were cut with cryomicrotome and fixed with ice-cold acetone. Masson trichrome staining was performed to analyse the amount of fibrosis in the tissues. Immunohistochemistry was performed to measure CMC cross-sectional area by using mouse-anti-dystrophin antibody (1:500 dilution, NCL-Dys 2, Novocastra). Rabbit-anti-Ki67 antibody (1:300, ab1667, Abcam) was used to evaluate the effects of DOX and sACVR2B-Fc on the cell proliferation. Sections were imaged with Zeiss Axioimager microscope, and CMC size was calculated using Cell Profiler software.

### Statistical analysis

Multiple group comparisons except microarray (see details above) were conducted with general linear model analysis of variance followed by Bonferroni post hoc test or by non-parametric Kruskal–Wallis test followed by Holm–Bonferroni corrected Mann–Whitney *U*-test as post hoc when appropriate. For two-group comparisons, a two-tailed unpaired Student's *t*-test or non-parametric Mann–Whitney *U*-test was used. Data were checked for normality and for the equality of variances. The level of significance in these analyses was set at  $P < 0.05$ . Data are expressed as means  $\pm$  SEM if not otherwise mentioned. Statistical analyses were performed with IBM SPSS STATISTICS version 24 for Windows (SPSS, Chicago, IL).

## Results

### ACVR2B blocking can prevent chemotherapy-induced skeletal muscle but not cardiac atrophy

At 4 weeks, chemotherapy-induced atrophy was almost identical between skeletal and cardiac muscles (*Figure 1B*). In skeletal muscle, sACVR2B-Fc treatment effectively prevented the loss of muscle mass and was able to even increase muscle mass (*Figure 1B*). However, sACVR2B-Fc was unable to fully block the cardiac atrophy, although the weight loss was

slightly less consistent in DOX + sACVR2B ( $P = 0.165$ ) when compared with DOX alone ( $P = 0.030$ ). Furthermore, CMC cross-sectional area was not increased by sACVR2B (Online Resource 2: *Supplementary Figure S1A*).

### Larger transcriptomic changes in skeletal muscle than in the heart in response to doxorubicin chemotherapy

Whole-genome microarray analysis using  $FDR < 0.05$  and fold change  $\geq 1.2$  criteria showed that 485 and 40 annotated transcripts were up-regulated and 473 and 24 were down-regulated by DOX in skeletal muscle and heart, respectively, at 20 h after a single DOX injection. Out of these genes, there were 21 and 6 genes that were up-regulated or down-regulated, respectively, by DOX in both muscle and the heart (Online Resource 3: *Supplementary Figure S2A* and *S2B*). In addition to having much larger number of genes altered, the genes with largest changes showed more robust response in skeletal muscle as compared with the heart (*Figure 2A–2D*).

Of the most up-regulated genes, a well-known cell-cycle inhibitor *p21/Cdkn1a* was highly up-regulated by DOX injection in both muscle and the heart (*Figure 2A* and *2C*), and this was validated by qPCR (*Figure 3A*). Interestingly, this response was significantly decreased by sACVR2B-Fc treatment preceding DOX administration in skeletal muscle (*Figure 3A*). sACVR2B-Fc alone did not, however, decrease *p21/Cdkn1a* below healthy controls (*Figure 3A*). Moreover, DNA-damage response indicator *Redd1/Ddit4* was up-regulated in both skeletal and heart muscle as published earlier,<sup>4,5</sup> and blocking ACVR2B ligands attenuated this response in skeletal muscle as published earlier<sup>4</sup> without an effect in the heart (Online Resource 2: *Supplementary Figure S1B*).

#### Tceal7 and Ccl21 mRNAs are regulated by sACVR2B-Fc

One hundred eighteen and 1 annotated transcripts were up-regulated, and 84 and 2 transcripts were down-regulated in DOX + sACVR2B-Fc-treated mice when compared with DOX alone in muscle and the heart, respectively. In skeletal muscle, the gene with the highest increase by sACVR2B-Fc in microarray (*Figure 2E*) was *Tceal7* [transcription elongation factor A], a protein involved in skeletal muscle development and regeneration,<sup>38</sup> and this finding was further confirmed by qPCR (*Figure 3B*). The expression level of *Tceal7* in the heart was very low and could not be analysed reliably. The only significantly up-regulated gene by sACVR2B-Fc in the heart was *Vsig4* (3.52-fold,  $FDR < 0.001$ ), which remained unchanged in skeletal muscle. Of the five annotated probes down-regulated by sACVR2B-Fc in the heart, four were probes for *Ccl21* gene and the response of this gene was also validated by qPCR in both tissues (*Figure 3C*). sACVR2B-Fc treatment alone also increased the

expression of *Tceal7* and decreased the expression of *Ccl21* (*Figure 3B* and *3C*), confirming that these effects are due to the blocking of activin receptor type IIB ligands. Potassium voltage-gated channel, Isk-related subfamily, member 1 (*Kne1*) was another gene decreased by sACVR2B-Fc in the heart (0.55-fold,  $FDR = 0.01$ ) without an effect in skeletal muscle. Transcripts, which showed the largest down-regulation by sACVR2B-Fc in muscle, are shown in *Figure 2F*.

There were 22 and 17 genes that were up-regulated or down-regulated, respectively, by DOX in skeletal muscle, and whose expression was normalized by sACVR2B-Fc treatment (Online Resource 3: *Supplementary Figure S2C* and *S2D*). An interesting gene among these was transferrin receptor, as iron metabolism has been shown to be affected and to play a role in DOX-induced toxicity.<sup>39</sup> In both muscle and the heart transferrin receptor mRNA decreased by DOX and in both tissues, but especially in skeletal muscle, this was rescued by sACVR2B-Fc (*Figure 3D*). The increase in transferrin receptor by sACVR2B-Fc was translated into protein level as well, especially in skeletal muscle (*Figure 3E*).

#### PGC-1 gene expression

As microarray platforms do not have probes for most of the recently identified PGC-1 $\alpha$  isoforms, we analysed them by qPCR. In skeletal muscle, *Pgc-1 $\alpha$  exon 1a* (*Ppargc1a* exon 1a) and *Pgc-1 $\alpha$  exon 1c* isoforms as well as *Pgc-1 $\beta$*  (*Ppargc1b*) mRNA decreased by DOX ( $P < 0.05$ ), and only the N-truncated *Pgc-1 $\alpha$*  isoforms remained unchanged (*Figure 4A–4D*). In contrast, in the heart, there was an overall increase by DOX in *Pgc-1 $\alpha$*  isoforms (*Figure 4A–4D*). No effect of sACVR2B-Fc was observed in either tissue type (*Figure 4A–4D*).

#### Heart protein synthesis and ubiquitin ligases

We recently reported that skeletal muscle protein synthesis was decreased by DOX and this could be restored by sACVR2B-Fc.<sup>4</sup> In this study, we analysed protein synthesis in the heart in response to DOX and sACVR2B-Fc. Unlike in skeletal muscle, there was no consistent effect of either DOX or sACVR2B-Fc on puromycin incorporation into proteins, a marker of protein synthesis, in the heart (*Figure 5A*). The level of ubiquitinated proteins was also unchanged in the heart (*Figure 5B*) similarly as previously published in skeletal muscle.<sup>4</sup> E3 ubiquitin ligase *Atrogin1* mRNA increased by DOX in both tissues, but more robustly in the skeletal muscle (*Figure 5C*). Interestingly, sACVR2B-Fc prevented the increase in *Atrogin1* mRNA in muscle (*Figure 5C*). *Murf1* mRNA showed a small decrease by DOX in the heart (*Figure 5C*), while as previously published in skeletal muscle, *Murf1* mRNA was unaltered by DOX, but decreased due to sACVR2B-Fc.<sup>4</sup>

### Muscle doxorubicin content is unaltered by sACVR2B-Fc

To analyse whether the strong effects of sACVR2B-Fc were simply due to attenuated DOX levels in the combination group, DOX concentration in gastrocnemius muscle after the acute DOX treatment was analysed. We found that DOX content at 20 h post-injection did not differ between the DOX and DOX + sACVR2B administered mice (Figure 5D),

suggesting that sACVR2B-Fc effects are not due to altered tissue concentration of DOX.

### Pathway analysis shows similar responses in skeletal muscle and the heart

To identify affected pathways, further analyses were conducted by using an unbiased gene clustering analysis with

**Figure 2** Top 10 genes with largest response to doxorubicin in skeletal muscle (A and B) and in the heart (C and D). Top 10 genes with largest change by sACVR2B-Fc in skeletal muscle (E and F). C = CTRL, D = DOX, A = DOX + sACVR2B. \*, \*\*, or \*\*\* = significant ( $P < 0.05$ ,  $P < 0.01$ , or  $P < 0.001$ , respectively) adjusted difference (false discovery rate).  $n = 5$  per group.

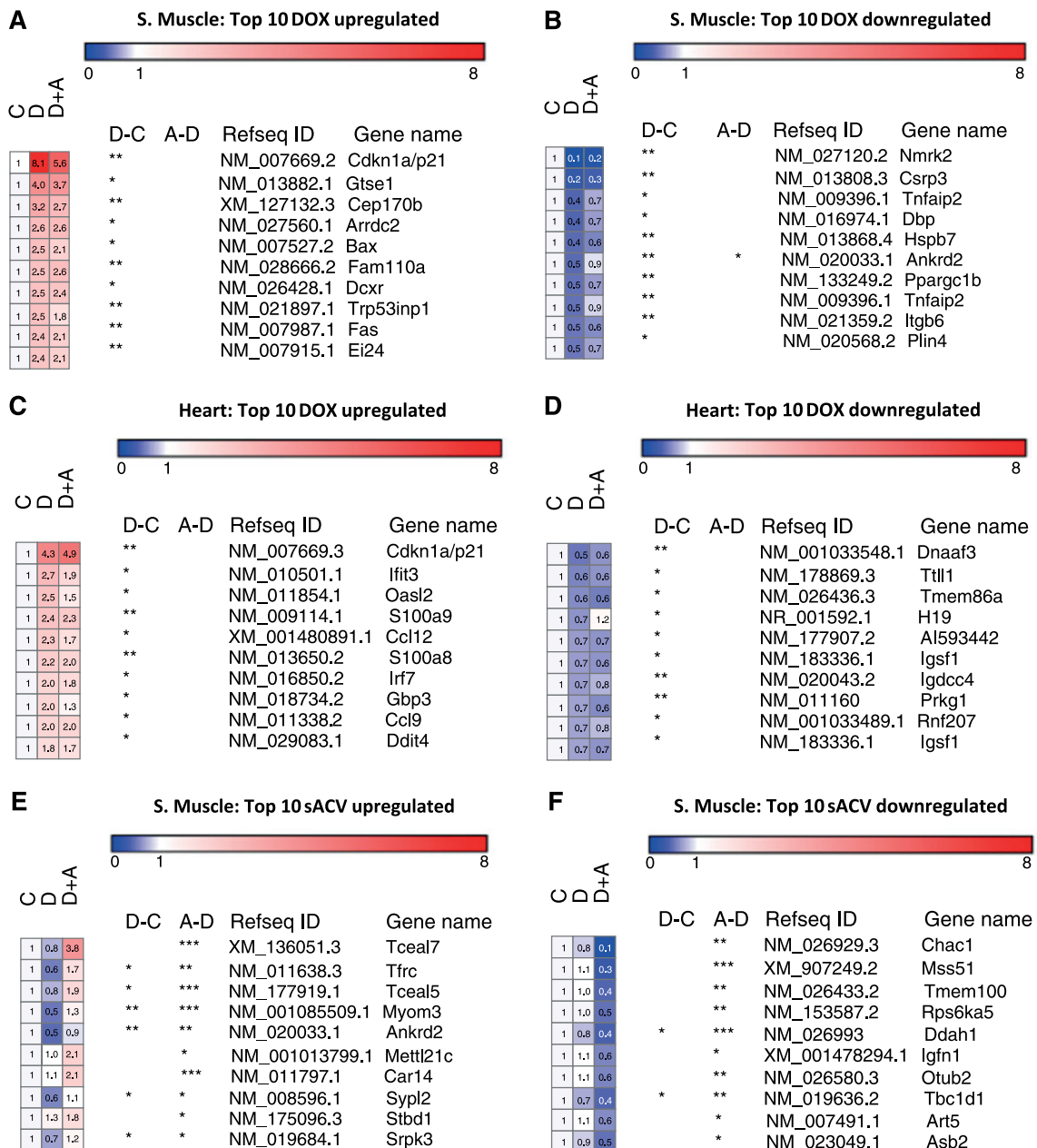
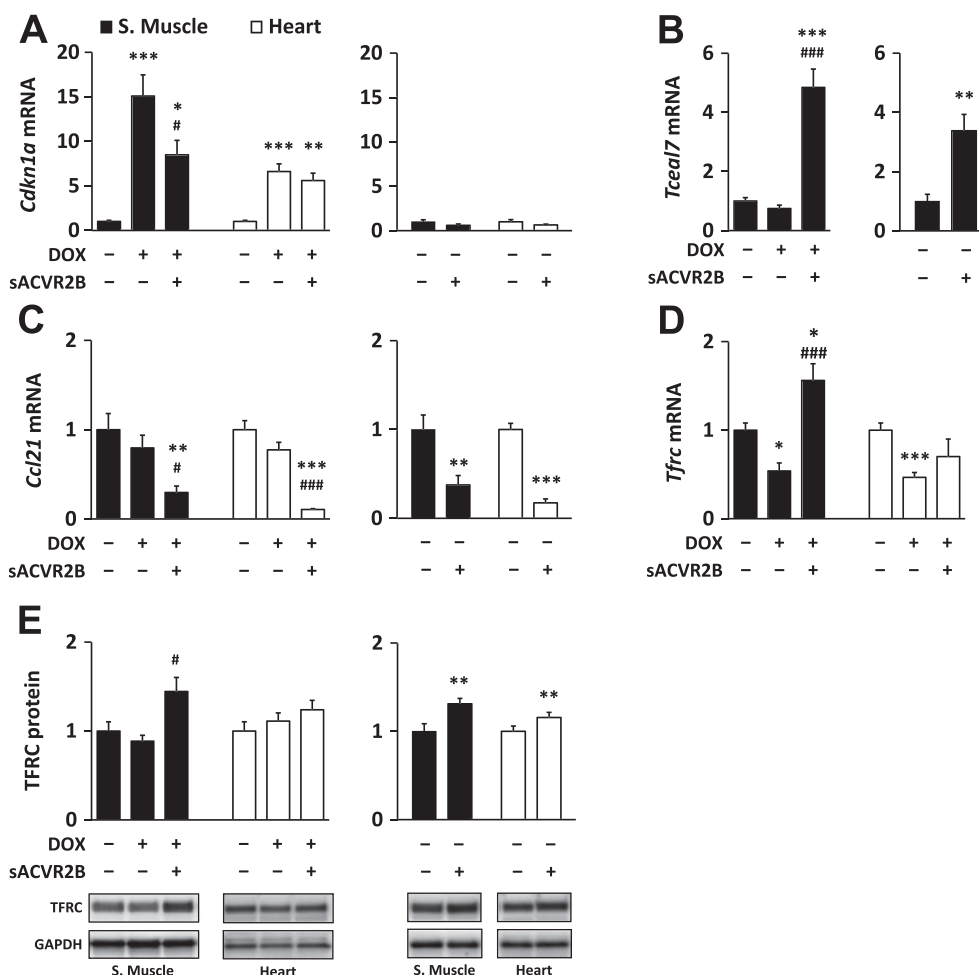


**Figure 3** Doxorubicin alters the gene expression of (A) *Cdkn1a* (p21), while sACVR2B-Fc increases (B) *Tceal7* in skeletal muscle and attenuates (C) *Ccl21* mRNA levels. (D) Doxorubicin decreases transferrin receptor (*Tfrc*) mRNA in both tissues while its mRNA and protein (E) levels are increased by sACVR2B-Fc. *Tceal7* was expressed in heart only very weakly, and thus, it was not analysed. The values are presented as fold changes compared with the control group. For multiple group comparisons, general linear model analysis of variance with Bonferroni post hoc test (A and B) or Kruskal-Wallis test with Holm-Bonferroni corrected Mann-Whitney *U* post hoc test (C-E) were used. For two-group comparisons, the Student's *t*-test (A-C) or non-parametric Mann-Whitney *U*-test (E) were used. \*, \*\*, or \*\*\* = significant ( $P < 0.05$ ,  $P < 0.01$ , or  $P < 0.001$ , respectively) difference to respective CTRL. # or ### = significant ( $P < 0.05$  and  $P < 0.001$ , respectively) difference to respective DOX.  $n = 7-9$  per group in the doxorubicin experiment and  $n = 5-6$  per group in the sACVR2B-Fc alone vs. PBS experiment.



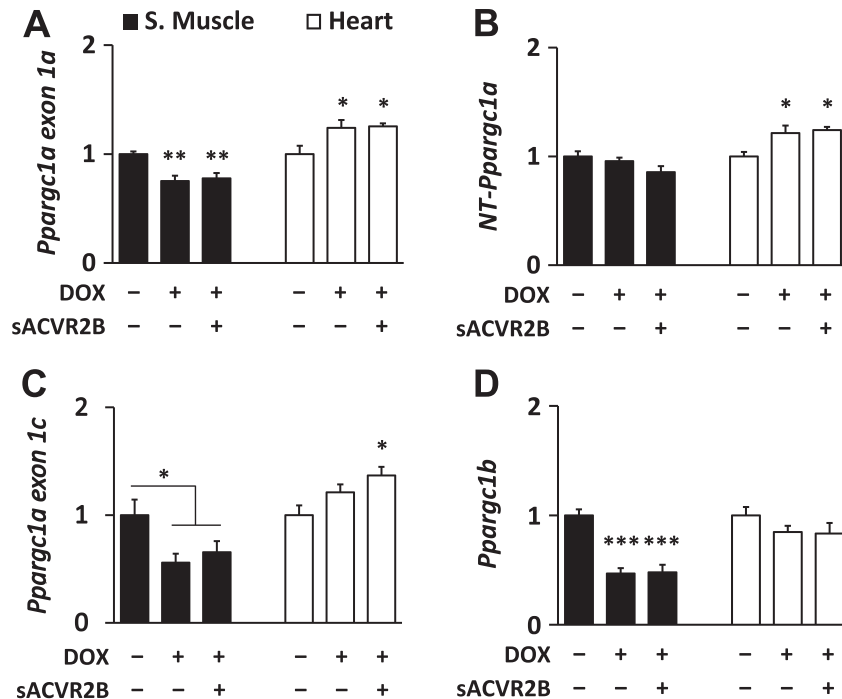
GSEA.<sup>35</sup> In GSEA analysis, 72 and 51 gene sets were up-regulated and 17 and 0 down-regulated ( $FDR < 0.05$ ) in skeletal muscles and hearts of DOX-injected mice, respectively (Online Resource 4: *Supplementary Figure S3A* and *S3B*). It was evident that p53/p63 pathways/gene sets were activated in both skeletal muscle and the heart (*Figure 6A* and *6B*). Also, pathways related to RNA polymerase and transcription were up-regulated in both tissues (*Figure 6A* and *6B*). In skeletal muscle the most down-regulated pathways were related to extracellular proteins, collagens, and their regulation (*Figure 6A*). Same pathways tended to be decreased also in the heart after DOX-injection, but less significantly than in skeletal muscle ( $FDR > 0.05$ ). No sign of fibrosis was observed with Masson trichrome staining either in skeletal muscle or

in the heart at 4 weeks (Online Resource 2: *Supplementary Figure S1C*).

Correspondingly, nine gene sets were up-regulated and six down-regulated ( $FDR < 0.05$ ) in DOX + sACVR2B when compared with DOX alone in skeletal muscle without any affected gene sets in the heart (*Figure 6C*). In muscle, the most activated gene sets were related to translation capacity and efficiency, and the most down-regulated ones to extracellular proteins, and especially proteoglycans and extracellular matrix glycoproteins. Of the gene sets that were down-regulated by DOX in skeletal muscle, p38-MAPK pathway was significantly increased by DOX + sACVR2B when compared with DOX alone (*Figure 6C* and Online Resource 4: *Supplementary Figure S3C* and *S3D*).



**Figure 4** (A–D) Doxorubicin differentially alters the gene expression of *Ppargc1* (PGC-1) mRNA isoforms in muscle and the heart. Notice that in (C) *Ppargc1a* exon 1c, the \* in S. muscle with lines depicts the doxorubicin effect of both doxorubicin groups pooled when compared with control without treatments. General linear model analysis of variance with Bonferroni post hoc test was used. \*, \*\*, or \*\*\* = significant ( $P < 0.05$ ,  $P < 0.01$ , or  $P < 0.001$ , respectively) difference to respective CTRL.  $n = 6–9$  per group.



As sACVR2B prevented the DOX-induced increase in the cell cycle inhibitor p21, we stained muscle and heart sections with Ki67 antibody. DOX treatment had no significant effect on the number of Ki67-positive nuclei, but surprisingly, sACVR2B significantly increased Ki67-positive nuclei in both muscle and the heart (Online Resource 2: *Supplementary Figure S1D*).

### Transcription factor analysis

Next, to gain insight into the key mediators of the effects of DOX and sACVR2B-Fc, a TF analysis was conducted. For this analysis, the gene lists of FDR  $< 0.05$  up-regulated or down-regulated genes with at least 1.5-fold change were loaded to iRegulon software. As a common TF up-regulated by DOX in both the muscle and the heart, p53 was again identified (Online Resource 5: *Supplementary Table S1*). mRNA expression changes of genes containing p53 targeted motifs in microarray ( $>1.5$ -fold increase DOX vs. Control) are shown in *Figure 7A* and *7B*. *p21/Cdkn1a* and *Redd1/Ddit4* rankings were high in both tissues suggesting that p53-REDD1-p21 pathway is the main common pathway activated by DOX in skeletal and cardiac muscles. p53 itself is mainly post-transcriptionally regulated, and indeed, its protein content was increased in both tissues after DOX (*Figure 7C*). However,

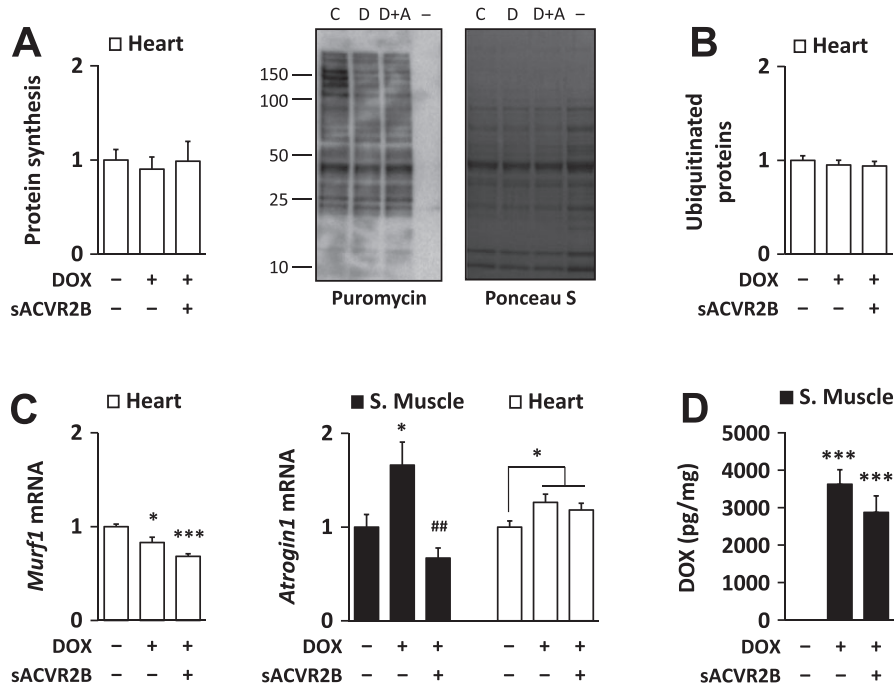
sACVR2B-Fc completely blocked this response in both tissues (*Figure 7C*). This is in line with the expression changes downstream of p53, as *p21/Cdkn1a* mRNA up-regulated in response to DOX was attenuated by sACVR2B-Fc, especially in skeletal muscle (*Figure 3A*).

Other notable TFs affected by DOX were MyoD in skeletal muscle and Stat3 in the heart. MyoD binding site was enriched in iRegulon by DOX (Online Resource 5: *Supplementary Table S1*). This result was associated with increased *Myod1* mRNA by DOX in both microarray and in qPCR (Online Resource 6: *Supplementary Figure S4A*). On the other hand, Stat3 binding site was strongly enriched in the heart, but not in skeletal muscle (Online Resource 5: *Supplementary Table S1*) without changes in the phosphorylation of Stat3 (Online Resource 6: *Supplementary Figure S4B*).

### Gene expression of ACVR2B and its ligands in muscle and in heart and in response to doxorubicin and sACVR2B-Fc

The difference in the response to ACVR2B ligand blocking between skeletal muscle and the heart could be explained by different expression level of activin receptor IIB or its ligands or their responses to DOX. First, we compared the mRNA levels in muscle and heart tissues of young healthy mice

**Figure 5** (A) Doxorubicin administration and sACVR2B-Fc treatment did not alter heart protein synthesis. Protein synthesis relative to doxorubicin was analysed with puromycin incorporation method. Representative blot (left) with Ponceau S staining (right). (– = negative control for puromycin). Doxorubicin administration had no effect on the amount of ubiquitinated proteins in the heart (B) despite minor changes in the mRNA expression of E3 ubiquitin ligases MuRF1 and Atrogin1 (C). (D) sACVR2B-Fc treatment did not alter doxorubicin levels in gastrocnemius muscle at the 20 h timepoint after doxorubicin-administration, when the RNA and protein samples were also taken. Kruskal-Wallis test with Holm-Bonferroni corrected Mann-Whitney *U* post hoc test (A and B), and general linear model analysis of variance with Bonferroni post hoc test (C and D) were used. Doxorubicin effect in Atrogin1 expression in the heart was evaluated with Student's *t*-test. *n* = 7–9 per group in the doxorubicin experiment. Regarding doxorubicin experiment, muscle results of *Murf1* can be found as Supporting Information in earlier publication.<sup>4</sup>



(*n* = 12). Myostatin (*Gdf8*) mRNA expression was ~18-fold higher in skeletal muscle than in the heart ( $P < 0.001$ ; Figure 8A). The expression levels of *Activin A* (*Inhibin βA*), *Gdf11*, and activin receptor IIb (*Acvr2b*) mRNAs were relatively low in both tissues, especially in skeletal muscle that had lower mRNA of these genes than the heart ( $P < 0.005$ ; Figure 8A). Next, we analysed the responses of these ligands to the treatments. sACVR2B-Fc increased *Gdf8* mRNA but decreased *Acvr2b* mRNA exclusively in skeletal muscle without effects on *Activin A* or *Gdf11* mRNA (Figure 8B–E). DOX slightly decreased *Activin A* and *Gdf11* mRNA in skeletal muscle without an effect on *Gdf8* or *Acvr2b* mRNA expression (Figure 8B–E).

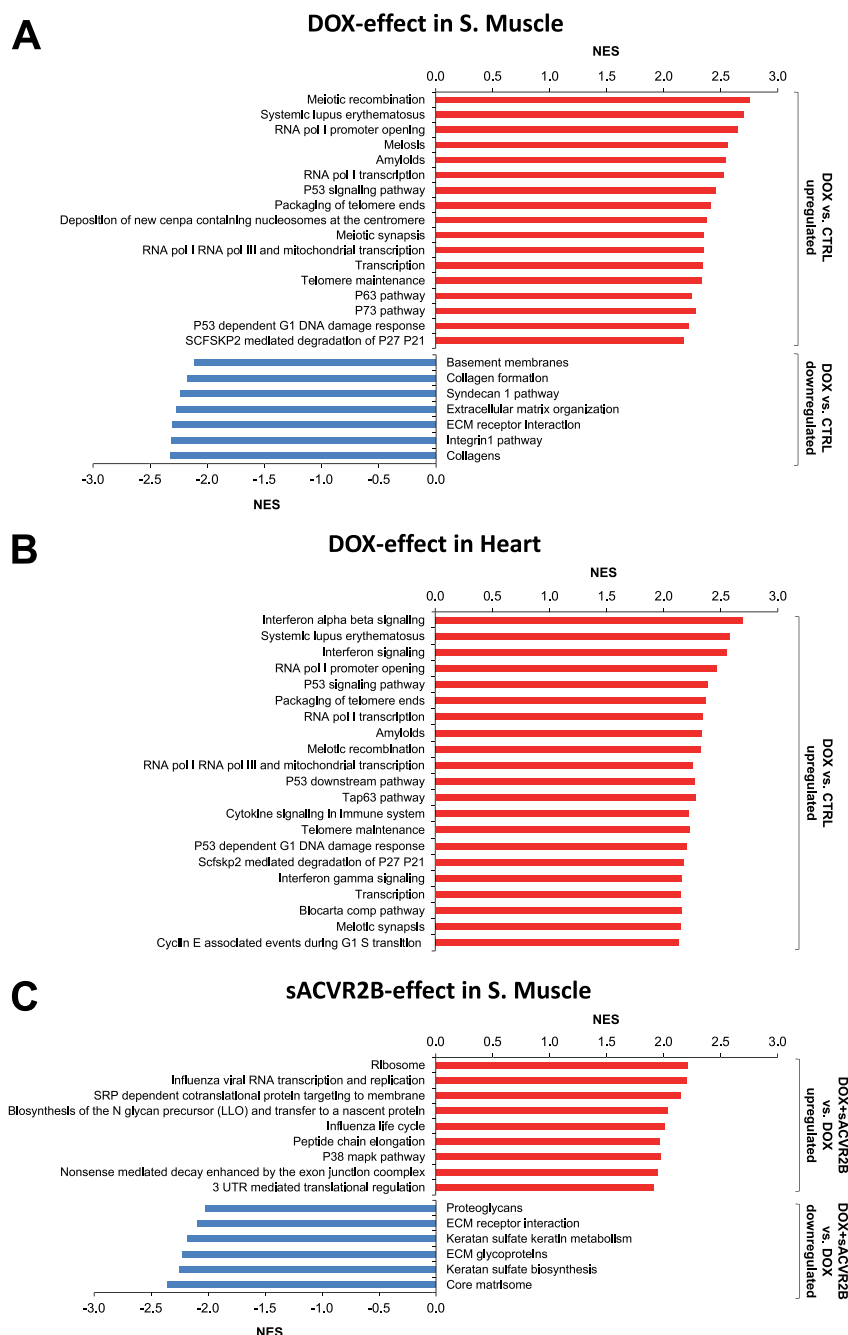
## Discussion

The present study reports common and unique changes in skeletal muscle and the heart after DOX chemotherapy alone and in combination with activin receptor ligand blocking. DOX treatment induced similar tissue wasting in both heart and skeletal muscles; however, changes in the whole-genome

transcriptome were much greater in skeletal muscle. We identified p53-p21-REDD1 as the main common pathway activated by DOX in both skeletal and cardiac muscles, and this was attenuated by blocking the activin receptor IIB ligands. Although a few novel targets were found in the heart, the blocking of sACVR2B ligands had markedly stronger effects in skeletal muscle than in the heart.

To the best of our knowledge, this was the first omics-based study comparing the effects of chemotherapy and activin receptor ligand blocking in the heart and skeletal muscle. Previously, the effects of DOX on heart transcriptome have been investigated<sup>9,40</sup> and the effects of cancer cachexia without chemotherapy have been compared in cardiac and skeletal muscles.<sup>41</sup> Moreover, we and others have investigated skeletal muscle transcriptome after blocking or deleting activin receptor ligands with different strategies.<sup>4,21,37</sup> However, we are unaware of any omics-based DOX studies in skeletal muscle. Here we found that after a cumulative dose of 24 mg/kg of DOX, skeletal muscle and heart wasting at 4 weeks after starting the treatment were almost identical, supporting previous findings in rats.<sup>11</sup> Regarding quality and functional aspects, previous studies comparing the degree of toxicity in skeletal muscle and in the heart have provided

**Figure 6** Gene set enrichment analysis was conducted from the microarray results. Positive and negative enrichment scores denote a large number of genes up-regulated or down-regulated, respectively, in the given gene set. Gene sets with false discovery rate < 0.001 are presented for the doxorubicin effects in muscle (A) and the heart (B). Normalized enrichment score (NES)-values of up-regulated gene sets in doxorubicin-treated mice (DOX vs. CTRL) are expressed as red bars and NES-values of down-regulated gene sets as blue bars. There was no significant enrichment of gene sets down-regulated by doxorubicin in the heart (B). For the sACVR2B-Fc effects, gene sets with false discovery rate < 0.05 are presented (C). NES-values of up-regulated gene sets in treated mice (DOX + sACVR2B vs. DOX) are expressed as red bars and NES-values of down-regulated gene sets as blue bars. There was no significant enrichment of gene sets altered by sACVR2B-Fc at false discovery rate < 0.05 in the heart.

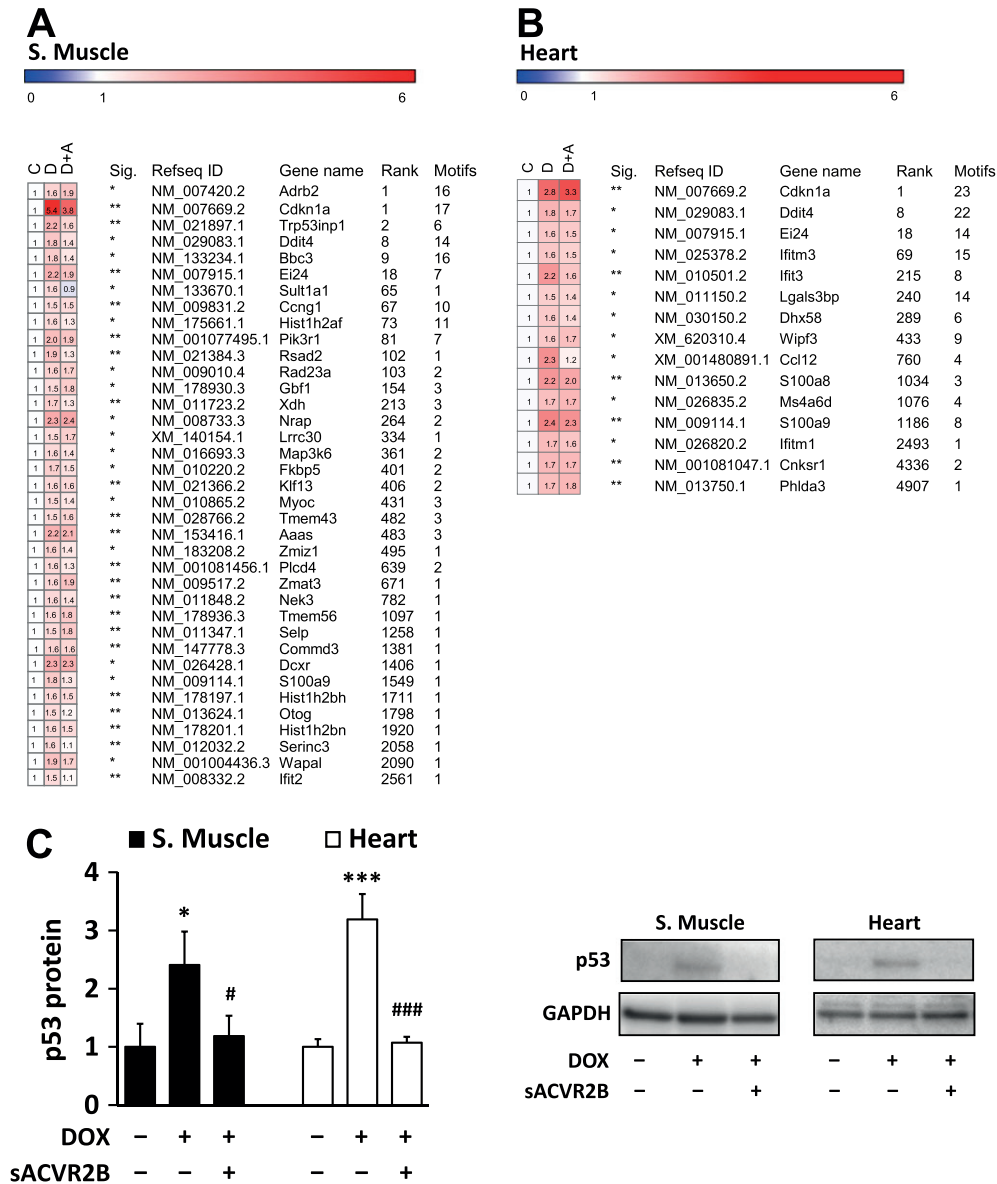


contrasting results.<sup>2,3,11,12</sup> Perhaps surprisingly, in our study, skeletal muscles showed much more robust changes in transcript expression after DOX administration when compared with the heart. Interestingly, in line with our findings, a recent

study reported that muscle transcriptome was much more responsive to C26 cancer cachexia than that of the heart.<sup>41</sup>

Why the DOX-induced changes, especially in transcriptomics, were much larger in skeletal muscle even though the

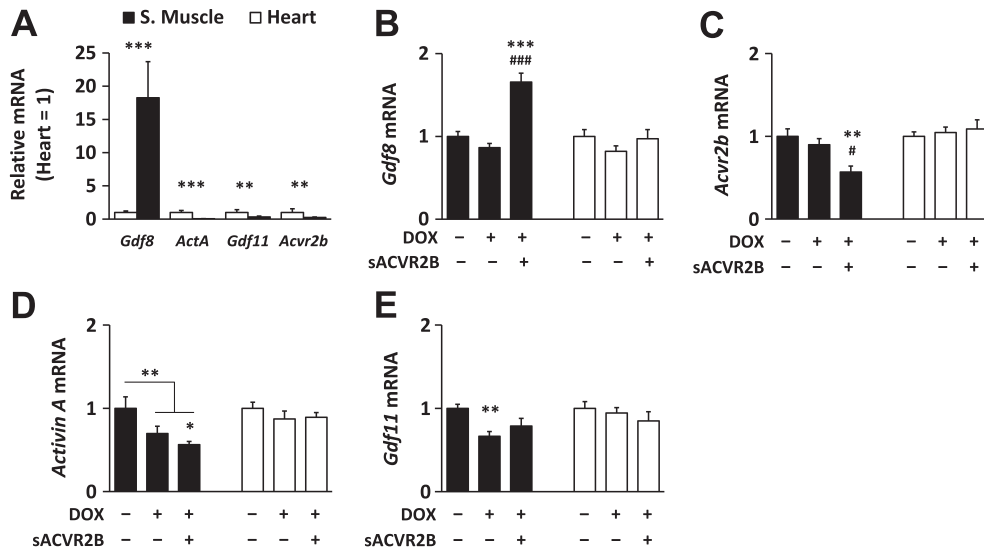
**Figure 7** mRNA expression changes of genes containing p53 targeted motifs (DOX vs. CTRL fold change > 1.5 and false discovery rate < 0.05) (A) in skeletal muscle and (B) in the heart. C = control, D = DOX, and D + A = DOX + sACVR2B. Sig. designates p-adjusted false discovery rate of the difference between the doxorubicin and controls (\* = false discovery rate < 0.05, \*\* = false discovery rate < 0.01, \*\*\* = false discovery rate < 0.001). Rank = the rank number (all genes in the genome) of likelihood of being a p53 target. Motifs = the number of p53 associated motifs found in regulatory sequence. The table presents results of mean of probes with multiple transcripts.  $n = 5$  per group. (C) The effects of DOX and combined DOX + sACVR2B on p53 protein level. Kruskal-Wallis test with Holm-Bonferroni corrected Mann-Whitney  $U$  post hoc test was used.  $n = 8-9$  in heart and 4-6 in skeletal muscle.



loss of tissue mass was equal? Skeletal muscle tissue has a tremendous regeneration capacity after muscle damage compared with the heart.<sup>13,14</sup> One of the most important factors in skeletal muscle regeneration/restoration is a skeletal muscle-specific protein MyoD that activates skeletal muscle-specific transcription,<sup>42</sup> and is required for muscle regeneration after injury.<sup>43</sup> MyoD target genes and *Myod* mRNA itself were induced in skeletal muscle in DOX-injected mice, possibly reflecting regeneration process in skeletal muscle by

activated satellite cells.<sup>43</sup> This response is probably secondary to the myocyte damage,<sup>2,10</sup> as at least in vitro in myoblasts, DOX per se can inhibit MyoD expression.<sup>44</sup> *Tceal7* was the most induced gene by sACVR2B-Fc in skeletal muscle. TCEAL7 is a protein expressed mainly in skeletal muscle, and it is up-regulated after muscle injury serving as an enhancer of muscle cell differentiation.<sup>38</sup> This may be one of the mechanisms how new myofibre nuclei can be acquired with sACVR2B.<sup>22</sup>

**Figure 8** (A) Activin receptor type IIB and its major ligands are differentially expressed in the heart and skeletal muscle. The effects of doxorubicin and sACVR2B-Fc administration on mRNA expression of (B) *Gdf8* (myostatin), (C) *Acrv2b*, (D) *Activin A*, and (E) *Gdf11* in skeletal muscle and the heart.  $n = 12$  per group in muscle and heart comparison (A),  $n = 6-9$  per group in the doxorubicin experiment (B-E). For multiple group comparisons, general linear model analysis of variance with Bonferroni post hoc test was used (B-E). For two-group comparisons, the non-parametric Mann-Whitney *U*-test (A) or Student's *t*-test (doxorubicin effect in D) were used.



REDD1<sup>45</sup> and p21<sup>46</sup> are downstream targets of p53. The present results suggest that p53-p21-REDD1 is the main pathway activated by DOX in both skeletal and cardiac muscles. DOX has been shown to increase nuclear accumulation and DNA binding of p53,<sup>47</sup> which at least in part mediates cardiac wasting.<sup>48</sup> Interestingly, sACVR2B-Fc completely prevented DOX-induced increase in p53 protein in both tissues and attenuated the increase in p21 mRNA in skeletal muscle. Our results show that sACVR2B-Fc does not induce its effect via modulating DOX-levels in muscles. Instead, decreased level of ACVR2B ligands such as myostatin can directly affect cell cycle regulation.<sup>49</sup> We found that sACVR2B-Fc increased Ki67-positive cells in both tissues. In skeletal muscle, this may indicate increased proliferation of at least satellite cells,<sup>22</sup> although most of the Ki67 staining was observed in myofibre and CMC nuclei. In addition to changes in proliferating cells, the increased Ki67 staining by sACVR2B-Fc may also reflect ribosomal RNA transcription.<sup>50</sup> In our pathway analyses, gene sets related to translation capacity or efficiency were enriched in skeletal muscle by sACVR2B-Fc. Knowing the importance of mTOR and ribosomes and their biogenesis in muscle protein synthesis and in muscle hypertrophy,<sup>51</sup> this may be causally linked with the increased muscle protein synthesis and mTORC1 signalling that we showed earlier.<sup>4</sup>

Downstream of p53, cell cycle arrest and increased reactive oxygen species are thought to be mediated, at least in part, by cyclin-dependent kinase inhibitor p21<sup>46</sup> and REDD1/DDIT4.<sup>45,52</sup> These responses can be important in

preventing proliferation of cells with harmful alterations in their DNA. This may, however, also be detrimental as some of the proliferating cells would aid recovery of skeletal muscle and the heart.<sup>53</sup> In the heart, absence of p53 may prevent at least part of the DOX-induced injury.<sup>54</sup> In skeletal muscle, overexpression of p53 is sufficient to induce muscle atrophy and muscle is partially resistant to certain types of atrophy stimuli in the absence of p53.<sup>55</sup> Interestingly, Fox et al. showed that p53 specifically targeted to muscle fibres mediates atrophy through p21, and that p21 alone is sufficient to decrease muscle fibre size.<sup>55</sup> Thus, the evidence suggests that increased p53 and its downstream signalling in skeletal muscle mainly acts by provoking muscle loss and injury rather than being protective. Our present results indicate that sACVR2B-Fc acts in part via inhibiting increased p53 signalling and thus may have a protecting role in the muscles and the heart.

Another common effect of sACVR2B-Fc was decreased expression of *Ccl21* mRNA. CCL21 is a chemokine that is increased in the heart and in serum of clinical and pre-clinical heart-failure, and its high levels are associated with increased all-cause mortality in patients with heart pathologies.<sup>56,57</sup> Thus, our results indicate that activin receptor ligand blocking attenuates pathological cytokine responses in both tissues. However, based on the present data, we cannot conclude the effect of this directly on heart or skeletal muscle function.

Blocking of activin receptor ligands had only minor effects in the heart. However, it may still have certain protective

effects in CMCs, as indicated by the effects on p53 and *Ccl21*. The ~18-fold higher myostatin expression in skeletal muscle (see *Figure 8A*) may be one important reason why sACVR2B-Fc has more pronounced effects in skeletal muscle than in the heart. The difference is not, however, explained by different protein<sup>18</sup> or gene expression levels of activin receptor IIB or its other ligands activin A and GDF11, as their mRNA levels were low in these tissues and if anything, higher in the heart. Also, their gene expression was not affected by DOX. Myostatin is activated after cleavage of its prodomain by BMP1/tolloid proteinases.<sup>26</sup> Our microarray data suggest that the expression level of these (TLL1, TLL2, and TLD/BMP1 found on our array chip) did not differ between skeletal muscle and the heart (<http://www.ncbi.nlm.nih.gov/geo/>; accession no. GSE77745 and GSE97642).

One of the main reasons for DOX-induced cardiotoxicity is thought to be mitochondrial iron accumulation.<sup>39</sup> DOX-induced iron uptake has been shown to be mediated, in part, by transferrin receptor-dependent mechanism.<sup>58</sup> Muscle-specific lack of transferrin receptor leads to decreased muscle growth and other metabolic changes, and surprisingly, many other tissues are affected as well.<sup>59</sup> Our present study showed that transferrin receptor mRNA was decreased by DOX in both tissues. Surprisingly, especially in skeletal muscle and to a small extent also in the heart, sACVR2B-Fc was able to increase the transferrin receptor mRNA and protein levels. This opens up interesting ideas for further studies to elucidate the role of transferrin receptor in muscle wasting and the role of activin receptor ligands in this regulation.

Interestingly, some of the responses were to the opposite directions between the tissues. Most of the PGC-1 mRNA isoforms were decreased by DOX in skeletal muscle, while in the heart, they tended to increase. PGC-1 $\alpha$  regulates for instance mitochondrial biogenesis, angiogenesis, and to some extent also muscle hypertrophy.<sup>60</sup> The observed differences support the recent evidence suggesting that PGC-1 $\alpha$  may have different functions in skeletal muscle and the heart.<sup>61</sup> Downstream genes of Stat3 TF were up-regulated specifically in the heart. This may reflect heart's response to attenuate cardiotoxicity as Stat3 overexpression in the heart has been shown to decrease DOX-induced cardiomyopathy.<sup>62</sup>

The importance of ACVR2B ligands in skeletal muscle is rather well studied. In addition, severe cardiac defects are observed in ACVR2B knockout mice<sup>24</sup> showing that ACVR2B signalling is important also for the heart development. In many pathological conditions or when cardiac load is increased, myostatin expression is induced in the heart,<sup>26,27</sup> which may be sufficient to decrease both cardiac and skeletal muscle size.<sup>25</sup> Myostatin inhibition has had variable effects on heart size depending on the model used.<sup>18,25,63</sup> Based on recent evidence, GDF11 that has high homology with myostatin, and is also a ligand for ACVR2B, may be more potent in inducing cardiac atrophy than myostatin.<sup>18</sup> Of other

ACVR2B ligands, also elevated serum activin A levels have been reported in heart failure,<sup>64</sup> and heart size is decreased in situations with large increases in systemic activin A levels.<sup>22,28</sup> Moreover, activin A and cancer-induced decrease in heart size can be prevented with strategies that block ACVR2B ligands.<sup>22</sup> In the present study, sACVR2B-Fc treatment increased skeletal muscle mass without a significant effect on heart mass. The small effect of sACVR2B-Fc in the heart supports earlier findings, in which blocking of activin receptor ligands in mice without cardiac atrophy had very small or no effect on heart size.<sup>20,65,66</sup> The present study showed that there was also no effect of DOX or sACVR2B-Fc on cardiac protein synthesis or CMC size unlike in skeletal muscle.<sup>4</sup> In skeletal muscle, also large *de novo* increase in size by blocking or deleting activin receptor ligands is possible without endogenous changes in myostatin, GDF11, or activin A expression as shown in the present study. Identifying the receptor and ligand preference in the heart vs. muscle will be of importance, as several pre-clinical and clinical experiments with blockers of these ligands and their receptors are currently ongoing.

In conclusion, the present results demonstrate that cardiac and skeletal muscles displayed similar atrophy due to the DOX treatment. However, the transcriptional changes were much greater in skeletal muscle, which may be attributed to the different regeneration capacity of these two tissues. On the other hand, p53-p21-REDD1 signalling was strongly induced in both tissues, and this could be attenuated by activin receptor ligand blocking, especially in skeletal muscle. Smaller effect of blocking these ligands in the heart may be explained in part by higher gene expression of myostatin in skeletal muscle. Taken together, the present study emphasizes that therapeutic strategies should not assume that skeletal and cardiac muscles show similar responses to different atrophy conditions.

## Acknowledgements

Director of the Wihuri Research Institute Kari Alitalo is thanked for providing resources and valuable comments on the study design. We also thank Dr. Philippe Pierre for kindly providing the anti-puromycin antibody. We acknowledge Maria Arrano de Kivikko, Kirsi Lintula, Arja Pasternack, Jouko Laitila, Juho Hyödynmaa, and Markus Ritvos for their valuable help and technical assistance. Biomedicum Functional Genomics Unit and Biomedicum Imaging Unit are thanked for core services and technical support.

The authors certify that they comply with the ethical guidelines for authorship and publishing of the *Journal of Cachexia, Sarcopenia and Muscle*.<sup>67</sup>

This work was supported by the Academy of Finland (grant nos. 275922 and 297245) and Jenny and Antti Wihuri Foundation.

## Online supplementary material

Additional Supporting Information may be found online in the supporting information tab for this article.

**Figure S1.** (A) Cardiomyocyte size at 2 weeks, (B) *Redd1* (*Ddit4*) mRNA acutely, (C) fibrosis at 4 weeks, and (d) ki67 at 2 weeks (both tissues, left panel) and acutely (right panel) in the heart after single doxorubicin and sACVR2B-Fc injection. In *Figure 1C*, representative images of stained transverse heart section and tibialis anterior muscle of different groups show no marked fibrosis at this timepoint (scalebar 50  $\mu$ m). In *Figure 1D*, lower panel shows representative Ki67 staining in muscle and in the heart (scalebar 100  $\mu$ m). The  $n = 4-8$  per group in cardiomyocyte and ki67,  $n = 9-10$  in fibrosis, and in REDD1  $n = 6-9$  per group). Bonferroni post hoc tests. \*, \*\*, or \*\*\* = significant ( $P < 0.05$ ,  $P < 0.01$ , or  $P < 0.001$ , respectively) difference to respective CTRL. # or ### = significant ( $P < 0.05$ ,  $P < 0.001$ , respectively) difference to respective doxorubicin. Notice that muscle results of *Redd1* can be found from a previous publication [4].

**Figure S2.** Venn graphs for individual gene transcripts changed by doxorubicin (A) in skeletal muscle (tibialis anterior) and (B) in the heart and (C-F) the effects of sACVR2B-Fc in tibialis anterior at adjusted false discovery rate  $< 0.05$ ,

fold change  $\geq 1.2$ .

**Figure S3.** Venn graphs for comparison of gene set enrichment analysis identified gene sets and pathways in skeletal muscle and the heart (false discovery rate  $< 0.05$ ) (A-C and E). p38 MAPK pathway was down-regulated by doxorubicin and restored by sACVR2B-Fc treatment in skeletal muscle as (D).

**Table S1.** These tables present top 10 identified transcription factors that may be involved in regulation of co-expressed genes in question. The program searched the regulatory motifs from each gene 500 bp upstream from transcription start site. Motif collection involved 9713 position weight matrices. D = doxorubicin, C = CTRL, A = doxorubicin + sACVR2B-Fc. NES = enrichment score threshold.

**Figure S4.** (A) *Myod* mRNA levels in skeletal muscle ( $n = 8$  per group) and (B) p-STAT3(Tyr750)/total STAT3 protein levels in skeletal muscle and the heart ( $n = 7-9$  per group).

## Conflict of interest

Juha Hulmi, Tuuli Nissinen, Markus Räsänen, Joni Degerman, Julia Lautaoja, Karthik Hemanthakumar, Janne Backman, Olli Ritvos, Mika Silvennoinen, and Riikka Kivelä declare that they have no conflicts of interest.

## References

- Kazemi-Bajestani SM, Mazurak VC, Baracos V. Computed tomography-defined muscle and fat wasting are associated with cancer clinical outcomes. *Semin Cell Dev Biol* 2016;**54**:2-10.
- Doroshov JH, Tallent C, Schechter JE. Ultrastructural features of Adriamycin-induced skeletal and cardiac muscle toxicity. *Am J Pathol* 1985;**118**:288-297.
- Ito H, Miller SC, Billingham ME, Akimoto H, Torti SV, Wade R, et al. Doxorubicin selectively inhibits muscle gene expression in cardiac muscle cells in vivo and in vitro. *Proc Natl Acad Sci U S A* 1990;**87**:4275-4279.
- Nissinen TA, Degerman J, Rasanen M, Poikonen AR, Koskinen S, Mervaala E, et al. Systemic blockade of ACVR2B ligands prevents chemotherapy-induced muscle wasting by restoring muscle protein synthesis without affecting oxidative capacity or atrogenes. *Sci Rep* 2016;**6**:32695.
- Rasanen M, Degerman J, Nissinen TA, Miinalainen I, Kerkela R, Siltanen A, et al. VEGF-B gene therapy inhibits doxorubicin-induced cardiotoxicity by endothelial protection. *Proc Natl Acad Sci U S A* 2016;**113**:13144-13149.
- Murphy KT. The pathogenesis and treatment of cardiac atrophy in cancer cachexia. *Am J Physiol Heart Circ Physiol* 2016;**310**:H466-H477.
- Tacar O, Sriamornsak P, Dass CR. Doxorubicin: an update on anticancer molecular action, toxicity and novel drug delivery systems. *J Pharm Pharmacol* 2013;**65**:157-170.
- Mitry MA, Edwards JG. Doxorubicin induced heart failure: phenotype and molecular mechanisms. *Int J Cardiol Heart Vasc* 2016;**10**:17-24.
- Zhang S, Liu X, Bawa-Khalife T, Lu LS, Lyu YL, Liu LF, et al. Identification of the molecular basis of doxorubicin-induced cardiotoxicity. *Nat Med* 2012;**18**:1639-1642.
- Gilliam LA, St Clair DK. Chemotherapy-induced weakness and fatigue in skeletal muscle: the role of oxidative stress. *Antioxid Redox Signal* 2011;**15**:2543-2563.
- Hydock DS, Lien CY, Jensen BT, Schneider CM, Hayward R. Characterization of the effect of in vivo doxorubicin treatment on skeletal muscle function in the rat. *Anticancer Res* 2011;**31**:2023-2028.
- Min K, Kwon OS, Smuder AJ, Wiggs MP, Sollanek KJ, Christou DD, et al. Increased mitochondrial emission of reactive oxygen species and calpain activation are required for doxorubicin-induced cardiac and skeletal muscle myopathy. *J Physiol* 2015;**593**:2017-2036.
- Sommese L, Zullo A, Schiano C, Mancini FP, Napoli C. Possible muscle repair in the human cardiovascular System. *Stem Cell Rev* 2017;**13**:170-191.
- Grounds MD. The need to more precisely define aspects of skeletal muscle regeneration. *Int J Biochem Cell Biol* 2014;**56**:56-65.
- d'Albis A, Couteaux R, Janmot C, Roulet A, Mira JC. Regeneration after cardiotoxin injury of innervated and denervated slow and fast muscles of mammals. Myosin isoform analysis. *Eur J Biochem* 1988;**174**:103-110.
- McPherron AC, Lawler AM, Lee SJ. Regulation of skeletal muscle mass in mice by a new TGF-beta superfamily member. *Nature* 1997;**387**:83-90.
- Chen JL, Walton KL, Winbanks CE, Murphy KT, Thomson RE, Mankanji Y, et al. Elevated expression of activins promotes muscle wasting and cachexia. *FASEB J* 2014;**28**:1711-1723.
- Hammers DW, Merscham-Banda M, Hsiao JY, Engst S, Hartman JJ, Sweeney HL. Supraphysiological levels of GDF11 induce striated muscle atrophy. *EMBO Mol Med* 2017;**9**:531-544.
- Lee SJ, Reed LA, Davies MV, Girgenrath S, Goad ME, Tomkinson KN, et al. Regulation of muscle growth by multiple ligands signaling through activin type II receptors. *Proc Natl Acad Sci U S A* 2005;**102**:18117-18122.
- Hulmi JJ, Oliveira BM, Silvennoinen M, Hoogaars WM, Ma H, Pierre P, et al. Muscle protein synthesis, mTORC1/MAPK/

- Hippo signaling, and capillary density are altered by blocking of myostatin and activins. *Am J Physiol Endocrinol Metab* 2013;**304**:E41–E50.
21. Rahimov F, King OD, Warsing LC, Powell RE, Emerson CP Jr, Kunkel LM, et al. Gene expression profiling of skeletal muscles treated with a soluble activin type IIB receptor. *Physiol Genomics* 2011;**43**:398–407.
  22. Zhou X, Wang JL, Lu J, Song Y, Kwak KS, Jiao Q, et al. Reversal of cancer cachexia and muscle wasting by ActRIIB antagonism leads to prolonged survival. *Cell* 2010;**142**:531–543.
  23. Toledo M, Busquets S, Penna F, Zhou X, Marmonti E, Betancourt A, et al. Complete reversal of muscle wasting in experimental cancer cachexia: additive effects of activin type II receptor inhibition and beta-2 agonist. *Int J Cancer* 2016;**138**:2021–2029.
  24. Oh SP, Li E. The signaling pathway mediated by the type IIB activin receptor controls axial patterning and lateral asymmetry in the mouse. *Genes Dev* 1997;**11**:1812–1826.
  25. Heineke J, Auger-Messier M, Xu J, Sargent M, York A, Welle S, et al. Genetic deletion of myostatin from the heart prevents skeletal muscle atrophy in heart failure. *Circulation* 2010;**121**:419–425.
  26. Breitbart A, Auger-Messier M, Molkenstein JD, Heineke J. Myostatin from the heart: local and systemic actions in cardiac failure and muscle wasting. *Am J Physiol Heart Circ Physiol* 2011;**300**:H1973–H1982.
  27. Bish LT, George I, Maybaum S, Yang J, Chen JM, Sweeney HL. Myostatin is elevated in congenital heart disease and after mechanical unloading. *PLoS One* 2011;**6**:e23818.
  28. Chen JL, Walton KL, Qian H, Colgan TD, Hagg A, Watt MJ, et al. Differential effects of IL6 and activin A in the development of cancer-associated cachexia. *Cancer Res* 2016;**76**:5372–5382.
  29. Morissette MR, Cook SA, Foo S, McKoy G, Ashida N, Novikov M, et al. Myostatin regulates cardiomyocyte growth through modulation of Akt signaling. *Circ Res* 2006;**99**:15–24.
  30. Vejpongsa P, Yeh ET. Prevention of anthracycline-induced cardiotoxicity: challenges and opportunities. *J Am Coll Cardiol* 2014;**64**:938–945.
  31. Schmidt EK, Clavarino G, Ceppi M, Pierre P. SUNSET, a nonradioactive method to monitor protein synthesis. *Nat Methods* 2009;**6**:275–277.
  32. Goodman CA, Mabrey DM, Frey JW, Miu MH, Schmidt EK, Pierre P, et al. Novel insights into the regulation of skeletal muscle protein synthesis as revealed by a new nonradioactive in vivo technique. *FASEB J* 2011;**25**:1028–1039.
  33. Kallio MA, Tuimala JT, Hupponen T, Klemela P, Gentile M, Scheinin I, et al. Chipster: user-friendly analysis software for microarray and other high-throughput data. *BMC Genomics* 2011;**12**: 507–2164–12–507.
  34. Janky R, Verfaillie A, Imrichova H, Van de Sande B, Standaert L, Christiaens V, et al. iRegulon: from a gene list to a gene regulatory network using large motif and track collections. *PLoS Comput Biol* 2014;**10**:e1003731.
  35. Subramanian A, Tamayo P, Mootha VK, Mukherjee S, Ebert BL, Gillette MA, et al. Gene set enrichment analysis: a knowledge-based approach for interpreting genome-wide expression profiles. *Proc Natl Acad Sci U S A* 2005;**102**:15545–15550.
  36. Kivela R, Silvennoinen M, Lehti M, Rinnankoski-Tuikka R, Purhonen T, Ketola T, et al. Gene expression centroids that link with low intrinsic aerobic exercise capacity and complex disease risk. *FASEB J* 2010;**24**:4565–4574.
  37. Kainulainen H, Papaioannou KG, Silvennoinen M, Autio R, Saarela J, Oliveira BM, et al. Myostatin/activin blocking combined with exercise reconditions skeletal muscle expression profile of mdx mice. *Mol Cell Endocrinol* 2015;**399**:131–142.
  38. Shi X, Garry DJ. Myogenic regulatory factors transactivate the Tceal7 gene and modulate muscle differentiation. *Biochem J* 2010;**428**:213–221.
  39. Ichikawa Y, Ghanefar M, Bayeva M, Wu R, Khechaduri A, Naga Prasad SV, et al. Cardiotoxicity of doxorubicin is mediated through mitochondrial iron accumulation. *J Clin Invest* 2014;**124**:617–630.
  40. Yi X, Bekeredjian R, DeFilippis NJ, Siddiquee Z, Fernandez E, Shohet RV. Transcriptional analysis of doxorubicin-induced cardiotoxicity. *Am J Physiol Heart Circ Physiol* 2006;**290**:H1098–H1102.
  41. Shum AM, Fung DC, Corley SM, McGill MC, Bentley NL, Tan TC, et al. Cardiac and skeletal muscles show molecularly distinct responses to cancer cachexia. *Physiol Genomics* 2015;**47**:588–599.
  42. Olson EN. Regulation of muscle transcription by the MyoD family. The heart of the matter. *Circ Res* 1993;**72**:1–6.
  43. Megeney LA, Kablar B, Garrett K, Anderson JE, Rudnicki MA. MyoD is required for myogenic stem cell function in adult skeletal muscle. *Genes Dev* 1996;**10**:1173–1183.
  44. Kurabayashi M, Jeyaseelan R, Kedes L. Anti-neoplastic agent doxorubicin inhibits myogenic differentiation of C2 myoblasts. *J Biol Chem* 1993;**268**:5524–5529.
  45. Ellisen LW, Ramsayer KD, Johannessen CM, Yang A, Beppu H, Minda K, et al. REDD1, a developmentally regulated transcriptional target of p63 and p53, links p63 to regulation of reactive oxygen species. *Mol Cell* 2002;**10**:995–1005.
  46. Deng C, Zhang P, Harper JW, Elledge SJ, Leder P. Mice lacking p21CIP1/WAF1 undergo normal development, but are defective in G1 checkpoint control. *Cell* 1995;**82**:675–684.
  47. Kurz EU, Douglas P, Lees-Miller SP. Doxorubicin activates ATM-dependent phosphorylation of multiple downstream targets in part through the generation of reactive oxygen species. *J Biol Chem* 2004;**279**:53272–53281.
  48. Zhu W, Soonthara MH, Chen H, Shen W, Payne RM, Liechty EA, et al. Acute doxorubicin cardiotoxicity is associated with p53-induced inhibition of the mammalian target of rapamycin pathway. *Circulation* 2009;**119**:99–106.
  49. Patel AK, Tripathi AK, Patel UA, Shah RK, Joshi CG. Myostatin knockdown and its effect on myogenic gene expression program in stably transfected goat myoblasts. *In Vitro Cell Dev Biol Anim* 2014;**50**:587–596.
  50. Bullwinkel J, Baron-Luhr B, Ludemann A, Wohlenberg C, Gerdes J, Scholzen T. Ki-67 protein is associated with ribosomal RNA transcription in quiescent and proliferating cells. *J Cell Physiol* 2006;**206**:624–635.
  51. von Walden F, Liu C, Aurigemma N, Nader GA. mTOR signaling regulates myotube hypertrophy by modulating protein synthesis, rDNA transcription, and chromatin remodeling. *Am J Physiol Cell Physiol* 2016;**311**:C663–C672.
  52. Shoshani T, Faerman A, Mett I, Zelin E, Tenne T, Gorodin S, et al. Identification of a novel hypoxia-inducible factor 1-responsive gene, RTP801, involved in apoptosis. *Mol Cell Biol* 2002;**22**:2283–2293.
  53. Tidball JG, Villalta SA. Regulatory interactions between muscle and the immune system during muscle regeneration. *Am J Physiol Regul Integr Comp Physiol* 2010;**298**:R1173–R1187.
  54. Velez JM, Miriyala S, Nithipongvanitch R, Noel T, Plablueng CD, Oberley T, et al. p53 Regulates oxidative stress-mediated retrograde signaling: a novel mechanism for chemotherapy-induced cardiac injury. *PLoS One* 2011;**6**:e18005.
  55. Fox DK, Ebert SM, Bongers KS, Dyle MC, Bullard SA, Dierdorff JM, et al. p53 and ATF4 mediate distinct and additive pathways to skeletal muscle atrophy during limb immobilization. *Am J Physiol Endocrinol Metab* 2014;**307**:E245–E261.
  56. Yndestad A, Finsen AV, Ueland T, Husberg C, Dahl CP, Oie E, et al. The homeostatic chemokine CCL21 predicts mortality and may play a pathogenic role in heart failure. *PLoS One* 2012;**7**:e33038.
  57. Finsen AV, Ueland T, Sjaastad I, Ranheim T, Ahmed MS, Dahl CP, et al. The homeostatic chemokine CCL21 predicts mortality in aortic stenosis patients and modulates left ventricular remodeling. *PLoS One* 2014;**9**: e112172.
  58. Kotamraju S, Chitambar CR, Kalivendi SV, Joseph J, Kalyanaraman B. Transferrin receptor-dependent iron uptake is responsible for doxorubicin-mediated apoptosis in endothelial cells: role of oxidant-induced iron signaling in apoptosis. *J Biol Chem* 2002;**277**:17179–17187.
  59. Barrientos T, Laothamatas I, Koves TR, Soderblom EJ, Bryan M, Moseley MA, et al. Metabolic catastrophe in mice lacking transferrin receptor in muscle. *EBioMedicine* 2015;**2**:1705–1717.
  60. Martinez-Redondo V, Pettersson AT, Ruas JL. The hitchhiker's guide to PGC-1alpha isoform structure and biological functions. *Diabetologia* 2015;**58**:1969–1977.
  61. Mutikainen M, Tuomainen T, Naumenko N, Huusko J, Smirin B, Laidinen S, et al. Peroxisome proliferator-activated receptor-gamma coactivator 1 alpha1 induces a



- cardiac excitation-contraction coupling phenotype without metabolic remodelling. *J Physiol* 2016;**594**:7049–7071.
62. Kunisada K, Negoro S, Tone E, Funamoto M, Osugi T, Yamada S, et al. Signal transducer and activator of transcription 3 in the heart transduces not only a hypertrophic signal but a protective signal against doxorubicin-induced cardiomyopathy. *Proc Natl Acad Sci U S A* 2000;**97**:315–319.
63. Biesemann N, Mendler L, Wietelmann A, Hermann S, Schafers M, Kruger M, et al. Myostatin regulates energy homeostasis in the heart and prevents heart failure. *Circ Res* 2014;**115**:296–310.
64. Yndestad A, Ueland T, Oie E, Florholmen G, Halvorsen B, Attramadal H, et al. Elevated levels of activin A in heart failure: potential role in myocardial remodeling. *Circulation* 2004;**109**:1379–1385.
65. Hulmi JJ, Oliveira BM, Silvennoinen M, Hoogaars WM, Pasternack A, Kainulainen H, et al. Exercise restores decreased physical activity levels and increases markers of autophagy and oxidative capacity in myostatin/activin-blocked mdx mice. *Am J Physiol Endocrinol Metab* 2013;**305**:E171–E182.
66. Morine KJ, Bish LT, Selsby JT, Gazzara JA, Pendrak K, Sleeper MM, et al. Activin IIB receptor blockade attenuates dystrophic pathology in a mouse model of Duchenne muscular dystrophy. *Muscle Nerve* 2010;**42**:722–730.
67. von Haehling S, Morley JE, Coats AJ, Anker SD. Ethical guidelines for publishing in the Journal of Cachexia, Sarcopenia and Muscle: update 2015. *J Cachexia Sarcopenia Muscle* 2015;**6**:315–316.



### III

## **TREATING CACHEXIA USING SOLUBLE ACVR2B IMPROVES SURVIVAL, ALTERS MTOR LOCALIZATION, AND ATTENUATES LIVER AND SPLEEN RESPONSES**

by

Nissinen, T.A., Hentilä, J., Penna, F., Lampinen, A., Lautaoja, J.H.,  
Fachada, V., Holopainen, T., Ritvos, O., Kivelä, R. & Hulmi, J.J. 2018

Journal of Cachexia, Sarcopenia and Muscle vol 9, 514–529

<https://doi.org/10.1002/jcsm.12310>

Reproduced with kind permission by John Wiley & Sons Ltd.

Published under CC BY-NC 4.0 license.



# Treating cachexia using soluble ACVR2B improves survival, alters mTOR localization, and attenuates liver and spleen responses

Tuuli A. Nissinen<sup>1\*</sup> , Jaakko Hentilä<sup>1</sup>, Fabio Penna<sup>2</sup>, Anita Lampinen<sup>1</sup>, Juulia H. Lautaoja<sup>1</sup>, Vasco Fachada<sup>1</sup>, Tanja Holopainen<sup>3</sup>, Olli Ritvos<sup>4</sup>, Riikka Kivelä<sup>3</sup> & Juha J. Hulmi<sup>1,4\*</sup> 

<sup>1</sup>Neuromuscular Research Center, Biology of Physical Activity, Faculty of Sport and Health Sciences, University of Jyväskylä, Rautpohjankatu 8, Jyväskylä 40014, Finland, <sup>2</sup>Department of Clinical and Biological Sciences, University of Turin, Corso Raffaello, Turin 10125, Italy, <sup>3</sup>Translational Cancer Biology Program, Research Programs Unit, Faculty of Medicine, University of Helsinki, and Wihuri Research Institute, Haartmaninkatu 8, Helsinki 00290, Finland, <sup>4</sup>Department of Physiology, Faculty of Medicine, University of Helsinki, Haartmaninkatu 8, Helsinki 00290, Finland

## Abstract

**Background** Cancer cachexia increases morbidity and mortality, and blocking of activin receptor ligands has improved survival in experimental cancer. However, the underlying mechanisms have not yet been fully uncovered.

**Methods** The effects of blocking activin receptor type 2 (ACVR2) ligands on both muscle and non-muscle tissues were investigated in a preclinical model of cancer cachexia using a recombinant soluble ACVR2B (sACVR2B-Fc). Treatment with sACVR2B-Fc was applied either only before the tumour formation or with continued treatment both before and after tumour formation. The potential roles of muscle and non-muscle tissues in cancer cachexia were investigated in order to understand the possible mechanisms of improved survival mediated by ACVR2 ligand blocking.

**Results** Blocking of ACVR2 ligands improved survival in tumour-bearing mice only when the mice were treated both before and after the tumour formation. This occurred without effects on tumour growth, production of pro-inflammatory cytokines or the level of physical activity. ACVR2 ligand blocking was associated with increased muscle (limb and diaphragm) mass and attenuation of both hepatic protein synthesis and splenomegaly. Especially, the effects on the liver and the spleen were observed independent of the treatment protocol. The prevention of splenomegaly by sACVR2B-Fc was not explained by decreased markers of myeloid-derived suppressor cells. Decreased tibialis anterior, diaphragm, and heart protein synthesis were observed in cachectic mice. This was associated with decreased mechanistic target of rapamycin (mTOR) colocalization with late-endosomes/lysosomes, which correlated with cachexia and reduced muscle protein synthesis.

**Conclusions** The prolonged survival with continued ACVR2 ligand blocking could potentially be attributed in part to the maintenance of limb and respiratory muscle mass, but many observed non-muscle effects suggest that the effect may be more complex than previously thought. Our novel finding showing decreased mTOR localization in skeletal muscle with lysosomes/late-endosomes in cancer opens up new research questions and possible treatment options for cachexia.

**Keywords** Activin; Myostatin; MDSC; Protein synthesis; Acute phase response; Physical activity

Received: 24 January 2018; Revised: 20 March 2018; Accepted: 27 March 2018

\*Correspondence to: Tuuli Nissinen and Juha Hulmi, Neuromuscular Research Center, Faculty of Sport and Health Sciences, University of Jyväskylä, Jyväskylä, Finland.  
Email: tuuli.a.m.nissinen@jyu.fi; juha.hulmi@jyu.fi

## Introduction

Cancer cachexia is a debilitating condition without an effective treatment. It is usually associated with marked loss of muscle and fat mass, reduced physical activity and function,

decreased tolerance to cancer therapies and increased mortality.<sup>1,2</sup> Skeletal muscle has been an underappreciated tissue in health and disease,<sup>3</sup> but a growing body of evidence suggests a beneficial role for treating muscle tissue in cachectic conditions associated with different diseases, such as cancer.<sup>4</sup>

Muscle wasting in cancer cachexia is a consequence of decreased muscle protein synthesis,<sup>5,6</sup> impaired regeneration<sup>7</sup> and/or increased protein degradation,<sup>6</sup> but their relative importance and mechanisms are not well known. One possible mechanism for muscle wasting in cachexia is increased signalling through activin receptor ligands, such as myostatin and activins.<sup>8–11</sup> Myostatin and activins negatively regulate muscle mass through binding to their receptors activin receptor type 2 (ACVR2) A and B.<sup>12,13</sup> Blocking these ligands or their receptors can increase muscle mass and prevent muscle wasting in various animal models,<sup>12–16</sup> but also in humans.<sup>17,18</sup>

Prevention of cancer associated cachexia by blocking ACVR2 ligands with either soluble receptor (sACVR2B)<sup>9,16</sup> or neutralizing antibody against the receptors<sup>14</sup> has previously been shown to improve survival without an effect on primary tumour growth in preclinical animal models. In addition, many other strategies to prevent muscle loss in different experimental models suggest causality between reduced muscle loss and survival in cachexia. For example, inhibition of NF- $\kappa$ B signalling reduced denervation- and Lewis lung carcinoma (LLC) tumour-induced muscle loss which was associated with improved survival rate.<sup>19</sup> Blocking GDF15, and consequently cachexia, significantly improved survival in fibrosarcoma (HT-1080) and in LNCaP tumour-bearing mice.<sup>20</sup> Furthermore, preventing the loss of muscle mass in C26 tumour-bearing mice by histone deacetylase inhibitor<sup>21</sup> and by inhibiting TWEAK/Fn14 signalling in the tumour<sup>22</sup> have prolonged survival.

If indeed treating cachexia and especially muscle loss by strategies such as blocking ACVR2 ligands can improve survival in cancer, this may occur at least in part through preventing the loss of respiratory muscle mass and function.<sup>23</sup> However, also other factors, such as haematological changes, acute phase response (APR), inflammatory cytokines, and myeloid-derived suppressor cells (MDSCs), have recently been identified as potential contributors to either the development of cancer cachexia or to the poor prognosis associated with it.<sup>24–28</sup> The contribution of these factors to the improved survival, when treating cachexia by blocking of ACVR2 ligands, is unknown.

In the present study, we aimed to study the effects of blocking ACVR2 ligands in a preclinical model of cancer cachexia on both muscle and non-muscle tissues. Two different treatment protocols were applied to compare the effects of blocking ACVR2 ligands only before the tumour formation, and thus increasing muscle size only prior to the onset of cachexia, or continued treatment both before and after the onset of cachexia. This comparison was performed to investigate whether increased muscle mass alone before the onset of cachexia is enough for the improved survival or if the continued treatment is crucial. We aimed to gain more insight into the potential mechanisms of muscle wasting and the role of non-muscle tissues in cancer cachexia, in order to understand the sACVR2B-mediated improved survival.

## Materials and methods

### Animals

BALB/c (BALB/cAnNCrI) male mice aged 5–6 weeks (Charles River Laboratories, Germany) were used in all experiments. Mice were housed under standard conditions (temperature 22°C, 12:12 h light/dark cycle) with free access to food pellets (R36; 4% fat, 55.7% carbohydrate, 18.5% protein, 3 kcal/g, Labfor, Stockholm Sweden) and water.

The treatment of the animals was in strict accordance with the European Convention for the protection of vertebrate animals used for experimental and other scientific purposes. The protocols were approved by the National Animal Experiment Board, and all the experiments were carried out in accordance with the guidelines of that committee (permit number: ESAVI/10137/04.10.07/2014) and with the ethical standards laid down in the 1964 Declaration of Helsinki and its later amendments.

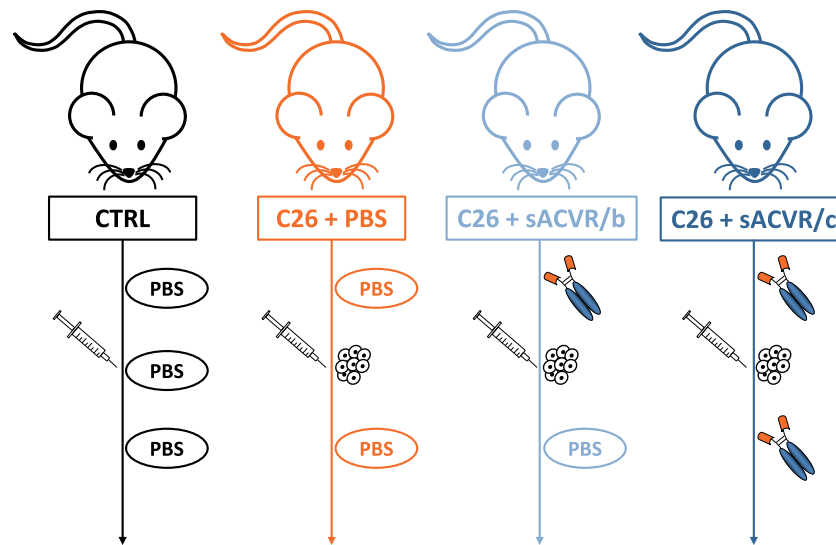
### Tumour cell culture

Colon 26 carcinoma (C26) cells (provided by Dr Fabio Penna, obtained from Prof. Mario P. Colombo and originally characterized by Corbett et al.<sup>29</sup>) were maintained in complete Dulbecco's Modified Eagle's Medium (high glucose, GlutaMAX™ Supplement, pyruvate, Gibco™, Life Technologies) supplemented with penicillin (100 U/mL), streptomycin (100 µg/mL), and 10% FBS. Our pilot experiments showed that injecting mice with C26 cells ( $5 \times 10^5$ ), resulted in marked cachexia and considerably higher tumour gene expression of *Activin A*, *Interleukin-6 (Il-6)* and *Myostatin* in comparison to our previously conducted experiment using the LLC tumour model (*Online Resource 1: Figure S1*) with the same number of cells injected ( $5 \times 10^5$ ), but larger tumour<sup>15</sup> (data not shown).

### Experimental design

The mice were randomized into one of four groups (matched by body weight): (i) healthy control mice (CTRL), (ii) C26 tumour-bearing mice receiving vehicle treatment throughout the experiment (C26 + PBS), (iii) C26 tumour-bearing mice receiving sACVR2B-Fc treatment before tumour formation (until Day 1 after C26 cell inoculation) followed by vehicle treatment until the end of the experiment (C26 + sACVR/b), and (iv) C26 tumour-bearing mice receiving continued sACVR2B-Fc treatment throughout the experiment (C26 + sACVR/c). The experimental design and the treatment protocols are shown in *Figure 1*. Body mass and food intake of the mice were monitored daily in all the experiments.

**Figure 1** Schematic representation of the experimental design and the treatments. C26 cells were injected on Day 0, and sACVR2B-Fc or PBS vehicle were administered on Days -11, -7, -3, 1, 5, and 9 in all experiments.



### Survival experiment

The mice were followed until the predetermined humane end-point criteria were fulfilled, or until 3 weeks after C26 cell inoculation at the latest, to investigate survival. The end-point criteria combined the body mass loss and the overall condition of the mice. In the evaluation of the overall health status of the mice, the following aspects were taken into account in addition to the body mass loss: appearance and posture (lack of grooming, piloerection, and hunched posture), natural and provoked behaviour (inactivity, impaired locomotion, and reduced reactivity to external stimuli), and food intake/ability to eat and drink. Mice were euthanized when two researchers confirmed the fulfilment of the end-point criteria. During the experiment, seven mice needed to be euthanized due to reasons unrelated to study purposes (e.g. tumour ulceration or self-mutilation), and three mice were excluded from analysis due to delayed tumour growth. This did not have any major effect on the results.

### Short-term experiments

To study the potential mechanisms, another experiment was conducted with a predetermined end-point at Day 11 after C26 cell inoculation (Figure 1). This experiment was repeated with three groups: CTRL, C26 + PBS and C26 + sACVR/c groups in order to replicate the findings of the first short-term experiment and to collect more samples and data for further analysis.

### Experimental treatments

An intraperitoneal injection of sACVR2B-Fc (5 mg/kg) or PBS (100  $\mu$ l) was administered twice a week, three times before and three times after C26 cell inoculation (on Days -11, -7, -3, 1, 5, and 9) in all experiments (Figure 1). On Day 0, mice were anaesthetized by intraperitoneal administration of ketamine and xylazine (Ketaminol® and Rompun®, respectively) and inoculated with  $5 \times 10^5$  C26 cells in 100  $\mu$ l of PBS (tumour-bearing mice) or with an equal volume of vehicle (PBS) only (CTRL) into the intrascapular subcutis.

### The production of soluble ACVR2B

The ectodomain of ACVR2B was fused with an IgG1 Fc domain and the fusion protein was expressed *in house* in Chinese hamster ovary cells grown in a suspension culture as explained earlier in detail.<sup>30</sup> The protein is similar but not identical to that originally generated by Lee and colleagues.<sup>12</sup>

### Home cage physical activity

Home cage physical activity was recorded by our validated force plate system as previously described<sup>31,32</sup> at baseline and on Day 10 after C26 cell inoculation (22 h recording). The mice were housed in pairs and the activity index of each cage reflects the total locomotive activity in all directions (y, x, and z axes) of the two mice housing the same cage (from the same experimental group).

### Tissue collection

At the end of each experiment, the mice were anaesthetized by an intraperitoneal injection of ketamine and xylazine (Ketaminol® and Rompun®, respectively) and euthanized by cardiac puncture followed by cervical dislocation. A sample of the collected blood was taken to EDTA tubes for the analysis of basic haematology. The rest of the blood was collected in serum collection tubes, and centrifuged at 2000 g for 10 min (Biofuge 13, Heraeus). The diaphragm, the heart, tibialis anterior (TA), and gastrocnemius muscles, as well as the liver, the spleen, epididymal fat pads, and the tumour were rapidly excised, weighed, and snap-frozen in liquid nitrogen. The right TA and a sample of the spleen were embedded in Tissue-Tek® O.C.T. compound and snap-frozen in isopentane cooled with liquid nitrogen. All tissue masses were normalized to the length of the tibia (TL, mm), which was unaltered by the tumour or the continued sACVR2B-Fc treatment, but slightly increased in the C26 + sACVR/b group as compared to C26 + PBS (*Online Resource 3: Figure S2*).

### Muscle protein synthesis: in vivo surface sensing of translation

Muscle protein synthesis was analysed using surface sensing of translation method<sup>33,34</sup> as earlier in our laboratory.<sup>15,30,35</sup> Briefly, on Day 11 after C26 cell inoculation, mice were anaesthetized and subsequently injected i.p. with 0.040 µmol/g puromycin (Calbiochem, Darmstadt, Germany) dissolved in 200 µl of PBS. At exactly 25 min after puromycin administration, mice were euthanized by cardiac puncture followed by cervical dislocation. The left TA muscle and the heart, the diaphragm, as well as a sample of the median lobe of the liver were isolated, weighed and snap-frozen in liquid nitrogen at exactly 30, 35, and 40 min, respectively, after puromycin administration.

### Basic haematology

Basic haematology was analysed from whole blood (EDTA) samples diluted 1:25 in saline solution with an automated haematology analyser (Sysmex XP 300 analyzer Sysmex Inc, Kobe, Japan). For the analysis of the platelet count, whole blood was diluted 1:250 due to high platelet counts in the samples.

### Multiplex cytokine assay

A multiplex cytokine assay (Q-Plex Array 16-plex ELISA, Quansys Biosciences, Logan, Utah, USA) was performed in

accordance with manufacturer's instructions from 25 µl of serum at 11 days post cancer cell inoculation.

### RNA extraction, cDNA synthesis, and quantitative real-time PCR

Total RNA was extracted from tumour, gastrocnemius, and spleen samples using QIAzol and purified with RNeasy Universal Plus kit (Qiagen) according to manufacturer's instructions resulting in high quality RNA. RNA was reverse transcribed to complementary DNA (cDNA) with iScript™ Advanced cDNA Synthesis Kit (Bio-Rad Laboratories) following kit instructions. Real-time qPCR was performed according to standard procedures using iQ SYBR Supermix (Bio-Rad Laboratories) and CFX96 Real-Time PCR Detection System combined with CFX Manager software (Bio-Rad Laboratories). Data analysis was carried out by using efficiency corrected  $\Delta\Delta C_t$  method. Based on the lowest variation between and within the groups of the potential housekeeping genes (*Rn18S*, *Gapdh*, *36b4*, or *Tbp*), *Tbp* was selected for the spleen whereas *36b4* was chosen for the tumour and the muscle. Primers used are listed in *Online Resource 2: Supplementary methods (Table S1)*.

### Protein extraction and content

Tibialis anterior (TA), diaphragm, heart, and liver samples were homogenized in ice-cold buffer with proper protease and phosphatase inhibitors and further treated as earlier<sup>30</sup> with slight modifications. The samples were centrifuged at 500 g for 5 min at +4°C for the analysis of the protein synthesis, and at 10 000 g for 10 min at +4°C for other analyses. Total protein content was determined using the bicinchoninic acid protein assay (Pierce, Thermo Scientific) with an automated KoneLab device (Thermo Scientific).

### Citrate synthase activity assay

Citrate synthase activity was measured from TA, diaphragm, and heart homogenates using a kit (Sigma-Aldrich) with an automated KoneLab device (Thermo Scientific).

### Western blotting

Western blot analysis was performed as previously described.<sup>15,30,36</sup> Briefly, tissue homogenates containing 30 µg of protein were solubilized in Laemmli sample buffer and heated at 95°C (except at 50°C for the analysis of OXPHOS proteins) to denature proteins, separated by SDS-PAGE and then transferred to PVDF membrane followed by overnight probing with primary antibodies at +4°C. Proteins were visualized by enhanced chemiluminescence using a ChemiDoc

XRS device and quantified with Quantity One software version 4.6.3 (Bio-Rad Laboratories, Hercules, California, USA). In the case of the analysis of puromycin-incorporated proteins and ubiquitinated proteins, the intensity of the whole lane was quantified. Ponceau S staining and GAPDH were used as loading controls and all the protein level results were normalized to the mean of Ponceau S and GAPDH. Antibodies used are listed in *Online Resource 2: Supplementary methods*.

### Histology and immunohistochemistry

For histological analysis, 10 µm thick frozen sections were cut from O.C.T.-embedded (Tissue-Tek) TA and spleen samples. Antibodies used in the immunofluorescence analyses are listed in *Online Resource 2: Supplementary methods*.

For mechanistic target of rapamycin (mTOR)-LAMP2 colocalization analysis, TA sections were air-dried and fixed in  $-20^{\circ}\text{C}$  acetone for 10 min. After PBS washes, sections were blocked with 5% goat serum and 0.3% CHAPS in PBS for 1 h, washed with PBS, and incubated overnight at  $+4^{\circ}\text{C}$  with primary antibodies against mTOR, dystrophin, and LAMP2 diluted in PBS containing 0.5% BSA and 0.3% CHAPS. After PBS washes, sections were incubated with secondary antibodies (Goat anti-rabbit Alexa Fluor 555, Goat anti-mouse Alexa Fluor 405 and Goat anti-rat Alexa Fluor 488) for 1 h at room temperature, washed and mounted.

Spleen sections were stained using haematoxylin and eosin for basic histology. For immunofluorescence staining, frozen sections were air-dried for 15 min and fixed with 4% PFA for 10 min, followed by washes with PBS. The sections were blocked with 5% goat serum in PBS for 1 h, washed with PBS, and incubated with primary antibodies against LY-6G and LY-6C (GR-1) or CD11b diluted in 0.5% BSA in PBS at  $+4^{\circ}\text{C}$  overnight. After washing, the sections were incubated with Alexa fluorochrome conjugated secondary antibody (Goat anti-rat Alexa Fluor 488) diluted in 5% goat serum in PBS for 1 h.

The samples were mounted with Mowiol-DABCO. Fluorescently labelled samples were imaged using Zeiss LSM 700 confocal microscope and analysed from 10 images (mTOR-LAMP2) or from 6–11 images (CD11b and GR-1) in each sample using ImageJ. The colocalization of mTOR with LAMP2 was analysed according to Costes et al.<sup>37</sup> using the Colocalization Threshold plugin. All the steps were performed blinded to the sample identification.

### Statistical analyses

Differences in survival were analysed with the Kaplan–Meier method [log-rank (Mantel-Cox) test]. Cox regression analysis was used to determine factors predicting survival. The C26

cancer effect (CTRL vs. C26 + PBS or CTRL vs. C26 groups pooled) was examined with Student's *t*-test or non-parametric Mann–Whitney *U* test, and the effect of sACVR2B-Fc in the tumour-bearing groups with one-way analysis of variance or Kruskal–Wallis test followed by Holm–Bonferroni corrected LSD or Mann–Whitney *U* post hoc tests, respectively, when appropriate. Pearson correlation coefficient was used to analyse correlations. Statistical significance was set at  $P < 0.05$ . All values are presented as means  $\pm$  SEM unless otherwise stated.

## Results

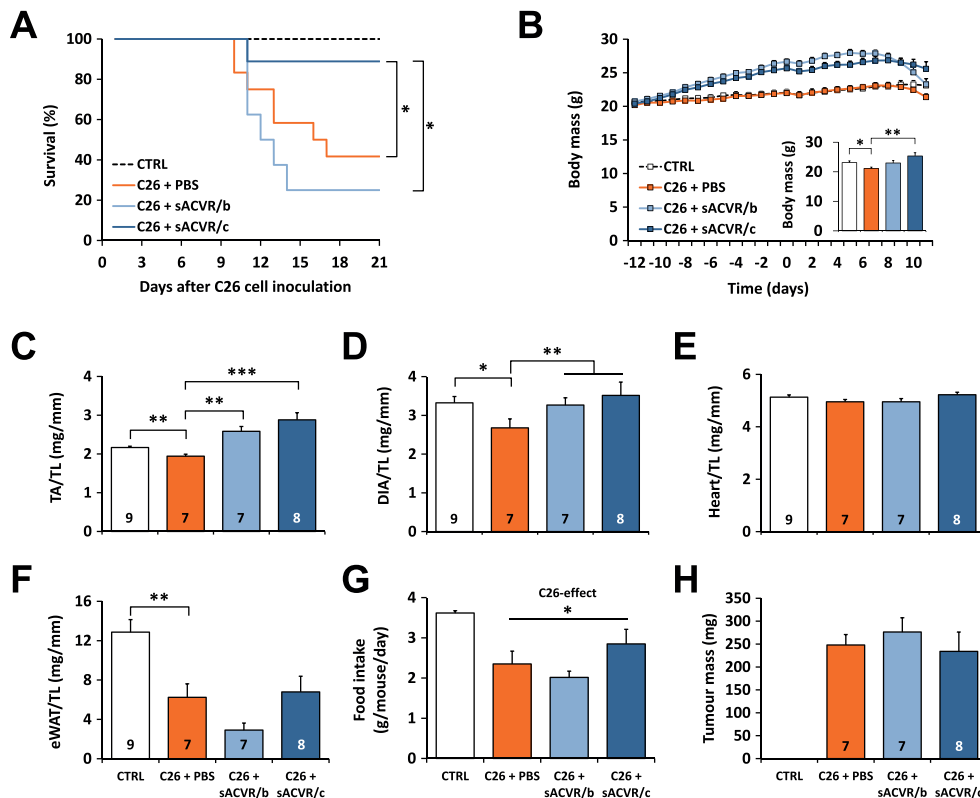
### Blocking activin receptor type 2B ligands improves survival of C26 tumour-bearing mice

Mice treated with sACVR2B started to gain body mass soon after the beginning of the treatment (*Online Resource 3: Figure S2*). The body mass of the tumour-bearing mice started to decrease after C26 cell inoculation. There was no significant difference in the survival time between C26 + PBS and C26 + sACVR/b groups (*Figure 2A*). However, the survival was significantly improved when sACVR2B-Fc administration was continued also after tumour formation (*Figure 2A*).

To study the potential mechanisms underlying the improved survival with only the continued sACVR2B-Fc administration, another experiment was conducted. Associations between the body mass change and survival time were analysed with Cox regression analysis, which revealed that especially the body weight change from Day 10 to Day 11 after cancer cell inoculation predicted survival ( $B = 1.82$ ,  $P < 0.001$ ). Thus, Day 11 was determined as the end-point for the second experiment to target the early phase of cachexia. At this time point, vehicle treated tumour-bearing mice exhibited cachexia manifested by significantly decreased body mass accompanied by lower TA, diaphragm, and adipose tissue mass compared with healthy controls (*Figure 2B–F*, Body mass in *Online Resource 3: Figure S2*). Both sACVR2B-Fc administered groups had significantly greater TA masses compared with vehicle treated tumour-bearing controls, and similar trend was also apparent in diaphragm (*Figure 2C and 2D*). sACVR2B-Fc administration had no effect on adipose tissue mass when compared to the PBS-treated mice, but discontinuation of the treatment seemed to result in more prominent fat wasting compared with the continued treatment (ns) (*Figure 2F*). Increased fat wasting together with non-significantly smaller muscle masses compared with continued treatment protocol probably explains why body mass had started to decrease especially rapidly in C26 + sACVR/b group. Heart mass



**Figure 2** The effects of sACVR2B-Fc administration on survival, tissue masses and food intake in C26 cancer cachexia. (A) A 3-week Kaplan–Meier survival curve (log-rank (Mantel-Cox) test).  $N = 6, 12, 8,$  and  $9$  in CTRL, C26 + PBS, C26 + sACVR/b, and C26 + sACVR/c, respectively. (B) Body mass and the final tumour-free body mass, in the short-term experiment. There was a significant time  $\times$  group interaction ( $P = 0.006$ , repeated measures ANOVA). Masses of (C) tibialis anterior (TA), (D) diaphragm (DIA), (E) the heart, and (F) epididymal white adipose tissue (eWAT) normalized to the length of the tibia in mm (TL) at 11 days after C26 cell inoculation. (G) Average food intake during Days 8–10 of the short term experiment, in which  $N = 3$ –4 cages/group, 2 mice/cage. (H) Tumour mass on Day 11 after C26 cell inoculation. \*, \*\* and \*\*\* =  $P < 0.05, 0.01$  and  $0.001$ , respectively. CTRL vs. C26 + PBS difference was analysed by Student's  $t$ -test (B–G), and differences between the C26-groups with one-way ANOVA with Holm–Bonferroni corrected LSD (B–H). Lines without vertical ends show a pooled effect: (D) sACVR2B-Fc combined and (G) C26-groups combined. N-sizes are depicted in the bar graphs.



was unaffected by the tumour and the sACVR2B-Fc administration at this time point (Figure 2E), although mild cardiac cachexia was observed in our pilot study at 2 weeks after cancer cell inoculation (Online Resource 1: Figure S1). During the last days of the experiment, all tumour-bearing groups had reduced food intake compared to healthy controls (Figure 2G).

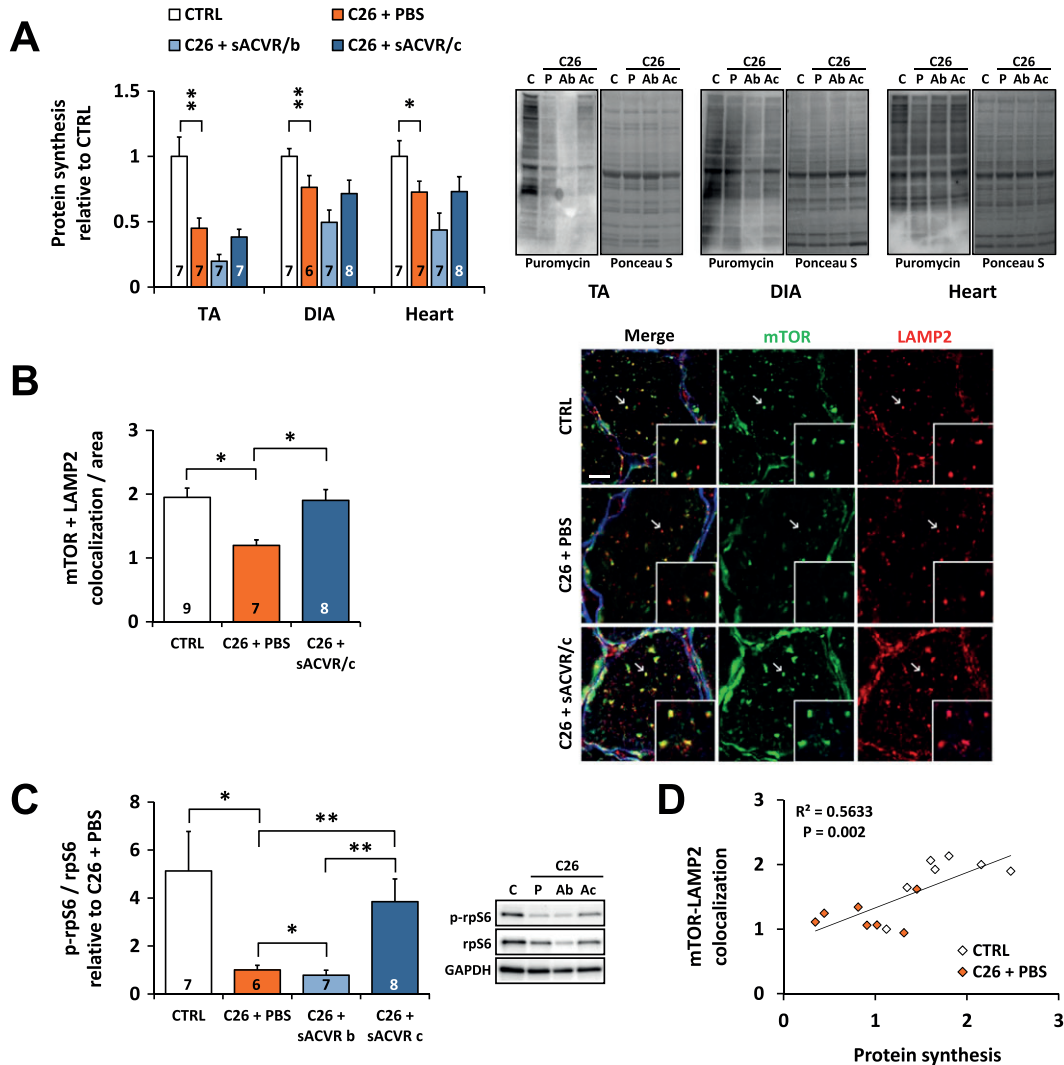
Administration of sACVR2B-Fc had no effect on tumour mass (Figure 2H). To find out if the mRNA expression of the potential cachexia-inducing factors was nonetheless modulated by sACVR2B-Fc administration, gene expressions were analysed from the tumours. Consistent with no effects on tumour mass, sACVR2B-Fc administration had no major effect on tumour *Activin A* (*Inhibin  $\beta$ A*) mRNA expression, but it increased *Il-6* mRNA expression independent of the treatment protocol (Online Resource 3: Figure S2). In the gastrocnemius muscles of the tumour-bearing mice, the mRNA expression of

*Activin A* slightly, but significantly decreased while *Il-6* strongly increased and *Myostatin* (*Gdf8*) tended to increase without an effect of the treatment (Online Resource 3: Figure S2).

#### *Muscle protein synthesis and mTOR signalling are decreased in C26 cancer cachexia alongside reduced mTOR localization to lysosomes/late-endosomes*

To clarify the mechanisms underlying C26 cancer-induced muscle atrophy, muscle protein synthesis was analysed from TA, diaphragm, and the heart. Tumour-bearing mice had markedly blunted protein synthesis in all of these tissues and especially in TA, whereas sACVR2B-Fc administration had no effect (Figure 3A). The mTOR, a regulator of protein synthesis, is at least in part regulated by its subcellular

**Figure 3** Decreased protein synthesis is associated with altered mTOR localization in the tumour-bearing mice at 11 days after C26 cell inoculation. (A) Protein synthesis analysed by SUnSET in TA, diaphragm (DIA) and the heart (left) and the representative blots (right, C = CTRL, P = C26 + PBS, Ab = C26 + sACVR/b, Ac = C26 + sACVR/c). (B) Quantification of mTOR-LAMP2 colocalization in TA and the representative images (scale bar = 10  $\mu$ m). Membranes were excluded from the analysis, but this did not have major impact on the results (data not shown). (C) Phosphorylation of rpS6 on Ser240/244 in TA (left) and the representative blots (right). (D) Correlation between mTOR-LAMP2 colocalization and protein synthesis in CTRL and C26 + PBS groups (Pearson correlation coefficient). \* and \*\* =  $P < 0.05$  and  $0.01$ , respectively. Kruskal–Wallis with Holm–Bonferroni corrected Mann–Whitney  $U$  (A, C); Student’s  $t$ -test (B, C26- and sACVR2B-Fc-effects). Lines without vertical ends show a pooled effect of all C26-groups combined. N-sizes are depicted in the bar graphs.



localization: localization to the lysosomal/late-endosome membrane is associated with mTOR activation.<sup>38,39</sup> To analyse whether decreased muscle protein synthesis was associated with altered mTOR localization, TA cross-sections were labelled with antibodies against mTOR and a lysosome/late-endosome marker LAMP2. The results demonstrate that colocalization of mTOR with LAMP2 was decreased in the tumour-bearing mice compared with the control group and restored by continued sACVR2B-Fc administration (Figure 3B), reflecting the levels of phosphorylation of ribosomal

protein S6, a marker of mTOR signalling (Figure 3C). Also the phosphorylation of S6 kinase 1 at Thr389 was decreased in the tumour-bearing mice without consistent restoration by the continued sACVR2B-Fc treatment (Online Resource 4: Figure S3). The total amount of mTOR analysed with western blotting was similar between the groups (data not shown). Interestingly, mTOR colocalization with LAMP2 correlated well with muscle protein synthesis ( $r = 0.751$ ;  $P < 0.01$ , Figure 3D) and the body mass change of the last day ( $r = 0.630$ ;  $P < 0.01$ ) in the untreated mice.

**C26 cancer cachexia is associated with elevated content of ubiquitinated proteins in skeletal muscle**

The content of ubiquitinated proteins was slightly but significantly increased in TA and diaphragm of the tumour-bearing mice (*Online Resource 4: Figure S3*). In line with this result, the mRNA expression of the major muscle-specific E3 ubiquitin ligases *Murf1* and *Atrogin1* was markedly increased in the tumour-bearing mice, similar trend being observed also in recently characterized muscle ubiquitin ligase of the SCF complex in atrophy-1 (*Musa1*)<sup>40</sup> (*Online Resource 4: Figure S3*). sACVR2B-Fc administration did not have significant effects on the markers of ubiquitin–proteasome system (*Online Resource 4: Figure S3*). Other protein degradation pathways may also contribute to muscle atrophy in tumour-bearing mice. Indeed, our data suggests potentially increased autophagy in tumour-bearing mice (Hentilä et al. unpublished observations).

**Reduced physical activity in C26 cancer cachexia is not rescued by soluble ACVR2B and is associated with minor alterations in skeletal muscle oxidative properties**

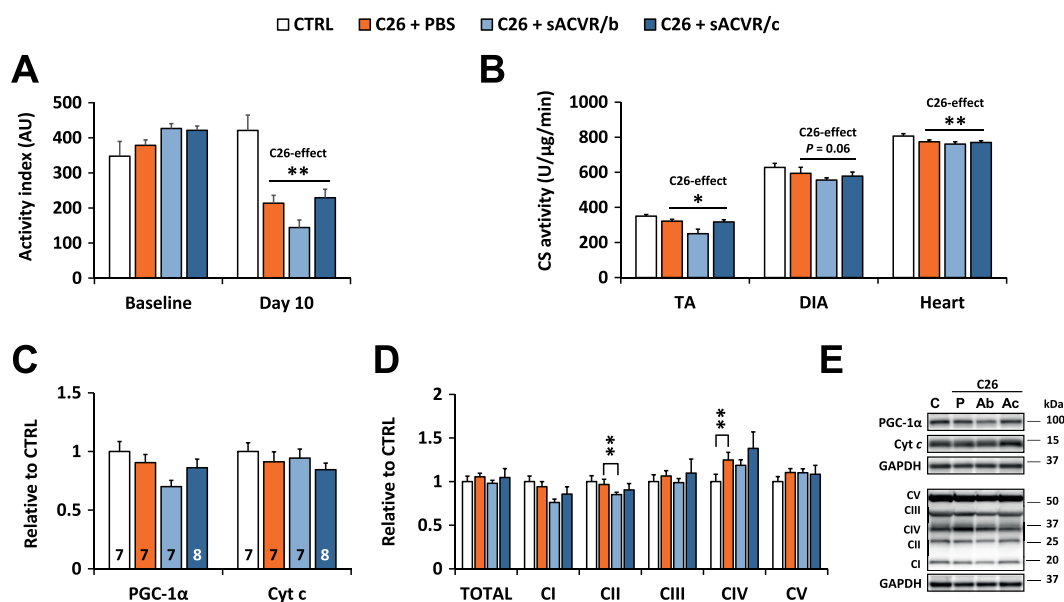
Home cage physical activity of the mice was recorded at baseline and on Day 10 after the injection of cancer cells

or vehicle control. On Day 10, the tumour-bearing mice were significantly less active compared with the control mice, and sACVR2B-Fc administration had no effect on the level of physical activity (*Figure 4A*). Reduced physical activity was accompanied by minor decreases in citrate synthase activity, but not in the markers of mitochondrial content in skeletal muscle and the heart of the tumour-bearing mice compared with healthy controls (*Figure 4B–E, Online Resource 5: Figure S4*). However, OXPHOS complex IV subunit 1 (MTCO1) was increased in tumour-bearing mice in both skeletal muscle and the heart (*Figure 4D and 4E; Online Resource 5: Figure S4*).

**Increased circulating levels of pro-inflammatory cytokines are not affected by blocking activin receptor ligands**

To investigate the possible effects of C26 cancer and sACVR2B-Fc administration on circulating cytokines, a multiplex assay was conducted. Of the 16 cytokines analysed, the levels of pro-inflammatory IL-6 and monocyte chemoattractant protein (MCP-1), also known as Chemokine (C-C motif) ligand 2 (CCL2), were highly elevated ( $P < 0.001$ ) in the sera of the C26 mice while chemokine RANTES (CCL5) was decreased from already low values of the healthy mice (*Online Resource 6: Table S2*). The sACVR2B treatment did not have any effect on IL-6 ( $P = 0.67$ ) or on

**Figure 4** Home cage physical activity and muscle oxidative properties at early phase of C26 cancer cachexia. (A) Activity indexes (AU) at baseline and at Day 10 after C26 cell injection.  $N = 2–3$  cages/group, 2 mice/cage. This result was replicated in the second short-term experiment (data not shown). (B) Citrate synthase activities in TA, diaphragm, and the heart on Day 11 after C26 cell injection. (C) PGC-1 $\alpha$  and cytochrome (Cyt) *c*, and (D) mitochondrial OXPHOS protein content in TA on Day 11 after C26 cell inoculation. (E) Representative blots. \* and \*\* =  $P < 0.05$  and  $0.01$ , respectively. C26-effect was analysed by Student’s *t*-test (A, B), and group differences by Kruskal–Wallis with Holm–Bonferroni corrected Mann–Whitney *U* (C, D).  $N = 7–9$ /group.



RANTES ( $P = 0.89$ ), while it even further increased MCP-1 ( $P = 0.042$ ), when the treatment was continued (*Online Resource 6: Table S2*). The treatment with sACVR2B-Fc also resulted in slightly elevated serum IL-1 $\beta$  ( $P < 0.05$ ) independent of the treatment protocol, but its levels were very close to the detection limit in most of the samples (*Online Resource 6: Table S2*).

### Increased hepatic protein synthesis and acute phase response in tumour-bearing mice are partially blocked by soluble ACVR2B

Liver mass was unaltered by C26 tumour and the treatments (*Figure 5A*). However, C26 tumour-bearing mice had significantly increased liver protein synthesis (*Figure 5B*) supported by increased phosphorylation of ribosomal protein S6, a marker of mTOR signalling (*Figure 5C*). This cancer effect was attenuated by sACVR2B-Fc administration independent of the treatment protocol (*Figure 5B and 5C*). Administration of sACVR2B-Fc alone in healthy mice did not affect liver protein synthesis as analysed from our previous experiment<sup>30</sup> (data not shown).

In line with increased protein synthesis, the C26 tumour-bearing mice had increased levels of fibrinogen and serpinA3N compared to healthy controls together with the increased phosphorylation of Stat3 indicating activation of APR (*Figure 5C*). Increased Stat3 phosphorylation was

partially attenuated by sACVR2B-Fc administration (*Figure 5C*). The protein contents of fibrinogen and serpinA3N correlated with the body mass loss during the last day in the tumour-bearing mice ( $r = -0.659$ ,  $P = 0.001$ , and  $r = -0.845$ ,  $P < 0.001$ , respectively).

### C26 cancer associated splenomegaly is partially prevented by soluble ACVR2B independent of splenic myeloid-derived suppressor cells

C26 tumour-bearing mice treated with PBS had significantly (over 2.5-fold) increased spleen mass compared with healthy control mice, which was partially prevented by sACVR2B-Fc administration independent of the treatment protocol (*Figure 6A*). We replicated the experiment with all groups except the discontinued sACVR2B-Fc treatment and showed again the same effects (*Online Resource 7: Figure S5*). Analysis of the spleen histology from this experiment revealed well-organized and clear red and white pulp areas in the control mice whereas in the tumour-bearing mice, moderate structural disorganization of the white pulp areas occurred, especially in sACVR2B treated mice (*Figure 6B*). To identify possible myeloid-derived suppressor cell (MDSC) expansion, spleen tissue was more specifically labelled with antibodies against GR-1 (LY-6C/G) and CD11b and the expression of typical MDSC marker genes was analysed by qPCR.<sup>42</sup> The density of CD11b positive cells (count/area) was increased

**Figure 5** Liver mass, protein synthesis and markers of acute phase response on Day 11 after C26 cell injection. (A) Liver mass normalized to the length of the tibia (TL). (B) Liver protein synthesis (left) and representative blots (right). (C) Phosphorylation of rpS6 on Ser240/244 and Stat3 on Tyr705, and protein contents of fibrinogen and serpinA3N in liver (left) and the representative blots (right).  $N = 6-9$ /group. \*\* and \*\*\* =  $P < 0.01$  and  $0.001$ , respectively. Student's  $t$ -test and one-way ANOVA with Holm-Bonferroni corrected LSD (A), Kruskal-Wallis with Holm-Bonferroni corrected Mann-Whitney  $U$  (B, C). Lines without vertical ends in (C) show a pooled effect of both sACVR2B-Fc groups combined. N-sizes are depicted in the bar graphs.

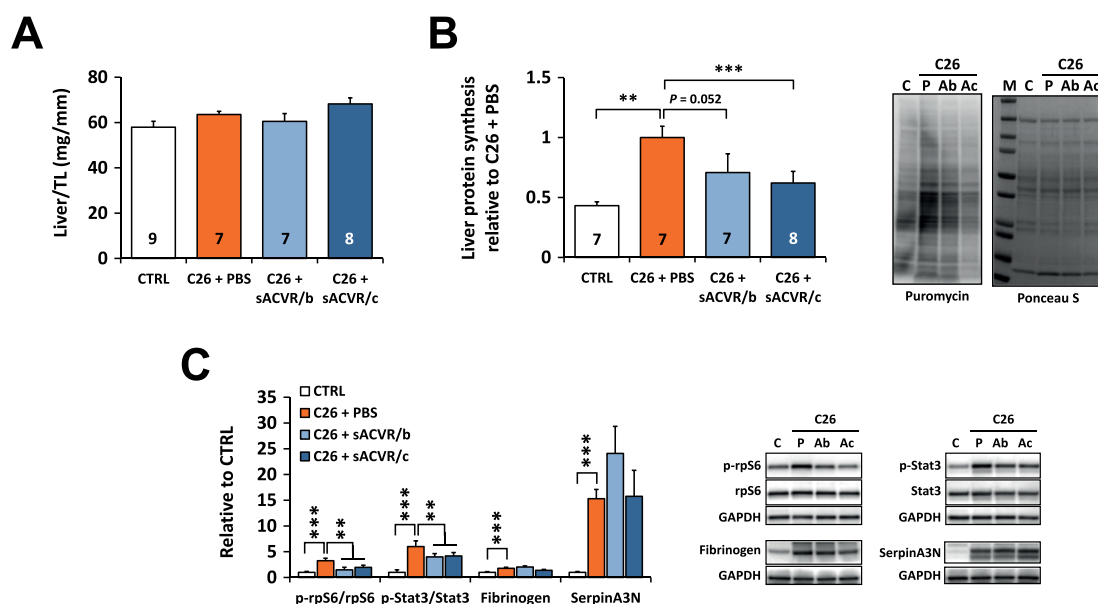
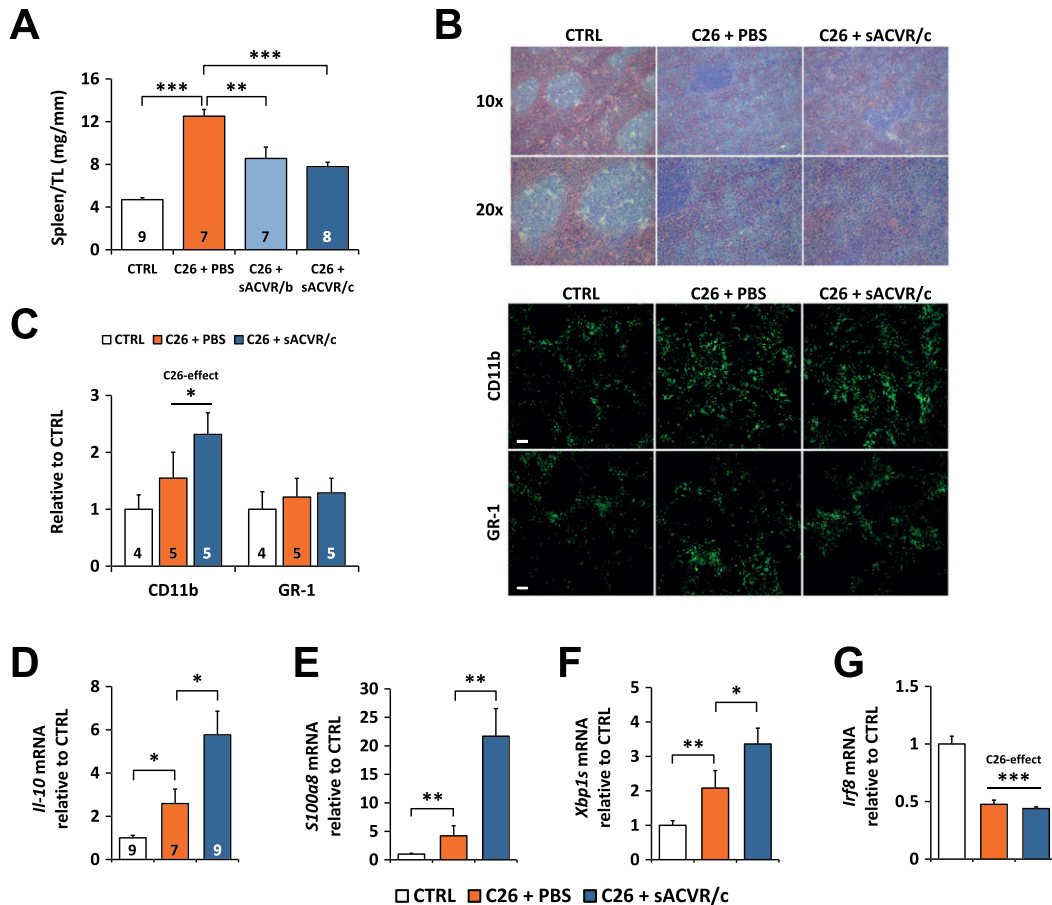


**Figure 6** Administration of sACVR2B-Fc attenuates C26 cancer-induced splenomegaly independent of splenic MDSCs. (A) Spleen mass normalized to the length of the tibia (TL) on Day 11 after C26 cell injection. (B) Haematoxylin and eosin staining of the spleen on Day 13 after C26 cell injection. (C) CD11b and GR-1 (LY-6C/G) count in spleen on Day 13 after C26 cell injection and representative immunofluorescence images. Scale bar = 100  $\mu$ m. The mRNA expression of MDSC markers (D) interleukin-10 (*Il-10*), (E) S100 calcium binding protein A8 (*S100a8*), and (F) the splice variant of X-box Binding Protein 1 (*Xbp1s*) as well as (G) Interferon Regulatory Factor 8 (*Irf8*), a negative regulator of MDSCs,<sup>41</sup> on Day 13 after C26 cell injection. \*, \*\*, and \*\*\* =  $P < 0.05$ , 0.01, and 0.001, respectively. Student's *t*-test and one-way ANOVA with Holm–Bonferroni corrected LSD (A, C, D), Mann–Whitney *U* (E–G). Lines without vertical ends show a pooled effect of all C26-groups combined. N-sizes are depicted in the bar graphs.  $N = 7$ – $9$ /group in (E–G).



in the C26 tumour-bearing mice compared with the control mice without changes in the density of GR-1 (LY-6C/G) positive cells (Figure 6C). As spleen size was increased in the tumour-bearing mice, counts/area were multiplied by the spleen mass to get an idea of the total abundance of CD11b and GR-1 (LY-6C/G) positive cells. This analysis showed a more pronounced increase in both CD11b and GR-1 (LY-6C/G) positive cells in the tumour-bearing mice (Online Resource 7: Figure S5).

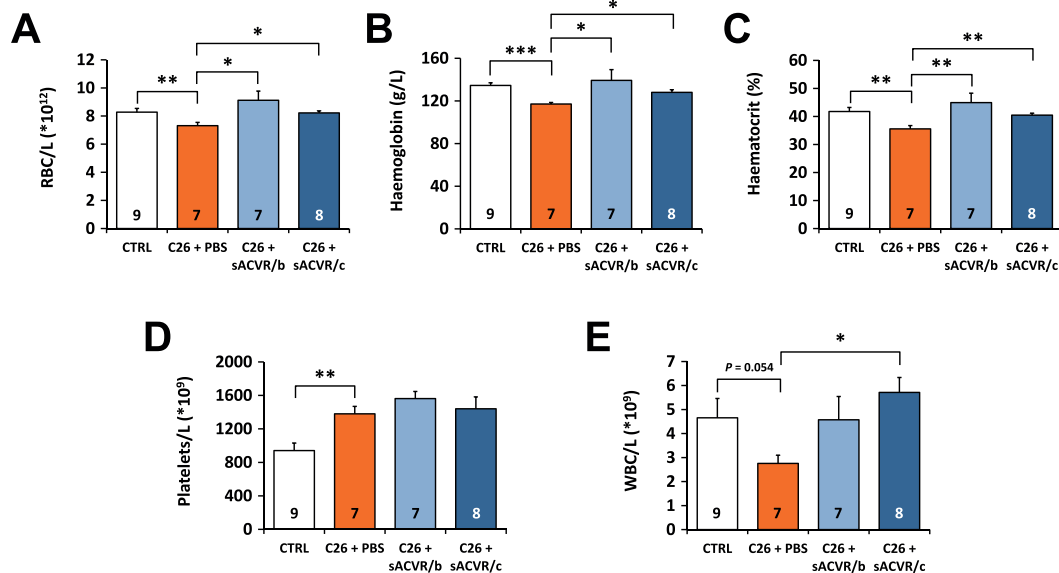
The expression of genes previously related to presence and development of MDSCs<sup>42</sup> was increased in the tumour-bearing mice, and this effect was even more pronounced in the sACVR2B-Fc treated mice (Figure 6D–G). These results suggest an increased abundance of splenic MDSCs in the tumour-bearing mice, and this effect is even accentuated by sACVR2B administration. Thus, changes in MDSCs do not explain the effect of sACVR2B-Fc on the

spleen mass, and the cell population responsible for this effect is still to be identified. Nevertheless, as a possible mechanism, sACVR2B-Fc treated group showed increased mRNA expression of Cyclin Dependent Kinase Inhibitor 1A (*Cdkn1a/p21*), an inhibitor of proliferation (Online Resource 7: Figure S5).

### Activin receptor ligand blocking reverses the mild anaemia observed in tumour-bearing mice

In the tumour-bearing mice, red blood cell count, haemoglobin, and haematocrit were slightly, but significantly decreased (Figure 7A–C). All of these parameters were at least partially restored by sACVR2B-Fc administration (Figure 7A–C). In contrast, platelet count was robustly augmented in the tumour-bearing mice independent of

**Figure 7** Haematological parameters in C26 tumour-bearing mice and the effects of sACVR2B-Fc. (A) Red blood cell count (RBC), (B) haemoglobin, (C) haematocrit, (D) platelet count, and (E) white blood cell count (WBC) on Day 11 after C26 cell injection. \*, \*\*, and \*\*\* =  $P < 0.05$ ,  $0.01$  and  $0.001$ , respectively. Kruskal–Wallis with Holm–Bonferroni corrected Mann–Whitney  $U$  (A–C) or Student's  $t$ -test and one-way ANOVA with Holm–Bonferroni corrected LSD (D, E). N-sizes are depicted in the bar graphs. These results were replicated in the second short-term experiment (data not shown).



sACVR2B-Fc administration (Figure 7D). White blood cell count tended to increase by continued sACVR2B-Fc administration (Figure 7E).

## Discussion

In the present study, we show that preventing cachexia by continued blocking of ACVR2B ligands improved survival in tumour-bearing mice without affecting primary tumour growth similarly as earlier.<sup>9,14,16</sup> These findings together with results from treatments affecting other pathways<sup>19–22</sup> as well as epidemiological evidence in humans<sup>2</sup> have led to suggestions for a possible causal link between preservation of muscle mass and improved survival.<sup>4</sup> This hypothesis is in part supported by the present study showing that increasing muscle mass and maintaining it by continued blocking of ACVR2B ligands improves survival. In comparison, the discontinuation of the treatment before the tumour formation led to a systematically worse outcome and also shorter survival. This may be due to the fact that the discontinuation of the treatment may in itself have adverse effects on the host or because larger muscles at the onset of the disease may result in more robust cachexia, as shown earlier.<sup>43</sup> Nevertheless, if the preservation of muscle *per se* indeed improved survival, the exact mechanisms still remain unresolved. It is possible, for instance, that the preservation of some specific vital muscles, such as the major respiratory muscles,<sup>44,45</sup> is paramount

rather than muscle tissue in general. Indeed, diaphragm atrophy and weakness accompanied by ventilatory dysfunction have been reported in C26 tumour-bearing mice.<sup>46,47</sup> Interestingly, ACVR2 ligand blocking restored diaphragm mass in the present study, which may at least in part have explained the prolonged survival of these mice, although the differences between the treatment protocols were quite marginal at the time point investigated.

In addition to skeletal muscles, cardiac cachexia and associated pathological changes such as arrhythmias may be linked to survival in cancer cachexia.<sup>48,49</sup> In our hands, however, the C26 tumour burden resulted in only mild cardiac cachexia and sACVR2B treatment did not affect heart size, similarly as earlier.<sup>35</sup> This differs from the results of Zhou *et al.* who reported significant cardiac atrophy which was fully reversed by sACVR2B. This may be explained by more severe cachexia that was treated with higher doses of sACVR2B-Fc.<sup>9</sup> However, we have recently demonstrated that sACVR2B-Fc has markedly smaller effects on cardiac than skeletal muscle in chemotherapy-induced cachexia model.<sup>35</sup> Future studies should better elucidate the effects of blocking ACVR2 ligands on the heart and the importance of cardiac cachexia on cancer prognosis.

Liver acute phase response (APR) has been associated with impaired survival in cancer cachexia in humans.<sup>26</sup> It is an early-defence system driven by cytokines such as IL-6, which induces Stat3 activation and consequently increased expression of acute phase proteins.<sup>26,50</sup> We showed induced hepatic APR in tumour-bearing mice supporting previous

findings.<sup>25</sup> Also the liver protein synthesis was increased in the tumour-bearing mice, a finding that is consistent with an earlier study with C26 cancer,<sup>51</sup> and also with human cancer cachexia, assuming that increased synthesis of circulating fibrinogen reflects mainly increased liver protein synthesis.<sup>52</sup> Increased liver protein synthesis in tumour-bearing mice may reflect increased synthesis of exported APR proteins, because no significant changes in liver mass were observed in any of the experiments. Both ACVR2 ligand blocking protocols reduced the increased protein synthesis and Stat3 phosphorylation again without an effect on liver mass. Although no differences in these results were observed between the two treated groups, the discontinued sACVR2B-Fc treatment was associated with much worse prognosis perhaps arguing against these hepatic changes being important for the survival benefit of continued ACVR2 ligand blocking. Interestingly, however, the level of hepatic APR proteins correlated with body mass loss suggesting that the importance of these pathways should be further investigated in the future as well as the mechanisms of blocking ACVR2 ligands on liver protein synthesis in cancer.

Pro-inflammatory cytokines are thought to be important for the development of cancer cachexia<sup>53</sup> and on its prognosis.<sup>27,54</sup> Of multiple cytokines analysed, IL-6 and MCP-1 were strongly elevated in the sera of the C26 tumour-bearing mice, which is in agreement with previous findings in the same experimental model.<sup>9,20</sup> In humans, high levels of MCP-1<sup>27</sup> and IL-6<sup>54</sup> have been related to shorter survival time in pancreatic ductal adenocarcinoma and lung cancer, respectively. Recently, elevated MCP-1 was associated with cachexia in treatment naïve pancreatic cancer patients.<sup>55</sup> However, in the present study, these responses were not attenuated by the sACVR2B treatment suggesting that continued blocking of ACVR2B pathway enhances survival and prevents muscle loss independent of the elevated circulating pro-inflammatory cytokines similarly as suggested by Zhou et al. based on IL-6, IL-1 $\beta$ , and TNF- $\alpha$ .<sup>9</sup> Continued sACVR2B-Fc treatment even increased serum MCP-1 and IL-1 $\beta$ , but the mechanism and physiological importance of this effect is unknown and further studies are needed. We also analysed sera from the survival experiment at the day of euthanasia ( $n = 4-5$  per group), where MCP-1 was even further elevated in the C26 + sACVR/c group of mice. This may be due to prolonged survival and thus more advanced disease at euthanasia (data not shown).

Interestingly, increased spleen size (splenomegaly) typically observed in experimental cancer,<sup>28,56,57</sup> was attenuated in sACVR2B-Fc treated mice. In addition, expansion of splenic MDSCs has previously been associated with potential effects on cachexia development and survival.<sup>28</sup> Interestingly, although the increase in spleen size was prevented, the markers of MDSCs in spleen were not decreased with ACVR2 ligand blocking. Moreover, the increase in spleen size was

prevented by sACVR2B-Fc treatment independent of the treatment protocol suggesting that spleen may not play a major role in enhanced survival with the continued ACVR2 ligand blocking. Nevertheless, an overall reduction in red pulp area by sACVR2B was recently observed in an animal model of  $\beta$ -thalassemia intermedia, and this was associated with alleviation of anaemia and splenomegaly.<sup>58</sup> We found that the white pulp areas were clearly visible in healthy control mice, whereas in the tumour-bearing mice, these areas were disorganized, and this tended to occur especially in sACVR2B treated mice. We also found changes in basic haematological parameters such as decreased blood haemoglobin and haematocrit in C26 tumour-bearing mice, which is in line with previous studies,<sup>59</sup> and those were reversed in the sACVR2B treated mice. Importantly, however, these factors did not differ between the treated groups, at least at this time point where the loss of body mass had already started with the discontinued treatment, suggesting that the attenuation of anaemia unlikely results in improved survival with continued ACVR2 ligand blocking. However, the effect of preventing anaemia *per se* may have other benefits as erythropoietin can improve health in C26 tumour-bearing mice.<sup>24,60</sup>

Physical activity has been shown to be beneficial for health and also for cancer incidence and potentially for tumour host survival.<sup>61,62</sup> Our results showed that tumour-bearing mice were less active than healthy controls supporting earlier evidence of decreased physical activity in tumour-bearing mice.<sup>16,59,63</sup> Decreased physical activity was not due to muscle wasting *per se* as preventing muscle wasting by blocking ACVR2 ligands did not prevent the decrease in physical activity. Our results also argue against physical activity being an important factor for improved survival with continued sACVR2B-Fc treatment. Similar results of the effects of sACVR2B treatment on physical activity have been reported earlier in LLC tumour-bearing mice.<sup>16</sup> The reduction in physical activity was associated with only minor changes in some of the mitochondrial markers in skeletal muscle and the heart.

Similarly to Zhou et al.,<sup>9</sup> we report that sACVR2B-Fc did not affect C26 tumour mass showing that C26 tumour growth is not regulated by ACVR2 ligands. We extended this finding by showing that the gene expression of *Activin A* and *Il-6*, which are important proteins in cachexia,<sup>8</sup> were not reduced by sACVR2B-Fc further showing that sACVR2B-Fc improved survival in this experimental model of cancer without marked effects on the tumour. However, the circulating ACVR2 ligands may also be directly or indirectly related to the cancer prognosis at least in part independent of cachexia. High circulating *Activin A* levels predict poor prognosis in colorectal and lung cancer patients.<sup>10,64</sup> This may be explained by increased *Activin A* levels reflecting the severity or the extent of the cancer or cachexia. However, also direct effects of *Activin A*,<sup>65,66</sup> and perhaps of other ACVR2 ligands,

on non-muscle tissues may also affect survival in cancer cachexia, and thus more studies are needed to further investigate this phenomenon.

Muscle wasting in cancer cachexia can be attributed to decreased protein synthesis,<sup>5,6</sup> impaired regeneration<sup>7</sup> as well as increased protein degradation<sup>6</sup> in skeletal muscle. At the time point in which body mass loss started to accelerate and predicted survival, increased mRNA expression of muscle specific E3 ubiquitin ligases and the content of ubiquitinated proteins were observed, suggesting increased protein degradation via the ubiquitin-proteasome system. At the same time, robustly decreased muscle protein synthesis in TA, diaphragm, and the heart of the tumour-bearing mice was observed. In the present study, as predicted from decreased mTOR signalling activity, mTOR colocalization with the lysosomes/late-endosomes was decreased in skeletal muscles of C26 tumour-bearing mice. Interestingly, our correlation data suggests that this novel finding may explain at least in part the cachexia and decreased muscle protein synthesis in the untreated tumour-bearing mice. Targeting of mTOR to lysosomes/late-endosomes has previously been shown to be sufficient to activate mTOR signalling while mTOR inactivation by, e.g. amino acid starvation is associated with mTOR dissociation from lysosomes/late-endosomes.<sup>38,39</sup> Even though continued sACVR2B-Fc administration had no effect on protein synthesis at this time point, it was able to partially restore S6 phosphorylation and the colocalization of mTOR with the lysosomes/late-endosomes. The reason for this discordance is unknown, but may be due to decreased food intake or simply the refractory nature of cancer cachexia at this time point in most of the animals.<sup>67</sup> Indeed, the increased skeletal muscle masses with ACVR2B ligand blocking are probably due to earlier changes in protein synthesis and/or degradation, as we have previously reported increased protein synthesis with ACVR2B ligand blocking in healthy and chemotherapy receiving mice.<sup>15,30</sup>

In conclusion, we showed that increased muscle size with ACVR2 ligand blocking was associated with improved survival in C26 tumour-bearing mice only when the treatment was continued after the tumour formation. The prolonged survival could potentially be attributed in part to maintenance of muscle mass and, in theory, the respiratory muscle mass. However, more specific strategies in preventing total and specific loss of muscle (limb, respiratory, and heart) without possible non-muscle effects should be investigated in the future. Moreover, our results suggest that circulating pro-inflammatory cytokines, physical activity, or altered hepatic and splenic physiology may not be determining factors for improved survival with activin receptor ligand blocking. In addition, our novel result of decreased muscle protein synthesis and mTOR localization with lysosomes/late endosomes opens up possible future research questions and treatment options for cachexia.

## Acknowledgements

This work was supported by the Academy of Finland [grant No. 275922 (JJH) and 297245 (RK)], Cancer Society of Finland (JJH), and Jenny and Antti Wihuri Foundation (TAN, RK). We also thank Dr Philippe Pierre for kindly providing the anti-puromycin antibody. We acknowledge Arja Pasternack, Mika Silvennoinen, Maarit Lehti, Sanna Lensu, Sira Karvinen, Mervi Matero, Jouni Härkönen, Aila Ollikainen, Risto Puurtinen, Kaisa-Leena Tulla, Eliisa Kiukkanen, Minna Savela, and Jouni Tukiainen for their valuable help and technical assistance.

The authors certify that they comply with the ethical guidelines for authorship and publishing of the Journal of Cachexia, Sarcopenia, and Muscle.<sup>68</sup>

## Online supplementary material

Additional Supporting Information may be found online in the supporting information tab for this article.

**Figure S1** C26 cancer decreases (a) body mass (time x group interaction  $P < 0.001$ ) and masses of (b) tibialis anterior (TA), (c) gastrocnemius (GA), (d) heart and (e) epididymal fat (eWAT). TL = tibial length. C26 tumour expresses substantially higher levels of (f) *Activin A*, (g) *Il-6*, and (h) *Myostatin* mRNA than LLC tumour. \*, \*\* and \*\*\* =  $P < 0.05$ ,  $P < 0.01$  and  $P < 0.001$ , respectively. Students *t*-test (a–e), Mann-Whitney U (f–h). N-sizes are depicted in the bar graphs, except in (a) where  $N = 8$  per group. Data is presented as means  $\pm$  SEM, except in (a), where data is presented as mean  $\pm$  SD.

**Supplementary Table S1** Primer information for qPCR analyses.

**Figure S2** The effects of C26 cancer and sACVR2B-Fc administration on body mass and tumour and muscle gene expression. (a) Length of the tibia on day 11 after C26 cell inoculation. (b) Body masses in the survival experiment. Tumour (c) *Activin A* (*Inhibin  $\beta$ A*) and (d) *Il-6* mRNA expression. Gastrocnemius (e) *Activin A* (*Inhibin  $\beta$ A*), (f) *Il-6* and (g) *Myostatin* (*Gdf8*) mRNA expression at day 11 after tumour inoculation. C26 cells were inoculated at day 0. mRNA-results were normalized to *36b4* mRNA. FC = fold change. \* and \*\* =  $P < 0.05$ , and  $P < 0.01$ , respectively. Student's *t*-test and one-way ANOVA with Holm-Bonferroni corrected LSD (a, e–g). Kruskal-Wallis with Holm-Bonferroni corrected Mann-Whitney U (c, d). N-sizes are depicted in the bar graph except in (b) in which  $n = 6, 12, 8,$  and  $9$  in CTRL, C26 + PBS, C26 + sACVR/b, and C26 + sACVR/c, respectively.

**Figure S3** (a) Phosphorylation of S6K1 at Thr389 was decreased in tumour-bearing mice on day 11 after C26 cell inoculation. C26 cancer cachexia was associated with increased ubiquitinated proteins in (b) tibialis anterior and



(c) diaphragm, and increased mRNA expression of ubiquitin ligases (d) *Murf1*, (e) *Atrogin1* and (f) *Musa1*, which were not affected by sACVR2B-Fc administration in gastrocnemius on day 11 after C26 cell inoculation. C = CTRL, P = C26 + PBS, Ab = C26 + sACVR/b, Ac = C26 + sACVR/c. FC = fold change. \* and \*\* =  $P < 0.05$  and  $P < 0.01$ , respectively. Kruskal-Wallis with Holm-Bonferroni corrected Mann-Whitney U (a–e), Student's *t*-test and one-way ANOVA with Holm-Bonferroni corrected LSD (f). N-sizes are depicted in the bar graphs.

**Figure S4** Mitochondrial markers in the heart on day 11 after C26 cell injection. (a) PGC-1 $\alpha$  and cytochrome *c* (Cyt *c*) protein levels were not altered by the C26 tumour or the sACVR2B-Fc treatment in the heart. N-sizes are depicted in the bar graphs. (b) OXPHOS complex IV (MTCO1) was significantly increased in the hearts of the vehicle treated tumour-bearing mice (C26 + PBS). In addition, when all C26 tumour-bearing groups were pooled, a significant increase was seen also in complexes CI (NDUFB8) and CIII (UQCRC2) as well as the sum of all complexes (total). This pooled C26-effect is depicted by the lines without vertical ends.  $N = 7$ – $9$ /group. C = CTRL, P = C26 + PBS, Ab = C26 + sACVR/b, Ac = C26 + sACVR/c. \* and \*\*\* =  $P < 0.05$  and  $P < 0.001$ , respectively (Mann-Whitney U).

**Supplementary Table S2** Serum cytokine levels at 11 days after C26 cell injection.  $N = 8, 7, 6$  and  $8$  in CTRL, C26 + PBS, C26 + sACVR/b and C26 + sACVR/c groups, respectively. The values are presented in pg/ml. If over half of the values in the group were below or close to the detec-

tion limit, the concentration is not presented (depicted as N/A in the table). Cytokines with at least 3/4 of all values below or close to the detection limit are not shown (IL-1a, IL-2, IL-3, IL-4, IL-10, IL-17, IFN $\gamma$ , TNF- $\alpha$ , MIP-1a and GM-CSF). In statistical analysis, the C26-effect was analysed by pooling all the tumour-bearing groups. The sACVR-effect P-value designates the lowest sACVR2B-Fc P-value in comparison to C26 + PBS and if the significance is found, the sACVR2B-Fc group significantly different compared with C26 + PBS is indicated with \*.

**Figure S5** Effects of C26 tumour and sACVR2B-Fc on the spleen on day 13 after C26 cell inoculation. (a) C26 cancer-induced splenomegaly is attenuated by sACVR2B-Fc administration. Splenic (b) CD11b and (c) GR-1 contents were increased in C26 cancer when multiplied by spleen mass to reflect the total abundance of CD11b and GR-1 positive cells. (d) sACVR2B-Fc administration resulted in increased splenic *Cdkn1a* (*p21*) mRNA. \* and \*\* =  $P < 0.05$  and  $P < 0.01$ , respectively. C26 and sACVR2B-Fc effects were analysed with Student's *t*-test (a, b, d) or Mann-Whitney U test (c). N-sizes are depicted in the bar graphs.

## Conflict of interest

Tuuli A. Nissinen, Jaakko Hentilä, Fabio Penna, Anita Lampinen, Juulia H. Lautaoja, Vasco Fachada, Tanja Holopainen, Olli Ritvos, Riikka Kivelä, and Juha J. Hulmi declare that they have no conflicts of interest.

## References

1. Fearon K, Arends J, Baracos V. Understanding the mechanisms and treatment options in cancer cachexia. *Nat Rev Clin Oncol* 2013;**10**:90–99.
2. Kazemi-Bajestani SM, Mazurak VC, Baracos V. Computed tomography-defined muscle and fat wasting are associated with cancer clinical outcomes. *Semin Cell Dev Biol* 2015;**54**:2–10.
3. Wolfe RR. The underappreciated role of muscle in health and disease. *Am J Clin Nutr* 2006;**84**:475–482.
4. Lee SJ, Glass DJ. Treating cancer cachexia to treat cancer. *Skelet Muscle* 2011;**1**:2.
5. Horstman AM, Olde Damink SW, Schols AM, van Loon LJ. Is cancer cachexia attributed to impairments in basal or postprandial muscle protein metabolism? *Forum Nutr* 2016;**8**.
6. Smith KL, Tisdale MJ. Increased protein degradation and decreased protein synthesis in skeletal muscle during cancer cachexia. *Br J Cancer* 1993;**67**:680–685.
7. Talbert EE, Guttridge DC. Impaired regeneration: a role for the muscle microenvironment in cancer cachexia. *Semin Cell Dev Biol* 2016;**54**:82–91.
8. Chen JL, Walton KL, Qian H, Colgan TD, Hagg A, Watt MJ, et al. Differential Effects of IL6 and Activin A in the development of cancer-associated cachexia. *Cancer Res* 2016;**76**:5372–5382.
9. Zhou X, Wang JL, Lu J, Song Y, Kwak KS, Jiao Q, et al. Reversal of cancer cachexia and muscle wasting by ActRIIB antagonism leads to prolonged survival. *Cell* 2010;**142**:531–543.
10. Loumave A, de Barsey M, Nachit M, Lause P, van Maanen A, Trefois P, et al. Circulating Activin A predicts survival in cancer patients. *J Cachexia Sarcopenia Muscle* 2017;**8**:768–777.>
11. Costelli P, Muscaritoli M, Bonetto A, Penna F, Reffo P, Bossola M, et al. Muscle myostatin signalling is enhanced in experimental cancer cachexia. *Eur J Clin Invest* 2008;**38**:531–538.
12. Lee SJ, Reed LA, Davies MV, Girgenrath S, Goad ME, Tomkinson KN, et al. Regulation of muscle growth by multiple ligands signaling through activin type II receptors. *Proc Natl Acad Sci U S A* 2005;**102**:18117–18122.
13. Morvan F, Rondeau JM, Zou C, Minetti G, Scheufler C, Scharenberg M, et al. Blockade of activin type II receptors with a dual anti-ActRIIA/IIb antibody is critical to promote maximal skeletal muscle hypertrophy. *Proc Natl Acad Sci U S A* 2017;**114**:12448–12453.>
14. Hatakeyama S, Summermatter S, Jourdain M, Melly S, Minetti GC, Lach-Trifilieff E. ActRII blockade protects mice from cancer cachexia and prolongs survival in the presence of anti-cancer treatments. *Skelet Muscle* 2016;**6**:2.
15. Nissinen TA, Degerman J, Rasanen M, Poikonen AR, Koskinen S, Mervaala E, et al. Systemic blockade of ACVR2B ligands prevents chemotherapy-induced muscle wasting without affecting oxidative capacity or atrogenes. *Sci Rep* 2016;**6**:32695.
16. Toledo M, Busquets S, Penna F, Zhou X, Marmonti E, Betancourt A, et al. Complete reversal of muscle wasting in experimental cancer cachexia: additive effects of activin type II receptor inhibition and beta-2 agonist. *Int J Cancer* 2016;**138**:2021–2029.
17. Attie KM, Borgstein NG, Yang Y, Condon CH, Wilson DM, Pearsall AE, et al. A single ascending-dose study of muscle regulator

- ACE-031 in healthy volunteers. *Muscle Nerve* 2013;**47**:416–423.
18. Rooks D, Praestgaard J, Hariry S, Laurent D, Petricoul O, Perry RG, et al. Treatment of Sarcopenia with Bimagrumab: results from a Phase II, randomized, controlled, proof-of-concept study. *J Am Geriatr Soc* 2017;**65**:1988–1995.
  19. Cai D, Frantz JD, Tawa NE, Jr MPA, Oh BC, Lidov HG, et al. IKKbeta/NF-kappaB activation causes severe muscle wasting in mice. *Cell* 2004;**119**:285–298.
  20. Lerner L, Tao J, Liu Q, Nicoletti R, Feng B, Krieger B, et al. MAP3K11/GDF15 axis is a critical driver of cancer cachexia. *J Cachexia Sarcopenia Muscle* 2016;**7**:467–482.
  21. Tseng YC, Kulp SK, Lai IL, Hsu EC, He WA, Frankhouser DE, et al. Preclinical investigation of the novel histone deacetylase inhibitor AR-42 in the treatment of cancer-induced cachexia. *J Natl Cancer Inst* 2015;**107**:djv274.
  22. Johnston AJ, Murphy KT, Jenkinson L, Laine D, Emmrich K, Faou P, et al. Targeting of Fn14 prevents cancer-induced cachexia and prolongs survival. *Cell* 2015;**162**:1365–1378.
  23. Tisdale MJ. Mechanisms of cancer cachexia. *Physiol Rev* 2009;**89**:381–410.
  24. Penna F, Busquets S, Toledo M, Pin F, Massa D, Lopez-Soriano FJ, et al. Erythropoietin administration partially prevents adipose tissue loss in experimental cancer cachexia models. *J Lipid Res* 2013;**54**:3045–3051.
  25. Bonetto A, Aydogdu T, Kunzevitzky N, Guttridge DC, Khuri S, Koniaris LG, et al. STAT3 activation in skeletal muscle links muscle wasting and the acute phase response in cancer cachexia. *PLoS One* 2011;**6**:e22538.
  26. Stephens NA, Skipworth RJ, Fearon KC. Cachexia, survival and the acute phase response. *Curr Opin Support Palliat Care* 2008;**2**:267–274.
  27. Lewis HL, Chakedis JM, Talbert E, Haverick E, Rajasekera P, Hart P, et al. Perioperative cytokine levels portend early death after pancreatectomy for ductal adenocarcinoma. *J Surg Oncol* 2017; <https://doi.org/10.1002/jso.24940>.
  28. Cuenca AG, Cuenca AL, Winfield RD, Joiner DN, Gentile L, Delano MJ, et al. Novel role for tumor-induced expansion of myeloid-derived cells in cancer cachexia. *J Immunol* 2014;**192**:6111–6119.
  29. Corbett TH, Griswold DP, Roberts BJ, Peckham JC, Schabel FM. Tumor induction relationships in development of transplantable cancers of the colon in mice for chemotherapy assays, with a note on carcinogen structure. *Cancer Res* 1975;**35**:2434–2439.
  30. Hulmi JJ, Oliveira BM, Silvennoinen M, Hoogaars WM, Ma H, Pierre P, et al. Muscle protein synthesis, mTORC1/MAPK/Hippo signaling, and capillary density are altered by blocking of myostatin and activins. *Am J Physiol Endocrinol Metab* 2013;**304**:41.
  31. Kainulainen H, Papaioannou KG, Silvennoinen M, Autio R, Saarela J, Oliveira BM, et al. Myostatin/activin blocking combined with exercise reconditions skeletal muscle expression profile of mdx mice. *Mol Cell Endocrinol* 2015;**399**:131–142.
  32. Silvennoinen M, Rantalainen T, Kainulainen H. Validation of a method to measure total spontaneous physical activity of sedentary and voluntary running mice. *J Neurosci Methods* 2014;**235**:51–58.
  33. Goodman CA, Mabrey DM, Frey JW, Miu MH, Schmidt EK, Pierre P, et al. Novel insights into the regulation of skeletal muscle protein synthesis as revealed by a new nonradioactive in vivo technique. *FASEB J* 2011;**25**:1028–1039.
  34. Schmidt EK, Clavarino G, Ceppi M, Pierre P. SUnSET, a nonradioactive method to monitor protein synthesis. *Nat Methods* 2009;**6**:275–277.
  35. Hulmi JJ, Nissinen TA, Rasanen M, Degerman J, Lautaoja JH, Hemanthakumar KA, et al. Prevention of chemotherapy-induced cachexia by ACVR2B ligand blocking has different effects on heart and skeletal muscle. *J Cachexia Sarcopenia Muscle* 2017; <https://doi.org/10.1002/jcsm.12265>.
  36. Hulmi JJ, Oliveira BM, Silvennoinen M, Hoogaars WM, Pasternack A, Kainulainen H, et al. Exercise restores decreased physical activity levels and increases markers of autophagy and oxidative capacity in myostatin/activin-blocked mdx mice. *Am J Physiol Endocrinol Metab* 2013;**305**:171.
  37. Costes SV, Daelemans D, Cho EH, Dobbin Z, Pavlakis G, Lockett S. Automatic and quantitative measurement of protein-protein colocalization in live cells. *Biophys J* 2004;**86**:3993–4003.
  38. Jacobs BL, Goodman CA, Hornberger TA. The mechanical activation of mTOR signaling: an emerging role for late endosome/lysosomal targeting. *J Muscle Res Cell Motil* 2014;**35**:11–21.
  39. Sancak Y, Bar-Peled L, Zoncu R, Markhard AL, Nada S, Sabatini DM. Ragulator-Rag complex targets mTORC1 to the lysosomal surface and is necessary for its activation by amino acids. *Cell* 2010;**141**:290–303.
  40. Sartori R, Schirwis E, Blaauw B, Bortolanza S, Zhao J, Enzo E, et al. BMP signaling controls muscle mass. *Nat Genet* 2013;**45**:1309–1318.
  41. Waight JD, Netherby C, Hensen ML, Miller A, Hu Q, Liu S, et al. Myeloid-derived suppressor cell development is regulated by a STAT/IRF-8 axis. *J Clin Invest* 2013;**123**:4464–4478.
  42. Bronte V, Brandau S, Chen SH, Colombo MP, Frey AB, Greten TF, et al. Recommendations for myeloid-derived suppressor cell nomenclature and characterization standards. *Nat Commun* 2016;**7**:12150.
  43. Benny Klimek ME, Aydogdu T, Link MJ, Pons M, Koniaris LG, Zimmers TA. Acute inhibition of myostatin-family proteins preserves skeletal muscle in mouse models of cancer cachexia. *Biochem Biophys Res Commun* 2010;**391**:1548–1554.
  44. Azoulay E, Thierry G, Chevet S, Moreau D, Darmon M, Bergeron A, et al. The prognosis of acute respiratory failure in critically ill cancer patients. *Medicine (Baltimore)* 2004;**83**:360–370.
  45. Schapira DV, Studnicki J, Bradham DD, Wolff P, Jarrett A. Intensive care, survival, and expense of treating critically ill cancer patients. *JAMA* 1993;**269**:783–786.
  46. Murphy KT, Chee A, Trieu J, Naim T, Lynch GS. Importance of functional and metabolic impairments in the characterization of the C-26 murine model of cancer cachexia. *Dis Model Mech* 2012;**5**:533–545.
  47. Roberts BM, Ahn B, Smuder AJ, Al-Rajhi M, Gill LC, Beharry AW, et al. Diaphragm and ventilatory dysfunction during cancer cachexia. *FASEB J* 2013;**27**:2600–2610.
  48. Kalantar-Zadeh K, Rhee C, Sim JJ, Stenvinkel P, Anker SD, Kovesdy CP. Why cachexia kills: examining the causality of poor outcomes in wasting conditions. *J Cachexia Sarcopenia Muscle* 2013;**4**:89–94.
  49. Murphy KT. The pathogenesis and treatment of cardiac atrophy in cancer cachexia. *Am J Physiol Heart Circ Physiol* 2016;**310**:466.
  50. Cray C, Zaias J, Altman NH. Acute phase response in animals: a review. *Comp Med* 2009;**59**:517–526.
  51. Samuels SE, McLaren TA, Knowles AL, Stewart SA, Madelmont JC, Attaix D. Liver protein synthesis stays elevated after chemotherapy in tumour-bearing mice. *Cancer Lett* 2006;**239**:78–83.
  52. Barber MD, Fearon KC, McMillan DC, Slater C, Ross JA, Preston T. Liver export protein synthetic rates are increased by oral meal feeding in weight-losing cancer patients. *Am J Physiol Endocrinol Metab* 2000;**279**:707.
  53. Argiles JM, Busquets S, Toledo M, Lopez-Soriano FJ. The role of cytokines in cancer cachexia. *Curr Opin Support Palliat Care* 2009;**3**:263–268.
  54. Martin F, Santolaria F, Batista N, Milena A, Gonzalez-Reimers E, Brito MJ, et al. Cytokine levels (IL-6 and IFN-gamma), acute phase response and nutritional status as prognostic factors in lung cancer. *Cytokine* 1999;**11**:80–86.
  55. Talbert EE, Lewis HL, Farren MR, Ramsey ML, Chakedis JM, Rajasekera P, et al. Circulating monocyte chemoattractant protein-1 (MCP-1) is associated with cachexia in treatment-naive pancreatic cancer patients. *J Cachexia Sarcopenia Muscle* 2018; <https://doi.org/10.1002/jcsm.12251>.
  56. Aulino P, Berardi E, Cardillo VM, Rizzuto E, Perniconi B, Ramina C, et al. Molecular, cellular and physiological characterization of the cancer cachexia-inducing C26 colon carcinoma in mouse. *BMC Cancer* 2010;**10**:363.
  57. Mundy-Bosse BL, Lesinski GB, Jaime-Ramirez AC, Benninger K, Khan M, Kuppusamy P, et al. Myeloid-derived suppressor cell inhibition of the IFN response in tumor-bearing mice. *Cancer Res* 2011;**71**:5101–5110.
  58. Suragani RN, Cawley SM, Li R, Wallner S, Alexander MJ, Mulivor AW, et al. Modified activin receptor IIB ligand trap mitigates ineffective erythropoiesis and disease

- complications in murine beta-thalassemia. *Blood* 2014;**123**:3864–3872.
59. Toledo M, Penna F, Busquets S, Lopez-Soriano FJ, Argiles JM. Distinct behaviour of sorafenib in experimental cachexia-inducing tumours: the role of STAT3. *PLoS One* 2014;**9**:e113931.
60. Pin F, Busquets S, Toledo M, Camperi A, Lopez-Soriano FJ, Costelli P, et al. Combination of exercise training and erythropoietin prevents cancer-induced muscle alterations. *Oncotarget* 2015;**6**:43202–43215.
61. Friedenreich CM, Neilson HK, Farris MS, Courneya KS. Physical activity and cancer outcomes: a precision medicine approach. *Clin Cancer Res* 2016;**22**:4766–4775.
62. Moore SC, Lee IM, Weiderpass E, Campbell PT, Sampson JN, Kitahara CM, et al. Association of leisure-time physical activity with risk of 26 types of cancer in 1.44 million adults. *JAMA Intern Med* 2016;**176**:816–825.
63. van Norren K, Kegler D, Argiles JM, Luiking Y, Gorselink M, Laviano A, et al. Dietary supplementation with a specific combination of high protein, leucine, and fish oil improves muscle function and daily activity in tumour-bearing cachectic mice. *Br J Cancer* 2009;**100**:713–722.
64. Hoda MA, Rozsas A, Lang E, Klikovits T, Lohinai Z, Torok S, et al. High circulating Activin A level is associated with tumor progression and predicts poor prognosis in lung adenocarcinoma. *Oncotarget* 2016;**7**:13388–13399.
65. Antsiferova M, Huber M, Meyer M, Piwko-Czuchra A, Ramadan T, MacLeod AS, et al. Activin enhances skin tumourigenesis and malignant progression by inducing a pro-tumourigenic immune cell response. *Nat Commun* 2011;**2**:576.
66. Li Q, Kumar R, Underwood K, O'Connor AE, Loveland KL, Seehra JS, et al. Prevention of cachexia-like syndrome development and reduction of tumor progression in inhibin-deficient mice following administration of a chimeric activin receptor type II-murine Fc protein. *Mol Hum Reprod* 2007;**13**:675–683.
67. Fearon K, Strasser F, Anker SD, Bosaeus I, Bruera E, Fainsinger RL, et al. Definition and classification of cancer cachexia: an international consensus. *Lancet Oncol* 2011;**12**:489–495.
68. von Haehling S, Morley JE, Coats AJS, Anker SD. Ethical guidelines for publishing in the journal of cachexia, sarcopenia and muscle: update 2017. *J Cachexia Sarcopenia Muscle* 2017;**8**:1081–1083.



## IV

# **MUSCLE FOLLISTATIN GENE DELIVERY INCREASES MUSCLE PROTEIN SYNTHESIS INDEPENDENT OF PERIODICAL PHYSICAL INACTIVITY AND FASTING**

by

Nissinen, T.A., Hentilä, J., Fachada, V., Lautaoja, J.H., Pasternack, A.,  
Ritvos, O., Kivelä, R. & Hulmi, J.J. 2020

In revision.

Request a copy from the author.

